

aMazing pattern: spatial self-organization in peatlands

BuitenGewoon patroon: ruimtelijke zelforganisatie in venen

(met een samenvatting in het Nederlands)

The research presented in this thesis was supported by a personal VIDI grant from the Netherlands Organization of Scientific Research / Earth and Life Sciences (NWO-ALW) to Max Rietkerk.

Cover photographs: Photographs from maze patterning in a Siberian peatland. The front picture was taken from helicopter, the back picture was taken on the ground (both pictures by Maarten Eppinga).

Printed by: Gildeprint Drukkerijen BV, Enschede

ISBN: 978-94-90122-33-1

aMazing pattern: spatial self-organization in peatlands

Buitengewoon patroon: ruimtelijke zelforganisatie in venen

(met een samenvatting in het Nederlands)

Proefschrift

ter verkrijging van de graad van doctor aan de Universiteit Utrecht
op gezag van de Rector Magnificus, Prof. dr. J.C. Stoof, ingevolge
het besluit van het College van Promoties in het openbaar te
verdedigen op vrijdag 19 juni 2009 des middags te 12.45 uur

door

Maarten Boudewijn Eppinga

geboren op 15 juni 1982 te Woerden

Promotoren: Prof. dr. M.J. Wassen
Prof. dr. P.C. de Ruiter

Co-promotor: Dr. ir. M. Rietkerk

Contents

Chapter 1: Introduction	07
Chapter 2: Linking habitat modification to catastrophic shifts and vegetation patterns in bogs <i>Plant Ecology 200:53-68 (2009)</i>	37
Chapter 3: Regular surface patterning of peatlands: confronting theory with field data <i>Ecosystems 11:520-536 (2008)</i>	59
Chapter 4: Nutrients and hydrology indicate the driving mechanisms of peatland surface patterning <i>The American Naturalist 173: 803-818 (2009)</i>	97
Chapter 5: Resource contrast in patterned peatlands increases along an evapotranspiration gradient	157
Chapter 6: Synthesis and Perspectives	181
References	207
Summary	228
Nederlandse samenvatting	232
Nawoord	240
Curriculum Vitae	243
Publications	244



Introduction

Maarten B. Eppinga

Introduction

Environmental Science

Environmental science integrates the natural and social sciences in order to study human-environment interactions. This interdisciplinary science developed in the 1970s in response to the growing awareness of the complexity of environmental problems such as pollution of air (Patterson 1965) and water (Almer et al. 1974), global climate change (Wilson and Matthews 1970), accelerated exploitation of resources (Meadows et al. 1972) and the decrease of biodiversity through habitat destruction (Ehrlich and Ehrlich 1981; Pimm and Pimm 1982) and through invasions by exotic species (Elton 1958). In this time period, it also became clear that these changes in the environment were closely interrelated with socio-economic processes such as globalization, enhanced population growth and increased industrial production (Wilson and Matthews 1970; Meadows et al. 1972). Nowadays, there is a worldwide human domination of the environment through transformation of the land surface, alteration of the biogeochemical cycles and modification of the species composition of ecosystems (Vitousek et al. 1997). This has led to environmental problems as mentioned above, but also stresses the need for solutions in terms of sustainable management options for the environment (Kareiva et al. 2007). Studying these problems and solutions requires a scientific perspective that takes both natural and socio-economic dimensions of human-environment relations into account.

Environmental problems can be conveniently structured in a society-environment chain perspective (Verkroost 1997). The society-environment chain consists of four interrelated layers or subsystems: the political subsystem, the societal activities subsystem, the abiotic subsystem and the biotic subsystem (Fig. 1). The political subsystem aims to formulate policies and legislation to govern the societal activities subsystem. The societal activities subsystem encompasses all actions of the human population that lead to a change in the natural environment. The natural environment includes an abiotic subsystem and a biotic subsystem. An environmental problem emerges if human activities induce a change in the natural environment that is experienced as negative by society (e.g. Schot and Dijst 2000). The chain perspective can also be used in the context of solutions for environmental problems. Solving an environmental problem requires a change in the environment (the biotic and abiotic subsystems), which requires a change in societal activities, which could be achieved by formulating adequate environmental policy at the political subsystem level.

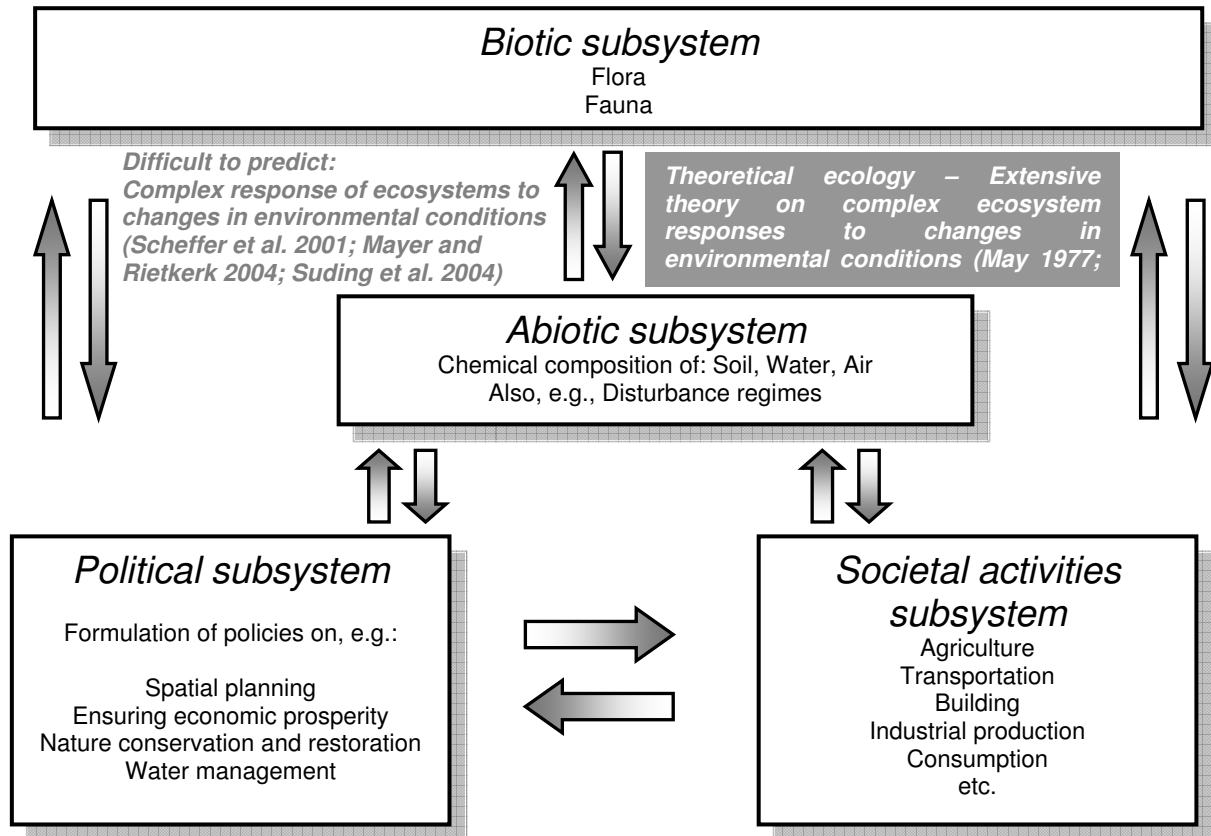


Figure 1: The society-environment chain perspective for environmental problems (Verkroost 1997). The diagram shows the main pathways through which humans influence the environment, and how changes in the environment may trigger societal action. A critical step in the chain includes the interrelationships between environmental conditions and the ecosystem response in terms of (a)biotic conditions. This step is often very difficult to assess due to the complex behavior of ecosystems. Therefore, it is useful to incorporate knowledge from theoretical ecology in this step. In theoretical ecology, much research has been devoted to better understand the response of complex systems to changes in environmental conditions.

The aims of environmental policy (political subsystem) are often set at the biotic subsystems level, for example by formulating goals in terms of preservation of species in pristine habitats (UNEP 1992), return of key species into degraded habitats (VROM 1991) or maintaining specific types of ecosystems (Ramsar Convention on Wetlands 1971). A critical step in formulating efficient and effective policies and management strategies, however, is to assess which environmental conditions are needed to achieve the goals set at the biotic subsystem level (Fig. 1). Societal activities are causing gradual environmental changes worldwide, such as changes in precipitation, temperature, land use and nutrient loading (Vitousek et al. 1997). The difficulty of making predictions originates from the complex response of many ecosystems to such gradual changes in environmental conditions (Scheffer et al. 2001; Mayer and Rietkerk 2004; Suding et al. 2004).

How to predict responses of complex systems to gradual changes is a well-developed field of research in theoretical ecology (May 1977; Tilman 1982; Levin 1998). Until now, however, there has been a limited effort to integrate theoretical modeling work with experimental approaches in real ecosystems. This thesis focuses on identifying the mechanisms that drive complex ecosystem behavior, using concepts developed in theoretical ecology. The work in this thesis will focus on applying concepts of theoretical ecology to better understand the functioning of peatland ecosystems. Peatlands are an interesting type of ecosystem to use as a case study for several reasons. First, peatlands provide an important ecosystem service (Costanza et al. 1998) as a large reservoir of carbon and a small sink of carbon dioxide (Gorham 1991). Second, peatlands are mostly situated at the latitudes at which the strongest effects of climate change will occur in the coming century (Houghton et al. 1995). Third, the surface of peatlands commonly shows spatial regular patterning, which may have been formed through a process of spatial self-organization (Rietkerk et al. 2004a). Spatial self-organization is one of the most obvious attributes of complex behavior of ecosystems (Levin 1998). Fourth, spatial patterning of peatlands has received a lot of attention during the last century, but an integrated approach of theory and experiments has rarely been used. Or, as Belyea and Lancaster (2002) formulated it: “*we are somewhat frustrated by a voluminous literature that seems to be concerned more with speculation on possible processes than with their investigation*”. I will now proceed with explaining the theoretical concepts that will be used in this study. To illustrate each theoretical concept, the text contains breakout boxes that address the concepts with a simple mathematical consumer-resource model (Boxes I-V). The breakout boxes provide additional information that is not essential to follow the main text.

Theoretical concepts

Positive feedback

Feedbacks occur when a system contains a loop of effects (e.g. Neutel et al. 2002). Positive feedbacks amplify small perturbations, destabilize the system globally and establish unstable equilibrium states (DeAngelis et al. 1986; Schröder et al. 2005). Global destabilization means that for all possible states, the system moves farther away from the unstable equilibrium state (e.g. Rosenzweig 1971). Negative feedbacks counteract deviations and stabilize the system locally, establishing the stable states (Schröder et al. 2005). Local stabilization means that for (at least) a subset of possible states, the system moves toward the stable equilibrium state (e.g. May 1977). Positive feedbacks play a major role in the organization of ecosystems

(DeAngelis and Post 1991; Wilson and Agnew 1992). In population dynamics, positive density dependence is the most common positive feedback (Berryman 2002). An example is the Allee effect: populations are suffering from decreased or even negative population growth rates at low densities (Allee 1931). In the following, the effect of feedbacks on consumer-resource dynamics will be examined.

The most simple consumer-resource interaction constitutes a negative feedback: an increase in consumer density decreases resource availability, which leads to a subsequent decrease in consumer density (the so-called type I functional response (Holling 1959), Fig. 2). In some ecosystems, however, the presence of a consumer may modulate the environment in a way that enables better access to resources (Fig. 2; Jones et al. 1994; Shachak et al. 2008). Such an environment-modulating species is referred to as an ecosystem engineer (Jones et al. 1994, 1997). There is some debate about the usefulness of the ecosystem engineer concept (e.g. Reichman and Seabloom 2002), but the main motivation is that it points out a contradiction with the classic view of the abiotic conditions determining the biotic environment (see e.g. Begon et al. 1990). The presence of ecosystem engineers may induce a positive feedback, if the positive effect of enhanced access to resources outweighs the negative effect of increased uptake of resources. In this case, an increase in the density of an ecosystem engineer may have a net positive effect on resource availability, which could lead to a further increase in the density of that ecosystem engineer (Fig. 2; Box I).

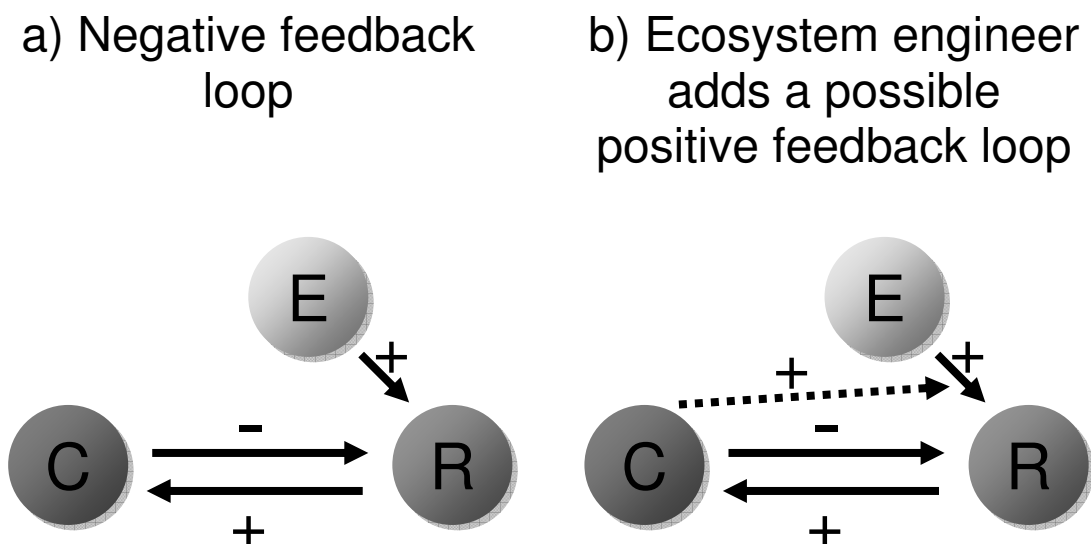


Figure 2: Illustrations of the possible feedback loops between consumers (C), resources (R) and the environment (E). a) The most simple consumer-resource interaction comprises a negative feedback. b) A consumer that functions as an ecosystem engineer may modulate the environment in a way that increases resource availability, which comprises a potential positive feedback loop.

Box I: Positive feedback governing consumer-resource dynamics

To illustrate the possibility of positive feedback governing consumer-resource dynamics let us consider a very simple consumer-resource system:

$$\frac{dR}{dt} = I - k_1 R - f(R)C$$

$$\frac{dC}{dt} = \alpha f(R)C - k_2 C$$

in which R is the resource density (units: $\text{g}\cdot\text{m}^{-2}$), and C is the consumer density ($\text{g}\cdot\text{m}^{-2}$), I is external resource input ($\text{g}\cdot\text{m}^{-2}\cdot\text{yr}^{-1}$), k_1 the resource depletion rate (yr^{-1}), k_2 is the consumer mortality rate (yr^{-1}) and α is an assimilation efficiency ($\text{g}\cdot\text{g}^{-1}$). The simplest consumer-resource interaction is a type I functional response (Holling 1959):

$$f(R) = k_3 R.$$

in which k_3 is the per capita consumption rate ($\text{m}^2\cdot\text{g}^{-1}\cdot\text{yr}^{-1}$). In this case, the per capita consumption rate increases linearly with resource density. A convenient way to analyze the model is through state space portraits (Fig. 1; Tilman 1982). In the consumer-resource system, a state consists of two components: a resource density and a consumer density. Now, for any particular state of the system, a state space portrait reveals to what direction the system will develop. The state space portrait also reveals the presence and position of equilibrium points. The state space portrait for the model with the Holling type I functional response shows that the consumer population is in equilibrium only at one specific resource density (Fig. 1a). Consequently, this is also the resource equilibrium density (Fig. 1a). Therefore there is a negative feedback: if the resource equilibrium is perturbed to a higher level, consumption exceeds resource production, and the resource density will return to the equilibrium. If the resource equilibrium is perturbed to a lower level, consumption is less than resource production, so the resource density will again return to the equilibrium. The state space portrait of this system reveals one globally attracting equilibrium with positive densities for both consumer and resource (Fig. 1a; Neutel et al. 1994) provided that the external resource input is large enough to maintain a consumer population.

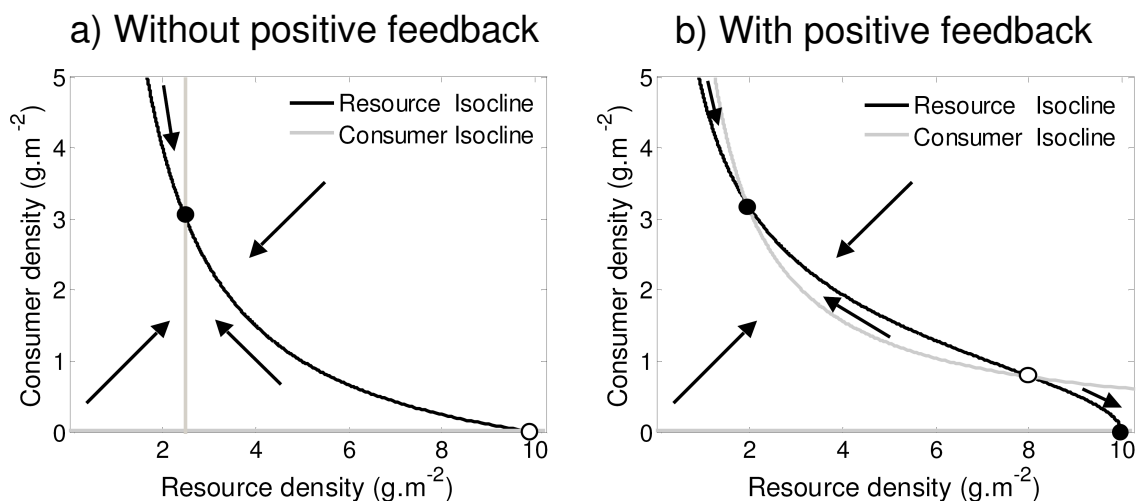


Figure 1: State space portraits showing the effect of positive feedback in a simple consumer resource model. a) A linear consumption response encompasses a negative feedback, which leads to one globally stable equilibrium (indicated with ●). b) A nonlinear consumption response encompasses a positive feedback, which destabilizes the system locally and creates an unstable equilibrium (○). Hence, two locally stable equilibria emerge due to the positive feedback. The following parameter values were used: $I=1$; $k_1=0.1$; $k_2=0.25$; $k_3=0.1$; $k_4=0.04$; $\alpha=1$.

In some ecosystems, however, the per capita consumption rate may be dependent of both consumer and resource density. Examples include indirect effects in trophic interactions (Neutel et al. 2007), or modification of the environment by an ecosystem engineer. Here, I would like to focus on the latter case. The simplest way to implement the effect of ecosystem engineering in this type of consumer-resource interaction in the model (without explicitly including the environment in the model as shown in Fig. 1) is as follows (Klausmeier 1999):

$$f(R, C) = k_4 RC$$

in which k_4 is a parameter determining how the per capita consumption rate depends on consumer density ($\text{m}^4 \cdot \text{g}^{-2} \cdot \text{yr}^{-1}$). In this case, the per capita consumption rate increases linearly with consumer density. This means that consumption rate becomes relatively low at low consumer densities, and relatively high at high consumer densities. Now, in the system an unstable equilibrium emerges (indicated with \circ in Fig. 1b). If the resource density is slightly decreased and the consumer density slightly increased from this unstable point, the decrease in resource loss ($k_1 R$) outweighs the effect of increased consumption ($k_4 RC^2$). This means that there is a positive feedback: an increase in consumers leads to an increase in resource use efficiency, which further stimulates the consumer population. The system will then develop toward a stable state with more consumers (Fig. 1b). On the other hand, if the resource density is slightly increased and the consumer density slightly decreased from the unstable equilibrium point, the increase in resource loss rate outweighs the effect of decreased consumption. Now, the positive feedback works the other way around: a decrease in consumers leads to a decrease in resource use efficiency, which further inhibits the consumer population. In this case, the system will develop toward a state without consumers (Fig. 1b). Hence, the state space portrait of this system reveals that there is a globally unstable equilibrium, which separates two locally stable equilibria: a stable state with consumers and a stable state without consumers (Fig. 1b). ■

Alternate stable states

The occurrence of positive feedback is a requirement for alternate stable states (DeAngelis et al. 1986). The concept of alternate stable states in ecosystems was first proposed theoretically by Lewontin (1969), and the practical relevance of this concept is still an issue of considerable interest and debate (Connell and Sousa 1983; Bertness et al. 2002; Scheffer and Carpenter 2003; Rietkerk et al. 2004b; Schröder et al. 2005; Kéfi et al. 2007b). Here I would like to focus on the simplest case of two alternate stable equilibria, referred to as bistability. If a system exhibits bistability, each stable state has its own *basin of attraction*, meaning a range of ecosystem states under which the system will develop towards this stable structure (Fig. 3; Lewontin 1969; Schröder et al. 2005). Consequently, if such stable structure is reached, the systems structure stays intact as long as conditions remain within the basin of attraction. Hence, systems may exist potentially indefinitely in contrasting states under the same external environmental conditions (Schröder et al. 2005). It should be noted that this kind of behaviour could already be observed in the earliest models in theoretical ecology (Lotka 1925; Volterra 1926).

In ecosystems, interactions between all the species and the environment may entail a large number of potential feedback mechanisms. A requirement for alternate stable states is that the effect of positive feedbacks dominates over the effect of negative feedbacks. Positive feedbacks between ecosystem engineers and the environment may especially dominate under stressful conditions, where it is of main importance to ameliorate abiotic conditions (Jones et al. 1994; Bruno 2003; Van Wesenbeeck et al. 2007). Hence, positive feedbacks may induce alternate stable states especially in harsh environments (Box II; Bertness and Callaway 1994; Bertness and Leonard 1997; Didham et al. 2005; but see Fukami and Lee 2006; Mason et al. 2007).

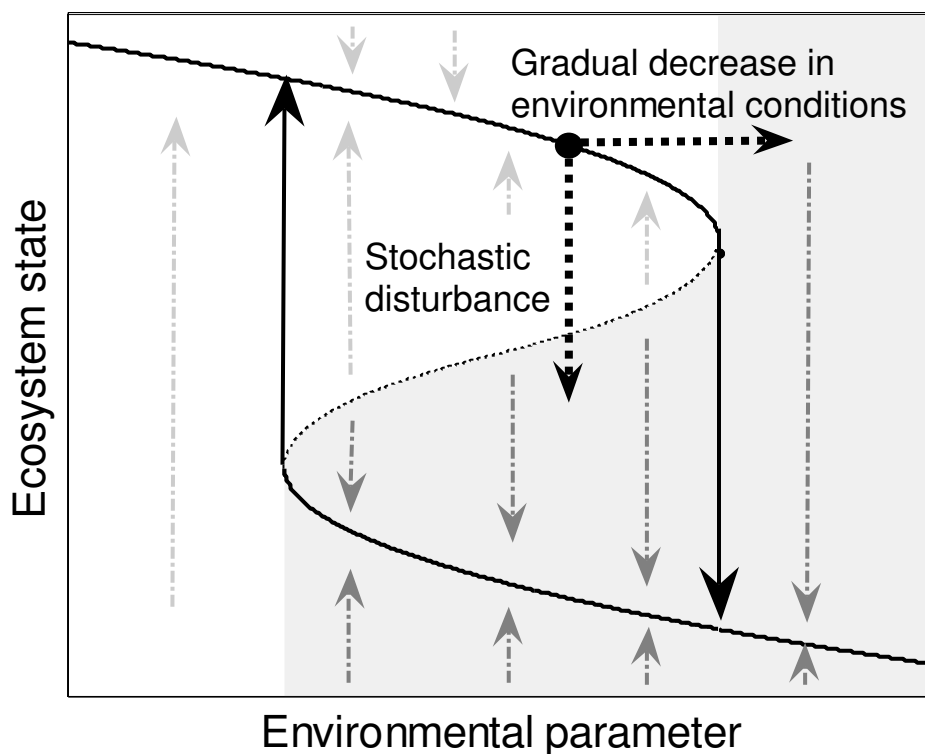


Figure 3: Conceptual graph of alternate stable ecosystem states (adapted from Schröder et al. 2005). Thick black lines indicate stable equilibria. For low values of the environmental parameter, only the upper ecosystem state exists, for high values only the lower ecosystem state. For each equilibrium there is a basin of attraction, meaning a range of ecosystem states that will develop toward the stable equilibrium. Here, the basin of attraction of the upper equilibrium is white shaded, the basin of attraction of the lower equilibrium is grey shaded. At intermediate values of the environmental parameter both stable equilibria exist, their basins of attraction being separated by an unstable equilibrium. A catastrophic shift from one state to the other can be triggered in two ways. First, there can be a perturbation of the current equilibrium (indicated with •) due to a stochastic disturbance. The fact that a system may not recover from the perturbation is referred to as hysteresis. Second, a gradual change in environmental conditions can lead the ecosystem to a point where the basin of attraction vanishes. At this point, there is an ecosystem shift toward the other equilibrium. Because the downward and upward shifts occur at different values of the environmental parameter, there is hysteresis.

Box II: Alternate stable states due to positive feedback

The state space portrait of the consumer-resource model with positive feedback (Box I) shows that this model version exhibits bistability. More specifically, there is a stable state with consumers and a stable state without consumers. We can use this model to investigate under which conditions positive feedbacks induce alternate stable ecosystem states. For this purpose, we adopt a quasi steady state approach (e.g. Edelstein-Keshet 1988): we assume that resource dynamics are much faster than consumer dynamics. With this assumption we can derive:

$$\hat{R} = \frac{I}{(k_1 + k_4 C^2)}$$

$$\frac{dC}{dt} = \frac{Ik_4 C^2}{(k_1 + k_4 C^2)} - k_2 C$$

where the hat indicates the equilibrium resource density. See Box I for the interpretation and dimensions of the parameters and variables. We can now draw a growth curve of the consumer as a function of consumer density only, which reveals that this type of consumer-resource interaction may induce positive density dependence (Fig. II). Whether this type of interaction indeed induces alternate stable states depends on the position of the unstable equilibrium. When the unstable equilibrium lies within the biologically realistic state space (that is at positive densities of the consumer), it means that there is a threshold consumer density below which it goes extinct, and above which it can survive (Fig. II). In this system, the position of the unstable equilibrium can be modified by the parameter k_2 which indicates the natural mortality rate of the consumer population. This parameter can be interpreted as a surrogate for habitat suitability or harshness of the environment. The basin of attraction of the state without consumers increases with larger values of k_2 (Fig. II), suggesting that especially in harsh environments, positive feedbacks may occur and induce alternate stable states.

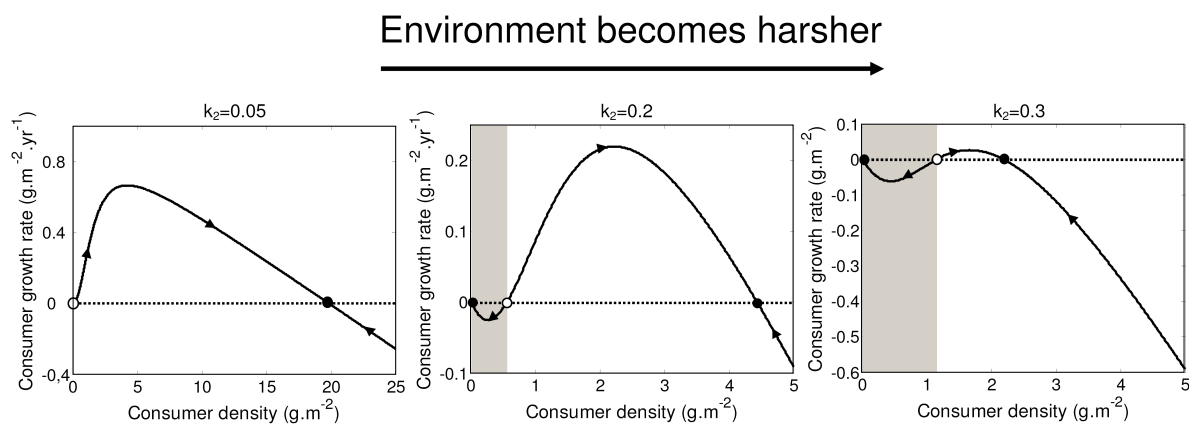


Figure II: The growth curves of the consumer populations along a gradient in harshness of the environment (mimicked by the parameter k_2 , other parameters have the same value as in Box II). The basin of attraction of the state without consumers is grey-hatched. Under benign conditions, the consumer will grow toward the carrying capacity already at very low densities (left panel). If the environment becomes harsher, positive density dependence emerges, leading to bistability between a state with and a state without consumers (middle panel). As harshness of the environment further increases, the basin of attraction of the ecosystem state without consumers increases as well (right panel). This suggests that alternate stable states are more likely to occur in harsher environments. ■

Catastrophic shifts

If a system reaches a stable equilibrium state or structure, the systems structure stays intact as long as conditions remain within the basin of attraction. However, when conditions reach the edge of this basin, only a small change can force the ecosystem into another basin of attraction. Basically, a shift toward another basin of attraction can be induced in two ways (Fig. 3; Box III; Holling 1996). First, a stochastic disturbance event may occur that affects the ecosystem state directly and pushes it outside the current basin of attraction (Fig. 3). Second, a gradual change in environmental (external) conditions may diminish the size of the basin of attraction of the current equilibrium until it vanishes completely (Fig. 3). Then, the system will be drawn towards another stable structure (Fig. 3). The latter switch between basins of attraction is known as passing a catastrophic bifurcation point (Kuznetsov 1995; Scheffer and Carpenter 2003).

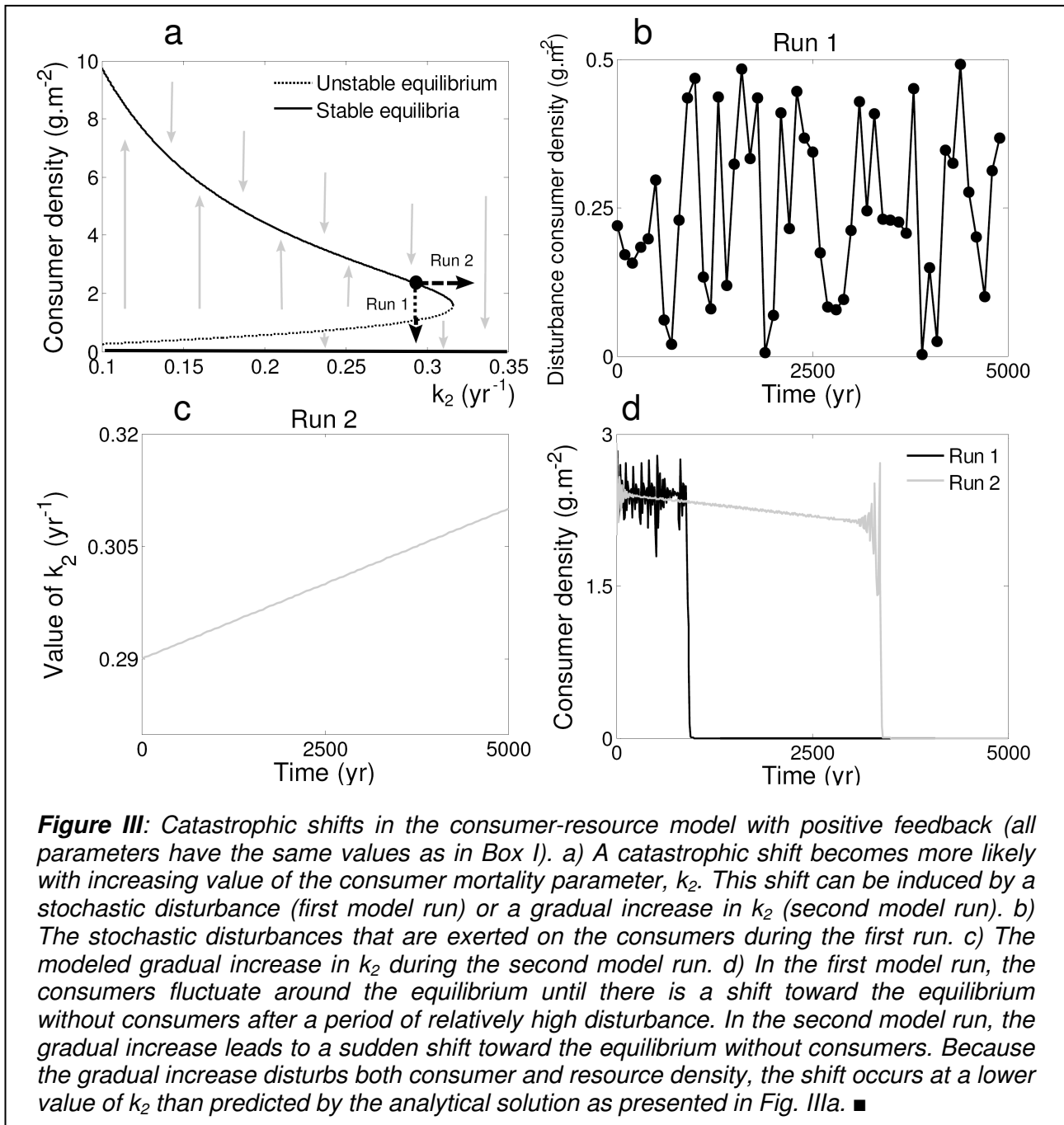
Ecologists have long recognized that gradual changes in environmental conditions can cause abrupt changes in ecosystems (Carpenter 2001). Passing a catastrophic bifurcation point can explain such “*Big effects from small causes*” (Ricker 1963), resulting from an ecosystems property of alternate stable states (Holling 1973). These ‘big effects’ are referred to as catastrophic shifts in ecosystem states, and several studies suggest that such shifts can occur in a large variety of different ecosystems, including lakes (Scheffer et al. 1993), coral reefs (Nystrom et al. 2000), fish populations in oceans (De Roos and Persson 2002), desert streams (Heffernan 2008), savanna woodlands (Van Langevelde et al. 2003), arid ecosystems (Rietkerk et al. 1997) and tidal flats (Van de Koppel et al. 2001). It is important to note that the term catastrophic refers to the nature of the change, not to the ecosystem development. The term can be somewhat misleading, because sometimes the occurrence of a catastrophic shift is desired and therefore stimulated (e.g. Meijer & Hosper 1997; Suding et al. 2004). However, most studies have focused on catastrophic shifts towards degraded ecosystem states (Rinaldi and Scheffer 2000; Scheffer et al. 2001; Mayer and Rietkerk 2004).

After an ecosystem shift, it may be very difficult to successfully restore the pre-shift state, even under environmental conditions in which it used to be present (Fig. 3). This phenomenon is referred to as hysteresis. Because of hysteretic and irreversible dynamics, the recovery from a catastrophic shift is not always achieved by restoring the environmental conditions that prevailed just before the shift took place. Restoring an ecosystem that has catastrophically degraded may therefore be very difficult or

expensive (Carpenter 2001), if it is possible at all. Hence, it is desirable to know whether an ecosystem is close to a catastrophic shift. Unfortunately, catastrophic shifts occur typically quite unannounced, and 'early warning signals' of approaching catastrophic change are difficult to obtain (Scheffer et al. 2001). Recent research aims to find indicators for catastrophic shifts by time-series analysis (Carpenter and Brock 2006; Van Nes and Scheffer 2007; Carpenter et al. 2008; Dakos et al. 2008; Guttal and Jayaprakash 2008; but see Biggs et al. 2009).

Box III: Catastrophic shifts in the consumer-resource system

Solving the equations of the consumer-resource model (Box I), yields the equilibrium densities of the resource and the consumer in terms of the model parameters. With these analytical expressions, the stable and unstable equilibrium consumer densities can be drawn for a range of values of the consumer mortality parameter, k_2 . It shows that the basin of attraction of the equilibrium with consumers decreases with increasing value of k_2 . This means that with increasing k_2 , the equilibrium becomes more vulnerable to changing conditions. As mentioned in the main text, a shift toward the basin of attraction to the other stable equilibrium can be induced in two ways. First, a stochastic disturbance event may occur that affects the ecosystem state directly and pushes it outside the current basin of attraction (Run 1 in Fig. IIIa). In the model, I mimicked stochastic disturbances by diminishing the consumer density once every hundred years by a random quantity between 0 and 0.5 g.m⁻² (Fig. IIIb). As a result, the consumer dynamics fluctuate around the equilibrium value, but during a period of relatively high disturbance, there is a sudden shift toward the state without consumers (Fig. IIIc). The second category of shifts originates from a gradual change in environmental (external) conditions (Fig. IIIc). Such a gradual change may diminish the size of the basin of attraction of the current equilibrium until it vanishes completely, and then the system will be drawn toward another equilibrium (Run 2 in Fig. IIIc). I mimicked a gradual change in the model by increasing the value of k_2 every hundred years with 0.0004 yr⁻¹. Note that a change in k_2 will change the density of both resources and consumers, meaning that there is a disturbance of the equilibrium. This disturbance exerts the final push toward the equilibrium without consumers, occurring before the value of k_2 has reached the catastrophic bifurcation point (Fig. IIIc).



Self-organized patchiness

The occurrence of catastrophic shifts between alternate stable states as discussed above is associated with the behavior of complex (eco)systems (Levin 1998). Complexity of (eco)systems can also reveal itself through spatial self-organization (Rohani et al. 1997; Levin 1998; Werner 1999). Spatial self-organization is the process where large-scale ordered spatial patterns emerge from disordered initial conditions through local interactions (Rietkerk and Van de Koppel 2008). This process is key to understanding ecological stability and diversity in ecosystems (Solé

and Bascompte 2006; Rietkerk and Van de Koppel 2008). A particular type of spatial self-organization is regular patterning of sessile biota. Such self-organized patchiness has been observed in various types of ecosystems (Fig. 4; Rietkerk and Van de Koppel 2008) including savanna (Lejeune et al. 2002), arid ecosystem (Klausmeier 1999), mussel bed (Gascoigne et al. 2005), ribbon forest (Hiemstra et al. 2006) and marsh tussocks (Van de Koppel and Crain 2006).

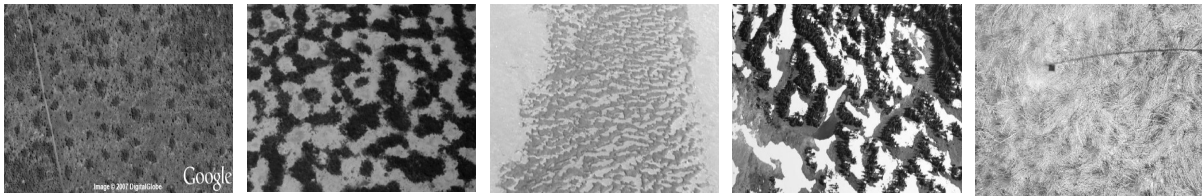


Figure 4: Self-organized patchiness in various types of ecosystems (Redrawn from Rietkerk and Van de Koppel 2008). From left to right: savanna, arid ecosystem, mussel bed, ribbon forest and marsh tussocks.

A recent review aimed to unravel the unifying principle of self-organized patchiness in these different ecosystems (Rietkerk and Van de Koppel 2008). The review revealed that the essential mechanism for self-organized patchiness is long-range inhibition (Box IV; Rietkerk and Van de Koppel 2008). Long-range inhibition means that consumers negatively influence habitat quality on a larger spatial scale than the patch-scale in which they are growing. One of the most obvious examples of long-range inhibition occurs when sessile consumers actively harvest resources from their surroundings. The fact that such a resource-concentration mechanism can lead to spatial pattern formation has long been recognized (Turing 1952; Nicolis and Prigogine 1977; Levin and Segel 1985; Murray 1989; Meinhardt 1995). A critical prerequisite for this type of dynamics to occur is that the resource transport is faster than consumer movement (Turing 1952). Self-organized patchiness can also occur in predator-prey systems (Hassell et al. 1994; Maron and Harrison 1997; De Roos et al. 1998). However, this is a different type of consumer-resource interaction, because the consumer (predator) movement is faster than resource (prey) movement. Therefore patterning in predator-prey systems is different from the self-organized patchiness of sessile consumers considered here.

Box IV: Self-organized patchiness: long-range inhibition is the key

Self-organized patchiness occurs in a spatially explicit version of the simple consumer-resource model with positive feedback. It is assumed that movement of both consumers and resources can be approximated by a diffusion term (Okubo 1989). Hence, the equations become:

$$\frac{\partial R}{\partial t} = I - k_1 R - f(R)C + D_R \left(\frac{\partial^2 R}{\partial x^2} + \frac{\partial^2 R}{\partial y^2} \right)$$

$$\frac{\partial C}{\partial t} = \alpha f(R)C - k_2 C + D_C \left(\frac{\partial^2 C}{\partial x^2} + \frac{\partial^2 C}{\partial y^2} \right)$$

In which D_R and D_C are the diffusion speeds of resources and consumers ($\text{m}^2.\text{yr}^{-1}$). Further, we assume that the resource diffuses hundred times faster than the consumer ($D_R = 100 \cdot D_C$). In this case, long-range inhibition occurs in the model because the consumer harvests resources from the surroundings, thereby actively depleting resources outside the consumer patches. Depending on environmental conditions, different kinds of patterns can be observed (Fig. IV), including spots, stripes and gaps. As an experiment, long-range inhibition can be switched off in the model as follows: instead of modeling resource transport explicitly, we calculated for each model grid cell what the transport of resources to this cell would be if it the grid cell was surrounded by four grid cells that are in the stable equilibrium state without consumers. In this way, each grid cell is able to harvest additional resources, but these resources are not coming from the surrounding grid cells. Under these conditions, pattern formation is no longer possible (Fig. IV), which agrees with the notion that self-organized patchiness is in essence driven by the long-range inhibition effect of consumers (Rietkerk and Van de Koppel 2008).

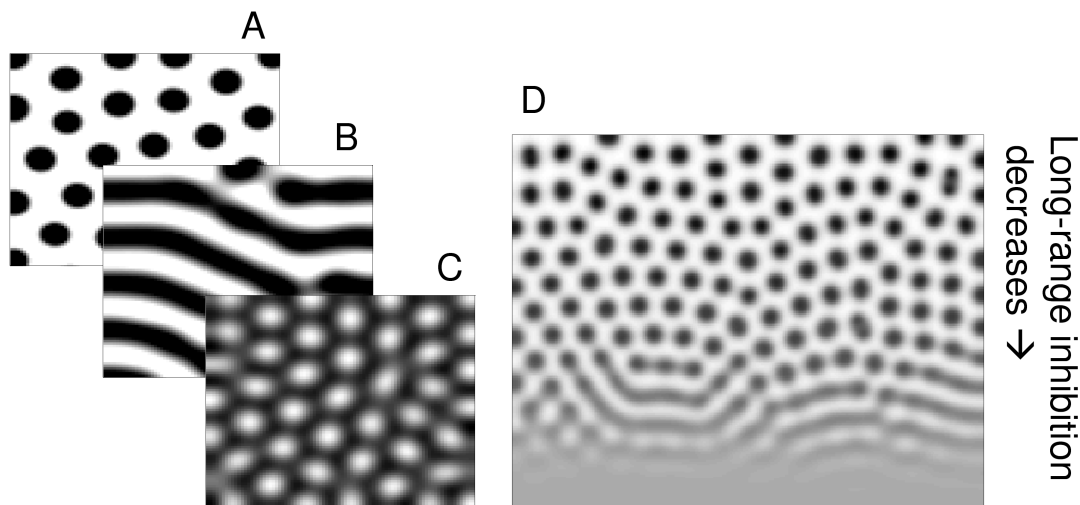


Figure IV: The various types of self-organized patchiness that can occur in the simple consumer-resource model with positive feedback. The panels show consumer density, with darker colors indicating higher density. Spots form when environmental conditions are relatively harsh (a, $k_2 = 0.2$). Spots comprise the final pattern before a catastrophic shift toward a state without consumers occurs. If environmental conditions are more benign, stripes can be observed (b, $k_2 = 0.14$). Gaps form if the conditions are most benign, but just not benign enough to support a uniform vegetation cover (c, $k_2 = 0.129$). The essential process that creates the self-organized patchiness is long-range inhibition (d, $k_2 = 0.2$). The diffusion speed was set at $0.5 \text{ m}^2.\text{yr}^{-1}$ for the consumer and $50 \text{ m}^2.\text{yr}^{-1}$ for the resource. The other parameters have the same values as in Box I. ■

Self-organized patchiness as an indicator of proximity to a catastrophic ecosystem shift

So far, two separate attributes of complex (eco)systems have been considered: catastrophic shifts between alternate stable ecosystem states and self-organized patchiness. A recently developed idea, however, is that these two attributes are mechanistically linked (Rietkerk et al. 2004b). This is because the resource concentration mechanism not only leads to long-range inhibition, but also to local facilitation of consumers living within or at the edge of the consumer patch. Due to this local facilitation effect, consumers growing in patterns may survive under environmental conditions that are too harsh to sustain a uniform consumer density (Box V; Rietkerk et al. 2002; Kéfi et al. 2007a).

Thus, under harsh conditions, two alternate stable states are possible: a state with no consumers and a state with patches of consumers, which survive through local facilitation by harvesting resources from the surroundings. This implies that if the environment changes from benign to harsh, the ecosystem properties change from only a stable consumer equilibrium to bistability between a patterned state and a state without consumers to only a stable state without consumers. This suggests that self-organized patchiness can be used as an indicator for proximity to catastrophic ecosystem shifts (Rietkerk et al. 2004b). A crucial prerequisite for this hypothesis, however, is that the self-organized consumer patterns are caused by a resource concentration mechanism, meaning that there is both local facilitation as well as long-range inhibition (Box V; Van de Koppel and Crain 2006).

Box V: Linking catastrophic shifts to self-organized patchiness

In the previous Boxes it has been shown that the consumer-resource model with positive feedback exhibits bistability (Boxes I, II), the potential of catastrophic shifts (Box III) and self-organized patchiness (Box IV). In the spatially explicit version of the model (Box IV), the resource concentration mechanism drives local facilitation and thereby a short-range positive feedback. Due to this facilitation process, the consumers are able to survive under harsher conditions than predicted by the mean field model (Fig. Va). This means that in the spatially explicit model, bistability emerges between a patterned consumer state and a state without consumers (Fig. Va). I will now show that patchiness only indicates proximity to catastrophic shifts if the patchiness is driven by a spatial process that includes local facilitation.

For this aim, I will introduce a slightly modified version of the consumer-resource model. Let us consider a new state variable that represents a dimensionless consumer inhibition factor, X . In ecological terms, an example of X could be plant litter, which accumulates due to the plant (consumer) presence and inhibits plant growth by decreasing light availability. If this new variable disperses faster than the consumers and resources, we introduce a long-range-inhibition mechanism in the model without a short-range facilitation effect (Van de Koppel and Crain 2006). Further, we assume equal dispersion rates of consumers and resources,

and a logistic growth rate for consumers (Van de Koppel and Crain 2006). Hence, the equations become:

$$\frac{\partial R}{\partial t} = I - k_1 R - k_4 RC(1 - C) + D_R \left(\frac{\partial^2 R}{\partial x^2} + \frac{\partial^2 R}{\partial y^2} \right)$$

$$\frac{\partial C}{\partial t} = k_4 RC(1 - C) - k_2 C - \frac{k_5 k_6 CX}{k_6 + X} + D_C \left(\frac{\partial^2 C}{\partial x^2} + \frac{\partial^2 C}{\partial y^2} \right)$$

$$\frac{\partial X}{\partial t} = k_2 C - k_7 X + D_X \left(\frac{\partial^2 X}{\partial x^2} + \frac{\partial^2 X}{\partial y^2} \right)$$

In which k_5 is the maximum consumer inhibition rate (yr^{-1}), k_6 is a saturation constant for the inhibition factor (dimensionless), k_7 is the removal rate of the inhibition factor (yr^{-1}), and D_X is the diffusion speed of the inhibition factor ($\text{m}^2 \cdot \text{yr}^{-1}$). Note that if the diffusion of the inhibition factor exceeds that of the consumer this induces a long-range inhibition effect. Moreover, the model is parameterized in such a way that there is no local facilitation effect. In this model with only long-range inhibition, patterns still form, but the pattern formation ceases before the consumer extinction threshold (Fig. Vb). Therefore, pattern formation that is induced solely by long-range inhibition does not indicate proximity to catastrophic shifts. These results concur the findings of Van de Koppel and Crain (2006). Only if local facilitation is included, the consumer is able to survive under conditions in which a uniform cover is no longer possible (Fig. Va vs. Fig. Vb). Hence, we conclude that a pattern that is induced by a spatially coupled feedback mechanism, meaning a combination of local facilitation and long-range inhibition, indicates proximity to a catastrophic shift.

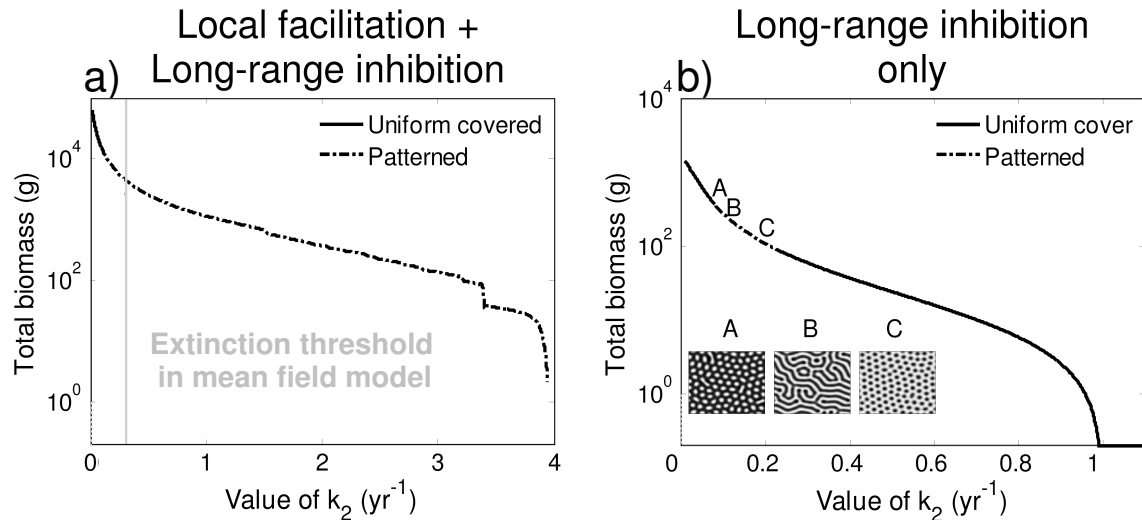


Figure V: The link between self-organized patchiness and catastrophic shifts. a) In the model with the resource concentration mechanism, there is a combination of short-range facilitation and long-range competition. Due to the facilitation effect, consumers can survive under harsher conditions than predicted by the mean field model. Thus, there is bistability between the patterned state and the state without consumers. In these cases, self-organized patchiness serves as an indicator for proximity to catastrophic shifts. The sequence of patterns in this model and the parameter values have been presented in Box IV. b) In a model without the facilitation mechanism, however, the same sequence of self-organized patchiness (gaps, stripes and spots) can still occur if there is a long-range inhibition effect, but only under intermediate stress conditions. The small panels show consumer density, with darker colors indicating higher density. If there is no local facilitation but only long-range inhibition, self-organized patchiness does not serve as an indicator to catastrophic shifts. Parameter values for this model simulation: $k_5 = 10$; $k_6 = 0.2$; $k_7 = 0.15$ $D_R = 0.5$; $D_X = 100$, other parameters as in Boxes I and IV. ■

Implications of the ecological theory for empirical studies

The ecological theory described above suggests that positive feedbacks play a major role in the organization of ecosystems. The occurrence of positive feedbacks may induce alternate stable ecosystem states. Due to alternate stable states, the response of ecosystems to gradual changes in environmental conditions may not be smooth, but relatively large and unexpected catastrophic shifts may occur. Unfortunately, these attributes are difficult to detect in real ecosystems. Whether positive feedbacks induce alternate stable states in a particular ecosystem requires an inventory of all the positive and negative feedbacks within that system. Also, catastrophic shifts typically occur unexpectedly, and are difficult to predict. On the contrary, self-organized vegetation patchiness in ecosystems is very clearly visible, and the pattern-forming mechanism may also be the driver of (short-range) positive feedback, alternate stable states and possibly catastrophic shifts. Ecological theory, however, has also revealed that this link does not hold for all types of pattern-forming mechanisms. It is therefore of key importance to identify the driving mechanism of pattern formation in empirical studies. If empirical research identifies the driving mechanism of a regular spatial ecosystem pattern, it can be assessed whether this ecosystem is likely to exhibit alternate stable states or not. Theoretical studies suggest that a resource concentration mechanism is a type of mechanism that induces alternate stable states. I will now proceed with describing peatlands, the ecosystem for which the theory will be empirically tested in this thesis.

Peatland ecosystems

Peatlands occupy less than two percent of the world's land surface yet contain about thirty percent of the global terrestrial carbon pool (Post et al. 1982, 1985; Gorham 1991; Bridgman et al. 2001). Peatlands are mainly situated on the northern hemisphere, in the boreal and subarctic region (Fig. 5). Carbon accumulates in peatlands because carbon uptake by plants exceeds losses of carbon to the atmosphere by decomposition. An important factor controlling decomposition losses from peatlands is the height of the seasonal minimum water table (Belyea and Malmer 2004). Below this height is the permanently saturated water table with low microbial activity and very slow decomposition. This layer is referred to as the catotelm (e.g. Holden and Burt 2003). Above the seasonal minimum water table is the aerated peat layer or acrotelm, with higher microbial activity and where decomposition takes place up to three orders of magnitude faster than in the catotelm (Ingram 1978). Hence, the most important carbon storing process in peatlands is plant litter at the bottom of the acrotelm becoming part of the catotelm

(Clymo 1984; Belyea and Clymo 2001; Belyea and Malmer 2004). Many different types of peatlands can be distinguished, but the most important distinction is between fens and bogs. Fens are peatlands in which plants have access to groundwater, whereas bogs depend entirely on rainwater as a water input.

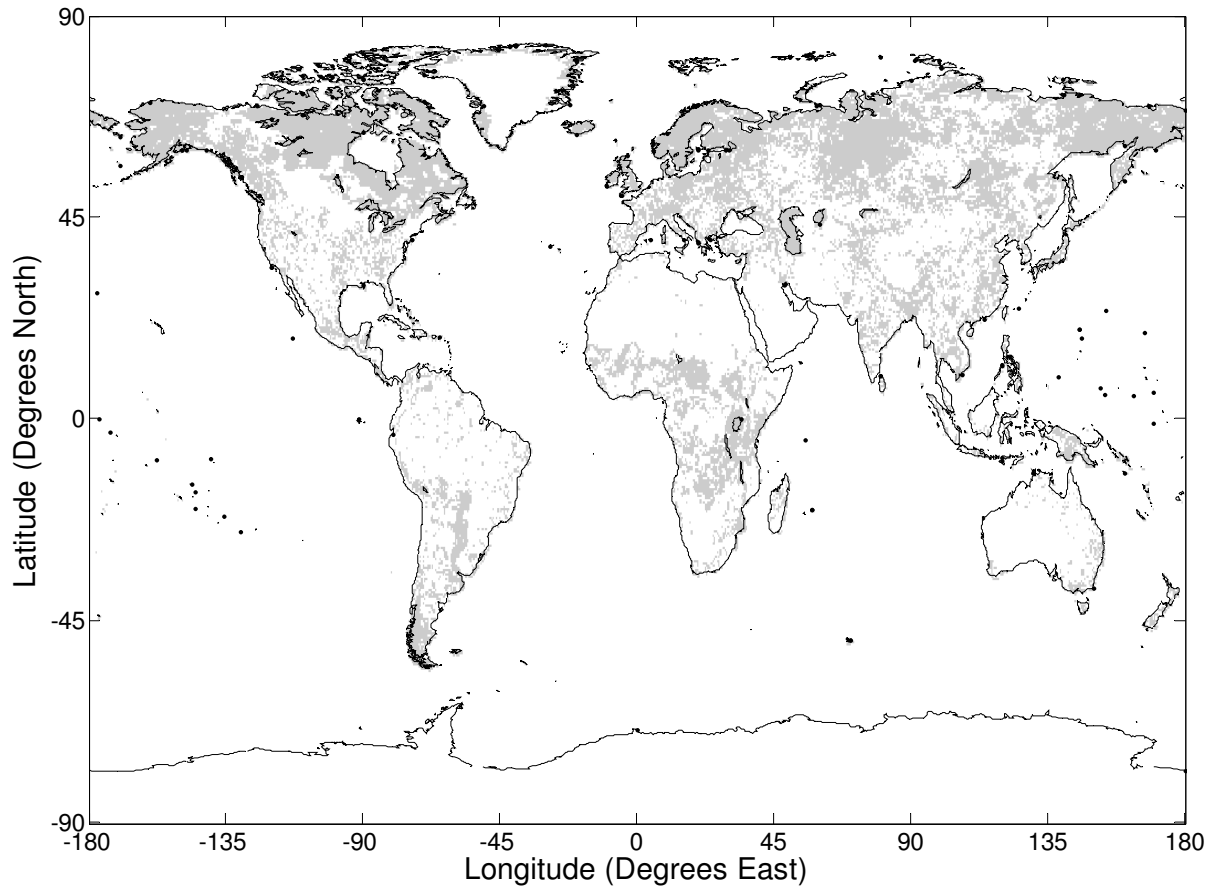


Figure 5: Global distribution of peatlands (grey shade). Data from the global wetland database (Lehner and Döll 2004).

The majority of peatlands is located in the altitudes expected to undergo the greatest changes in temperature and precipitation in the next decades (Houghton et al. 1995). More specifically, winter and summer temperatures are expected to increase and also significantly greater winter precipitation is predicted (Meehl et al. 2007; Roulet et al. 2007). The predictions for summer precipitation in northern regions, however, are less clear, particularly for northern Europe (Roulet et al. 2007). Further, gradual increases in atmospheric nutrient deposition may change peatland vegetation composition (Roelofs 1986; Lamers et al. 2000; Wassen et al. 2005). Due to these changes in environmental conditions peatlands may become significant sources for atmospheric carbon in the future (Yu et al. 2001; Heikkinen et al. 2004).

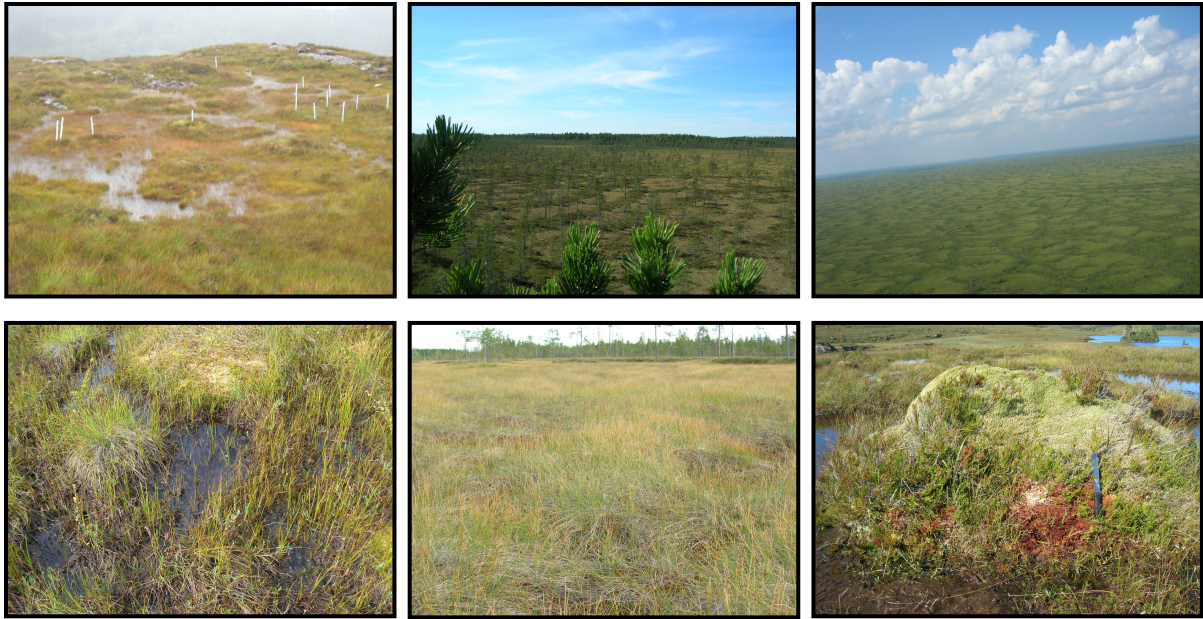


Figure 6: Self-organized patchiness in peatland ecosystems. Top row: large-scale patterns: individual hummocks, lawns and hollows (left panel), elevated strings perpendicular to peatland slopes (middle panel), a maze pattern of elevated ridges on relatively flat grounds (right panel). Bottom row: the large-scale patterns consist of spatial alternation of different microforms, ranging from (left to right) sparsely vegetated pools and hollows, slightly dryer lawns and densely vegetated, elevated hummocks.

Self-organized patchiness is commonly observed in peatlands (Fig. 6). These patterns consist of patches or microforms that differ in elevation and vegetation density. The wettest microforms are pools and hollows with sparse vegetation. Lawns are slightly dryer and have more vegetation. Hummocks are dry and elevated microforms, and have dense vegetation (Fig. 6). A considerable amount of attention has been paid to patterning in peatlands for more than a century (Nilsson 1899; Auer 1920; Malmström 1923; Foster et al. 1983; Seppälä and Koutaniemi 1985; Charman 2002). This has yielded many different hypotheses about the origin of peatland patterning, including simply following the mineral soil relief (Radforth 1969), solifluction (Pearsall 1956), ice thrust (Williams 1959), frost heaving (Tricart 1969), ponding of water behind poorly permeable peat (Kulczyński 1949; Swanson and Grigal 1988; Couwenberg 2005; Couwenberg and Joosten 2005), interception of floating plant litter by elevated patches during (spring) floods (Nilsson 1899; Sakaguchi 1980; Seppälä and Koutaniemi 1985; Larsen et al. 2007), and differential rates of peat formation in wetter and dryer areas (Foster et al. 1983; Foster and King 1984; Glaser 1992b; Belyea and Clymo 2001).

Peatlands are generally considered to be a harsh environment due to nutrient-poor conditions (Van Breemen 1995). Therefore it has been recently proposed that

peatland patterning may be driven by a resource-concentration mechanism, as previously suggested for other types of ecosystems (Fig. 7; Rietkerk et al. 2004a). The hypothesized mechanism works as follows: the presence of vascular plants (especially trees and shrubs) may increase evapotranspiration rates (Souch et al. 1998; Takagi et al. 1999; Frankl and Schmeidl 2000; Andersen et al. 2005). This induces a water flow from areas with low vascular plant biomass toward areas with high vascular plant biomass. Because this water contains dissolved nutrients, there is a net nutrient transport toward areas with higher vascular plant biomass. In short, vascular plants harvest nutrients from their surroundings, through higher evapotranspiration (Rietkerk et al. 2004a). This mechanism was coined the *nutrient accumulation mechanism* (Rietkerk et al. 2004a).

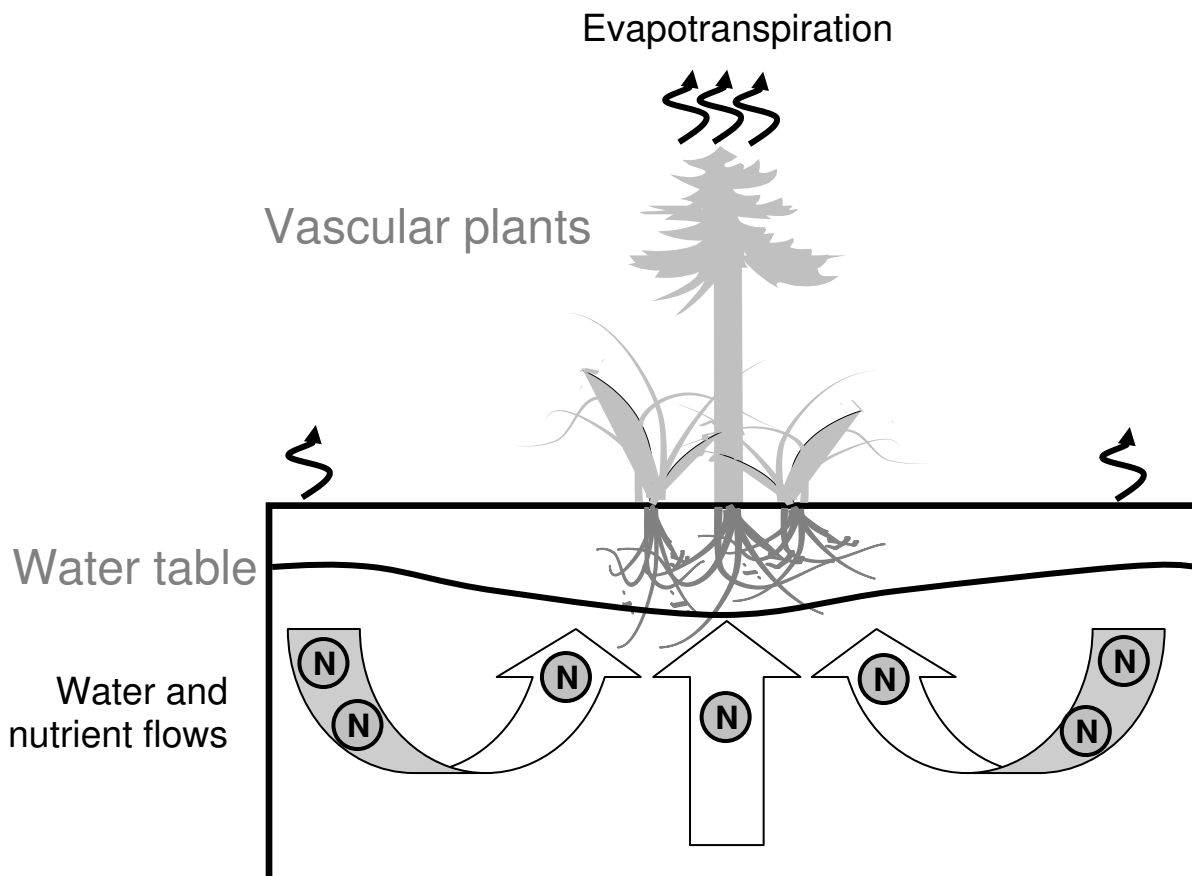


Figure 7: Schematic representation of the nutrient accumulation mechanism (Rietkerk et al. 2004a): vascular plant may increase evapotranspiration rates. As result, they may attract water from their surroundings. Nutrients are dissolved in this water, meaning that vascular plants harvest resources from their surroundings.

Thus, self-organized patchiness has been observed in peatlands (Fig. 6), and this patchiness may be caused by a resource concentration mechanism (the nutrient accumulation mechanism, Fig. 7). According to the previously explained theoretical concepts, occurrence of such a resource concentration mechanism induces local

facilitation, and hence a short-range positive feedback (Box V). This short-range positive feedback may induce alternate stable states (Boxes I-III), and the possibility of catastrophic shifts between these states in response to changes in environmental conditions (Boxes III - V), such as climate change. It should be noted, however, that empirical evidence for the nutrient accumulation mechanism is still lacking, and many alternative mechanisms for peatland patchiness have been proposed.

Problem definition

Predicting how anthropogenic-induced gradual changes in abiotic conditions affect ecosystem functioning is one of the key challenges in ecology and environmental sciences. Peatland ecosystems have been an important terrestrial carbon sink, but concern has risen that these systems may switch from being carbon sinks to becoming carbon sources due to changes in environmental conditions, notably global climate change. For many ecosystems, the response to gradual changes in environmental conditions may not be smooth, but rapid and almost irreversible shifts in ecosystem states may occur. Early warning signals for such catastrophic shifts are difficult to obtain. Recent research suggests that self-organized patchiness can serve as such an indicator. Self-organized patchiness is also commonly observed in peatland ecosystems. Hence, the following problem definition can be derived:

Self-organized patchiness is commonly observed in peatlands. Despite more than a century of research on this phenomenon, the driving mechanisms of peatland patterning remain elusive. It is therefore not known if patterning in peatlands is driven by a nutrient accumulation mechanism and whether or not peatland patterns may serve as an indicator for catastrophic shifts in peatland ecosystems, as possibly induced by global climate change.

Aim of this thesis

In order to address the current gap in knowledge as indicated in the problem definition, the following aim is formulated:

The aim of this thesis is to investigate whether the nutrient accumulation is a likely explanation for peatland patterning. Further, we aim to investigate whether self-organized patchiness in peatlands could serve as an indicator for proximity to catastrophic shifts in peatland ecosystem states.

Research questions

In order to reach the aim of the thesis, the research can be divided in seeking answers to the following research questions:

1. Are the theoretical concepts positive feedback, alternate stable states and catastrophic shift relevant for the case of spatial patterning of peatland ecosystems?
2. Do observations of water flow and the distribution of nutrients in patterned peatlands corroborate with predictions of models that imply the nutrient accumulation mechanism?
3. Through which variables can we discriminate the nutrient accumulation mechanism from alternative mechanisms as crucial drivers for peatland patterning?
4. Is the presence or absence of the nutrient accumulation mechanism indeed reflected in field data on the spatial variation of key variables in patterned peatlands?
5. What alternative stable states and concomitant catastrophic shifts could occur in peatland ecosystems, and can spatial patterns serve as an indicator of proximity to such shifts?

Research approach

Synergy through integration of theoretical and empirical parts

In this thesis, a combination of theoretical and empirical approaches will be adopted (Fig. 8). The theoretical parts consist of the development of mathematical models. The aim of these models is to generate hypotheses that can be tested in the field. For this aim, the mathematical models are kept as simple as possible. The empirical testing of model predictions will be aimed at falsifying the generated hypotheses (Popper 1968). Interpretation of current patterns benefits from such a priori construction of hypotheses (Chamberlin 1890; Platt 1964; Popper 1968; Loehle 1987). This method of hypothesis testing, in line with the idea of strong inference (Platt 1964), differs fundamentally from hypothesis generation based on a posteriori interpretation of data (Belyea and Lancaster 2002). This thesis aims at empirical testing of a priori formulated hypotheses that were generated with theoretical modeling (Fig. 8). In turn, the empirical results obtained in the field will be used to refine or develop new hypotheses (Fig. 8; Weiner 1995). There has also been some criticism of the use of strong inference in ecology (e.g. Quinn and Dunham 1983; Roughgarden 1983). A basic argument is that strong inference assumes that competing hypotheses are mutually exclusive, whereas in ecosystems, several independent mechanisms often contribute to an observed phenomenon that could, in theory, also be explained by each mechanism in isolation (Scheffer 1999). In this thesis this problem will be addressed by also analyzing the effect of multiple mechanisms in a full-factorial model design (Fig. 8).

The empirical tests in this thesis comprise field measurements in patterned peatlands. A limitation of field measurements is that cause-effect relationships and feedback processes cannot be measured directly. Such relationships could be identified in manipulative experiments. However, the long time span associated with peatland pattern formation limits the possibilities of such field manipulations (Moore and Bellamy 1974). Further, the spatial scale of the patterns of interest (Fig. 6) limits the possibilities for laboratory experiments. Moreover, previous studies have shown that it is very difficult to transport larger mesocosms ($\sim 1 \text{ m}^2$) into the laboratory without changing the properties of the peat matrix (Heijmans et al. 2001). Therefore, field measurements are chosen instead and the aim of the empirical tests is set relatively simple: measure the model state variables in the field, and compare whether the spatial variation in these variables is consistent for models and field observations (Shachak et al. 2008; Van der Valk and Warner 2009). The sampling campaigns in this thesis consist of transect-based samplings through peatland

patterns. It is known that the small-scale spatial variability in peatlands is enormous (Ohlson and Økland 1998), meaning that a lot of observations are needed to distinguish discernable trends. Therefore, we mainly focus in this thesis on taking a lot of relatively simple measurements (but a few detailed measurements are done as well). This combined modeling-measuring approach can create synergy between the theoretical and empirical parts of the research. The results of the theoretical chapters determine the design and target the key variables of interest for the empirical sampling campaigns (Fig. 8). In turn, the theoretical models are based, adjusted and improved with the empirical data (Fig. 8).

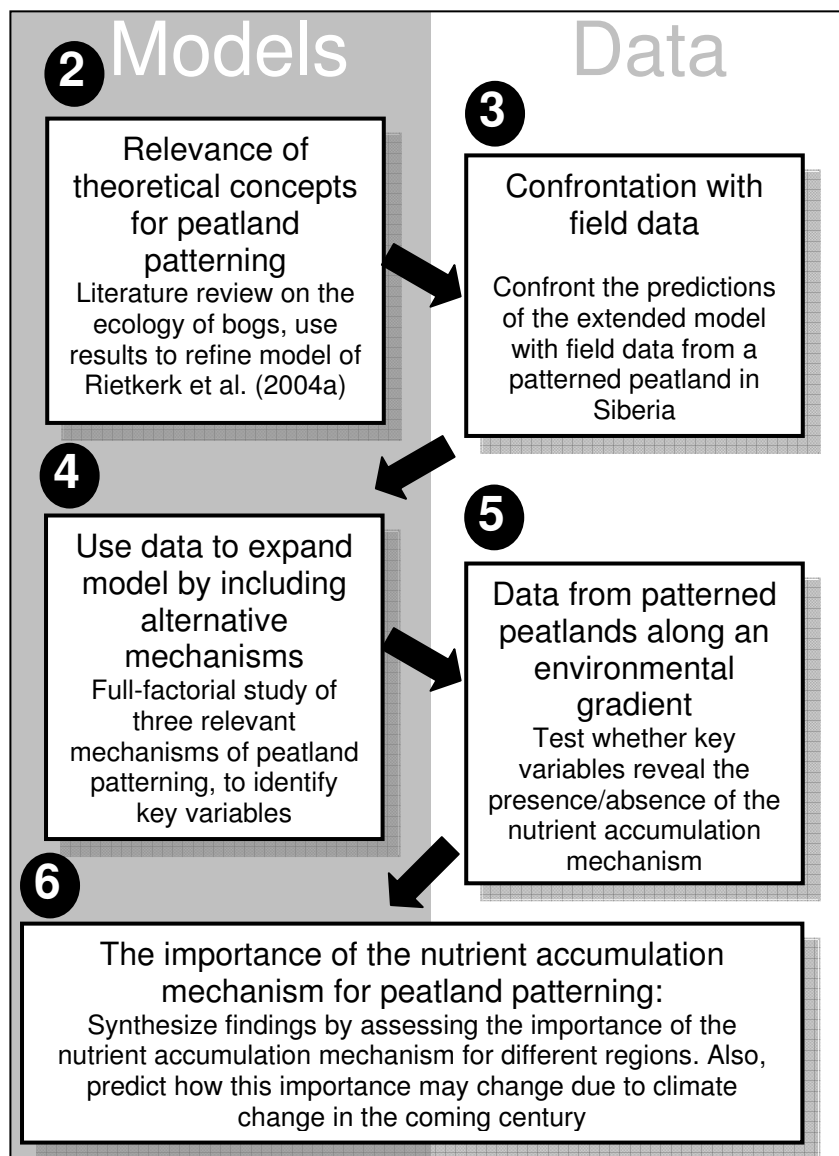


Figure 8: Schematic diagram of the integration of theory and empirical data gathering in this thesis. In the theoretical chapters, mathematical models are developed, that serve to formulate hypotheses and structure and focus the empirical sampling campaign. The empirical data is used to guide further model improvement.

Outline of the thesis

In Chapter 2, we analyze whether the theoretical concepts outlined in this Chapter 1 are indeed relevant for the ecosystem under study: peatlands. Thereby Chapter 2 answers the first research question by means of a literature review on the ecology of bogs. Also in this chapter, we will use this information to refine the mathematical model previously published in Rietkerk et al. (2004a).

In Chapter 3, we answer the second research question. We test the theoretical predictions generated by the model of Chapter 2. Until now, the only comparison that has been made is between the state variable biomass in the model and aerial pictures from patterned peatlands in Siberia (Rietkerk et al. 2004a). In Chapter 3, we test in a patterned peatland in the Great Vasyugan Bog of Western-Siberia whether model predictions and field observations also agree for the other model state variables: nutrients and water table level. Further, we test whether field data agrees with an alternative peatland model (Belyea and Clymo 2001).

In Chapter 4, we improved the mathematical model, based on the empirical data described in Chapter 3. The most important modification in Chapter 4 is that the model is extended in a way that two alternative mechanisms for peatland patterning (Swanson and Grigal 1988; Belyea and Clymo 2001) can also be studied. In the analyses, we answer the third research question by identifying key variables that can reflect the presence or absence for each of the three mechanisms. Thus, this extended model generated new hypotheses that could be tested in the field.

The aim of Chapter 5 is to test the theoretical predictions by the models in Chapter 4. To test these predictions, we compared peatland patterns along an environmental gradient. We measured nutrients and hydrology in patterned peatland sites in Scotland, Sweden and Siberia, which comprised a gradient in the importance of evapotranspiration to the water balance. Especially for Scotland we expect the peatland patterning to be driven by another mechanism than the nutrient accumulation mechanism. The model results from Chapter 4 suggest that in such cases the patterns in nutrients and hydrochemistry should be different as compared to sites where the mechanism is present. Thus, the comparison between sites along an environmental gradient enables answering of the fourth research question.

Finally in the Synthesis & Perspectives (Chapter 6), I will turn back to the question whether the nutrient accumulation mechanism explains peatland patterning, and how this differs between peatland regions (Fig. 8). Further, I will discuss whether patterns can serve as an indicator for catastrophic shifts. Thus, in Chapter 6 I will answer the final research question.

Glossary

Alternate stable states: alternative combinations of ecosystem states and environmental conditions that may persist at a particular spatial extent and temporal scale.

Bifurcation point: a specific setting of external conditions at which the stability of an equilibrium is lost; as a result, the system develops into another equilibrium state.

Bog: particular type of peatland in which plants depend entirely on precipitation for water input.

Catastrophic shift: a sudden shift in ecosystem status caused by passing a threshold where core ecosystem functions, structures and processes are fundamentally changed.

Complex systems: class of systems in which system characteristics at higher levels emerge from localized interactions and selection processes acting at lower levels. This complexity makes it more difficult to understand or predict the system's behavior.

Ecosystem engineer: an organism that directly or indirectly modulates the availability of resources to other species, by causing physical state changes in biotic or abiotic materials.

Ecosystem resilience: an ecosystem is resilient if it remains in the same domain of attraction and quickly returns to the same state after a disturbance.

Fen: particular type of peatland in which plants have access to both groundwater and precipitation as water sources.

Hysteresis: a property of systems that can follow different paths when increasing and when relaxing a perturbation. As a result, the state of a system cannot be predicted from external conditions only, but it depends on its history.

Long-range competition: the process where organisms, by depleting resources, constrain the establishment and survival of other organisms over a larger scale than the patch-scale on which they occur.

Maze pattern: type of self-organized patchiness in peatlands, which occurs on relatively flat ground. In a maze pattern, densely vegetated ridges occur within a matrix of more sparsely vegetated hollows. The ridges are connected in an almost continuous network without clear orientation, but occasionally the ridges form dead ends, somewhat resembling the corridors within a maze.

Mire: natural systems that actively sequester carbon as peat through water logging of organic matter (dead plant roots and litter). Hence, mires require a positive water balance,

Peatlands: ecosystems that have accumulated peat soils, but that are not necessarily still actively forming peat.

Positive feedback: a loop of effects that reinforce each other. Due to positive feedback an initial perturbation of a system's equilibrium may be amplified.

Resource concentration mechanism: this mechanism occurs when the presence of a functional group of organisms initiates a transport of resources from outside the patches in which they are present toward the inside of these patches.

Scale-dependent feedback: the strength and sign of a feedback between organisms and their environment varies with distance.

Short-range facilitation: the process where organisms, by creating favourable environmental conditions over a short range, help the establishment and survival of other organisms and themselves close-by.

Self-organized patchiness: particular type of spatial self-organization of sessile biota consisting of a two-phase mosaic of high- and low-density patches.

Spatial self-organization: the process where large-scale ordered spatial patterns emerge from disordered initial conditions through local interactions.



2

Linking habitat modification to catastrophic shifts and vegetation patterns in bogs

Maarten B. Eppinga, Max Rietkerk,
Martin J. Wassen & Peter C. De Ruiter

Plant Ecology 200: 53-68 (2009)

Linking habitat modification to catastrophic shifts and vegetation patterns in bogs

Abstract

Paleoecological studies indicate that peatland ecosystems may exhibit bistability. This would mean that these systems are resilient to gradual changes in climate, until environmental thresholds are passed. Then, ecosystem stability is lost and rapid shifts in surface and vegetation structure at landscape scale occur. Another remarkable feature is the commonly observed self-organized spatial vegetation patterning, such as string-flark and maze patterns. Bistability and spatial self-organization may be mechanistically linked, the crucial mechanism being scale dependent (locally positive and longer-range negative) feedback between vegetation and the peatland environment. Focusing on bogs, a previous model study shows that nutrient accumulation by vascular plants can induce such scale-dependent feedback driving pattern formation. However, stability of bog microforms such as hummocks and hollows has been attributed to different local interactions between *Sphagnum*, vascular plants and the bog environment. Here we analyze both local and longer-range interactions in bogs to investigate the possible contribution of these different interactions to vegetation patterning and stability. This is done by a literature review, and subsequently these findings are incorporated in the original model. When *Sphagnum* and encompassing local interactions are included in this model, the boundaries between vegetation types become sharper and also the parameter region of bistability drastically increases. These results imply that vegetation patterning and stability of bogs could be synergistically governed by local and longer-range interactions. Studying the relative effect of these interactions is therefore suggested to be an important component of future predictions on the response of peatland ecosystems to climatic changes.

Introduction

Northern peatlands occupy less than 2% of the land surface yet contain about 30% of the total terrestrial carbon pool (Gorham 1991), and are located in the altitudes expected to undergo the greatest increase in temperature and precipitation in the next decades (Houghton et al. 1995). Higher temperatures and longer thaw seasons may alter internal peatland dynamics in a way that increases emission of carbon dioxide and methane from these systems (Bridgham et al. 1995). Therefore concern has risen that peatlands may switch from sinks to sources of atmospheric carbon under such changing climate (Yu et al. 2001). An important factor controlling the rate of carbon sequestration is the peatland surface structure (Belyea and Malmer 2004). This structure comprises distinct microforms (order of magnitude: m), ranging from wet depressions (hollows or pools) to dry hummocks (e.g. Belyea and Clymo 2001). Focusing on peatland bogs, the hollows are usually dominated by species of the genus *Sphagnum* growing with sedges, while vascular plants mostly grow on the hummocks, coexisting with different species of *Sphagnum* (Wallén et al. 1988; Van Breemen 1995). Both these functional groups are actively modifying the bog habitat and thereby bog hydrology and peat accumulation.

The aim of this review Chapter is to gain insight in the possible effect of habitat modification by *Sphagnum* and vascular plants on peatland dynamics and also spatial self-organization, especially focusing on peatland bogs. First we discuss how paleoecological studies indicate that peatland dynamics may be governed by catastrophic shifts, and that self-organized vegetation patchiness might indicate proximity to such shifts. Then we review literature synthesizing bog habitat modification by *Sphagnum* and vascular plants. Subsequently, habitat modification is linked to spatial self-organization of bogs. As an illustration, we include habitat modification by *Sphagnum* and vascular plants in a simple and generic way in the analytical bog model of Rietkerk et al. (2004a), to illustrate its effect on bog dynamics and spatial self-organization. The results will be discussed from the perspective of the role of habitat modification in the response of bogs to climate change.

Catastrophic shifts in peatlands

A paleoecological study revealed that the current microtopography of hummocks and hollows of a Scottish mire has persisted for 5000 years (Moore 1977). In an Irish mire, Walker and Walker (1961) found stratigraphic evidence that microforms had remained at the same position over time. Similar conclusions are drawn from other

study sites (e.g. Sjörs 1961; Casparie 1972; Boatman and Tomlinson 1973; Frenzel 1983), and there is a general agreement that these different microforms are remarkably resilient to changes in environmental conditions (Belyea and Clymo 2001; Nungesser 2003), such as climate change.

However, this resilience is lost when changes in climate pass environmental thresholds, at which the peatland surface structure may abruptly shift to another stable state, with a different microstructure dominating the landscape (Belyea and Malmer 2004). If hollows dominate the landscape, it can be characterized as open treeless mire, while domination of hummocks with trees can be regarded as mire woodland (e.g. Alexandrov and Logofet 1994; Ohlson et al. 2001). Rapid transitions from open treeless mires to mire woodlands have been reported in paleoecological studies (see references in: Frankl and Schmeidl 2000; Ohlson et al. 2001). However, the reverse transition from mire woodland to treeless mire can also occur (Clymo and Hayward 1982; Svensson 1995; Van Breemen 1995; Ohlson et al. 2001). These transitions in microforms and vegetation also result in rapid changes in decomposition rates and carbon sequestration, stressing the urgent need for a better understanding of environmental thresholds in peatlands, and the way its surface structure and vegetation respond to climatic changes (Belyea and Malmer 2004).

A growing body of research suggests that these kinds of nonlinear responses of ecosystems to gradual changes in environmental conditions are associated with the occurrence of alternate stable ecosystem states (Scheffer et al. 2001). This concept was introduced by Lewontin (1969), and is still an issue of considerable interest and debate (Bertness et al. 2002). Alternate stable states mean that given the same set of environmental conditions, an ecosystem has more than one possible stable structure. Each stable structure has its own basin of attraction, meaning a certain range of ecosystem states that will always develop towards this stable structure (Lewontin 1969). Consequently, if such stable structure is reached, the ecosystem is resilient to perturbations within that basin of attraction.

However, changes in environmental conditions can alter the sizes of basins of attraction. Such changes may decrease a basin of attraction until it vanishes. When this point is reached, the ecosystem will be drawn towards another stable structure.

This threshold where the basin of attraction of the current ecosystem equilibrium disappears is known as a catastrophic bifurcation point (Kuznetsov 1995; Scheffer and Carpenter 2003). Ecologists have long recognized that gradual changes in environmental conditions can cause abrupt changes in ecosystems (Carpenter 1999). The passing of a catastrophic bifurcation point can explain such “Big effects from small causes” (Ricker 1963). These “Big effects” are referred to as catastrophic shifts in ecosystem states (Scheffer et al. 2001).

The term catastrophic shift comes from catastrophe theory. Catastrophe theory originated as a branch of mathematics studying bifurcations between different equilibria due to gradual changes (Thom 1975; Zeeman 1976). The theory is also useful for studying ecosystems with alternate stable equilibria (Loehle 1989). It is important to note that a catastrophic shift of an ecosystem into a different equilibrium does not necessarily imply a disaster or dramatic event, but it refers to the nature of the change. The term can therefore be a bit confusing, because sometimes the occurrence of a catastrophic shift is desired, and therefore stimulated (e.g. Meijer and Hoesper 1997).

The existence of alternate stable ecosystem states and catastrophic shifts implies that the state of an ecosystem cannot only be explained by the current environmental conditions, because the current ecosystem state also depends on its history. This phenomenon is known as hysteresis. Reversing a catastrophic shift is not achieved by simply restoring the environmental conditions that prevailed just before the shift took place because of such hysteretic dynamics. Restoring an ecosystem that has catastrophically degraded may therefore be very difficult or expensive (Carpenter 2001), if it is possible at all. Therefore, it is desirable to know whether ecosystems are close to a catastrophic shift. Unfortunately, catastrophic shifts are typically unpredictable, and “early warning signals” of approaching catastrophic change are difficult to obtain (Scheffer et al. 2001).

Vegetation patterning in peatlands

Recently, it has been suggested that the formation of self-organized vegetation patterns in peatlands indicate proximity to catastrophic shifts (Rietkerk et al. 2004b). Interesting observations in this respect are the rapid transition from a homogenous

hummock state into the current patterned state of a Swedish bog (Belyea and Malmer 2004), and the loss of surface patterning within 50 years in another Swedish mire (Gunnarsson et al. 2000). Self-organized patchiness in peatlands consists of a spatially regular two-phase mosaic of typical hummock and hollow vegetation (Rietkerk et al. 2004a). Patterned peatlands have been observed in North America (e.g. Heinselman 1963), Europe (e.g. Sjörs 1961), Asia (e.g. Sakaguchi 1980) and also on the Southern Hemisphere (Mark et al. 1995), including tropical mires (Backéus 1989). Two types of patterns ($10^2 - 10^3$ m) can be observed (Sjörs 1983; Wallén et al. 1988; Rietkerk et al. 2004a; Fig. 1): string and flark patterns on slopes and maze patterns on relatively flat mire parts.

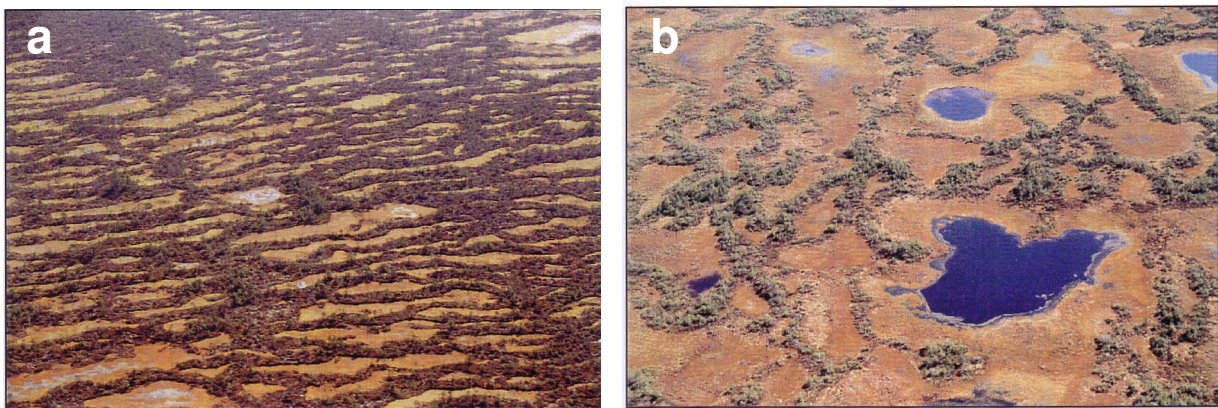


Figure 1: Photographs of hummock-hollow complexes on the slope (a) and the central part (b) of a watershed bog in the great Vasyugan area, Siberia (Courtesy W. Bleuten and E.D. Lapshina). Hummocks are covered with dwarf shrubs, *Pinus sylvestris*, *P. sibirica* and *Sphagnum fuscum*, hollows are occupied by *S. balticum*, *S. majus*, *S. jensii*, *S. papillosum*, *Carex limosa* and *Rhynchospora alba* (Semenova and Lapshina 2001; E.D. Lapshina, pers. comm.).

String and flark patterns consist of linearly merged hummocks (strings) alternating with linearly merged hollows (flarks), oriented along the topographic contours of peatland slopes. The origin of string and flark patterns has received considerable attention during the last century (Charman 2002), which has resulted in many hypotheses involving physical and biotic processes to explain the development of this peatland patterning (Seppälä and Koutaniemi 1985; Glaser 1992b; Belyea and Lancaster 2002). We restrict our discussion to biotic processes since these are currently thought to be governing peatland patterning (Seppälä and Koutaniemi 1985; Charman 2002).

A detailed hypothesis on initiation of flarks was derived from stratigraphical analyses in North America (Foster et al. 1983; Foster and King 1984; Glaser 1992b). It consists of three elements: (1) Initial accumulation of peat, converting channeled water flow into sheet flow; (2) Amplification of the surface microtopography because

of slower peat accumulation in hollows as compared to hummocks, and higher resistance of hollows to infiltration. Adjacent hollows merge into linear flarks; (3) Subsequent enlargement of flarks. Water chemistry (Glaser 1992b) and vegetation changes (Glaser et al. 1981; Glaser 1987, 1992b) in North American patterned fens could be explained with this hypothesis. Spatial analysis of a bog pool complex in Scotland confirmed most elements of this hypothesis (Belyea and Lancaster 2002).

Related to this hypothesis is the idea that differences in hydraulic conductivity may induce pattern formation. The hydraulic conductivity of hummocks is lower than that of hollows (Ivanov 1981); therefore water flow tends to pond up behind hummocks, causing hollow formation upslope (Couwenberg 2005, and references therein). Other studies focus on the initiation of strings, emphasizing the importance of spring floods in string formation (Sakaguchi 1980; Seppälä & Koutaniemi 1985). During these floods slush and plant remains are transported towards elevations on the mire surface, thereby amplifying the surface microtopography. These hypotheses have in common that they suggest that topographic differences on the peatland slope are amplified by local feedbacks between hydrology, peat accumulation and vegetation. As a result, hummocks and hollows develop in the landscape. Given the anisotropy (that is unidirectional water flow) on peatland slopes, linear features will develop over time.

Maze patterns on relatively flat mire parts consist of merged hummocks that are star or net-like. These patterns have been reported less frequently in literature, but they cover extensive areas in the Vasyugan area in Siberia for example (Semenova and Lapshina 2001; Rietkerk et al. 2004a; Fig. 1). The formation of spatially regular maze patterns on flat mire parts cannot be fully explained by the feedbacks described above, because unidirectional water flow is lacking (Rietkerk et al. 2004a). A putative mechanism inducing maze patterning is accumulation of nutrients under and near vascular plants through the advective transport of nutrients driven by transpiration of vascular plants (Rietkerk et al. 2004a; Wetzel et al. 2005).

The crucial mechanisms linking self-organized patchiness to catastrophic shifts are scale-dependent (that is locally positive and longer-range negative) feedbacks between the environment and plant species that actively modify this environment (Rietkerk et al. 2004b). This scale dependency arises when plants withdraw resources from their surroundings, leading to local resource accumulation, and longer-range resource depletion. Hence there is a local positive effect, and a longer-range negative effect. Nutrient accumulation by vascular plants is an example of such a scale-dependent feedback.

However, several models (Logofet and Alexandrov 1988; Alexandrov and Logofet 1994; Hilbert et al. 2000; Belyea and Clymo 2001), field experiments (Belyea and Clymo 2001) and studies on string-flark patterning (Foster et al. 1983; Glaser 1992b) suggest that the observed stability of peatland microforms results from more local feedbacks between hydrology and peat accumulation, resulting in alternate stable microstates of hummocks and hollows. In the following we speak of local processes when there is a short-range self-enforcing effect that does not induce effects on a longer range.

Focusing our current study on bogs, both the hollow-species of *Sphagnum*, from here referred to as *Sphagnum*, (Clymo and Hayward 1982; Svensson 1995; Van Breemen 1995) and vascular plants (most research focusing on *Pinus sylvestris*; Frankl and Schmeidl 2000; Ohlson et al. 2001) actively modify their habitat and thereby bog hydrology and peat accumulation. Therefore we will now summarize findings in literature providing a more detailed overview of the habitat modification by these two functional groups.

Bog habitat modification by *Sphagnum* and vascular plants

The pivotal environmental variables determining growth of *Sphagnum* and vascular plants in bogs are temperature, light availability, nutrient availability, pH and the level of the water table (Malmer 1962; Clymo 1970; Ivanov 1981; Clymo and Hayward 1982; Ingram 1983; Hayward and Clymo 1983; Backéus 1985; Rydin and McDonald 1985; Wallén et al. 1988; Økland 1990; Alexandrov and Logofet 1994; Belyea 1996; Gunnarsson and Rydin 1998; Frankl and Schmeidl 2000; Limpens et al. 2003; Nungesser 2003). The physiological characteristics of both *Sphagnum* and vascular plants drive ecosystem processes that change the pivotal environmental variables of bog ecosystems in a way that favors their own functional group, but disfavors the other functional group (Fig. 2).

It is important to note that neither functional group forms pure stands in bog ecosystems; the hollows are usually dominated by *Sphagnum* growing with sedges, while different species of *Sphagnum* occur on the higher vascular plant-dominated hummocks. However, we assume that the effect of each functional group on the environment is determined by the effect of its dominant species. This simplifying assumption is made to enable the subsequent coupling of our findings to an analytical mathematical model. The effect of *Sphagnum* and vascular plants on the bog environment will now be discussed in more detail for each of the five pivotal environmental variables.

Light availability

Using different strategies (Clymo and Hayward 1982; Svensson 1995; Fig. 2), both *Sphagnum* and vascular plants shape light availability in a way that suppresses the other functional group. Extensive *Sphagnum* growth hampers establishment of vascular plants (Ohlson et al. 2001), because it forms a thick carpet that overgrows small vascular plants (Malmer et al. 2003). On the other hand, when vascular plants have successfully established and reach above the *Sphagnum* carpet, it decreases *Sphagnum* development through shading and burial by aboveground litter (Hayward and Clymo 1983; Wallén et al. 1988; Malmer et al. 1994; Lamers et al. 2000; Berendse et al. 2001; Malmer et al. 2003). It can be concluded that *Sphagnum* and vascular plants modify the environment in opposite directions. As a result, interspecific competition for light exceeds intraspecific competition. Also, dominance of the functional groups may alter during the growing season.

Acidity (pH)

Sphagnum is considered an important source of acidity in bog waters (Siegel et al. 2006). It has long been suggested that the acidifying capability of *Sphagnum* stems from its high cation-exchange capacity, because of the considerable amounts of polyuronic acids in the tissue (e.g. Clymo 1964; Clymo and Hayward 1982; Van Breemen 1995). However, more rigorous geochemical studies strongly suggest that organic acids are the primary acidifying agent in bogs (Gorham et al. 1986; Reeve et al. 1996; Glaser et al. 2004; Siegel et al. 2006). Organic acids are believed to result from humification of *Sphagnum* (Hemond 1980), leading to a local decrease in mire water pH (Bragazza et al. 1998). It can thus be concluded that *Sphagnum* actively acidifies its environment, which is unfavorable for vascular plant growth (Van Breemen 1995). Thereby *Sphagnum* negatively affects vascular plants.

Water table

Compared to vascular plants, *Sphagnum* is less productive (Verry and Urban 1992). Therefore, relatively small yearly precipitation excess is needed for *Sphagnum* dominated bogs to maintain or decrease the distance between the bog surface and the water table. Moreover, *Sphagnum* litter decays slowly and is easily collapsible (Coulson and Butterfield 1978; Johnson and Damman 1993; Van Breemen 1995; Hobbie 1996), meaning that it stimulates the formation of peat with small porosity. This means that little water is needed for this low permeable peat to become waterlogged, so this characteristic of *Sphagnum* also promotes a higher water table (Van Breemen 1995). On the other hand, vascular plants stimulate a lowering of the

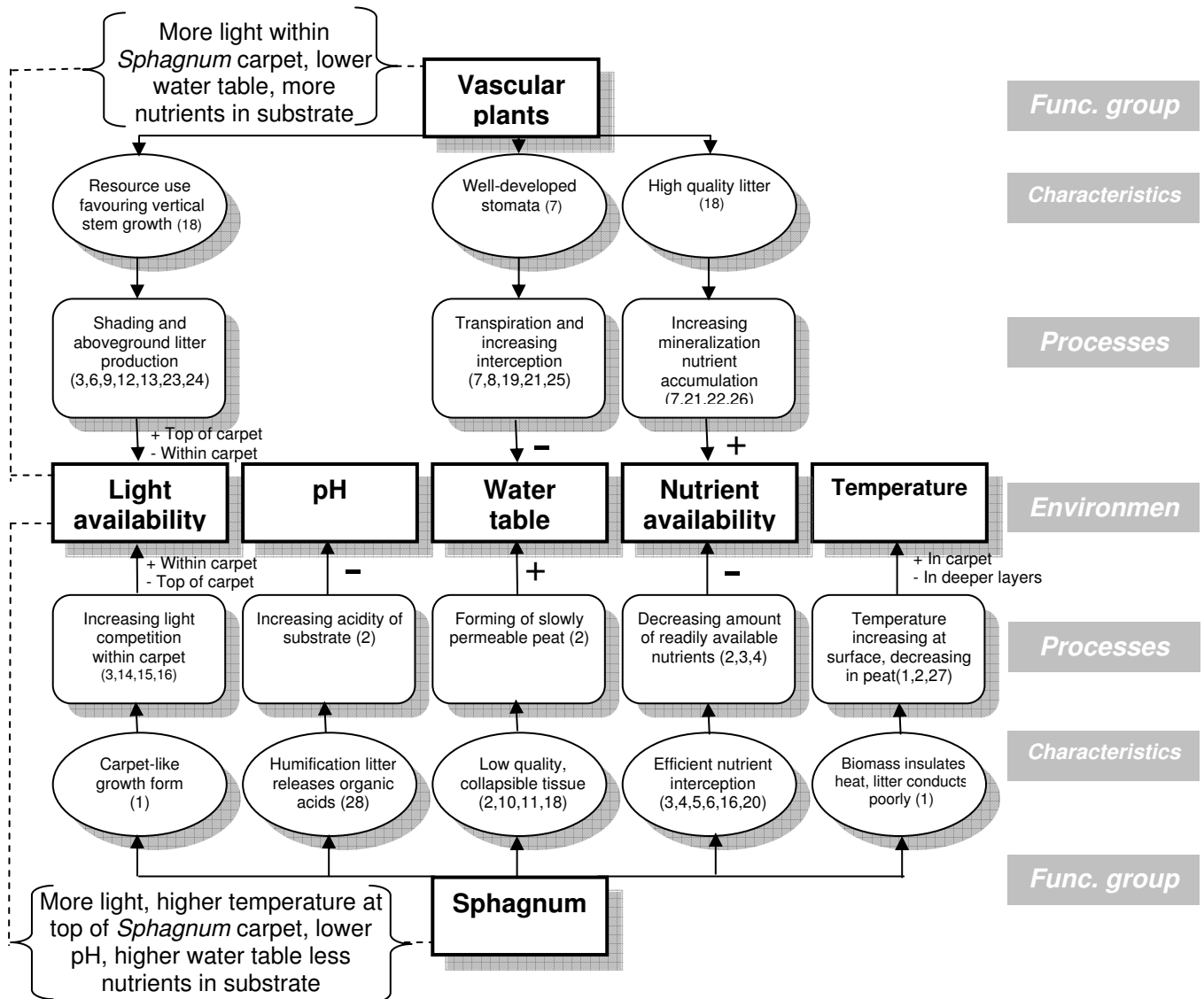


Figure 2: Habitat modification by *Sphagnum* and vascular plants in bogs. The ovals show the main functional characteristics of the two functional groups. The rounded rectangles show the resulting ecological processes. Solid arrows show relations and effects, the dashed arrows the feedbacks. The pivotal environmental variables are depicted in the rectangles. Minus signs mean a decreasing/lowering effect, plus signs an increasing/stimulating effect. Both plus and minus signs mean that the effect differs at the top or within the *Sphagnum* carpet (in case of light availability) or differs between the *Sphagnum* carpet and lower peat layers (in case of temperature). References; 1: Clymo and Hayward (1982) 2: Van Breemen (1995) 3: Malmer et al. (2003) 4: Rydin and Clymo (1989) 5: Clymo (1970) 6: Malmer et al. (1994) 7: Marschner (1995) 8: Ingram (1983) 9: Wallén et al. (1988) 10: Coulson and Butterfield (1978) 11: Johnson and Damman (1993) 12: Hayward and Clymo (1983) 13: Murray et al. (1993) 14: Backéus (1985) 15: Redbo-Torstensson (1994) 16: Svensson (1995) 17: Gunnarsson and Rydin (1998) 18: Hobbie (1996) 19: Frankl and Schmeidl (2000) 20: Heijmans et al. (2002) 21: Rietkerk et al. (2004a) 22: Belyea and Clymo (2001) 23: Lamers et al. (2000) 24: Berendse et al. (2001) 25: Rutter (1963) 26: Fitter and Hay (1983) 27: Williams (1970) 28: Hemond (1980)

water table by increasing the rate of evapotranspiration (Ingram 1983; Marschner 1995; Frankl and Schmeidl 2000; Rietkerk et al. 2004a), and the canopy of trees diminishes the amount of precipitation that reaches the surface (Rutter 1963). It can thus be concluded that *Sphagnum* promotes submergence, while vascular plant growth stimulates water table drawdown. Both functional groups are thus modifying the environment but in opposite directions, thereby negatively affecting each other. If a functional group increases in density, it modifies its environment towards better growing conditions for itself and creates worse conditions for the competing functional group. Moreover, if a functional group increases in density, it can better counteract adverse effects of the opposite modifications by the competing functional group.

Nutrient availability

The competition for nutrients in bogs is asymmetric, because *Sphagnum* acts as an effective filter intercepting and effectively recycling all nutrient inputs from atmospheric deposition (Clymo 1970; Rydin and Clymo 1989; Malmer et al. 1994; Svensson 1995; Heijmans et al. 2002; Malmer et al. 2003), while vascular plants mainly depend on nutrients that are released via mineralization of the peat (Malmer et al. 1994; Malmer et al. 2003). Apart from the effective interception, *Sphagnum* peat sequesters mineral nutrients from the acrotelm, and the low quality litter input of *Sphagnum* reduces mineralization rates in this layer (Malmer et al. 1994; Van Breemen 1995; Malmer et al. 2003). On the other hand, the previously discussed lowering effect on water table height by vascular plants, together with their deposit of high quality litter, promotes an increase in mineralization rate (Hobbie 1996; Belyea and Clymo 2001). Furthermore, vascular plants may attract and accumulate nutrients from the surrounding environment through advective transport by groundwater, which is driven by the active transpiration of vascular plants (Marschner 1995; Rietkerk et al. 2004a; Wetzel et al. 2005). Moreover, when trees die and fall down on the bog surface, the logs provide a nutrient rich environment suitable for successful colonization by vascular plants (Agnew et al. 1993). It can thus be concluded that nutrients in the substrate only affect vascular plant growth. *Sphagnum* decreases this nutrient availability, while vascular plants increase nutrient release rates in the substrate. Both functional groups thus modify the environment in opposite directions. If vascular plants increase in density, they modify the environment towards better growing conditions for themselves, and they can better counteract nutrient depleting effects of modification by *Sphagnum*. If *Sphagnum* increases in density it makes growing conditions for vascular plants worse.

Temperature

The living top layer (< 5cm) of the *Sphagnum* carpet tends to be relatively warm, thereby lengthening its growing season (Clymo and Hayward 1982; Van Breemen 1995). On the other hand, *Sphagnum* peat conducts heat poorly. Vascular plants mainly extend their root system in the upper peat layer (Backéus 1986; Laiho and Finer 1996; Gunnarsson and Rydin 1998). Because vascular plant growth depends on the functioning of belowground roots, a substrate that is dominated by *Sphagnum* peat leaves a relatively short growing season for vascular plants (Williams 1970; Van Breemen 1995). So, the characteristics of the living *Sphagnum* layer lengthen the growing season for *Sphagnum* itself, while the peat that is formed by its remains shortens the growing season of vascular plants. So concerning temperature, *Sphagnum* modifies the environment in a way that positively affects itself, and negatively influences vascular plants.

Linking habitat modification to vegetation patchiness

In general, competition for resources drives intraspecific competition within functional groups, and therefore negative feedback. However, in bogs, the different pathways to habitat modification (Fig. 2) show that both *Sphagnum* and vascular plants also modify their habitat towards better growing conditions for themselves, or suppress the other functional group. These positive effects give the possibility of bistability, because with a small change in biota or environment the system may switch between alternate stable states (Odum 1971; Wilson and Agnew 1992). Following Wilson and Agnew (1992), different types of these vegetation switches can be distinguished. A one sided switch (also called type I switch) means that a functional group changes an environmental factor to its own advantage in patches where it is present. Two type I switches may be involved in bogs, namely the modification of temperature and pH by *Sphagnum* (Fig. 3). A reaction switch (type II) refers to a process of a functional group changing an environmental factor to its own advantage in patches where it is present, and also changes this factor outside the patch, but in opposite direction. A type II switch in this system involves vascular plants increasing nutrient concentrations in patches where they are present through advective transport, but thereby decreasing nutrient concentrations farther away from these patches (Fig. 3).

A symmetric switch (type III) means that a functional group changes an environmental factor to its own advantage in its patches, and another functional group simultaneously changes the same environmental factor in its patches, but in the opposite direction. Three type III switches can be distinguished; *Sphagnum*

changes light availability, distance to the water table, and nutrient availability in a way that favors their own growth, while vascular plants do the same by modifying these environmental variables in the opposite directions (Fig. 3).

The concept of different types of vegetation switches is useful, because it enables separation of local and longer-range processes. The type I and type III switches only act within vegetation patches, and therefore agree with our definition of local. Hence, they cannot explain spatial regularity in vegetation patchiness (Wilson and Agnew 1992; Rietkerk et al. 2004a,b). The type II switch results from a short-range positive effect (inside the vegetation patch), and a longer-range (outside this patch) negative effect. Therefore, this type of switch can explain spatial regularity in vegetation patterns, which in turn may indicate proximity to catastrophic thresholds in ecosystems (Rietkerk et al. 2004b).

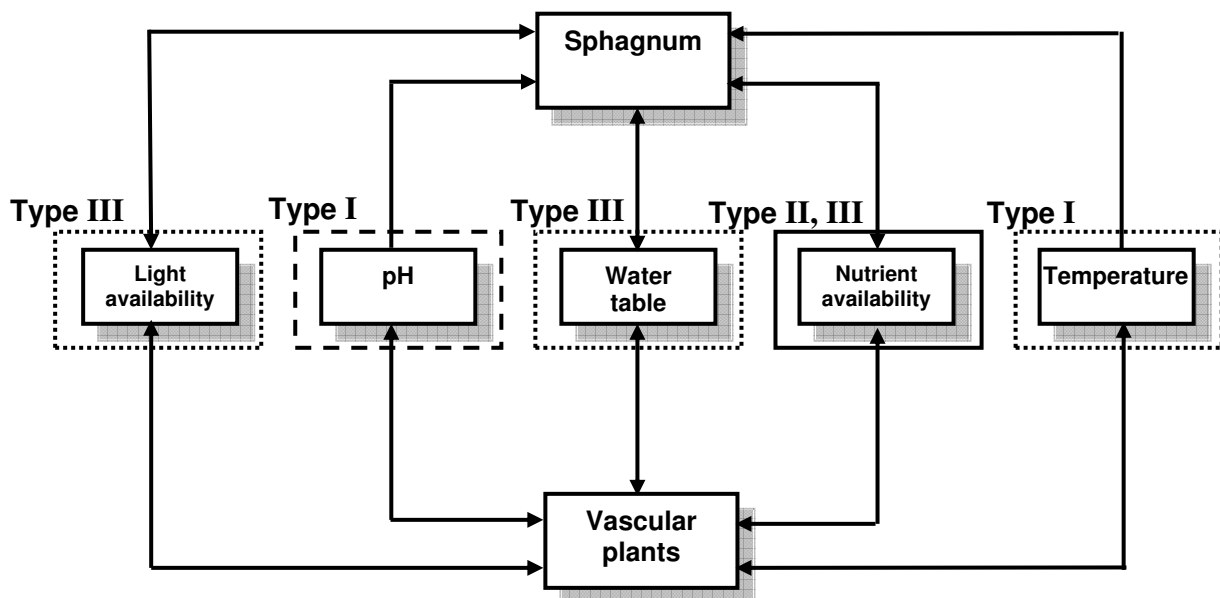


Figure 3: Vegetation switch analysis of the bog ecosystem. Romans indicate the three different types of switches that are distinguished here (following Wilson and Agnew, 1992). I: One sided switches; Sphagnum changes temperature and pH in a way that stimulates their own growth in the patch where they are present. II: Reaction switch; Vascular plants increase nutrient concentrations in the patches where they are present, but thereby decreasing nutrient concentrations at further distances. III: Symmetric switches; Sphagnum changes light availability, water table, and nutrient availability in a way that favors their own growth. Vascular plants do the same, by modifying these variables in the opposite directions.

A general model on bog dynamics

As an illustration, we will now include the discussed interactions between *Sphagnum*, vascular plants and the bog environment in an analytical bog model, disentangling

the effect of the previously discussed local and longer-range processes on self-organized patchiness and stability of bog ecosystems. The simplifying assumption of considering functional vegetation groups enables the inclusion of *Sphagnum* and the effects of habitat modification in a simple and generic way in the model of Rietkerk et al. (2004a). In the following, we investigate how this extension affects model results (see appendix 2A for all analytical details).

Competition between *Sphagnum* and vascular plants in bogs occurs mainly through habitat modification (Fig. 2). Modeling competition through modification of biotic or abiotic habitat components requires a different approach than the standard competition model (e.g. Eppinga et al. 2006). In the standard Lotka-Volterra approach, the relative loss rate (i.e. the damage that is exerted by 1 unit of biomass of the competitor) is modeled as a linearly increasing function of biomass (Fig. 4a). However, the analysis presented here suggests that vascular plants are negatively affected by modification of pH and temperature by *Sphagnum* (Fig. 2); therefore we assume that provided that *Sphagnum* is present, vascular plant biomass is lost through these effects (Fig. 4a). Also, we model modification by both functional groups of water table, nutrients and light availability in a different way than Lotka-Volterra competition. For these factors, the damage that is exerted by the competitor is saturating, meaning that there is a decreasing relative competitive effect with increasing density of the functional group.

Simulations of the Rietkerk et al. (2004a) model (from here referred to as the original model) show that vascular plant biomass develops in a spatially regular structure (Rietkerk et al. 2004a; Fig. 4b). However, apart from spatial regularity, other conspicuous features of vegetation patterns in bogs are the sharp boundaries between different functional groups (Fig. 1). In the original model nutrient accumulation by vascular plants induces a type II switch, which drives the formation of a spatially regular pattern but does not drive the formation of sharply bounded patches of vascular plants (Rietkerk et al. 2004a; Fig. 4b).

If we now include competition between *Sphagnum* and vascular plants inducing a type III switch, we see that because of this switch, sharper transitions occur in the vegetation pattern, as observed in the field (Fig. 4b). This result is in compliance with the assertion that a type III switch can sharpen vegetation boundaries and can create a stable vegetation mosaic (Wilson and Agnew 1992). If we subsequently introduce the type I switch exerted by *Sphagnum* in the model, the *Sphagnum* patches in the

pattern expand (Fig. 4b), which is in compliance with the findings of Wilson and Agnew (1992). At a certain point in time, however, the expansion of *Sphagnum* patches in the model stops, meaning that at this moment the type II and type III switches outweigh the effect of the type I switch.

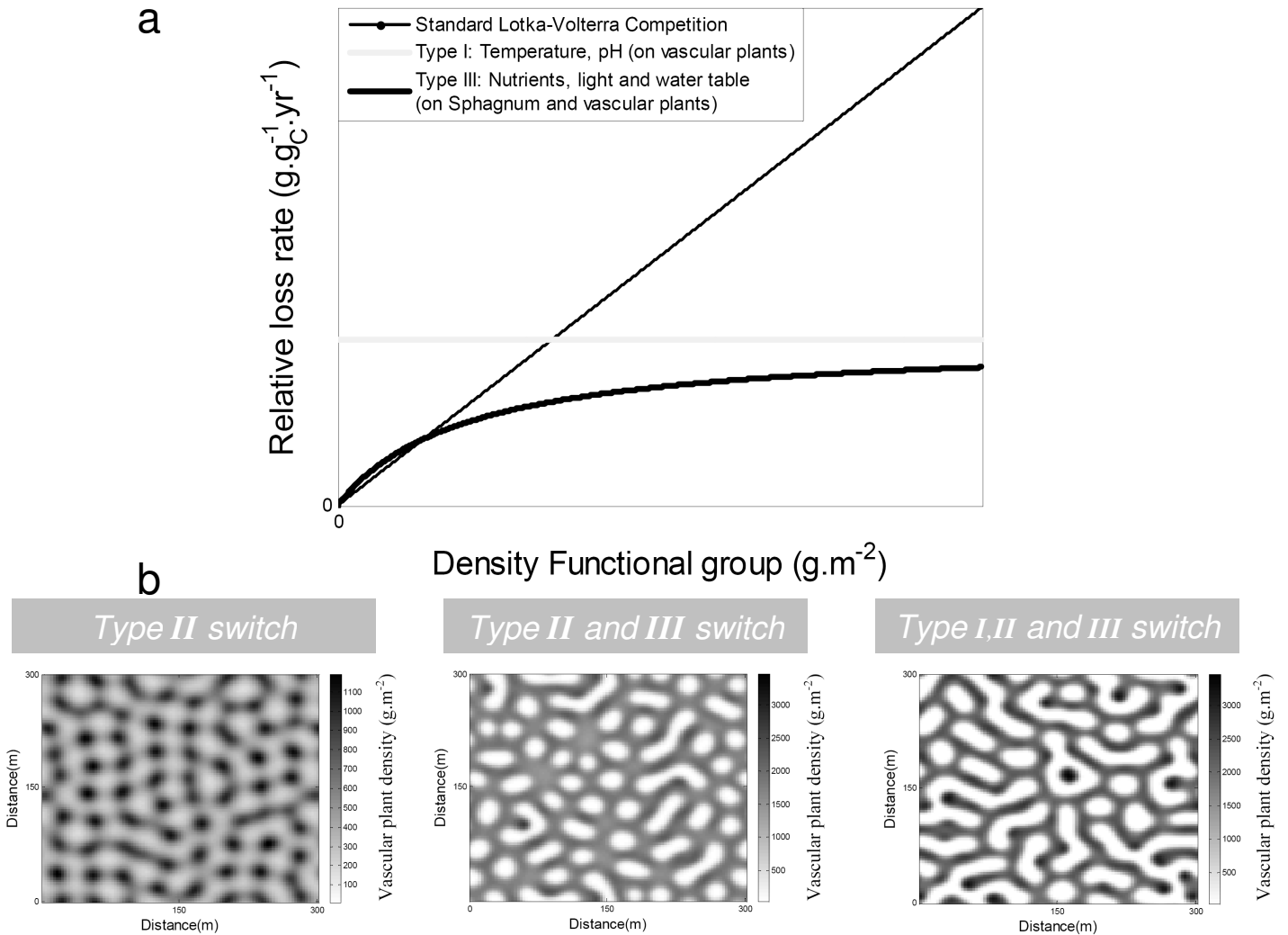


Figure 4: (a) Conceptual graph showing the difference between competition caused by type I and type III switches and the standard Lotka-Volterra approach. The relative loss rate indicates the damage that is exerted by 1 unit of biomass of the competitor. In the standard Lotka-Volterra approach, the relative loss rate increases linearly with biomass. For type I competition the relative loss rate is constant, for type III competition it is saturating. (b) Effect of vegetation switches on vegetation patchiness. The model of Rietkerk et al. (2004a) included only a type II switch, which drives the formation of a regular pattern, but not sharp transitions between vegetation types (left panel, $N_{in} = 1.4 \text{ g}_N \cdot \text{m}^{-2} \cdot \text{yr}^{-1}$). Extending this model by incorporation of competition between Sphagnum and vascular plants inducing a type III switch sharpens vegetation boundaries (middle panel, $N_{in} = 3.4 \text{ g}_N \cdot \text{m}^{-2} \cdot \text{yr}^{-1}$). When the model is further extended with Sphagnum affecting vascular plants in a way that induces a type I switch, the Sphagnum patches expand (right panel $N_{in} = 3.4 \text{ g}_N \cdot \text{m}^{-2} \cdot \text{yr}^{-1}$).

Apart from the self-organized vegetation patchiness becoming more pronounced, the parameter region in which hysteresis occurs increases (Fig. 5). In most of this region, vascular plants could stably exist in the original model, but can now become excluded by *Sphagnum* because of the type I and type III switches. Note that the vegetation state of only *Sphagnum* is a stable equilibrium for the entire parameter region examined (Fig. 5b). However, the negative slope of the separatrix shows that when nutrient input increases, the basin of attraction of this equilibrium becomes smaller (Fig. 5b). This means that a smaller amount of vascular plants biomass is needed to invade the system. So, local habitat modification and scale-dependent feedback synergistically affect pattern formation and stability in the model system (Fig. 5). The model results show that when approaching the catastrophic bifurcation point, a distinct sequence of different self-organized vegetation patterns can be observed (Fig. 5).

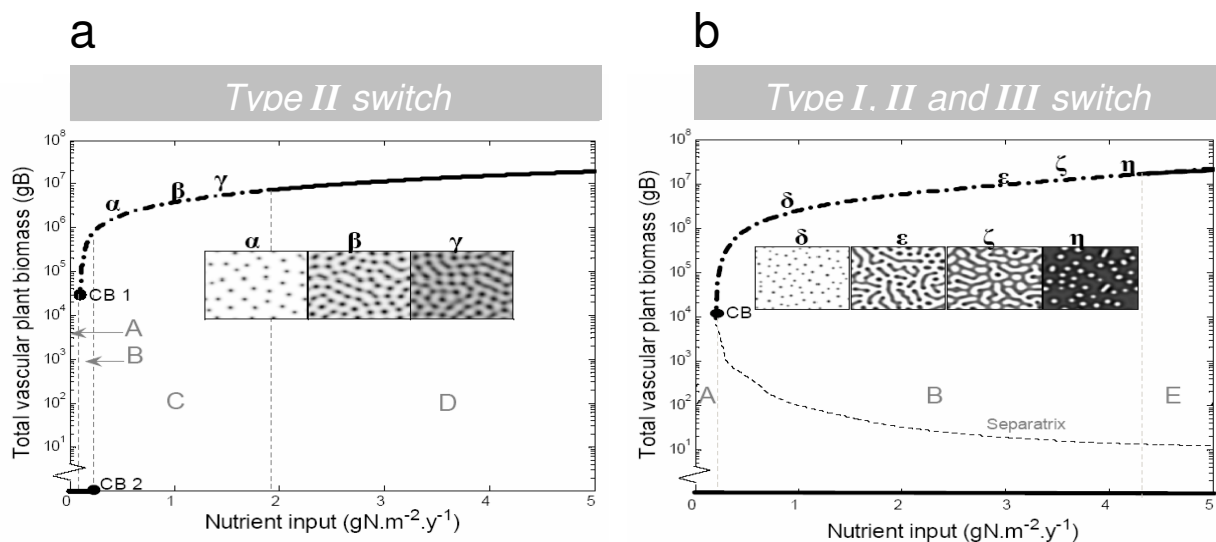


Figure 5: Bifurcation diagrams. Full black lines depict mean field equilibria, dashed black lines patterned equilibria. The black dotted line is a separatrix. (a) The original model by Rietkerk et al. (2004a), which only contains the nutrient accumulation mechanism. Along a gradient of nutrient input, four situations can be distinguished; A: Low nutrient input where vascular plants cannot exist. B: Region of nutrient input rates where no vascular plants or vascular plants growing in a pattern are both stable equilibria. C: Nutrient input range where vascular plants always exist and grow in patterns. D: Nutrient input region where vascular plants always exist, forming a homogeneous cover CB 1 is the catastrophic bifurcation point where vascular plants go extinct. CB 2 is the catastrophic bifurcation point where vascular plants always invade the system. (b) The original model extended with *Sphagnum* and habitat modification by *Sphagnum* and vascular plants. In parameter region E, there is bistability between homogeneous *Sphagnum* cover and homogenous vascular plant cover. The separatrix denotes the basins of attraction of the equilibria. Ecosystem states above the separatrix evolve towards the equilibrium with vascular plants; ecosystem states below the separatrix evolve to the equilibrium without vascular plants. CB is the catastrophic bifurcation point where vascular plants go extinct.

On slopes (see appendix 2A for modeling details), the model generates string and flark patterns (Fig. 6). Similar to the simulations on flat surfaces, vascular plants become more pronouncedly present with increasing nutrient input. First, the number of the vascular plant dominated strings increases, and the width of *Sphagnum* dominated flarks decreases. If nutrient input is further increased, the width of the strings increases (Fig. 6).

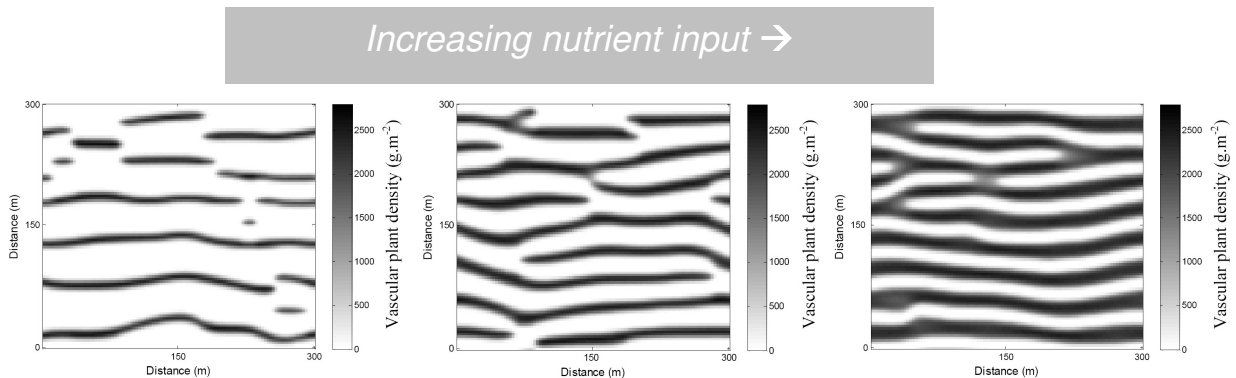


Figure 6: Linear vegetation patterns emerging on bog slopes, using the model with all three types of vegetation switches. Slopes are mimicked by modeling unidirectional water flow (cf. Rietkerk et al. 2004a). With increasing nutrient input rate, vascular plants increase in dominance. First, the main mode of expansion is an increase in the number of vascular plant dominated strings. With nutrient input rates increasing further, the width of the individual strings increases. Nutrient input rates were set as follows; Left Window: $1.4 \text{ g}_N \cdot \text{m}^{-2} \cdot \text{yr}^{-1}$ Middle Window: $2.4 \text{ g}_N \cdot \text{m}^{-2} \cdot \text{yr}^{-1}$ Right Window: $3.4 \text{ g}_N \cdot \text{m}^{-2} \cdot \text{yr}^{-1}$.

The impact of future climate change on bogs

The literature survey presented here suggests that the pivotal environmental variables in bogs are subject to modification by *Sphagnum* and vascular plants. These processes could have an important effect on the vegetation patchiness and stability of bogs. The analysis revealed that both local and spatial vegetation switches might be involved in the abrupt transitions in vegetation and surface structure of bog ecosystems. These transitions can be abrupt in space (vegetation patchiness) and time (catastrophic shifts). The model results suggest that because of incorporation of local habitat modification, vegetation boundaries become sharper and also the parameter region of bistability drastically increases, suggesting that local and longer-range interactions between the vegetation and the bog environment synergistically govern pattern formation and stability.

It would be interesting to expand our current model to examine how expected increases in annual temperature and precipitation in the boreal zone (Houghton et al.

1995; Hadley Centre Coupled Model Version 3 (HadCM3)) may alter the pivotal environmental variables in bogs. Both *Sphagnum* and vascular plants can amplify such external changes (Fig. 2). For example, an increase in temperature lengthens the growing season and increases mineralization rates (Aerts et al. 1992; Gunnarsson et al. 2004), which favors vascular plants (Backéus 1985). The accompanying decrease in *Sphagnum* might be self-enforcing because the temperature switch becomes less effective; a smaller proportion of *Sphagnum* in the peat layer leads to warmer conditions in the rooting zone of vascular plants, which further lengthens the growing season of vascular plants. An accompanying amplifying effect could be that this increasing vascular plant density generates higher nutrient availability because of the nutrient switch. The latter switch could also amplify increased nutrient availability via atmospheric deposition (Gunnarsson et al. 2004). Moreover, at high atmospheric deposition rates, *Sphagnum* is not capable of intercepting all nutrients (Lamers et al. 2000; Berendse et al. 2001; Malmer et al. 2003), meaning that nutrients will leach into the rooting zone of vascular plants (Aerts et al. 1992). Our current model results suggest that a *Sphagnum* dominated bog becomes more susceptible for invasion by vascular plants with increasing nutrient input (Fig. 5b). This result is in compliance with the notion that increased N-deposition could be one reason for the decrease in *Sphagnum* and rapid expansion of vascular plants that has been observed in many bogs in recent decades (Aaby 1994; Frankl and Schmeidl 2000; Gunnarsson et al. 2002; Malmer et al. 2003).

On the other hand, increases in precipitation may lead to a higher water table, favoring the more pronounced hollow species of *Sphagnum* (Belyea and Malmer 2004), which in turn can stimulate further submergence through the water table switch. Very high water tables can lead to substantial dieback of higher vascular plants (Gunnarsson and Rydin 1998). So, the response of bogs to future climatic changes is not straightforwardly determined, because it involves the study of the relative importance of different processes possibly inducing vegetation switches. Another difficulty in such predictions is that the relative importance of different processes (Fig. 2) is probably site-specific. For example, in relatively nutrient-rich mires, Malmer et al. (2003) found that the competition between *Sphagnum* and vascular plants for light was more important than for nutrients, while we expect the opposite to be true for the oligotrophic patterned bogs in the Vasyugan area in Siberia.

Our model results include linear patterning on slopes (Fig. 6), as is also found in models simulating local changes in hydrology (Swanson and Grigal 1988; Couwenberg 2005; Couwenberg and Joosten 2005). These models have the advantage of predicting linear patterning in both bogs and fens. On the other hand, our model simulating local resource accumulation has the advantage of predicting patterning on both slopes and flatter parts of peatland bogs dominated by *Sphagnum*. Formulation of such multiple independent hypotheses about possible different mechanisms driving the spatial self-organization of bogs will benefit the interpretations of self-organized vegetation patterns in bogs (Belyea and Lancaster 2002), which is necessary to identify whether these vegetation patterns can serve as indicators of proximity to catastrophic shifts or climate change.

Studying the interactions that drive pattern formation in peatlands can contribute to a better understanding of the ecosystem's functioning in general. The interactions between *Sphagnum* and vascular plants may induce vegetation switches that can drive such pattern formation. In general, these switches are expected to be important driving forces behind the rapid and nonlinear responses of peatland vegetation to climatic changes (Frankl and Schmeidl 2000; Ohlson et al. 2001; Belyea and Malmer 2004). Hence, interactions between *Sphagnum* and vascular plants exert a strong influence on the carbon accumulation rate in peatlands (Malmer et al. 2003), and therefore need to be taken into account in future predictions on the response of these systems to climatic changes.

Appendix 2A: Analytical details of the model

The competition effect of *Sphagnum* on vascular plants exhibiting a type I switch (Fig. 4a) is modeled by the following term:

$$c_{BS}S \tag{I}$$

in which S is the density of *Sphagnum* (units: $g_S \cdot m^{-2}$) and c_{BS} the type I coefficient, representing the relative amount of vascular plant biomass that cannot grow because of the acidifying and substrate-temperature decreasing effect of *Sphagnum* ($g_B \cdot g_S^{-1} \cdot yr^{-1}$). Now, both *Sphagnum* and vascular plants are affected by competition that induces type III switches, which can be converged in the following term in the equation for vascular plant growth:

$$\frac{\kappa_{BS}BS}{H_B + B} \tag{II}$$

Where B is the vascular plant density ($\text{g}_B \cdot \text{m}^{-2}$), κ_{BS} is the type III coefficient for vascular plants, representing the relative amount of vascular plant biomass that cannot grow because of the overgrowing (light) and submergence stimulating (water table) and available nutrient decreasing effect of *Sphagnum* ($\text{g}_B \cdot \text{g}_S^{-1} \cdot \text{yr}^{-1}$). H_B is the type III half-saturation density for vascular plants ($\text{g}_B \cdot \text{m}^{-2}$).

In similar vein, we derive the type III competition term affecting *Sphagnum* growth:

$$\frac{\kappa_{SB} SB}{H_S + S} \quad (\text{III})$$

With κ_{SB} being the type III feedback coefficient for *Sphagnum* ($\text{g}_S \cdot \text{g}_B^{-1} \cdot \text{yr}^{-1}$), and H_S the half saturation density ($\text{g}_S \cdot \text{m}^{-2}$), respectively.

For low atmospheric nutrient input rates, it is reasonable to assume that *Sphagnum* intercepts all nutrients from atmospheric deposition (Malmer et al. 2003). Assuming a constant deposition rate, we describe *Sphagnum* development by logistic growth. The lateral expansion of *Sphagnum* is modeled as a diffusion term (Okubo 1989; cf. Rietkerk et al. 2002; Rietkerk et al. 2004a). Including all terms in the equations for vascular plants, nutrients and height of the water table that were derived in Rietkerk et al. (2004a), we have obtained the following model:

$$\frac{\partial S}{\partial t} = r_s S \left(1 - \frac{S}{S_{\max}} \right) - \frac{\kappa_{SB} SB}{H_S + S} + D_S \left(\frac{\partial^2 S}{\partial x^2} + \frac{\partial^2 S}{\partial y^2} \right) \quad (\text{IV})$$

$$\frac{\partial B}{\partial t} = r_B [N] f(h(H)) B - dB - bB - c_{BS} S - \frac{\kappa_{BS} BS}{H_B + B} + D_B \left(\frac{\partial^2 B}{\partial x^2} + \frac{\partial^2 B}{\partial y^2} \right) \quad (\text{V})$$

$$\frac{\partial [N]}{\partial t} = \frac{N_{in} - u[N] B f(h(H)) + \frac{dB}{r_B} - r_N N - [N] \theta \frac{\partial H}{\partial t}}{H \theta} + D_N \left(\frac{\partial^2 [N]}{\partial x^2} + \frac{\partial^2 [N]}{\partial y^2} \right) + \frac{k}{\theta} \left(\frac{\partial}{\partial x} \left([N] \frac{\partial H}{\partial x} \right) + \frac{\partial}{\partial y} \left([N] \frac{\partial H}{\partial y} \right) \right) \quad (\text{VI})$$

$$\frac{\partial H}{\partial t} = \frac{p}{\theta} - \frac{t_v B f(h(H))}{\theta} - \frac{e f(h(H))}{\theta} + \frac{k}{\theta} \left(\frac{\partial}{\partial x} \left(H \frac{\partial H}{\partial x} \right) + \frac{\partial}{\partial y} \left(H \frac{\partial H}{\partial y} \right) \right) \quad (\text{VII})$$

in which r_s is a *Sphagnum* growth parameter (yr^{-1}), S_{\max} is the carrying capacity of *Sphagnum* ($\text{g}_S \cdot \text{m}^{-2}$), $[N]$ is the nutrient concentration in the groundwater ($\text{g}_N \cdot \text{m}^{-3}$), H is the hydraulic head (m), t is time (yr), r_B is the vascular plant growth parameter ($\text{m}^3 \cdot \text{g}_N^{-1} \cdot \text{yr}^{-1}$), d is the vascular plant mortality rate (yr^{-1}), b is the rate of nutrient loss from the landscape (yr^{-1}), N_{in} is the nutrient input rate ($\text{g}_N \cdot \text{m}^{-2} \cdot \text{yr}^{-1}$), u is a plant uptake parameter ($\text{m}^3 \cdot \text{g}_B^{-1} \cdot \text{yr}^{-1}$), r_N is a nutrient loss parameter (yr^{-1}), p is the precipitation rate ($\text{m} \cdot \text{yr}^{-1}$), θ is soil porosity (dimensionless), t_v depicts the vascular plant transpiration rate ($\text{m}^3 \cdot \text{g}_B^{-1} \cdot \text{yr}^{-1}$), e is an evaporation parameter ($\text{m} \cdot \text{yr}^{-1}$), D_S is the diffusion coefficient for *Sphagnum* biomass ($\text{m}^2 \cdot \text{yr}^{-1}$), D_B is the diffusion coefficient for

vascular plant biomass ($\text{m}^2.\text{yr}^{-1}$), D_N is the diffusion coefficient for nutrients ($\text{m}^2.\text{yr}^{-1}$) and k is the hydraulic conductivity ($\text{m}.\text{yr}^{-1}$). $f(h(H))$ is a dimensionless soil water stress function that is defined as follows:

$$f(h(H)) = 1, \quad H - z \geq h_1 \quad (\text{VIII})$$

$$f(h(H)) = 0, \quad H - z \leq h_2 \quad (\text{IX})$$

$$f(h(H)) = \frac{H - z - h_2}{h_1 - h_2}, \quad h_1 \leq H - z \leq h_2 \quad (\text{X})$$

in which h_1 is the pressure head below which soil water stress occurs (m), h_2 is the rooting depth of vascular plants (m) and z is a reference height (m). All parameter values follow Rietkerk et al. (2004a). To the newly introduced parameters, we assigned the following values: $r_s=0.2$, $S_{max}=800$, $D_S=0.2$, $\kappa_{BS}=0.5$, $c_{BS}=0.1$, $\kappa_{SB}=0.1$, $H_B=800$, $H_S=300$ (Van Breemen 1995; Ohlson et al. 2001). The value of N_{in} is varied for the simulations presented in the figures, values are given in the captions. In model runs simulating vegetation dynamics on a bog slope, water flow was set in one direction (cf. Rietkerk et al. 2004a).

Acknowledgments

The authors thank Wladimir Bleuten and Elena Lapshina for sharing their photographs. Aat Barendregt, Yuki Fujita, Sonia Kéfi, Jasper Van Belle, Ton Verkroost and three anonymous reviewers provided comments that improved the manuscript. The research of MBE and MR is supported by a VIDI grant from the Research Council Earth and Life Sciences of the Netherlands Organization of Scientific Research to MR.



3

Regular surface patterning of peatlands: Confronting theory with field data

Maarten B. Eppinga, Max Rietkerk, Wiebe Borren,
Elena D. Lapshina, Wladimir Bleuten
& Martin J. Wassen

Ecosystems 11: 520-536 (2008)

Regular surface patterning of peatlands: confronting theory with field data

Abstract

Regular spatial patterns of sharply bounded ridges and hollows are frequently observed in peatlands and ask for an explanation in terms of underlying structuring processes. Simulation models suggest that spatial regularity of peatland patterns could be driven by an evapotranspiration-induced scale-dependent feedback (locally positive, longer-range negative) between ridge vegetation and nutrient availability. The sharp boundaries between ridges and hollows could be induced by a positive feedback between net rate of peat formation and acrotelm thickness. Theory also predicts how scale-dependent and positive feedback drive underlying patterns in nutrients, hydrology and hydrochemistry, but these predictions have not yet been tested empirically. The aim of this study was to provide an empirical test for the theoretical predictions; therefore we measured underlying patterns in nutrients, hydrology and hydrochemistry across a maze-patterned peatland in the Great Vasyugan Bog, Siberia. The field data corroborated predicted patterns as induced by scale-dependent feedback; nutrient concentrations were higher on ridges than in hollows. Moreover, diurnal dynamics in water table level clearly corresponded to evapotranspiration and showed that water levels in two ridges were lower than in the hollow in between. Also, the data on hydrochemistry suggested that evapotranspiration rates were higher on ridges. The bimodal frequency distribution in acrotelm thickness indicated sharp boundaries between ridges and hollows, supporting occurrence of positive feedback. Moreover, nutrient content in plant tissue was most strongly associated with acrotelm thickness, supporting the view that positive feedback further amplifies ridge-hollow differences in nutrient status. Our measurements are consistent with the hypothesis that the combination of scale-dependent and positive feedback induces peatland patterning.

Introduction

Spatial surface patterning is one of the most striking features of boreal peatland ecosystems, and a considerable amount of attention has been paid to this phenomenon in the peatland literature of the last century (Foster et al. 1983; Charman 2002). Analysis of spatial peatland patterns provides a means for testing hypotheses about underlying structuring processes (Belyea and Lancaster 2002). The recently established view of peatlands as complex adaptive systems has emphasized the need for a better understanding of these structuring processes to predict the response of peatland ecosystems to external forcing such as global climate change (Levin 1998; Belyea and Malmer 2004; Belyea and Baird 2006; Chapter 2).

A common feature of peatlands is the spatially irregular patterning of distinct microforms (hummocks and hollows, characteristic spatial scale 10^1 - 10^2 m², Belyea and Clymo 2001). Hummocks are elevated above hollows because hummocks have a thicker acrotelm, which is an aerobic layer consisting of active peat-forming vascular plants and mosses, together with slightly decomposed litter. Hollows have a much thinner acrotelm or no acrotelm at all. Below the acrotelm the water-saturated peat layer or catotelm is situated. This means that the acrotelm-catotelm boundary is determined by the seasonal minimum water table (e.g. Holden and Burt 2003). The structuring process that could explain the formation of hummocks and hollows is a positive feedback between net rate of peat formation and acrotelm thickness on slightly elevated, dryer sites, mainly because of increased production of vascular plants (Wallén 1987; Wallén et al. 1988; Belyea and Clymo 2001). Thus, slight differences between more densely vegetated dryer sites and more sparsely vegetated wetter sites may further amplify and lead to spatial patterning of sharply bounded microforms. From here we refer to this process as the positive feedback.

Less common, but still frequently observed, are two types of regular spatial peatland patterning that occur on the mesotope scale (10^4 - 10^6 m², Sjörs 1983; Wallén et al. 1988). The first type comprises merged hummocks forming linear strings alternating with lower and wetter hollows, oriented along the contours of mire slopes. On flat parts of mires the second type of regular patterning is observed; merged hummocks forming ridges that are star or net-like, enclosed by lower and wetter hollows. This study focuses on the latter pattern, which is also referred to as maze patterns (Rietkerk et al. 2004a).

In the Great Vasyugan Bog, Western Siberia, extensive areas with maze patterning occur (Rietkerk et al. 2004a). Characteristic features of maze patterns are the spatial regularity and the sharp boundaries between different vegetation communities occupying ridges and hollows. The positive feedback cannot explain spatial regularity in peatland patterning (Rietkerk et al. 2004a). Instead, recent modeling studies suggest that the spatial regularity of maze patterns could be induced by nutrient accumulation under ridges, which is driven by increased evapotranspiration rates by vascular plants (especially shrubs and trees) that grow on these ridges (Rietkerk et al. 2004a). This structuring process would imply that because of higher evapotranspiration rates, there is a net flow of water and dissolved nutrients toward ridges. Subsequently, the nutrients become trapped on ridges through uptake by vascular plants. So, during their lifespan, vascular plants that grow on ridges accumulate nutrients originating from outside the ridge. Nutrients become available again through mineralization of vascular plant litter, but this only increases nutrient availability on the local scale (within the ridge). Models predict that this local recycling effect outweighs the effect of nutrient uptake, meaning that nutrient concentrations in the mire water under ridges also increase (Rietkerk et al. 2004a; Chapter 2; see appendix 3A for details). Because higher nutrient availability will lead to an increase in vascular plant biomass, this is a self-reinforcing process. This self-reinforcing process has a positive effect on nutrient concentration and plant growth on the local scale (inside the ridge) but a negative effect on a longer range (outside the ridge). From here we refer to this process as the scale-dependent feedback. Although the scale-dependent feedback provides an explanation for the spatial regularity of maze patterns, it cannot explain the sharp boundaries between ridges and hollows as observed in the field (Chapter 2).

So, on the one hand the positive feedback explains the distinct differentiation of the peatland surface into sharply bounded hummocks and hollows, but cannot explain spatial regularity (Table 1). On the other hand, the scale-dependent feedback explains spatial regularity, but cannot explain the sharp boundaries between ridges and hollows (Table 1). Because maze patterns comprise both features, it has been suggested that the positive and the scale-dependent feedback may synergistically govern this type of spatial patterning in peatlands (Chapter 2).

This hypothesis has mainly emerged from simulation modeling, but has not yet been tested empirically. The aim of the present study was to test whether underlying patterns in nutrients and hydrology corroborate the hypothesis that a combination of the positive and the scale-dependent feedback drives spatial surface patterning,

using field data from a maze-patterned peatland. Previous models and other studies provide clear indications of how the maze pattern of ridges and hollows should be related to the associated underlying patterns in nutrients, hydrology and hydrochemistry in case of the occurrence of the two types of feedbacks (see references in Table 1; appendix 3A). Therefore, we measured nutrient concentrations in water and plant tissue, diurnal dynamics in water table level and analyzed mire water chemistry across various transects through a maze-patterned peatland in the Great Vasyugan Bog. By comparing the measurements with the predictions (Table 1), it could then be inferred whether the combination of feedbacks is a likely explanation for maze patterning.

Hypothesized feedback	Expected vegetation pattern	Expected nutrient concentration pattern in water	Expected nutrient concentration pattern in plant tissue	Expected pattern in hydrology (and hydrochemistry)
Acrotelm thickness – Productivity (positive feedback)	Sharply bounded hummock and hollows (Spatial scale: 10^1 - 10^2 m ²) randomly distributed over mire surface ^{1,2,3}	Higher nutrient concentrations under hummocks because of larger decomposition rates ^{1,4}	Higher nutrient content in hummock vegetation because of higher nutrient concentrations in water ^{5,6,7}	Differential submergence rates create small-scale hydraulic gradients, with highest heads under hummocks ^{1,8} (no specific pattern for hydrochemistry)
Evapotranspiration-Nutrient accumulation (scale-dependent feedback)	Hummocks merged to ridges forming regular maze patterns (10^4 - 10^6 m ²), but no sharp ridge-hollow boundaries ^{2,3,4}	Higher nutrient concentrations under ridges because of transport from surroundings ^{2,3,9,10,11}	Higher nutrient content in ridge vegetation because of higher nutrient concentrations in water ^{5,6,7}	Lower water table levels under ridges ^{2,3,4,9,10,11,12} (Higher EC, higher concentration conservative solutes under ridges ^{13,14})

Table 1: Proposed feedbacks that might synergistically govern maze patterning in peatlands, and how the occurrence of these feedbacks in the field would be reflected in underlying patterns in nutrients, hydrology and hydrochemistry. References: 1: Belyea and Clymo (2001) 2: Rietkerk et al. (2004a) 3: Rietkerk et al. (2004b) 4: Chapter 2 (this thesis) 5: Craft et al. (1995) 6: Wassen et al. (1995) 7: Shaver et al. (1998) 8: Ivanov (1981) 9: Reed and Ross (2004) 10: Wetzel et al. (2005) 11: Ross et al. (2006) 12: Frankl and Schmeidl (2000) 13: McCarthy et al. (1993) 14: Bleuten (2001).

Previous studies suggest that the scale-dependent feedback induces a lower water table level under ridges than in hollows, and, because of local recycling effects, higher nutrient concentration in mire water on ridges as compared to hollows (Table

1; appendix 3A). Nutrient enrichment experiments and correlation studies suggest that an increase in nutrient availability also increases nutrient content within plant tissue (Craft et al. 1995; Wassen et al. 1995; Shaver et al. 1998). The scale-dependent feedback would further imply that higher evapotranspiration rates are reflected by both higher electrical conductivity and higher concentration of conservative solutes (chloride, sodium) in the mire water under ridges as compared to hollows (Table 1).

The presence of the positive feedback would imply that cumulative decomposition (i.e. the amount of mass decomposed within the entire acrotelm) increases with acrotelm thickness (Belyea and Clymo 2001). With increasing cumulative decomposition the nutrient availability on ridges is also expected to increase (appendix 3A), so the mire water under ridges would have a higher concentration of nutrients as compared to hollows, and therefore the nutrient content of plant species may be higher when growing on ridges (Craft et al. 1995; Wassen et al. 1995; Shaver et al. 1998). Also, the pressure on the peat at the acrotelm-catotelm boundary increases with acrotelm thickness. With higher pressure, this layer becomes more compressed and the effective pore space decreases (Ivanov 1981; Belyea and Clymo 2001). This means that for a given amount of water input, the water table rise will be larger in microforms with a thicker acrotelm (ridges). As a result, hydraulic gradients could develop that initiate a net water flux from ridges to hollows (Table 1). So, the scale-dependent feedback and the positive feedback would induce similar patterns in nutrient concentration in water and nutrient content of plant tissue, but lead to contradictory hypotheses on patterns in water table level (Table 1).

Material and Methods

Study site

The Great Vasyugan Bog (55-59 °N, 76-83 °E) is the largest undisturbed peat complex in the world, covering an area of more than $5 \cdot 10^4$ km² (Lapshina et al. 2001a). The area is situated at the water divide between the rivers Ob and Irtysh, approximately 200 km northeast of Novosibirsk (Fig. 1a). Permafrost disappeared in this region 11000 years ago, and about 500 years later peat accumulation commenced on the sandy loam mineral sub-soil (Lapshina et al. 2001b). Current climate is typically continental, with a mean monthly temperature ranging between ca. -20 °C and ca. +18 °C (Semenova and Lapshina 2001). The frost-free period in this region lasts 100-120 days, which keeps the growing season relatively short (Semenova and Lapshina 2001). Contrary to most regions in the boreal zone, the precipitation excess is not very large: annual precipitation is 500 mm, whereas the

annual evapotranspiration is 300-500 mm (Semenova and Lapshina 2001). Within this area, the study was carried out on a maze-patterned plain (56°16'-56°20' N, 81°19'-81°36' E), which was accessed by helicopter. Here the current thickness of the peat layer is 3-4 m. During the measurement period from July 28 to July 31 2005, one precipitation event was recorded (on July 29). Averaged over two rain gauges (placed at 1.5 m above the mire surface, accuracy 0.1 mm) rainfall measured 0.9 mm. Mean temperature during this period at the Culym weather station (55°08' N 80°58' E; approximately 130 km from the study site) was 19.6 °C with extreme temperatures ranging from 15.8 °C to 25.0 °C.

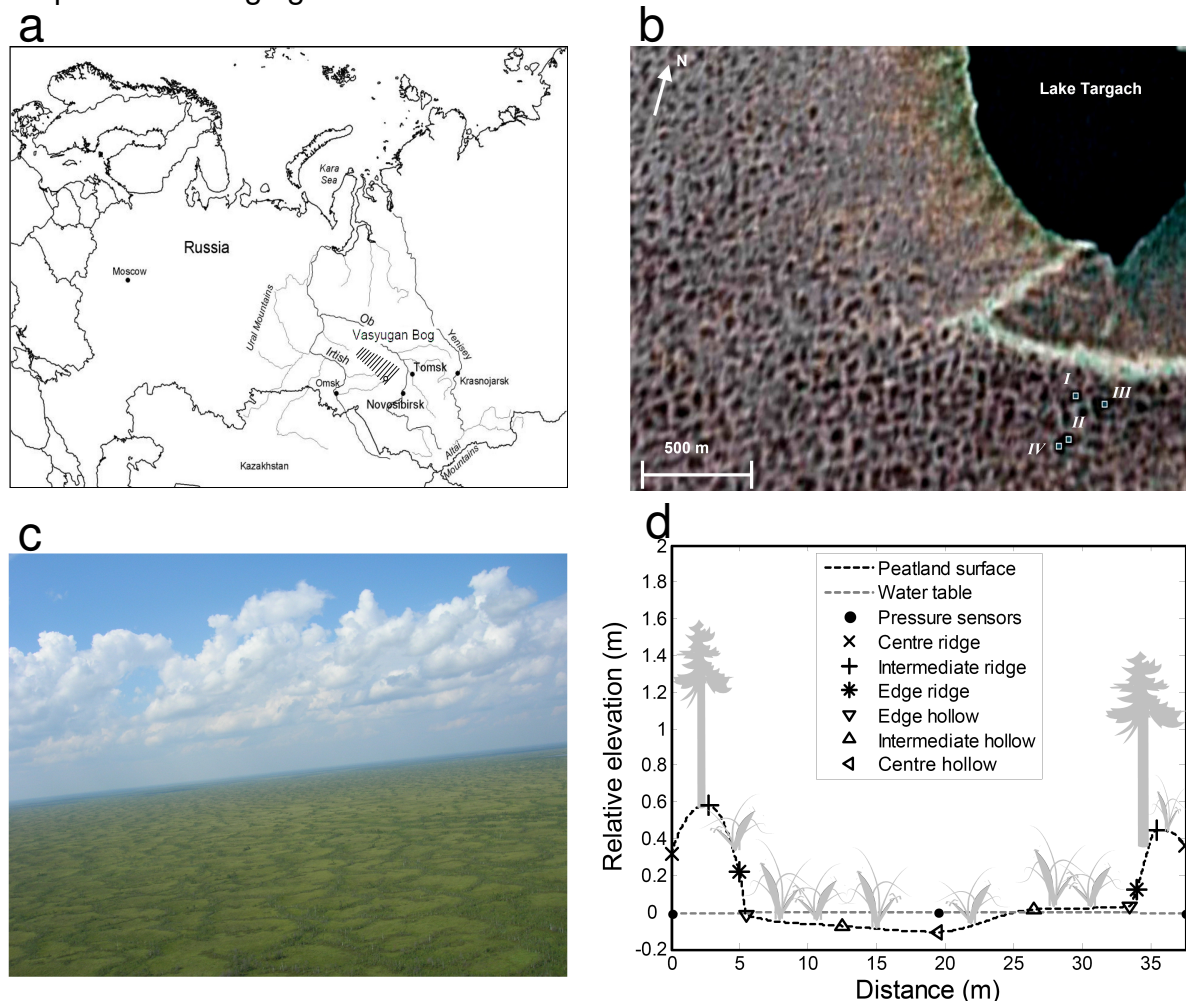


Figure 1: a) Location of the Great Vasyugan Bog, Siberia, indicated by the hatched area. The circle within the hatched area indicates the study site, a maze-patterned plain. b) Satellite image of the study site (accessed via Google Earth, coordinates: 56°16' N, 81°33' E). Roman numerals indicate junctions of the orthogonal transects that were used in the sampling campaign. Hydrological measurements were also carried out along a large North-South (491 m) and East-West transect (791 m), which crossed at point I. c) A photograph of the study site, taken from helicopter. d) Cross-section of transect I; a ridge-hollow-ridge sequence through the maze pattern. Markers indicate measured data (measured on the 28th of July, 2005), whereas dashed lines are shape-preserving interpolations. Elevations are relative to the water level in the hollow (which is set at 0). Vegetation is included as an illustration.

The regularly patterned area comprises approximately 100 km², and is clearly visible on satellite imagery (Fig. 1b) or from helicopter (Fig. 1c). Elevated ridges of widths ranging from 1 m to 15 m form the maze-like structure. The depth of the acrotelm in these ridges is 0.1-0.7 m. Vegetation on the lowest ridges is dominated by *Betula nana*, *Typha latifolia* and *Sphagnum obtusum*, *S. flexuosum*, *S. fallax*, *S. contortum* and *S. majus*. Higher ridges become dominated by *B. pubescens*, *Carex lasiocarpa*, *C. elata* ssp. *omskiana*, *S. warnstorffii* and *S. centrale*. Vegetation at the highest ridges is characterized by *Pinus sylvestris*, *Chamaedaphne calyculata*, *Ledum palustre*, *S. fuscum*, *S. magellanicum*, *S. russowii*, *S. capillifolium* and *S. angustifolium*. A previous study reports for bog ridges in other parts of southern Siberia an average aboveground density of dwarf shrubs and herbs of approximately 500 g.m⁻² (Vasiliev et al. 2001). In our study site, aboveground vascular plant biomass also includes trees. The ridges are embedded in a matrix of waterlogged hollows that have no acrotelm. The width of the hollows ranges from 25 m to 100 m. The vegetation in these hollows is dominated by *C. lasiocarpa*, at an average density of approximately 170 g.m⁻². Other species that frequently occur in hollows were *C. elata* ssp. *omskiana*, *Menyanthes trifoliata*, *Equisetum fluviatile* and the brown mosses *Scorpidium scorpioides* and *Campylium polygamum*. *C. lasiocarpa* is the only vascular plant species that is present in hollows and on all types of ridges.

Field measurements and laboratory analyses

Field measurements were taken along four pairs of two orthogonal transects through the surface pattern. A transect ranged from the middle of one ridge to the middle of the next ridge, so each transect contained the halves of two ridges and the hollow in between. The average transect length was 42 ± 12 m. The two orthogonal transects crossed in the centre of the hollow (centers are marked with I-IV in Fig. 1b). On each ridge, three measurement points were selected: the centre of the ridge, the edge of the ridge and a point in between these two (referred to as “intermediate”). The hollow in between these ridges was sampled on five points: the centre, the edges with the two ridges and a point in between the centre and each edge (“intermediate” class). Hence, one transect consisted of $3_{\text{ridge}}+5_{\text{hollow}}+3_{\text{ridge}}=11$ measurement points. Because the centre of the hollow was part of both orthogonal transects, the total number of measurement points for a pair of transects was 21. So in total, this would add up to $4*21=84$ measurement points. However, one of the ridges in the survey was too narrow to perform three measurements; therefore two measurement points were chosen instead (so $n_{\text{ridge}}=47$, $n_{\text{hollow}}=36$, $n_{\text{total}}=83$).

In the first transect, diurnal dynamics in water table level were measured at three points in a North-South transect, containing two ridges and the hollow in between. The position of the centre of this hollow is indicated with I in Fig. 1b. Total length of this three point transect was 37.5 m (Fig. 1d). At each point, water level dynamics were recorded with water pressure sensors (air pressure compensated Keller: accuracy 0.1 mm).

In order to have access to the mire water under ridges at the other measurement points, piezometers (0.3 m) were installed in small excavations. The piezometer mantles were covered with a filter (Eijkelkamp Agrisearch Equipment, The Netherlands). From these wells, water samples were taken and also distance to the mire surface was determined (see below). Because the water level in the hollows was at the mire surface, installing piezometers was not necessary for these measurement points.

On each measurement point we measured pH (WTW-pH96 with Ag/AgCl electrode), electrical conductivity (EC₂₅) and temperature (WTW-LF91) directly in the mire water (cf. Wassen and Joosten 1996). Alkalinity ([HCO₃⁻]) of the mire water was determined through acidimetric titration (Aquamerck alkalinity field set). We also determined the distance between the mire surface level and the water table (DWT). We measured the height where the hollow surface was strong enough to carry the probe of a sounding device, and this height was taken as the surface level. Within ridges, the water level was measured with the sounding device, and subsequently DWT was determined by eye, using the depth scale of the sounding device. The surface of the mire showed small-scale variability, so DWT was determined by the average value of this distance for three randomly selected points within a 0.5 m radius of the measurement point. The yearly minimum water level in this area is most often reached in August (Semenova and Lapshina 2001). Because the measurements took place at the last days of July, we think that DWT was close to the yearly lowest water table and therefore an appropriate estimate for the thickness of the acrotelm of the ridges.

At each measurement point a mire water sample was taken for laboratory analyses. Water samples were stored in polyethylene tubes that were rinsed with mire water. Within 8 hours, half of each water sample was acidified with 5 M HNO₃ (0.025 ml.ml⁻¹), the other half with 5 M H₂SO₄ (0.025 ml.ml⁻¹). After centrifugation in the laboratory, the HNO₃ acidified samples were analyzed using an Inductively Coupled Plasma

technique (ICP-OES), and the H₂SO₄ acidified water samples were analyzed for major ions using colorimetric titration (Auto-Analyzer). Inorganic nitrogen concentrations were calculated as $N_{\text{inorganic}} = N [\text{NO}_3^- + \text{NH}_4^+]$.

Furthermore, around each measurement point we harvested 10 healthy-looking shoots of *C. lasiocarpa*, the only vascular plant species that was present on all ridges and in hollows. In the laboratory, samples were dried for one week at 70 °C, weighed and ground. A subsample of 5-10 mg was used to determine C and N concentrations in the tissue, using a Dynamic Flash Combustion technique. Another subsample of ca. 125 mg was taken and digested in 2.5 ml of mixed acid consisting of 12.0 M HClO₄ and 14.5 M HNO₃ (mixing ratio 3:2), and 2.5 ml of 27.3 M HF. Then, the samples were kept in closed Teflon jars at 90 °C for 12 hours. Afterwards the lids were removed and the jars were heated to 160 °C for 8 hours. Subsequently 25 ml of 1.0 M HNO₃ was added, the jars were closed again and kept at 90 °C for 18 hours. The remaining solution was then used to determine P and K content of the plant tissue using the ICP-AES technique mentioned above.

The type of nutrient limitation was subsequently determined with a method based on N:P, N:K and K:P ratio in the plant tissue (Wassen et al. 2005). Critical values for these ratios were derived in Wassen et al. (2005); N:P ratio > 16 determines P-limitation, N:P ratios < 13.5 indicate N-limitation, and values in between, N and P co-limitation. N/P co-limitation means that there is no clear limitation either by N or P alone. (Co)-limitation by K occurs at N:K ratios > 2.1 or K:P ratios > 3.4 (Wassen et al. 2005).

Water level measurements were also made on a larger spatial scale. Therefore the previously described North-South transect was extended both to the North and the South to a total transect length of 491 m (NS) and perpendicular to that (crossing point I in Fig. 1b) an East –West oriented transect (EW) of 718 m length. The average wavelength of the pattern (measured as the length of a ridge-hollow sequence) did not differ for the NS and EW directions (NS: 51 ± 20 m EW: 57 ± 17 m, One-way ANOVA: $F_{1,19} = 0.543$ $p = 0.47$). Gauges were placed in each hollow and in each ridge along the transects (26 gauges along the EW transect, 21 along the NS transect) for measurement of the water level in a 0.2 – 0.4 m deep pit with a ruler (accuracy: 1 mm). Because this method is not as accurate as using water pressure sensors (that we used in small-scale transect I), the large-scale transect data could only identify large-scale gradients, rather than quantifying water level differences

between neighboring ridges and hollows. Gauge readings were made during three days (in the afternoon).

In order to evaluate the water level variation the water pressure sensors and gauges were tightly fixed to a 4 m long PVC tube founded in the mineral soil below the peat layers in order to secure the vertical position during the recording period. The relative elevations of gauges and sensors were determined once with a theodolite (Wild), the vertical position of which was stabilized by extending the tripod with three PVC rods (2 m) firmly pushed into the peat.

Comparisons and statistical treatment

First, we analyzed whether the surface pattern of our study site was indeed characterized by sharp boundaries between ridges and hollows. The occurrence of sharp boundaries between ridges and hollows would result in a distinct two-phase mosaic, whereas gradual transitions between ridges and hollows would result in a surface pattern in which intermediate phases also frequently occur (Chapter 2). Hence, the sharpness of boundaries between ridges and hollows can be assessed by analysis of the frequency distribution of surface elements (vascular plant biomass or acrotelm thickness): occurrence of sharp boundaries would result in a bimodal frequency distribution of surface elements, whereas gradual transitions would result in a unimodal distribution around the mean value of the surface element examined. We used the DWT data as a measure of acrotelm thickness, and tested for bimodality by fitting to the data both a normal distribution function and a bimodal distribution function given by:

$$P = qN[DWT, \mu_1, \sigma_1] + (1 - q)N[DWT, \mu_2, \sigma_2] \quad (I)$$

Where q is a constant between 0 and 1, N is the normal distribution with μ mean and standard deviation σ . Distributions were fitted using the maximum likelihood method (Sokal and Rohlf 1995). Significance of the bimodal distribution as compared to the unimodal model was determined by the log-likelihood ratio (Van de Koppel et al. 2001). For this analysis of the DWT data we used R Project software (Version 2.3.0, R Development Core Team 2006).

For nutrient concentrations and other characteristics of the mire water and for nutrient content of the plant tissue (*C. lasiocarpa*), we first tested for general differences between ridges and hollows. Also, we analyzed the spatial trend through

the peatland surface pattern, using an ordinal scale of six classes ranging from the ridge-centre to hollow-centre. Subsequently, we used electrical conductivity and, in absence of detectable chloride concentrations, the conservative solute sodium (cf. McCarthy et al. 1993) in the mire water as indicators for evapotranspiration rates. Sodium concentration of the mire water is a suitable indicator for evapotranspiration rate because adsorption processes usually do not influence it, and the amount of sodium uptake by plants is small (McCarthy et al. 1993; Bleuten 2001).

Further statistical analyses were done with the software SPSS (Version 11.0.1, SPSS Inc. 2001). For all comparisons, homogeneity of variances between groups was tested with the Levene test statistic. If variances were homoscedastic at the $\alpha = 0.05$ significance level, differences were tested with one-way ANOVA and in case of more than two groups also a Post Hoc Tukey HSD-test was carried out. Otherwise we turned to the nonparametric Mann-Whitney U test, and in case of more than two groups we performed pair wise Mann-Whitney U tests, and subsequently performed a Bonferroni adjustment.

To reveal the correlation structure in the dataset, we performed a Principal Component Analysis (PCA) using Varimax rotation. For this PCA, the hydrochemistry variables and the nutrient variables measured in plant tissue were tested for skewness. If $|\text{skewness}| > 1$ for a certain variable, it was log-transformed to approximate a normal distribution. Subsequently, all variables were standardized to zero mean and unit variance. The scores for each measurement point on the components extracted with the PCA were obtained using regression.

Results

Sharpness of boundaries within the surface pattern

The Distance to the Water Table data (DWT, indicating acrotelm thickness) showed a bimodal distribution (Fig. 2; $\chi^2=147.307$, degrees of freedom= 3, $p < 0.001$). Observations were either close to a positive acrotelm thickness around 0.43 m, which is the ridge state, or close to a negative acrotelm thickness (meaning that the water table was above the peatland surface) around -0.05 m, which is the hollow state. Despite the fact that edges of ridges and hollows were strongly represented in the dataset (31 out of 83 measurement points; 93 out of 249 DWT observations), the data contained relatively few observations of intermediate acrotelm thickness (Fig. 2).

This bimodality in the frequency distribution of acrotelm thickness corroborates the occurrence of sharp boundaries between ridges and hollows.

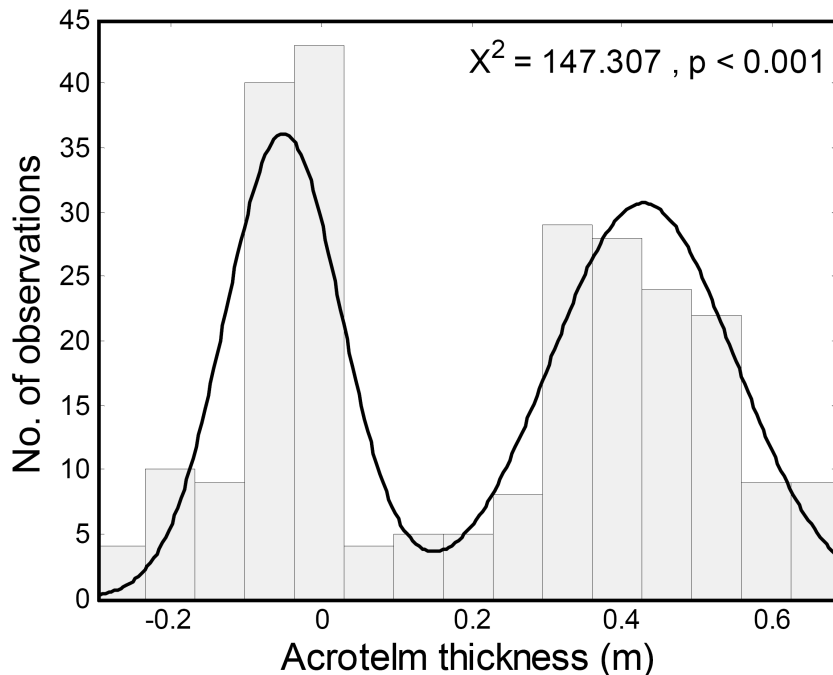


Figure 2: Grey bars show the frequency distribution of measured acrotelm thickness across a maze-patterned plain in the Great Vasyugan Bog, Siberia. Note that negative values of acrotelm thickness indicate that the water table was above the peatland surface. The full black line shows a bimodal fit: $P = qN[DWT, \mu_1, \sigma_1] + (1 - q)N[DWT, \mu_2, \sigma_2]$, where q is a constant between 0 and 1, N is the normal distribution with μ mean and standard deviation σ . (Parameter values: $q = 0.43$, $\mu_1 = -0.05$, $\sigma_1 = 0.08$, $\mu_2 = 0.43$, $\sigma_2 = 0.12$) Significance of the bimodal distribution as compared to the unimodal model was determined by the log-likelihood ratio. The bimodal distribution of acrotelm thickness indicates sharp transitions between ridges and hollows within the surface pattern.

Patterns in nutrients

Concentrations of nitrogen (N), phosphorus (P), and potassium (K) were higher in mire water under ridges than in hollows (Table 2). P concentrations showed the largest difference between ridges and hollows. Observing the spatial trend, there was a sharp decrease in N, P and K concentrations at the ridge-hollow interface (Fig. 3).

Both N and P content were higher in *C. lasiocarpa* shoots growing on ridges (Table 2). N:P ratios revealed that plant growth in the hollows was N/P co-limited at the edge of the hollows, and P-limited at larger distance from the ridge (Fig. 3). Growth on the ridges was N/P co-limited (Fig. 3). For P, there was a significant decline in tissue content within the ridge (from the centre to the edge, Fig. 3).

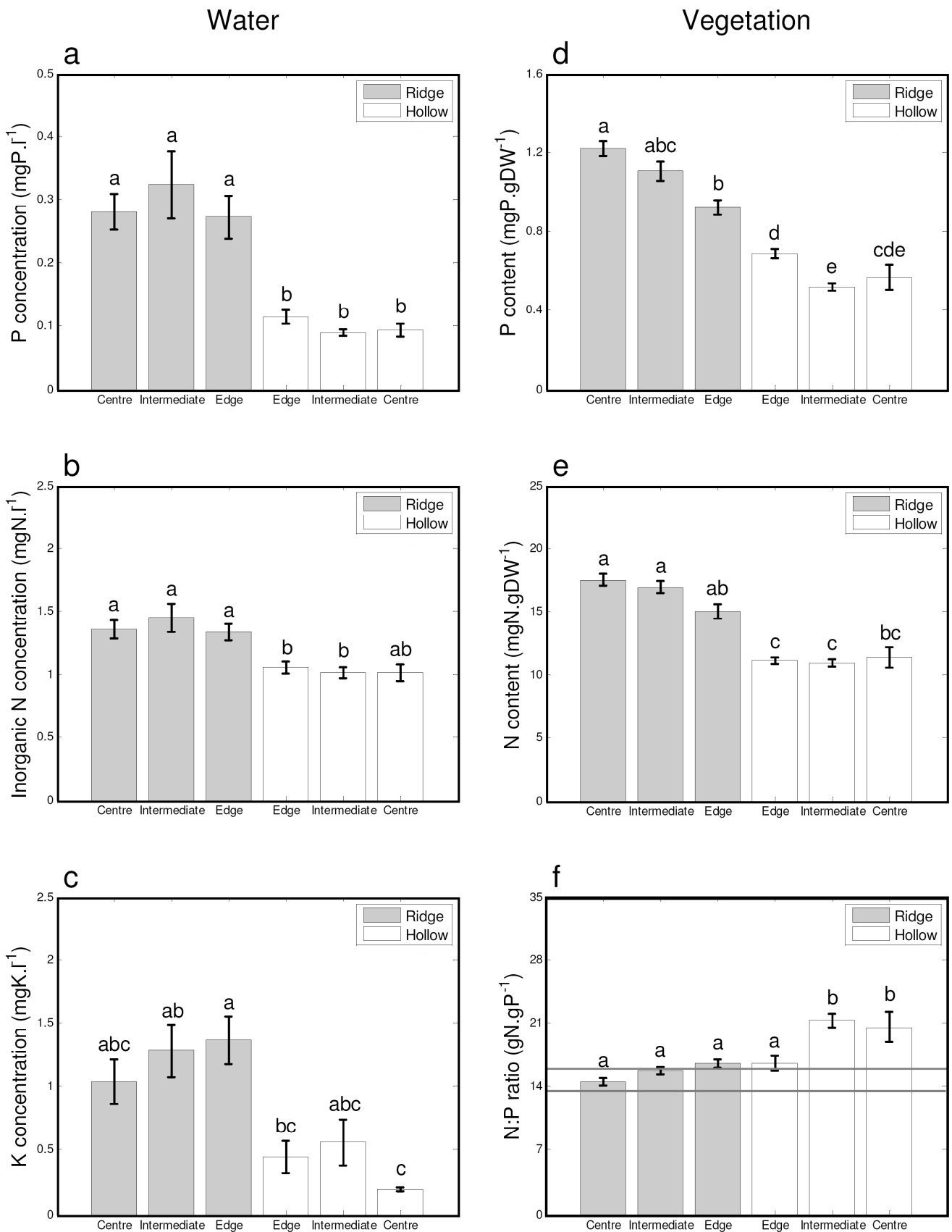


Figure 3: Nutrient concentrations measured in mire water and vegetation tissue (*Carex lasiocarpa*) of a maze-patterned plain in the Great Vasyugan Bog, Siberia. Error bars show ± 1 standard error. Bars with the same letter do not differ at the $p=0.05$ level. (a) The spatial trend in mire water phosphorus concentration shows a sharp decline at the ridge-hollow interface. (b) Inorganic nitrogen concentration shows a similar pattern, but relative

differences between ridges and hollows are smaller. (c) Potassium concentration shows high variation throughout the pattern, but a sharp decline in concentration at the ridge-hollow interface similar to phosphorus and inorganic nitrogen. (d) The spatial trend in phosphorus content of the vegetation tissue reveals a significant difference between the centre and the edge of the ridges. (e) The spatial trend in nitrogen reveals a similar pattern as phosphorus content. (f) Nutrient ratios in the plant tissue show that the ridge and the edge of the hollow are N/P co-limited, the intermediate and centre hollow classes are P-limited. Above the dashed line (N:P = 16), plant growth is P limited. Below the dotted line (N:P = 13.5), plant growth is N limited. In between the dotted and the dashed line, N/P co-limitation occurs.

For both N and P, there was a sharp decrease in tissue content at the ridge-hollow interface. P content was higher at the edge of the hollow as compared to the intermediate hollow class, which led to a similar N:P ratio on the edge of the hollow as compared to the ridge vegetation (but both N and P content were lower at the edge of the hollow as compared to the ridge). Analysis of the N:K and P:K ratios in the plant tissue revealed that growth was not (co)limited by K.

Patterns in hydrology

In the three-point transect, recorded water levels in both ridges were consistently lower than in the hollow (on average 5 mm, Fig. 4). The diurnal vertical dynamics in water level of both the hollow and the ridges corresponded to evapotranspiration, which was greatly reduced or ceased close to sunset (Fig. 4). The average evapotranspiration rate on ridges was estimated to be $9.1 \pm 2.3 \text{ mm}\cdot\text{d}^{-1}$ (see appendix 3B for calculations and further analyses of diurnal water table dynamics). Close to sunset, the daytime evapotranspiration was first replenished in the hollow (Fig. 4). During the night, there was a consistent rise of the water table in both ridges by advection from the hollow into the ridges (Fig. 4). The potential influxes of the main limiting nutrients into ridges were estimated to be $0.7 \pm 0.3 \text{ mgP}\cdot\text{m}^{-2}_{\text{ridge}}\cdot\text{d}^{-1}$ and $6.9 \pm 2.6 \text{ mgN}\cdot\text{m}^{-2}_{\text{ridge}}\cdot\text{d}^{-1}$ (appendix 3B). The trend of the head gradient in E-W direction was almost constant over time ($262 \cdot 10^{-7}$), indicating a steady flow in western direction (Fig. 5). With a hydraulic conductivity of the 'plant layer' (that is the active plant and litter layer in the hollows) of $548 \text{ m}\cdot\text{d}^{-1}$ (Borren and Bleuten 2006) and thickness of the 'plant layer' of 0.5 m the average westward water flux was approximately $0.007 \text{ m}^3\cdot\text{d}^{-1}\cdot\text{m}^{-1}$ across the flow direction. The hydraulic gradient in E-W direction was not smooth. Water level jumps seemed to occur at several points along the EW transect, coinciding with the occurrence of ridges (Fig. 5). This may indicate that water was dammed up at the ridges because of their lower hydraulic conductivity as compared to hollows (e.g. Swanson and Grigal 1988; Couwenberg and Joosten 2005). It is important to note, however, that the precision of our measurements on the large-scale transects was not high enough to confirm water

ponding in front of ridges. The gradient in NS direction was much smaller, decreasing in three days from $53 \cdot 10^{-7}$ to $42 \cdot 10^{-7}$ (data not shown), but this gradient was too small to enable conclusions about the general direction of water flow in NS direction.

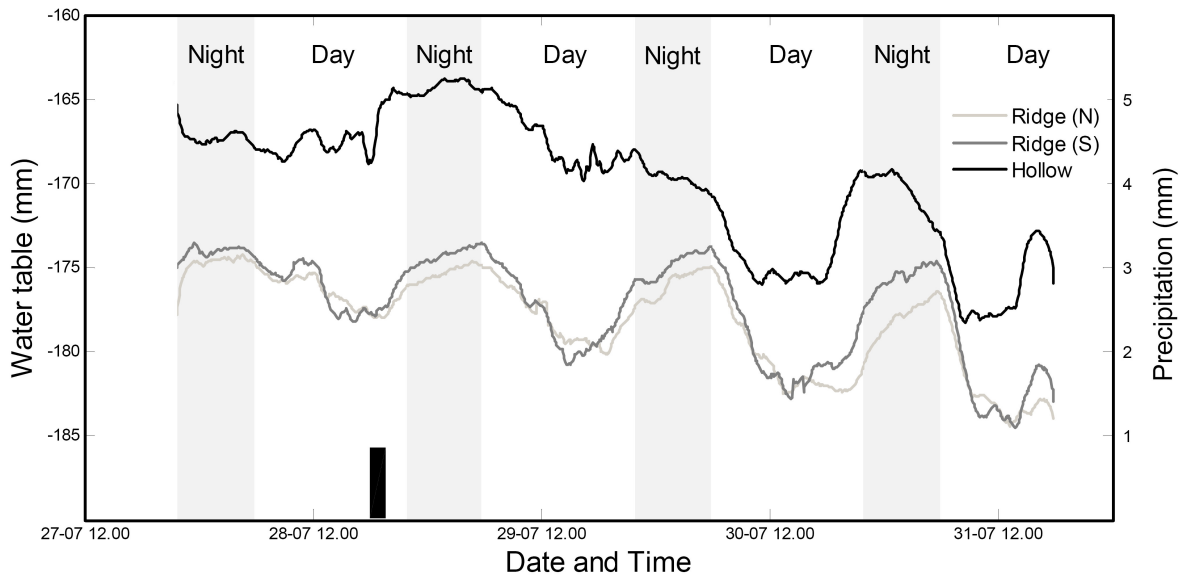


Figure 4: Diurnal dynamics in water table level for two ridges and the hollow in between, situated in a maze-patterned peatland in the Great Vasyugan Bog, Siberia. Water levels are measured relative to an arbitrary reference height. Grey areas show the period between sunset and sunrise (data from the Culym weather station). The higher water table in hollows indicates a continuous water flow towards the ridges. During the day inflow into the ridges is overcompensated by evapotranspiration losses. The transect is oriented in North-South direction. The distance between the northern (N) and southern (S) ridge is 37.5 m. The hollow measurement point is indicated as point I in Fig. 1b. The black bar indicates the occurrence of the only precipitation event (0.9 mm) during the study period.

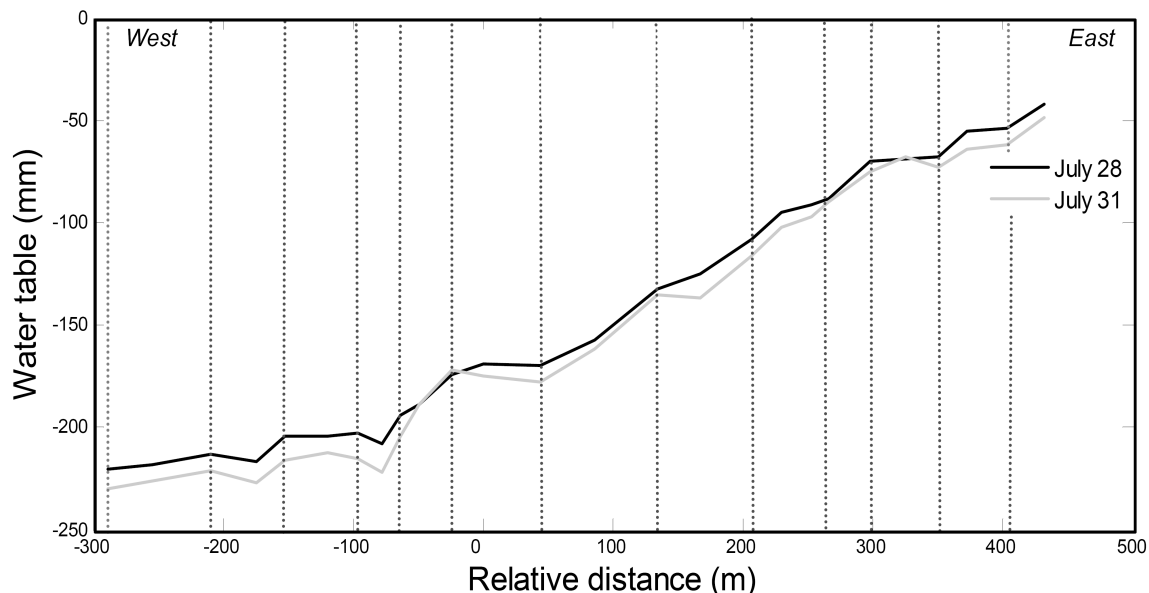


Figure 5: Measured water table level in a 791 m long transect through a maze-patterned peatland in the Vasyugan Bog, Siberia. Distance = 0 corresponds with point I in Fig. 1b. The transect is oriented in East-West direction. The vertical dotted lines indicate the occurrence of ridges. The small head gradient ($262 \cdot 10^{-7}$) indicates water flow in Westward direction. This head gradient was fairly constant during the measurement period (28-31 July 2005).

Patterns in hydrochemistry

The hydrochemistry of the mire water under ridges significantly differed from that under hollows (Table 2). In general mire water under ridges was characterized by a lower pH, temperature and alkalinity and higher concentrations of the solutes examined (Table 2). Also the indicators for evapotranspiration rates, electrical conductivity (EC) and sodium (Na), were higher in the mire water under ridges than that in hollows (Table 2).

Variable	Ridge (n=47)	Hollow (n=36)	Test statistic	p - value
Water (mg.l⁻¹)				
DWT (cm)	41 (13)	-7 (6)	U <0.001	< 0.001
PH (-)	4.93 (0.83)	5.64 (0.36)	U = 344	< 0.001
HCO ₃ ⁻ (mmol.l ⁻¹)	0.25 (0.16)	0.34 (0.08)	U = 599	0.017
EC (μS.cm ⁻¹)	53 (14)	48 (8)	U = 632	0.049
Temperature (°C)	16.76 (3.17)	21.63 (2.24)	U = 171	< 0.001
N _{inorg.}	1.38 (0.34)	1.03 (0.17)	U = 247	< 0.001
P	0.29 (0.16)	0.10 (0.04)	U = 67	< 0.001
Al	0.26 (0.15)	0.06 (0.03)	U = 41	< 0.001
Ca	6.15 (2.03)	5.39 (0.88)	U = 483	0.001
Fe	0.72 (0.48)	0.29 (0.12)	U = 106	< 0.001
K	1.23 (0.76)	0.46 (0.59)	F _{1,81} = 25	< 0.001
Mg	2.77 (0.56)	2.32 (0.29)	U = 377	< 0.001
Mn	0.33 (0.36)	0.11 (0.08)	U = 264	< 0.001
Na	1.55 (0.32)	1.35 (0.28)	F _{1,81} = 8.7	0.004
S	1.13 (0.15)	0.96 (0.09)	U = 302	< 0.001
Si	1.62 (0.76)	0.85 (0.14)	U = 104	< 0.001
Vegetation (mg.g⁻¹)				
P	1.05 (0.25)	0.60 (0.12)	U = 33	< 0.001
N	16.49 (2.29)	11.05 (1.11)	U = 35	< 0.001
K	11.18 (2.45)	8.89 (0.96)	U = 176	< 0.001
C	454 (19)	462 (18)	F _{1,81} = 4.1	0.047

Table 2: Measured values of water and vegetation variables on ridges and hollows of a maze-patterned plain in the Great Vasyugan Bog, Siberia. Water variables have subscript *aq*, and are depicted in mg.l⁻¹ unless indicated differently. Values of the vegetation variables have subscript *veg*, and are given in mg.g⁻¹. Standard deviations are given between brackets. DWT means distance from the peatland surface to the water table. The F-statistic is presented for comparisons with one-way ANOVA, the U-statistic is presented for comparisons with the Mann-Whitney U-test

Correlation structure

The Principal Component Analysis revealed four components, which together explained more than 75 % of the variance in the data (Table 3). The first component (indicated I in Table 3, explaining 29.3 % of the total variance) showed that higher nutrient concentrations in the plant tissue were associated with larger DWT, lower temperature, lower alkalinity and lower pH, the latter four variables corresponding to

the hollow-ridge gradient. The second component (explaining 21.3 % of the total variance) revealed that concentrations of the nutrients N, P and K in the mire water were positively correlated with each other and also with other ions, including the conservative solute Na. The third component (explaining 13.3 % of the total variance) indicated that in the dataset, higher concentrations of the base cations Ca and Mg were positively correlated with each other, and also with Mn concentration in the mire water. Finally, the fourth component (explaining 12.5 % of the total variance) revealed that higher EC values of the mire water were associated with lower C content of the plant tissue.

Variable	I	II	III	IV
Cumulative variance explained (%)	29.3	50.6	63.9	76.4
N_{veg}	0.84	0.35	0.10	-0.03
P_{veg}	0.83	0.32	0.19	0.21
DWT	0.82	0.35	0.27	0.03
Temperature (°C)_{aq}	-0.81	-0.21	-0.01	-0.33
pH_{aq}	-0.72	-0.13	0.32	-0.22
K_{veg}	0.68	0.29	0.07	0.32
Al_{aq}	0.64	0.54	0.31	0.15
HCO₃_{aq}	-0.63	-0.09	0.53	-0.11
Si_{aq}	0.61	0.46	0.02	0.47
K_{aq}	0.26	0.84	0.14	0.07
Na_{aq}	0.16	0.72	-0.15	0.35
N_{aq}	0.33	0.72	0.14	0.03
P_{aq}	0.56	0.71	0.18	0.10
Fe_{aq}	0.34	0.61	0.50	-0.23
Ca_{aq}	-0.10	0.08	0.91	0.13
Mn_{aq}	0.23	0.52	0.65	-0.14
Mg_{aq}	0.35	0.11	0.65	0.46
EC_{aq}	0.11	0.18	-0.05	0.81
C_{veg}	-0.19	0.09	-0.11	-0.72
S_{aq}	0.32	0.56	0.11	0.59

Table 3: Correlation structure in variables measured in water and vegetation samples from a maze-patterned plain in the Great Vasyugan Bog, Siberia. For each variable, loadings on principal components (after Varimax rotation) are given. Highest eigenvector scores for each variable are depicted in bold. DWT means distance from the peatland surface to the water table.

In general, measurement points on ridges had higher scores on both the first and the second PCA component (Fig. 6). More detailed analysis of these scores revealed that the first component most clearly separates ridges from hollows (Fig. 6). Most ridge points (81%) exceeded the maximum score for hollows on the first component (Fig. 6). Although less clear, the second component also enabled separation between ridges and hollows: 25 % of the hollow points had a lower score than the minimum score for ridges (Fig. 6). Also, 15% of the ridges exceeded the maximum score for hollows on the second component (Fig. 6).

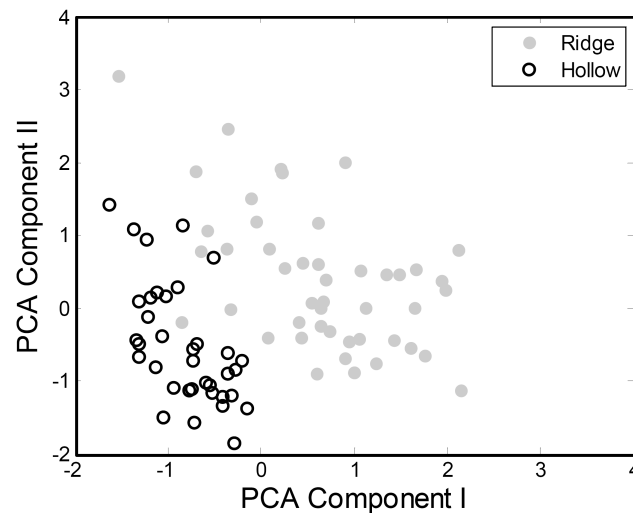


Figure 6: Results of a PCA (using Varimax rotation) of measurement points at ridges and hollows of a maze-patterned plain in the Great Vasyugan Bog, Siberia. The axes of the graph represent the first two components extracted with the PCA. Grey dots indicate ridges, black dots hollows. Ridges generally had higher scores on both components. The first component (reflecting a positive feedback between net rate of peat formation and acrotelm thickness) most clearly distinguished ridges from hollows.

Discussion

Patterns in nutrients, hydrology and hydrochemistry

Our field survey in a maze-patterned peatland corroborated the hypothesis that underlying patterns in nutrients, hydrology and hydrochemistry, together with the maze patterning of the peatland surface, could be induced by a combination of the evapotranspiration-induced scale-dependent feedback and the positive feedback (Table 1; Rietkerk et al. 2004a,b; Chapter 2). The measured diurnal dynamics in water table level clearly showed the effect of evapotranspiration on water table dynamics (Fig. 4; appendix 3B). During the measurement period, the water table under ridges was consistently lower than in the hollow in between. Inside the hollows the plant layer is very open and more or less floating, which results in a high hydraulic conductivity and a nearly horizontal water level. Therefore we expect that

inside hollows, (potential) water flow diverges toward the ridges. This is supported by the observation that during the nights, the water level consistently rose in both ridges, but it lowered in the hollow in between (Fig. 4; appendix 3B). The observed water table dynamics suggest that differences in water table level between ridges and hollows were maintained because losses through evapotranspiration on ridges exceeded the inflow received from hollows during the day (appendix 3B). Similar diurnal dynamics in water table level have been observed in other patterned wetland ecosystems than maze-patterned peatlands, notably in a linearly patterned part of a Swedish bog (Kellner and Halldin 2002), in tree islands and surrounding sloughs in the Florida Everglades (Reed and Ross 2004) and in tree islands and the surrounding swamps in the Okavango Delta (McCarthy et al. 1993). Islands or ridges having lower water tables than their surroundings, and this difference being maintained by higher evapotranspiration rates suggests that there is a continuous water flow from hollows to islands or ridges (Reed and Ross 2004), and thereby advective transport of nutrients and other solutes towards the islands or ridges (Wetzel et al. 2005; Ross et al. 2006).

The second component extracted with the PCA contained information on hydrochemistry, showing that nutrient concentrations in the mire water were associated with other, more conservative solutes such as sodium. This corroborates the notion that higher nutrient concentrations may be the result of higher evapotranspiration rates (McCarthy et al. 1993; Bleuten 2001). Also we measured higher EC of mire water under ridges as compared to hollows. Because the water table in hollows is above the surface, there could be a more direct influence of precipitation on the chemical composition of the water (e.g. Beltman and Rouwenhorst 1994), which could have contributed to the reported differences in mire water chemistry between ridges and hollows. However, nutrient concentration data in the mire water was in compliance with the independently gathered data on nutrient content in plant tissue (Fig. 3), which suggests that the data on hydrochemistry, together with the other lines of data, can indeed be used to identify processes governing maze pattern formation in our study site.

The occurrence of sharp boundaries between ridges and hollows (Fig. 2) corroborated the occurrence of the positive feedback in our study site. Moreover, the first component of the PCA revealed that both N and P content of the plant tissue were negatively correlated with mire water temperature and positively correlated to Distance to the Water Table (DWT). Because DWT indicates the thickness of the

acrotelm, this positive correlation corroborates the notion that enhanced cumulative decomposition could also contribute to the higher nutrient availability on ridges. This first component of the PCA most clearly separated ridges from hollows (Fig. 6), which supports the view that peatland surface patterning may be amplified by positive feedback between net rate of peat formation and acrotelm thickness.

In this study we used N and P content of the plant tissue as an indicator for nutrient availability. Although the nutrient content of the plant tissue is also influenced by the amount of carbon fixation and dry matter production, N and P content has been suggested to be a reliable indicator for nutrient availability (de Wit 1963; Vermeer and Berendse 1983; Wassen et al. 1995; U.S. EPA 2002). In particular P enrichment experiments commonly show that P content of the plant tissue increases with P availability, regardless of the plant growth response (Solander 1983; Verhoeven and Schmitz 1991; Craft et al. 1995). Increased P availability creates the possibility of luxury uptake, meaning that P is stored in vacuoles so that it can be used later (Davis 1991). For nitrogen, similar responses have been observed for N enrichment experiments (Shaver and Melillo 1984; Shaver et al. 1998), although luxury uptake of N is not always observed (Verhoeven and Schmitz 1991). In this study, we compared differences between ridges and hollows by sampling the same plant species (*C. lasiocarpa*) during the same period within the same study site, meaning that these other factors that could possibly influence the nutrient content of plant tissue were kept as similar as possible. Summarizing, we think that nutrient content of the plant tissue is a reliable indicator for nutrient availability within our study site. Based on the different lines of field data presented in this Chapter, the scale-dependent feedback and the positive feedback synergistically driving maze pattern formation seems a promising explanation for the maze-patterned peatland that was studied.

If peatland maze patterns were strongly associated with underlying patterns in nutrients, hydrology and hydrochemistry, one would expect that these underlying patterns could be distinguished from peatlands without regular spatial patterning. Indeed, the measured patterns in nutrients, hydrology and hydrochemistry in a maze-patterned peatland reported in this study are rather different from those reported for other peatland types. First, we found nutrient-richer conditions under elevated sites (ridges), instead of nutrient-poorer conditions (Couwenberg 2005, and references therein). Second, we found that water flow was directed from hollows to ridges, instead of the other way around (Ivanov 1981; Belyea and Clymo 2001). Third, our

hydrological measurements do not support observations that evapotranspiration rates are higher in hollows (Romanov 1968; Edom 2001; Belyea 2007).

On ridges, the presence of vascular plants may increase transpiration rates (Frankl and Schmeidl 2000), meaning that the evapotranspiration rate from ridges could exceed the potential open water evaporation rate (Souch et al. 1998; Andersen et al. 2005). On the other hand, lateral advection of warm air could induce a larger-scale oasis effect enhancing evaporation rates from hollows so that it also could exceed the potential open water evaporation rate (Price and Maloney 1994). Even without a clear difference in evapotranspiration rate between ridges and hollows, however, there could have been a net flux of water and nutrients from ridges to hollows during our study period. The reason for this is that our study was carried out in a period of net water loss (Fig. 4; appendix 3B). When the same amount of water is lost from ridges and hollows through evapotranspiration, the drop in water level is larger in the ridges than in the hollows because of their smaller effective porosity (Ivanov 1981; Belyea and Clymo 2001). It is important to note, however, that there is likely to be strong seasonal variation in the partitioning of evapotranspiration losses between evaporation and transpiration (Admiral and Lafleur 2007): especially in wet periods with precipitation excess (spring and fall), evaporation may be greatest. The differences in effective porosity, together with a higher evaporation rate in hollows, could therefore create a reversed net flux of water and nutrients (from ridges toward hollows) during spring and fall.

Summarizing, the diurnal dynamics of the water table as observed in this study (Fig. 4), may substantially differ from other parts of the season. Nevertheless, the hypothesized mechanism driving pattern formation concerns the spatial redistribution of nutrients stimulating vascular plant growth on ridges and inhibiting vascular plant growth outside ridges. This implies that a net flux of water and nutrients only amplifies patterning during periods of vascular plant growth, in which nutrients are trapped by the vascular plants (appendix 3A). During other parts of the season, this flux may be reversed, but this will not affect vascular plant growth and therefore it is not expected to exert a strong effect on the formation and development of maze patterning.

Alternative theories of peatland patterning

Our hypothesis that the scale-dependent feedback and the positive feedback may synergistically drive maze pattern formation in peatlands contributes to a

considerable body of theory on peatland pattern formation, which has mainly focused on the formation of linear patterns on slopes. It is interesting, however, to examine whether these two types of spatially regular patterning may be associated with similar mechanisms. Therefore, we will now discuss our field data with respect to theories and hypotheses on linear patterning as well.

For example, our data suggested that the ridges might dam the water upstream (Fig. 5), caused by the lower hydraulic conductivity of the ridges. It has been hypothesized that differences in hydraulic conductivity between ridges and hollows can contribute to linear pattern formation in systems with unidirectional water flow (i.e. on mire slopes, Foster et al. 1983; Glaser 1992b; Couwenberg 2005), but not maze pattern formation on flat parts of mires (Couwenberg and Joosten 2005). Interestingly, we did find a larger-scale hydraulic gradient over the EW transect in our study site (Fig. 5), which suggests a unidirectional water flow in western direction. So, we could distinguish two types of water flow in our study site; smaller-scale water flow directed to the ridges that is possibly driven by evapotranspiration (Fig. 4) and unidirectional water flow in western direction on a regional scale (Fig. 5). This regional gradient over the EW transect was 262×10^{-7} (Fig. 5). Although this regional gradient is similar to those seen in other patterned wetlands such as the Florida Everglades (Noe et al. 2001), it was relatively weak as compared to the smaller-scale gradient over our three-point transect ($\sim 2500 \times 10^{-7}$), which might explain the maze-pattern formation in our study site instead of linear patterning. With increasing slope it seems likely that the regional water flow would become the dominant process, leading to the formation of linear patterns. This notion stresses the importance of examining the effects of positive feedback, scale-dependent feedback and hydraulic conductivity feedback simultaneously in future models on peatland pattern formation, because the data from our study suggested that these mechanisms might operate simultaneously in reality. If this is indeed the case, the importance of each mechanism for pattern formation will probably be dependent on site-specific conditions (e.g. slope, vegetation types, climate).

There are also theories on peatland patterning that stress the importance of uplift of ridges by differential effects of frost heaving. Ridges remain frozen longer during the thaw season because the upper aerobic peat layer insulates the frost in ridges (Brown 1968; Moore and Bellamy 1974). The insulating capacity of ridges also became apparent in our study; during the relatively warm measurement period, water in the ridges was on average 5 °C colder than the mire water in hollows (Table 2).

Although differential effects of frost heaving cannot explain the formation of a spatially regular pattern, it may amplify existent spatial patterning in peatlands. The fact that we still encountered ice needles in the ridges at the end of July supports the idea that effects of frost heaving could be of secondary importance in peatland patterning.

Finally, some studies focus on the possible role of spring floods in pattern formation (Sakaguchi 1980; Seppälä and Koutaniemi 1985). During high water levels, as occurring with spring snowmelt, storage capacity in the hollows may be insufficient so that water can flow freely over the ridges (e.g. Quinton and Roulet 1998). These conditions probably also occur in our study site, because of the snow pack that develops in winter in this part of Siberia (Semenova and Lapshina 2001). During the spring floods, slush and plant remains could be transported towards elevations on the mire surface, thereby amplifying the surface microtopography.

Perspectives

This discussion reveals that although the field measurements presented here corroborate the hypothesis of the scale-dependent and the positive feedback synergistically governing maze pattern formation in peatlands, alternative hypotheses suggested to induce linear patterning cannot be ruled out. Previous theoretical predictions (Table 1) enabled an empirical test of our hypotheses by taking a ‘snapshot’ of the ecosystem state. The alternative mechanisms described above, however, require longer-term observations to identify the role of processes that occur on a seasonal timescale. The developmental processes driving peatland patterning has been the field of much speculation, but little actual experiment (Moore and Bellamy 1974; Belyea and Lancaster 2002). Therefore, we think that there are two promising avenues of future research.

First, a number of well-developed peatland simulation models exist (e.g. Hilbert et al. 2000; Belyea and Clymo 2001; Frohling et al. 2001; Pastor et al. 2002; Rietkerk et al. 2004a; Couwenberg and Joosten 2005), but there is no model yet that incorporates the processes mentioned above. Such a combined model would enable the on and off switching of different processes. One of the strengths of such “modeling experiments” is that they can show the effect of processes and factors that are difficult to disentangle by field manipulations of patterned peatlands.

Second, the problem could be tackled with empirical experiments under controlled circumstances. Such an approach could be used to measure process rates (e.g. evapotranspiration, hollow-ridge water flow, nutrient accumulation under ridges) and to identify causal relationships between these processes. This information is needed to assess the relative importance of the hypothesized feedbacks governing surface pattern formation in peatlands.

Appendix 3A: Model calculations leading to “Expected nutrient concentration pattern in water” (Column 3 in Table 1)

Table 1 in the main text of Chapter 3 presents how the positive feedback and the scale-dependent feedback are expected to drive underlying patterns in nutrients and hydrology. In this appendix, we explain how the hypotheses for “Expected nutrient concentration pattern in water” (Column 3 in Table 1) were derived from calculations using previously published model equations (Belyea and Clymo 2001; Rietkerk et al. 2004a). We show that the positive feedback predicts a positive effect on nutrient availability on hummocks and ridges, because increased mineralization outweighs increased productivity. Further, we show that the scale-dependent feedback has a positive effect on nutrient availability on ridges, because increased local recycling of plant litter outweighs increased vascular plant uptake.

Effect of the positive feedback

To study how the occurrence of the positive feedback would influence nutrient concentration in water, we used the positive feedback model of Belyea and Clymo (2001). This model includes two biological processes that would influence nutrient concentration in the opposite directions: plant production or primary productivity (uptake of nutrients) and decomposition (here assumed to lead to mineralization and release of nutrients). Decomposition involves competition between microbial biomass and (mainly vascular) plants for released nutrients. If litter quality is poor, decomposition may lead to immobilization of nutrients, whereas decomposition of high quality litter may lead to mineralization and release of nutrients. Litter quality can be indicated by C:N and C:P ratios (e.g. Köppisch 2001). Recently, Bragazza et al. (2007) found that in ombrotrophic habitats the decomposition of *Sphagnum* and vascular plant litter with C:N ratios of 56-75 and C:P ratios of 1030-1975 always leads to net mineralization of nutrients. In our vegetation samples, we measured

mean C:N ratios of 28 (ridges) and 42 (hollows), and mean C:P ratios of 438 (ridges) and 804 (hollows). Given this relatively high quality as compared to the litter in the experiment of Bragazza et al. (2007), the assumption that was made to formulate the hypotheses seems reasonable.

To quantify the balance between primary productivity and decomposition, we analyzed the model, which consists of one ordinary differential equation describing acrotelm growth rate:

$$\frac{dZ_A}{dt} = \frac{P - D_A}{\rho_D} - \frac{\Delta W_C}{\theta} \quad (\text{I})$$

Where Z_A is the acrotelm thickness (Units: m) and ΔW_C the catotelm's rate of water storage ($\text{m}\cdot\text{yr}^{-1}$). Further the model includes two biological processes; P is the net primary productivity ($\text{g}\cdot\text{m}^{-2}\cdot\text{yr}^{-1}$), D_A is the cumulative mass loss rate through decomposition in the acrotelm ($\text{g}\cdot\text{m}^{-2}\cdot\text{yr}^{-1}$). Also the model includes two characteristics of the peat; ρ_D is the dry bulk density at the acrotelm-catotelm boundary ($\text{g}\cdot\text{m}^{-3}$) θ is the effective porosity at the acrotelm-catotelm boundary (-). All these four terms are functions of the acrotelm thickness itself. The model has been parameterized with data from a field experiment on Ellergower Moss, an ombrotrophic peatland in Scotland (Belyea and Clymo 2001). For our purpose, we focused on the terms primary productivity and cumulative mass loss through decomposition:

$$D_A = (k_4 + k_5 Z_A)^2 \quad (\text{II})$$

$$P = (k_1 + k_2 Z_A - k_3 Z_A^2)^2 \quad (\text{III})$$

In which k_1, k_2, k_3, k_4 and k_5 are parameters that have been estimated by regression in the original study. How the balance between decomposition and plant production changes with increasing acrotelm thickness can be studied by the ratio of the derivatives to acrotelm of both components, which is given by:

$$\frac{\left(\frac{dP}{dZ_A}\right)}{\left(\frac{dD_A}{dZ_A}\right)} = \frac{dP}{dD_A} = \frac{(k_2 - 2k_3 Z_A)(k_1 + Z_A(k_2 - k_3 Z_A))}{k_5(k_4 + k_5 Z_A)} \quad (\text{IV})$$

If the value of this ratio is smaller than 1, an increase in acrotelm thickness leads to a larger increase in decomposition as compared to the increase in primary productivity. If the value of this ratio is larger than 1, an increase in acrotelm thickness leads to a larger increase in primary productivity as compared to the increase in decomposition. Provided that nutrients are mineralized instead of immobilized through decomposition

and that living and dead organic matter have the same C:Nutrient stoichiometry (a simplifying modeling assumption, as assumed in Rietkerk et al. 2004a; Chapter 2), a ratio smaller than 1 means that there is a relative increase in the amount of available nutrients. Using the parameter values of Belyea and Clymo (2001), we plotted the ratio as a function of acrotelm thickness (Fig. A1).

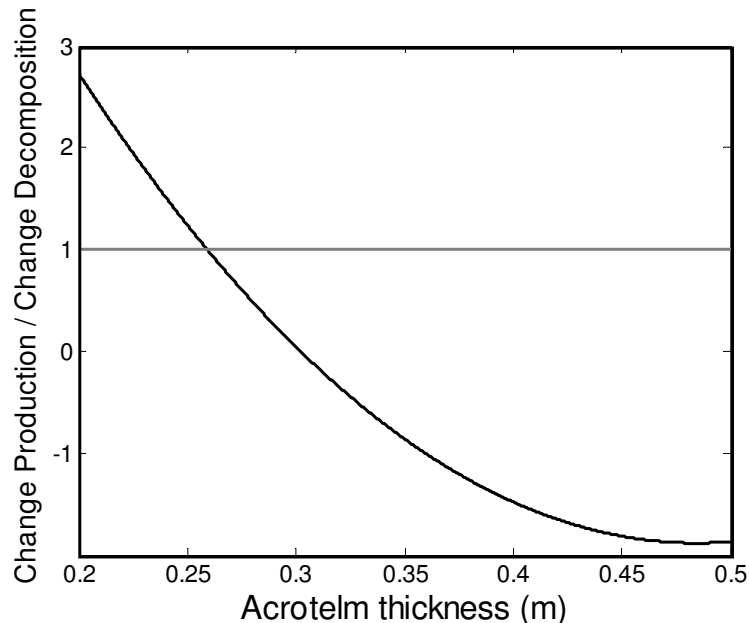


Figure A1: The ratio of change in primary production and change in decomposition as specified by the local positive feedback model of Belyea and Clymo (2001). If the value of the ratio is smaller than 1, an increase in acrotelm thickness implies that there will be a larger increase in nutrient release via mineralization as compared to the increase in nutrient uptake by plants. If the ratio is larger than 1, the increase in uptake of nutrients is larger than the increase in release of nutrients. Hence, an increase in acrotelm thickness would be expected to lead to an increase in nutrient availability when the ratio becomes smaller than 1. Using the parameter settings of Belyea and Clymo (2001) this threshold occurs at acrotelm thickness of approximately 0.25 m. If these parameters are varied up to 10% of the original value, the threshold occurs within the acrotelm thickness range of 0.20-0.33 m.

Figure A1 shows that if the acrotelm is thicker than approximately 0.25 m, the model predicts that with an increase in acrotelm thickness, decomposition increases more than production. Yet, it is important to note that this model has been specifically parameterized for one particular bog, so the parameters are likely to vary across peatland ecosystems. Therefore we performed a sensitivity analysis for this result. If all parameters are allowed to deviate (both increase and decrease) up to 10% of the original value, the following range of thresholds is observed: 0.20 - 0.33 m. Because the hummocks and ridges of patterned peatlands typically have an acrotelm thickness above this threshold range, we hypothesized that the positive feedback mechanism induces a higher nutrient availability with increasing acrotelm thickness (see Column 3 of Table 1 in the main text of Chapter 3).

Effect of the scale-dependent feedback

Models predict that occurrence of the scale-dependent feedback leads to patches of high vascular plant biomass to where nutrients are transported (Rietkerk et al. 2004a; Chapter 2). Here, we focused the analysis on the model of Rietkerk et al. (2004a), because this model aims to identify the effect of solely the scale-dependent feedback. The effect of an increase in vascular plant biomass on nutrient concentration in the mire water, however, is not straightforward, because it leads to increased nutrient depletion through plant uptake, but also to increased litter input and hence possibly to increased nutrient release through mineralization. Therefore, we analyzed how an increase in vascular plant biomass in a certain patch would alter the nutrient concentration in water of that patch, using the mean field model version of Rietkerk et al. (2004a). The reaction equations for vascular plant biomass, nutrient availability and hydraulic head are:

$$\frac{dN}{dt} = N_{in} - r_N N + \frac{duB}{g} - uB[N]f(h(H)) \quad (\text{V})$$

$$\theta \frac{dH}{dt} = P - E_T f(h(H)) - t_V B f(h(H)) \quad (\text{VI})$$

$$\frac{dB}{dt} = gB[N]f(h(H)) - dB - bB \quad (\text{VII})$$

In which N_{in} is the nutrient input rate ($\text{g}_N \cdot \text{m}^{-2} \cdot \text{yr}^{-1}$), t is time (yr), r_N is a nutrient loss parameter (yr^{-1}), u is a plant uptake parameter ($\text{m}^3 \cdot \text{g}_B^{-1} \cdot \text{yr}^{-1}$), θ is soil porosity (dimensionless), H is the hydraulic head (m), P is the precipitation rate ($\text{m} \cdot \text{yr}^{-1}$), E_T is an evaporation parameter, t_V depicts the vascular plant transpiration rate ($\text{m}^3 \cdot \text{g}_B^{-1} \cdot \text{yr}^{-1}$), B is vascular plant biomass density ($\text{g} \cdot \text{m}^{-2}$), g is a vascular plant growth parameter ($\text{m}^3 \cdot \text{g}_N^{-1} \cdot \text{yr}^{-1}$), d is the fractional return in litter (yr^{-1}), b is the rate of fractional export or loss from the landscape (yr^{-1}). N is the amount of nutrients in the mire water ($\text{g} \cdot \text{m}^{-2}$), $[N]$ is then the nutrient concentration in the mire water, which is defined as:

$$[N] \equiv \frac{N}{\theta H} \quad (\text{VIII})$$

Further, $f(h(H))$ is a dimensionless soil water stress function that is defined as follows:

$$f(h(H)) = 1, \quad H - z \geq h_1 \quad (\text{IX})$$

$$f(h(H)) = 0, \quad H - z \leq h_2 \quad (\text{X})$$

$$f(h(H)) = \frac{H - z - h_2}{h_1 - h_2}, \quad h_1 \leq H - z \leq h_2 \quad (\text{XI})$$

In which h_1 is the pressure head below which soil water stress occurs (m), h_2 is the rooting depth of vascular plants (m) and z is a reference height (m).

For brevity, we introduce:

$$x \equiv \frac{1}{h_1 - h_2} \quad (\text{XII})$$

$$y \equiv z + h_2 \quad (\text{XIII})$$

So that:

$$f(h(H)) = x(H - y) \quad (\text{XIV})$$

Now, solving eqs. (V), (VI) and (VII) after each other gave the equilibrium values for nutrient amount, hydraulic head and vascular plant biomass:

$$\hat{N} = \frac{(gN_{IN} + duB)\theta\hat{H}}{g(r_N\theta\hat{H} + xuB(\hat{H} - y))} \quad (\text{XV})$$

$$\hat{H} = \frac{P}{x(t_v B + E_T)} + y \quad (\text{XVI})$$

$$\hat{B} = \frac{gxN_{IN}P - r_N\theta(b+d)(P + xyE_T)}{xuP + r_N t_v xy\theta(b+d)} \quad (\text{XVII})$$

The above equations, however, only apply if the pressure head $H-z$ is between h_1 and h_2 (eq. (XI)). It follows from eq. (XVI) that $H-z$ is always larger than h_2 . Further, $H-z$ needs to be smaller than h_1 , which yields the following constraint on B :

$$B \geq \frac{P - E_T}{t_v} \quad (\text{XVIII})$$

By combining eqs. (VIII), (XV) and (XVI) and subsequent rearranging, we obtained an expression for the equilibrium nutrient concentration in the mire water, which depends on vascular plant biomass:

$$[\hat{N}] = \frac{(t_v B + E_T)(gN_{IN} + duB)x}{gP(r_N\theta + xuB) + gr_N\theta(t_v B + E_T)xy} \quad (\text{XIX})$$

Now, the relation between nutrient release and nutrient uptake could be studied analytically by examining the rate of change in nutrient concentration as a function of biomass density. First, we used the expression in eq. (XIX) to calculate the derivative to B :

$$\frac{d[N]}{dB}_{[N]=[\hat{N}]} = \frac{(gN_{IN}P(r_N t_V \theta - E_T ux) + du(r_N E_T P \theta + B P t_V (2r_N \theta + Bux) + r_N \theta (E_T + B t_V)^2 xy))x}{g(P(r_N \theta + Bux) + r_N \theta (E_T + B t_V)^2 xy)} \quad (XX)$$

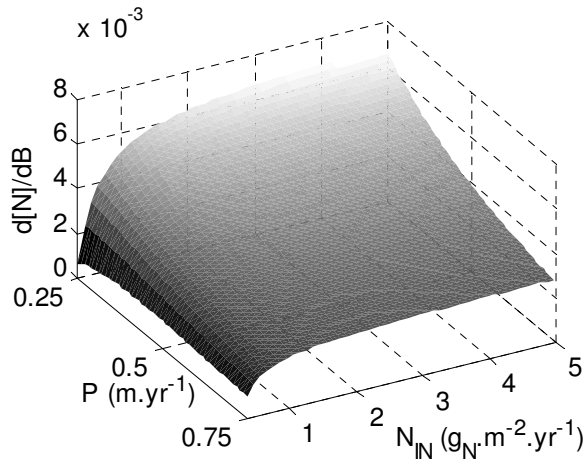
In case of the occurrence of the scale-dependent feedback, patches emerge that act as nutrient sinks, meaning that these patches receive an extra input of nutrients from their surroundings. Therefore these patches reach higher biomass density than the equilibrium density predicted by the mean field model (Rietkerk et al. 2004a). Combining eqs. (XVII) and (XX) yielded an analytical expression of the effect on such an increase in vascular biomass on the nutrient concentration in the mire water. If the sign of the derivative is positive, the increase in biomass increases nutrient concentration in the mire water, if the sign is negative, nutrient concentration in the mire water decreases. For almost the entire parameter range in precipitation and nutrient input rate that was studied in the original paper, the sign of the derivative is positive and the constraint given by eq. (XVIII) is satisfied if the predicted mean field density is larger than approximately $100 \text{ g}_B \cdot \text{m}^{-2}$ (calculated using eq. (XVII)). This is indeed the case in the parameter region where maze pattern formation occurs in the model (Rietkerk et al. 2004a).

Crucial for this positive sign of the derivative, however, is the effect of local recycling of nutrients by decomposition of vascular plant litter (Fig. A2). Without this process, eq. (XX) reduces to:

$$\frac{d[N]}{dB}_{\text{NoRECYCLING } [N]=[\hat{N}]} = \frac{N_{IN} P x (t_V r_N \theta - E_T ux)}{(P(r_N \theta + x u B) + r_N \theta (E_T + t_V B) xy)^2} \quad (XXI)$$

The sign of the right hand side of eq. (XXI) is determined by the second term in the numerator, which is always negative for the parameter regions that have been examined in the original paper (Fig. A2). Concluding, based on these model calculations and predictions we could hypothesize that occurrence of the scale-dependent feedback creates nutrient sinks and thereby patches of higher vascular plant density within the landscape. So, the main mechanism of nutrient accumulation from the surroundings in high-density patches is entrapment in the vascular plant tissue. Further, the vascular plant tissue in high-density patches contains nutrients that were partly imported from the surroundings, but these nutrients are recycled only locally. Therefore, occurrence of the scale-dependent feedback *indirectly* (meaning first taken up by plants, then locally released) increases nutrient concentration in the mire water under high-density patches.

With local recycling of plant litter



No local recycling of plant litter

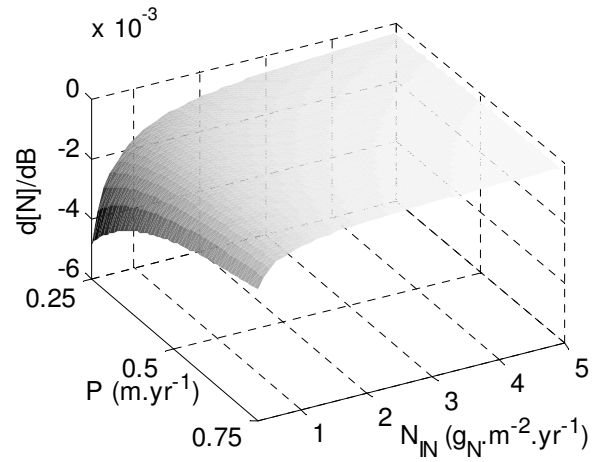


Figure A2: The relation between nutrient concentration in mire water and vascular plant biomass as predicted by a model that only mimics the occurrence of a scale-dependent feedback (Rietkerk et al. 2004a). Positive values of the derivative $\frac{d[N]}{dB}$ mean that if the vascular plant biomass exceeds the predicted mean field density (because of extra nutrient import from the surroundings), the equilibrium nutrient concentration in the mire water also increases. When the local recycling of plant litter is included in the model, $\frac{d[N]}{dB}$ is positive except for very small values of nutrient input rate (left panel), coinciding with predicted mean field vascular plant densities of $< 100 \text{ g}_B \cdot \text{m}^{-2}$ (calculated using eq. (XVII) in text). If local recycling is excluded from the model, the sign of $\frac{d[N]}{dB}$ is always negative (right panel), showing that the role of local recycling is essential in the model predictions on the effect of the scale dependent feedback on nutrient concentrations in the mire water.

Appendix 3B: Analysis of the diurnal water table dynamics

In this appendix, we discuss in more detail the hydrological processes that can be inferred from Figure 4 of the main text of Chapter 3. We show that our hydrological data can be used to estimate evapotranspiration rates on ridges and also to estimate flows of water and nutrients from hollows toward ridges. In summary, we found an evapotranspiration rate on ridges of $9.1 \pm 2.3 \text{ mm} \cdot \text{d}^{-1}$ and a net advection of $6.7 \pm 2.3 \text{ mm} \cdot \text{d}^{-1}$ from hollows toward ridges, yielding potential nutrient fluxes of $0.7 \pm 0.3 \text{ mgP} \cdot \text{m}^{-2} \cdot \text{ridge} \cdot \text{d}^{-1}$ and $6.9 \pm 2.6 \text{ mgN} \cdot \text{m}^{-2} \cdot \text{ridge} \cdot \text{d}^{-1}$.

The water balance in the ridges of our study site comprised gains via precipitation and advection and losses via evapotranspiration. The contribution of each these processes to the water balance changed during the day, as indicated by different segments in the water table graph (Fig. B1). After sunrise, losses by evapotranspiration exceeded the input through advection, causing the water table in ridges to drop (Fig. B1). In the afternoon, this pattern reversed; the input through advection exceeded losses through evapotranspiration, causing the water table in ridges to rise (Fig. B1). Previous studies indicate that evapotranspiration greatly reduces or ceases after sunset (Kim and Verma 1996; Reed and Ross 2004). Because the water table in ridges was well below the surface (see Table 1 in the main text of Chapter 3), it is likely that evapotranspiration from ridges ceased at night in our study site as well. Apart from one precipitation event during the study period, the rise of the water table in ridges could only be due to import of water from the surroundings by advection (Fig. B1).

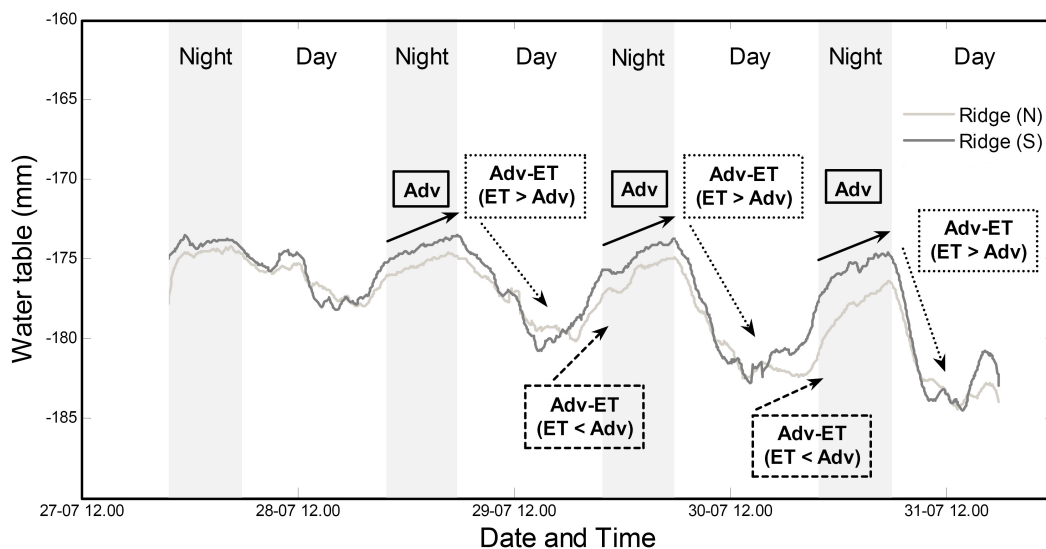


Figure B1: Diurnal dynamics in water table level under two ridges in a maze-patterned peatland in the Great Vasyugan Bog, Siberia. Water levels were measured relative to an arbitrary reference height. Grey areas show the period between sunset and sunrise (data from the Culym weather station). The water balance of the ridges comprised gains via precipitation and advection and losses via evapotranspiration. Full arrows indicate the nighttime period where the water balance comprised input via advection. Dotted arrows indicate the first period after sunrise, in which losses through evapotranspiration exceeded gains via advection, causing a drop in the water table. Dashed arrows indicate the second period after sunrise, in which losses through evapotranspiration were smaller than gains via advection, yielding a rising water table.

On average, water table level rose 2.4 ± 1.2 mm in ridges during the night (paired samples t-test, $t_7 = -5.556$, $p_{(\text{one-tailed})} < 0.001$), whereas water table level dropped 2.1 ± 1.6 mm in the hollow during the night (paired samples t-test, $t_3 = 2.705$, $p_{(\text{one-tailed})} =$

0.037). This means that the hydraulic head gradient between hollow and ridges decreased during the night (Fig. B2), which implies that the rate of advection also decreased during the night. We tested whether a quadratic fit (decreasing advection rate during the night) indeed explained the water table dynamics significantly better than a linear fit (constant advection rate during the night) using an extra sum of squares test (e.g. Kéfi et al. 2007b). Although a quadratic regression fitted best on most nighttime series, the effect of the type of regression (linear or quadratic) on the magnitude of the calculated average advection rate was small (Table B1). This suggested that it was reasonable to approximate advection into ridges as a constant rate, probably because of the high hydraulic conductivity of the hollows. For the last 3 nights of the study period, the average advection rate was $7.3 \pm 2.5 \text{ mm.d}^{-1}$ (the average of the upper six values in column 5 of Table B1).

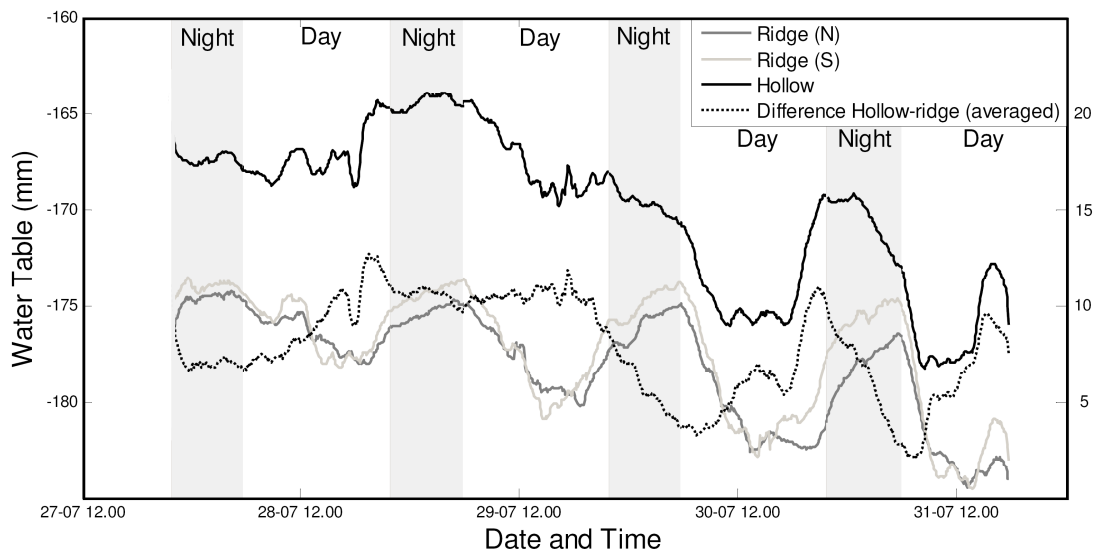


Figure B2: Diurnal dynamics in water table level under two ridges, the hollow in between and the resulting ridge-hollow gradient in hydraulic head (dotted line), as measured in a maze-patterned peatland in the Great Vasyugan Bog, Siberia. The gradient was calculated as the difference between water table level in the hollow and the average water table level under the two ridges. Water levels were measured relative to an arbitrary reference height. Grey areas show the period between sunset and sunrise (data from the Culym weather station). The difference in hydraulic head indicates a consistent flow from hollow toward ridges. Largest differences in hydraulic head occurred during the day, and the hydraulic head decreased during the night.

Observation	Ridge Position	Type of Regression	Degrees of Freedom	F	Slope (mm.d ⁻¹)	r ² _{adj}	p-value
Nighttime trend 28-29 July 2005	North	Quadratic	1, 92	1271	4.6 (4.6)	0.96	< 0.001
Nighttime trend 28-29 July 2005	South	Quadratic	1, 92	1549	4.8 (4.8)	0.97	< 0.001
Nighttime trend 29-30 July 2005	North	Quadratic	1, 93	453	8.1 (8.1)	0.90	< 0.001
Nighttime trend 29-30 July 2005	South	Linear	1, 94	881	7.6	0.90	< 0.001
Nighttime trend 30-31 July 2005	North	Quadratic	1, 94	1953	11.3 (11.5)	0.98	< 0.001
Nighttime trend 30-31 July 2005	South	Quadratic	1, 94	624	7.5 (7.7)	0.93	< 0.001
Overall trend (using daily minima)*	North	Linear	1, 2	155	-2.7	0.98	0.006
Overall trend (using daily minima)*	South	Linear	1, 2	51	-2.5	0.94	0.019

Table B1: Regressions of nighttime water table dynamics and overall trend in water table (using 4 daily minimum water table levels) for two ridges within the Great Vasyugan Bog, Siberia. Quadratic regressions were used if there was a significant increase in explained variance (using an extra sum of squares test and significance level $\alpha = 0.05$). In these cases the slope as estimated by linear regression is given between brackets. Nights were defined as the period between sunrise and sunset, according to data from the Culyum weather station.

* Corrected for the precipitation event on 28-07 2005. The amount of precipitation (0.9mm) divided by the assumed acrotelm porosity (0.92) was added to the daily minimum of 28-07 2005.

By selecting periods over which the water table rose and then fell to the same level and correcting for water input via precipitation during these periods, we could account for evapotranspiration losses in ridges. We selected periods in between the daily minimum water level in ridges (Fig. B3). During the measurement period, there was a net water loss from ridges, and the linear decline in daily minimum water level (Fig. B3) suggested that this loss rate was relatively constant; using linear regression the average loss rate from the two ridges was estimated to be $2.6 \pm 0.4 \text{ mm.d}^{-1}$ (Table B1). A constant advection input raising the water table with 7.3 mm.d^{-1} and a net lowering of the water of 2.6 mm.d^{-1} implied that evapotranspiration caused a drop in the water table at a rate of $9.9 \pm 2.5 \text{ mm.d}^{-1}$. The actual amount of water that was lost, however, was less, because a fraction of the substrate volume is occupied by peat. Assuming an acrotelm porosity of 0.92 (Nungesser 2003), this would yield a net advection toward ridges of $6.7 \pm 2.3 \text{ mm.d}^{-1}$. In similar vein, this would yield a net evapotranspiration rate of $9.1 \pm 2.3 \text{ mm.d}^{-1}$ from ridges. Interestingly, this estimated

evapotranspiration rate for our study site is higher than the measured maximal evapotranspiration rate (4.2 mm.d^{-1}) in a Siberian treeless bog without regular maze patterning (Shimoyama et al. 2004).

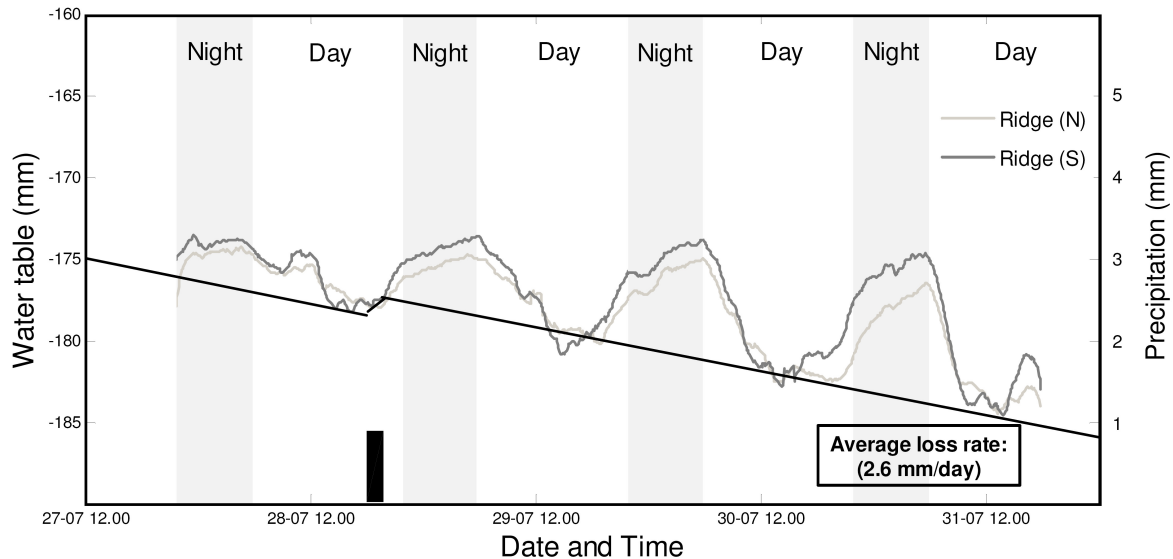


Figure B3: Diurnal dynamics in water table level under two ridges in a maze-patterned peatland in the Great Vasyugan Bog, Siberia. Water levels were measured relative to an arbitrary reference height. Grey areas show the period between sunset and sunrise (data from the Culym weather station). Corrected for the precipitation event, the trend in minimum daily water level shows that during the measurement period, there was a relatively constant loss of water from the ridges.

Assuming a water input of 6.7 mm.d^{-1} through advection, the daily influx of water from hollows toward ridges would be $0.0067 \times 1 \times 1 = 0.0067 \pm 0.0023 \text{ m}^3 \text{d}^{-1}$. In our study we measured an average concentration of $0.1 \pm 0.03 \text{ mgP.l}^{-1}$ and $1.0 \pm 0.2 \text{ mgN.l}^{-1}$ of the mire water in hollows (see Table 1 in the main text of Chapter 3). The maximum nutrient gain for ridges would be reached if no nutrients were immobilized during the transport from hollows toward ridges. In this case, the nutrient transport through advection would yield a net gain of nutrients in ridges of $0.7 \pm 0.3 \text{ mgP.m}^{-2} \text{ridge.d}^{-1}$ and $6.9 \pm 2.6 \text{ mgN.m}^{-2} \text{ridge.d}^{-1}$.

It is important to note some of the uncertainties in the above calculations. For example, the water pressure sensors were based on data measured in the centres of the ridges. It is likely that the water table level increases toward the edge of the ridge, which would affect advection and evapotranspiration rates. Further uncertainties arose from the measurement period being short, and the number of observations being small.

Acknowledgments

We thank Helen de Waard, Gijs Nobbe and Dineke van de Meent for help with the laboratory analyses, and Olga Pisarenko, Andrej Korolyuk and Jan Hrupacék for assistance in the field. We would also like to thank Lisa Belyea and Peter de Rooter for many comments that improved the manuscript, and Johan van de Koppel for writing the R-script for bimodality. The research of MBE and MR is supported by a VIDI grant from the Research Council Earth and Life Sciences of the Netherlands Organization of Scientific Research (NWO-ALW) to MR.



4

Nutrients and hydrology indicate the driving mechanisms of peatland surface patterning

Maarten B. Eppinga, Peter C. De Ruiter,
Martin J. Wassen & Max Rietkerk

The American Naturalist 173: 803-818 (2009)

Nutrients and hydrology indicate the driving mechanisms of peatland surface patterning

Abstract

Peatland surface patterning motivates studies that identify underlying structuring mechanisms. Theoretical studies so far suggest that different mechanisms may drive similar types of patterning. The long time-span associated with peatland surface pattern formation, however, limits possibilities for empirically testing model predictions by field manipulations. Here, we present a model that describes spatial interactions between vegetation, nutrients, hydrology and peat. We used this model to study pattern formation as driven by three different mechanisms: peat accumulation, water ponding, and nutrient accumulation. By on and off switching of each mechanism, we created a full-factorial design to see how these mechanisms affected surface patterning (pattern of vegetation and peat height) and underlying patterns in nutrients and hydrology. Results revealed that different combinations of structuring mechanisms lead to similar types of peatland surface patterning, but contrasting underlying patterns in nutrients and hydrology. These contrasting underlying patterns suggest that the presence or absence of the structuring mechanisms can be identified by relatively simple short-term field measurements of nutrients and hydrology, meaning that longer-term field manipulations can be circumvented. Therefore this study provides promising avenues for future empirical studies on peatland patterning.

Introduction

A key challenge in ecosystem ecology is to explain landscape-scale patterns that emerge from smaller-scale structuring mechanisms (Levin 1992; Solé and Bascompte 2006). Spatial vegetation patterns are among the most striking landscape-scale patterns and have been observed in a variety of ecosystems. Examples include arid ecosystems (Klausmeier 1999), savannas (Lejeune et al. 2002), ribbon forests (Hiemstra et al. 2006) and marsh tussocks (Van de Koppel and Crain 2006). Identification of the smaller-scale structuring mechanisms that explain these kinds of spatial vegetation patterning is important, because it also provides insight in other aspects of ecosystem functioning, such as responses to increased anthropogenic pressure or global climate change (Rietkerk et al. 2004b; Kéfi et al. 2007b; Scanlon et al. 2007). Spatial surface (and hence vegetation) patterning is also observed in boreal peatland ecosystems. A considerable amount of attention has been paid to this phenomenon in the peatland literature of the last century (Foster et al. 1983; Charman 2002). Several modeling studies (Swanson and Grigal 1988; Hilbert et al. 2000; Belyea and Clymo 2001; Rietkerk et al. 2004a; Couwenberg and Joosten 2005) suggest that these large-scale surface patterns emerge from smaller-scale structuring mechanisms (Belyea and Baird 2006). These models, however, focused on different kinds of peatland surface patterns and also suggested different kinds of structuring mechanisms. We will now explain these differences in more detail.

One of the most commonly observed patterns in peatlands is the spatial structure consisting of distinct microforms, namely hummocks and hollows with a characteristic spatial scale of 1-10 m (Belyea and Clymo 2001). Hummocks are elevated above hollows because of a thicker acrotelm, which is a layer of aerobic peat. Hollows have a much thinner acrotelm or no acrotelm at all. Below the acrotelm the water-saturated peat layer or catotelm is situated. This means that the acrotelm-catotelm boundary is determined by the seasonal minimum water table (e.g. Holden and Burt 2003). Plant growth in peatlands is limited by water stress, which can occur both at high water tables because of waterlogging and at low water tables because of desiccation (Ridolfi et al. 2006). Because plant production determines the organic matter input into the peat layer, peat growth is optimal at intermediate acrotelm thickness (Hilbert et al. 2000; Belyea and Clymo 2001). This implies that below the optimum acrotelm thickness for plant growth, there is a positive feedback between net rate of peat formation and acrotelm thickness, mainly because of increased production of vascular plants (Wallén et al. 1988; Belyea and Clymo 2001). This positive feedback

is a structuring mechanism that explains how peatland microforms may develop either into a wet, sparsely vegetated, low-productive state or a dry, densely vegetated, high-productive state. Thus, slight differences between wetter and dryer sites may further amplify and lead to spatial patterning of sharply bounded microforms. From here we refer to this structuring mechanism as the peat accumulation mechanism.

Another type of pattern comprises merged hummocks forming linear ridges alternating with lower and wetter hollows, oriented along the contours of mire slopes, with a characteristic spatial scale of 10^2 - 10^3 m (Sjörs 1983). A possible mechanism that can explain this type of patterning is a lower hydraulic conductivity of ridges as compared to hollows (Swanson and Grigal 1988). As a result of lower hydraulic conductivity, water may accumulate upslope of ridges, which stimulates the formation of hollows. Models show that such water ponding mechanism (cf. Rietkerk et al. 2004a), which originates from differences in hydraulic conductivity, can indeed explain the formation of ridge-hollow patterns on peatland slopes (Swanson and Grigal 1988; Couwenberg 2005; Couwenberg and Joosten 2005).

Furthermore, peatland maze patterns on flat ground consist of merged hummocks forming ridges that are star or net-like, enclosed by lower and wetter hollows (Wallén et al. 1988; Rietkerk et al. 2004a). The term “maze pattern” is used, because the densely vegetated ridges are connected in an almost continuous network without a clear orientation, but occasionally the bands form dead ends, somewhat resembling the corridors within a maze (Rietkerk et al. 2004a). In arid ecosystems similar patterns are called labyrinths (Rietkerk et al. 2002). Peatland maze patterning can be induced by nutrient accumulation under ridges, which is driven by increased evapotranspiration rates by vascular plants (especially shrubs and trees) that grow on these ridges (Rietkerk et al. 2004a; Wetzel et al. 2005; Ross et al. 2006). This structuring mechanism would imply that because of higher evapotranspiration rates, there is a net flow of water and dissolved nutrients toward ridges. Subsequently, the nutrients become trapped on ridges through uptake by vascular plants. Thus, during their lifespan, vascular plants that grow on ridges accumulate nutrients originating from outside the ridge. Nutrients become available again through mineralization of vascular plant litter, but this only increases nutrient availability on the local scale at which the litter is deposited (within the ridge). Models predict that this local recycling effect outweighs the effect of nutrient uptake, meaning that nutrient concentrations in the mire water under ridges also increase (Rietkerk et al. 2004a; Chapters 2 and 3). Because higher nutrient availability will lead to an increase in vascular plant biomass,

this is a self-reinforcing process, which will be referred to as the nutrient accumulation mechanism (cf. Rietkerk et al. 2004a). Models show that the nutrient accumulation mechanism could indeed explain the formation of maze patterns on flat ground (Rietkerk et al. 2004a; Chapter 2). Moreover, model simulations show that the nutrient accumulation mechanism may also drive the formation of individual hummocks on flat ground and linear ridge-hollow patterning on peatland slopes (Rietkerk et al. 2004a; Chapter 2). This means that the nutrient accumulation mechanism provides an alternative explanation for the types of patterning previously associated with the peat accumulation and water ponding mechanisms.

Thus, until now, three different structuring mechanisms for peatland patterning have been proposed and modeled, namely peat accumulation through differences in net rate of peat formation, water ponding through differences in hydraulic conductivity and nutrient accumulation through differences in evapotranspiration. These three mechanisms, however, are inextricably linked in nature: acrotelm thickness not only controls net rate of peat formation, but also affects evapotranspiration rates (Lafleur et al. 2005) and hydraulic conductivity of the peat (Romanov 1968; Ivanov 1981). In turn, evapotranspiration and hydraulic conductivity influence the water balance, and hence regulate acrotelm thickness (Hilbert et al. 2000; Belyea and Malmer 2004; Belyea and Baird 2006). The possibility of a combination of mechanisms together driving peatland surface patterning has also been suggested in previous theoretical (Larsen et al. 2007; Chapter 2) and empirical (Chapter 3) studies. Therefore, there is a need to investigate the interaction between these mechanisms with respect to peatland pattern formation, rather than studying the mechanisms in isolation using separate models. Furthermore, it is important to identify key variables in patterned peatlands that can be measured in order to accept one (combination of) structuring mechanism(s) and thereby reject other hypotheses. Until now, the theoretical models were too different from each other to be able to identify such key variables. In other words, the current lack of an integrated theoretical framework limits the inferential power of empirical research that is aimed at identifying and rejecting structuring mechanisms that drive peatland surface patterning.

The aim of this study was to integrate the three aforementioned mechanisms into one mechanistic model in order to study the interaction between these mechanisms, and to identify key variables that discriminate between likely and unlikely structuring mechanisms of a peatland surface pattern. More specifically, we aimed to derive hypotheses on the manner in which the occurrence of different structuring mechanisms would be reflected in peatland surface patterning and also in underlying

patterns in nutrients and hydrology. We developed a model framework that integrates the three mechanisms into one model. The model contained four state variables: vascular plant biomass, acrotelm thickness, groundwater table and available nutrient pool. Therefore, the model enabled predictions of how surface patterns (i.e. patterns in vegetation and peat height) are associated with underlying patterns in nutrients and hydrology. Each mechanism could be switched on or off, which allowed the performance of a full-factorial analysis. Model simulations were run both on flat ground and on peatland slopes.

The model

Model system and study approach

The study was designed to study the effects of three mechanisms on peatland pattern formation: peat accumulation, water ponding and nutrient accumulation. It should be noted that many other mechanisms have been proposed as explanations for pattern formation (see Chapters 2 and 3 for reviews), but in this study we focused on the three mechanisms that have been most prominently examined in recent model studies. We combined elements of the models of Hilbert et al. (2000), Belyea and Clymo (2001), Pastor et al. (2002), Rietkerk et al. (2004a) and Couwenberg (2005). In order to focus our study on the mechanisms of pattern formation, we made a number of simplifying assumptions of the peatland model system. First, we considered the water table in the modeled peatland area as being independent from the surroundings, meaning that larger-scale regional groundwater flows were not explicitly taken into account. Also, we assumed that the extent of the peatland area is fixed, meaning that we do consider vertical growth of the peatland but not lateral expansion of the peatland. It is well known that lateral peatland expansion and the regional geographical context of peatlands strongly interact with peatland hydrology and development (Ingram 1982; Clymo 1984; Belyea and Baird 2006), but taking into account these aspects would require site-specific model parameterization (Borren and Bleuten 2006). The aim of this study, however, was to answer general questions and not to focus on site-specific properties. Second, we followed Pastor et al. (2002), who formulated a model applicable to both fens and bogs. Pastor et al. (2002) could simulate the succession from fens to bogs by including a negative relationship between the thickness of the peat layer and the supply of nutrients by groundwater. In this study, however, we assumed a constant nutrient input rate that is independent of the peat layer thickness. This means that our model could be parameterized to resemble either a fen or a bog, but not the succession from one peatland type to the other during a model simulation. It should also be noted that such a transition also

strongly depends on larger-scale regional water flow (Glaser 1992a,b), which was not considered in this study (see above). Third, we distinguished the acrotelm and catotelm as distinct peat layers with different decomposition rates (Hilbert et al. 2000), but we did not consider heterogeneity within these layers. Small-scale heterogeneity in the peat layers could create preferential flow channels that greatly affect peatland transport processes (Holden 2005), but here we focused on the transport processes as generated by the three pattern-forming mechanisms of interest. Fourth, following Hilbert et al. (2000) and Rietkerk et al. (2004a), we considered only one functional plant group. Competition between functional plant groups can be important (Van Breemen 1995; Ohlson et al. 2001), and the species composition affects peat decomposability (Moore et al. 2007) and carbon sequestration rates (Belyea and Malmer 2004), but interactions between functional plant groups are beyond the scope of the current study. How competition between different functional plant groups may affect pattern formation is treated in detail elsewhere (Chapter 2).

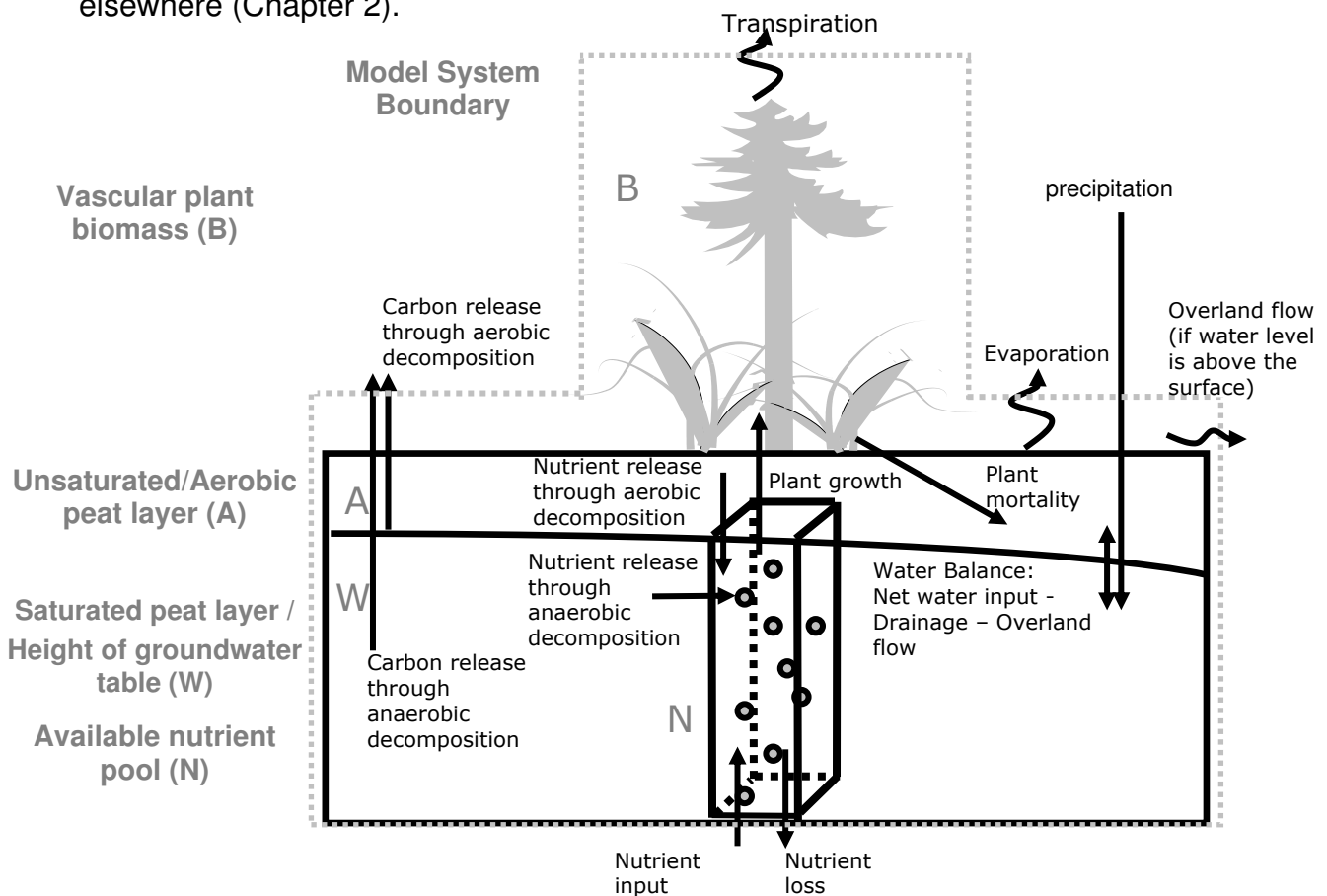


Figure 1: Schematic diagram of the state variables and the non-spatial processes in the model. (All spatial processes follow Rietkerk et al. (2004a) and Broelsma and Bierkens (2007)). The model consists of four state variables, represented by compartments in the diagram: vascular plant biomass, height/thickness of the aerobic peat layer (acrotelm),

height/thickness of the saturated peat layer (or: height of the water table), and available nutrient pool. Nutrient concentration in the groundwater is the quotient of the available nutrient pool and the height of the water table. Arrows indicate flows of biomass, water and nutrients from one compartment to the other, or flows crossing the model system boundaries. Decomposition processes involve two arrows: a release of nutrients and a loss of from the system of organic matter. Curled arrows indicate losses of water through evaporation, transpiration and overland flow.

Figure 1 shows a schematic diagram of the state variables and the non-spatial processes that were considered in this study. All spatial processes followed the model of Rietkerk et al. (2004a), except for the modeling of gravity-induced water flow on peatland slopes. For this process, we explicitly included a gradient in one direction in the impermeable mineral subsoil (see appendix 4A for analytical details; Brotsma and Bierkens 2007).

The null model contained none of the three mechanisms. The peat accumulation mechanism was introduced in the model by making plant growth most favorable at intermediate acrotelm thickness (Hilbert et al. 2000; Belyea and Clymo 2001). The water ponding mechanism was introduced in the model by letting hydraulic conductivity of the peat decrease with increasing acrotelm thickness (Romanov 1968; Couwenberg 2005). The nutrient accumulation mechanism was introduced in the model by letting transpiration rate increase with increasing vascular plant biomass (Rietkerk et al. 2004a). Thus, each mechanism could be switched on or off, which allowed the performance of a full-factorial analysis. In the following, we will first explain how the dynamics of the four state variables were modeled. Subsequently, we will explain how each of the three mechanisms was included in the model. The mathematical formulation of the null model is presented in Table 1. The explanation of the model parameters is presented in Table 2. The estimation of parameter values was based on literature and is explained in detail in appendix 4B. The full-factorial analysis of the effects of the three mechanisms on peatland pattern formation is specified in Table 3.

The null model

State Variable 1: Vascular plant biomass

Vascular plant dynamics comprise growth (the model term is indicated with I in Table 1), respiration (II), mortality (III) and dispersion (IV). Growth is limited by nutrient availability. We assumed that vascular plants grow faster when nutrient availability increases, asymptotically reaching a maximum growth rate at high levels of nutrient availability (e.g. DeAngelis 1992). Also, we assumed that plant growth is inhibited when the water conditions are not optimal; from here we refer to this process as

water stress. In this study, model parameters were set to mimic a vascular plant community, but the plant growth and water stress functions can also be adjusted to mimic *Sphagnum* species (Nungesser 2003).

In the null model, we assumed that water stress occurs as soon as the groundwater table drops below a certain depth. As the water table drops further, water stress increases linearly with depth until the rooting depth of the plant is reached: at this point plants can no longer grow (Feddes et al. 1978; Rodriguez-Iturbe and Porporato 2004). So, in the null model, water stress only occurs due to desiccation. Further, we assumed that mortality and mass loss through respiration increase linearly with increasing vascular plant biomass (Rietkerk et al. 2004a). Finally, the dispersion of vascular plants, either by seed dispersal or clonally, is approximated as a diffusion process (e.g. Okubo 1989). This means that the amount of dispersed biomass is linearly proportional to the gradient in biomass density.

State Variable 2: Acrotelm thickness

Acrotelm thickness dynamics include input of plant litter (V), decomposition losses (VI) and changes in the groundwater table (VII-X). Plant litter mass is converted into a height increase of the acrotelm by dividing this mass by the dry bulk density of the peat (Belyea and Clymo 2001). Dry bulk density generally increases with distance below the peatland surface, whereas effective porosity and hydraulic conductivity of peat generally decrease (e.g. Rycroft et al. 1975; Frolking et al. 2001). In this study, however, we did not take into account vertical variation in the peat layers. Hence, we made the simplifying modeling assumption that the peat characteristics bulk density, effective porosity and hydraulic conductivity do not vary vertically. Decomposition leads to mass loss from the peat layer, which implies a decrease in acrotelm thickness (Fig. 1). We assume that the amount of mass loss through decomposition increases linearly with layer thickness (Hilbert et al. 2000; Pastor 2002). Decay rate, however, is different for the two layers: acrotelm decay is faster than catotelm decay (Hilbert et al. 2000). Finally, we assumed that the groundwater table defines the acrotelm-catotelm boundary (Belyea and Malmer 2004), meaning that a change in the groundwater table affects acrotelm thickness. More specifically, acrotelm thickness decreases if the groundwater table rises, whereas acrotelm thickness increases when the groundwater table lowers (Hilbert et al. 2000)

State variable	Equation
Plant biomass (B)	$\frac{\partial B}{\partial t} = \underbrace{\frac{g[N]}{s+[N]} Bf^*}_{\text{I growth}} - \underbrace{bB}_{\text{II respiration}} - \underbrace{dB}_{\text{III mortality}} + \underbrace{D_B \left(\frac{\partial^2 B}{\partial x^2} + \frac{\partial^2 B}{\partial y^2} \right)}_{\text{IV dispersion}}$
Acrotelm thickness (A)	$\frac{\partial A}{\partial t} = \underbrace{\frac{dB}{\rho_D}}_{\text{V litter input}} - \underbrace{r_A A - r_w W}_{\text{VI decomposition}} - \underbrace{\frac{\Delta W_C^* - d_w W}{\theta}}_{\text{VII water input}} - \underbrace{\frac{\Delta W_C^* - d_w W}{\theta}}_{\text{VIII drainage}} - \underbrace{k^* \left(\frac{\partial}{\partial x} W \left(\frac{\partial W}{\partial x} \right) + \frac{\partial}{\partial y} W \left(\frac{\partial W}{\partial y} \right) \right)}_{\text{X Darcy flow}}$ <p style="text-align: right;">If A >= 0</p> $\frac{\partial A}{\partial t} = \frac{dB}{\rho_D} - r_w (A + W) - \underbrace{\frac{\Delta W_C^* - d_w W + oA}{\theta}}_{\text{IX overland flow}} - \underbrace{k^* \left(\frac{\partial}{\partial x} W \left(\frac{\partial W}{\partial x} \right) + \frac{\partial}{\partial y} W \left(\frac{\partial W}{\partial y} \right) \right)}_{\text{X Darcy flow}}$ <p style="text-align: right;">If A <= 0</p>
Groundwater table (W)	$\frac{\partial W}{\partial t} = \underbrace{\frac{\Delta W_C^* - d_w W}{\theta}}_{\text{XI water input}} - \underbrace{d_w W}_{\text{XII drainage}} + \underbrace{k^* \left(\frac{\partial}{\partial x} W \left(\frac{\partial W}{\partial x} \right) + \frac{\partial}{\partial y} W \left(\frac{\partial W}{\partial y} \right) \right)}_{\text{XIV Darcy flow}}$ <p style="text-align: right;">If A >= 0</p> $\frac{\partial W}{\partial t} = \frac{\Delta W_C^* - d_w W + oA}{\theta} + \underbrace{k^* \left(\frac{\partial}{\partial x} W \left(\frac{\partial W}{\partial x} \right) + \frac{\partial}{\partial y} W \left(\frac{\partial W}{\partial y} \right) \right)}_{\text{XIII overland flow}}$ <p style="text-align: right;">If A <= 0</p>
Nutrient availability (N)	$\frac{\partial N}{\partial t} = \underbrace{I_N}_{\text{XV nutrient input}} - \underbrace{r_N N}_{\text{XVI nutrient loss}} + \underbrace{\rho_D u (r_A A + r_w W)}_{\text{XVII decomposition}} - \underbrace{u \frac{g[N]}{s+[N]} Bf^*}_{\text{XVIII plant uptake}} + \underbrace{W \theta \left(D_N \left(\frac{\partial^2 [N]}{\partial x^2} + \frac{\partial^2 [N]}{\partial y^2} \right) + \frac{k^*}{\theta} \left(\frac{\partial}{\partial x} [N] \left(\frac{\partial W}{\partial x} \right) + \frac{\partial}{\partial y} [N] \left(\frac{\partial W}{\partial y} \right) \right) \right)}_{\text{XIX nutrient diffusion}} + \underbrace{\frac{k^*}{\theta} \left(\frac{\partial}{\partial x} [N] \left(\frac{\partial W}{\partial x} \right) + \frac{\partial}{\partial y} [N] \left(\frac{\partial W}{\partial y} \right) \right)}_{\text{XX nutrient advection (Darcy flow)}}$ <p style="text-align: right;">If A >= 0</p> $\frac{\partial N}{\partial t} = I_N - r_N N + \rho_D u (r_w (W + A)) - \underbrace{u \frac{g[N]}{s+[N]} Bf^*}_{\text{XVIII plant uptake}} + \underbrace{oA[N]}_{\text{XXI overland flow}} + W \theta \left(D_N \left(\frac{\partial^2 [N]}{\partial x^2} + \frac{\partial^2 [N]}{\partial y^2} \right) + \frac{k^*}{\theta} \left(\frac{\partial}{\partial x} [N] \left(\frac{\partial W}{\partial x} \right) + \frac{\partial}{\partial y} [N] \left(\frac{\partial W}{\partial y} \right) \right) \right)$ <p style="text-align: right;">If A <= 0</p>

Table 1: Null model equations. Symbols indicated with * vary for the different model versions, and are specified for each model version in Table 2.

Parameter	Interpretation	Units
g	Plant growth rate	yr^{-1}
b	Plant respiration rate	yr^{-1}
d	Plant mortality rate	yr^{-1}
s	Nutrient saturation constant	g.m^{-3}
D_B	Diffusion coefficient biomass	$\text{m}^2.\text{yr}^{-1}$
ρ_D	Peat dry bulk density	g.m^{-3}
r_A	Acrotelm decomposition rate	yr^{-1}
r_w	Catotelm decomposition rate	yr^{-1}
d_w	Drainage parameter	yr^{-1}
o	Overland flow parameter	yr^{-1}
θ	Peat porosity	-
I_N	Nutrient input rate	$\text{g.m}^{-2}.\text{yr}^{-1}$
r_N	Nutrient loss rate	yr^{-1}
u	Nutrient content organic matter	g.g^{-1}
D_N	Diffusion coefficient nutrients	$\text{m}^2.\text{yr}^{-1}$
P_{EXCESS}	Net water input (for null model)	m.yr^{-1}
A_{OPT}	Optimum distance water table for vegetation growth (for peat accumulation mechanism)	m
c	Controlling decline of evapotranspiration away from optimum (for peat accumulation mechanism)	-
y	Controlling width of evapotranspiration plateau close to optimum (for peat accumulation mechanism)	m^{-y}
t_V	Maximum transpiration rate (for nutrient accumulation mechanism)	$\text{m}^3.\text{g}^{-1}.\text{yr}^{-1}$
E_T	Maximum evaporation rate (for nutrient accumulation mechanism)	m.yr^{-1}
h_1	Distance to water table below which stress occurs (for nutrient accumulation mechanism)	m
h_2	Rooting depth (for nutrient accumulation mechanism)	m
z	Reference height (for nutrient accumulation mechanism)	m
P	Net water input rate (for nutrient accumulation mechanism)	m.yr^{-1}
k^*	Range of hydraulic conductivity (for water ponding mechanism)	m.yr^{-1}
k_0	Hydraulic conductivity (in null model)	m.yr^{-1}
k_{opt}	Hydraulic conductivity when distance to the water table equals A_{OPT} (for water ponding mechanism)	m.yr^{-1}
β	Controlling decline in hydraulic conductivity with increasing acrotelm thickness (for water ponding mechanism)	$\text{m}^{-2\beta}$
α	Angle of peatland slope (see appendix 4A)	Degrees
B	Vascular plant biomass	g.m^{-2}
A	Acrotelm thickness	m
W	Water table height	m
N	Available nutrient pool	g.m^{-2}
$[N]$	Nutrient concentration in the groundwater	g.m^{-3}
k^*	Hydraulic conductivity function	m.yr^{-1}
ΔW_C^*	Net water input rate	m.yr^{-1}
f^*	Function(s) for plant water stress and evaporation	-
f_{Plant}	Plant water stress function	-
f_{Evap}	Evaporation function	-

Table 2: Model parameters, state variables and functions and their interpretation

State Variable 3: Groundwater table

Groundwater table dynamics consist of water input (XI), losses of water from the peatland toward the surroundings (drainage) (XII), loss through overland flow (XIII) and lateral transport of water that is driven by differences in hydraulic head (XIV). We assumed that the long-term net water input rate is constant (Belyea and Clymo 2001), and that loss through drainage increases linearly with catotelm thickness (Hilbert et al. 2000). Also, when the water table is above the peatland surface (hollow state), it is indicated by a negative acrotelm thickness. In this case the porosity of this upper water layer is set to 1 (Hilbert et al. 2000), and limited infiltration capacity of hollows is mimicked by including a loss term through overland flow (Foster et al. 1983; Foster and King 1984; Glaser 1992b; Belyea 2007). Overland flow and drainage, however, are not modeled explicitly in this study, because these depend on the regional setting of the peatland (Ingram 1982; Clymo 1984; Belyea and Baird 2006). Hence, we modeled overland flow and drainage as water losses from the model. Lateral transport of water through the peat was described by Darcy's law (Rycroft et al. 1975; Rietkerk et al. 2004a; Borren and Bleuten 2006), meaning that lateral transport of water is driven by differences in hydraulic head.

State variable 4: Available nutrient pool

Available nutrient pool dynamics comprise external input (XV), nutrient losses (e.g. through leaching, XVI), release through decomposition (XVII), plant uptake (XVIII), diffusion due to nutrient concentration gradients (XIX), advection due to groundwater movement (XX) and loss of nutrients through overland flow (XXI). We model nutrients in the soluble reactive phase, which can be taken up by plants. Nutrient concentration is defined as the quotient of available nutrient pool and the amount of water (i.e. height of the water table multiplied by the effective porosity). We assumed that external input of nutrients into the system (e.g. by atmospheric deposition) is constant (Rietkerk et al. 2004a). We also assumed that decomposition leads to mineralization, meaning that nutrients become available for plants and that, for example, microbes do not immobilize them. In our model, nutrient content of the plant biomass does not change when it dies and turns into litter. Subsequently, the nutrient content of plant litter does not change during storage in acrotelm and catotelm (Rietkerk et al. 2004a; Chapter 3). Removal of nutrients through plant uptake was assumed proportional to plant growth. Further, we assumed that nutrient losses (e.g. by leaching) increase linearly with available nutrient pool (Pastor et al. 2002; Rietkerk et al. 2004a). We assumed that Fick's law could describe the nutrient diffusion process, meaning that the flux of nutrients increases linearly with increasing nutrient

concentration gradient (Rietkerk et al. 2004a). Finally, nutrients are dissolved in the groundwater, meaning that groundwater flow also implies advective transport of dissolved nutrients.

Mechanisms associated with peatland pattern formation

Mechanism 1: Peat accumulation

The peat accumulation mechanism was switched on by making plant growth most favorable at intermediate acrotelm thickness. Therefore, plant water stress needed to become a function of acrotelm thickness. For this we assumed that water stress occurs both at high water tables because of waterlogging and at low water tables because of desiccation. Therefore, the water stress function was modeled as an optimum curve, with highest values (least stress) occurring at intermediate acrotelm thickness (Fig. 2a; Hilbert et al. 2000; Belyea and Clymo 2001). It can be shown intuitively why this water stress function describes the peat accumulation mechanism. In the case that vascular plant biomass, available nutrient pool and groundwater table are in equilibrium, acrotelm thickness will reach equilibrium when input of plant litter equals losses through decomposition. Because plant litter production is linearly related to plant biomass (see section “Vascular plant biomass”), litter production will follow the same shape as the water stress function (Fig. 2a). Because decomposition is linearly related to acrotelm thickness (see section “Acrotelm thickness”), mass loss through decomposition will be a linear function of acrotelm thickness (Fig. 2a). Figure 2a shows that this yields three possible situations in which the acrotelm thickness is in equilibrium: a stable, low productive, wet state and a stable, higher productive dry state. In between there is a tipping point at which the acrotelm thickness is in equilibrium, but a slight perturbation will move the system toward one of the stable states. If acrotelm thickness increases at this tipping point, production exceeds decomposition and the acrotelm will grow toward the dry state. If acrotelm thickness decreases at this tipping point, decomposition exceeds production and the acrotelm will shrink toward the wet state. Further, the peat accumulation mechanism is also expressed by a negative relationship between evaporation rate and acrotelm thickness (Table 2; Hilbert et al. 2000).

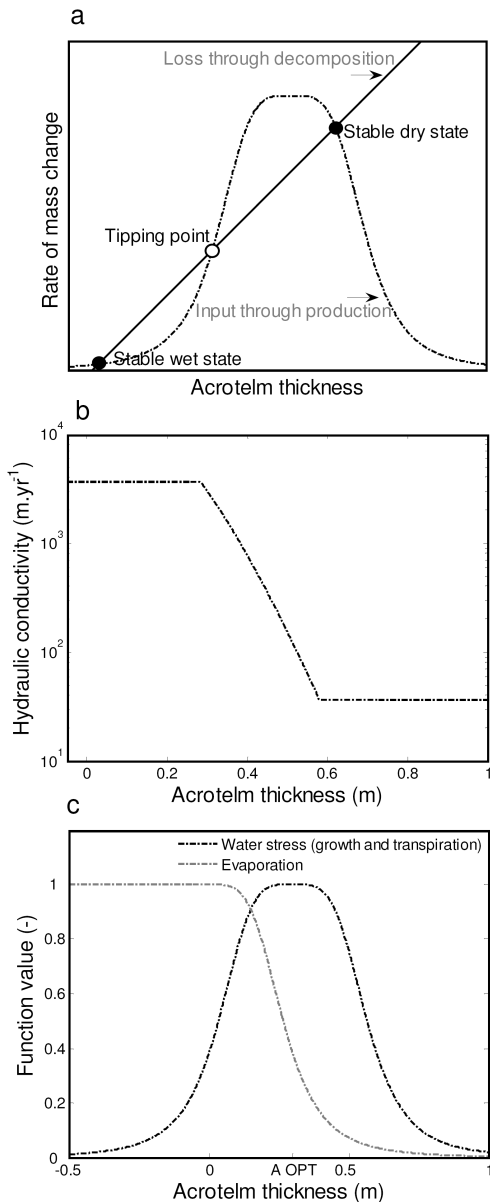


Figure 2: a) Conceptual graph illustrating the peat accumulation mechanism. Just above the tipping point, production exceeds decomposition; meaning development toward a stable dry state. Just below the tipping point, decomposition exceeds production; meaning development toward a stable wet state. b) If the water ponding mechanism is switched on, a negative relation between acrotelm thickness and hydraulic conductivity is assumed. The graph shows the specific numerical form of this relation, using the parameter values as specified in appendix 4B. Note that the y-axis is logarithmic. c) If the nutrient accumulation mechanism and the peat accumulation mechanism are both switched on, evaporation rate and vegetation water stress are controlled by acrotelm thickness. It is assumed that evaporation decreases with increasing acrotelm thickness. Water stress occurs when the water table is higher (inhibition because of waterlogging) or lower (inhibition because of desiccation) than the optimum acrotelm thickness A_{OPT} .

Mechanism 2: Water ponding

The water ponding mechanism can be switched on by letting hydraulic conductivity of the peat decrease with increasing acrotelm thickness. This decrease may be due to the increased degree of decomposition with depth (Ivanov 1981; Swanson and Grigal 1988), and due to increased pressure of the overlying peat mass (Belyea and Clymo 2001). Empirical studies indeed show that the hydraulic conductivity of the peat decreases with acrotelm thickness (Romanov 1968; Ivanov 1981), suggesting that the depth integrated conductivity (transmissivity) of the peat layer is lower for ridges and hummocks than for hollows (Ivanov 1981; Swanson and Grigal 1988; Couwenberg and Joosten 2005). We assumed that hydraulic conductivity exponentially increases with decreasing acrotelm thickness (Fig. 2b; Romanov

1968). To limit the number of parameters in the model, we scaled the hydraulic conductivity function relative to the acrotelm thickness for optimal plant growth (Table 3). Further, we assumed a maximum difference in hydraulic conductivity between hollows and hummocks of two orders of magnitude (Fig. 2b; Waddington and Roulet 1997; Givnish et al. 2008). It is important to note that we did not take into account vertical variations in hydraulic conductivity. We used the acrotelm thickness to calculate the hydraulic conductivity (Fig. 2b), and assumed that this calculated value was constant for the entire peat column. This approach is similar to the approach used in previous studies that modeled the water ponding mechanism (Swanson and Grigal 1988; Couwenberg 2005; Couwenberg and Joosten 2005). Instead of considering two vegetation states and two values of hydraulic conductivities, however, our model uses a functional relationship between conductivity and acrotelm thickness (Fig. 2b). Although this is a simplification of reality, this approach does introduce lower conductivity of hummocks/ridges as compared to hollows in the model, which subsequently affects lateral transport. So, this approach is suitable for our current purpose.

Mechanism 3: Nutrient accumulation

The nutrient accumulation mechanism was switched on by letting transpiration rate increase with increasing vascular plant biomass. This creates the possibility of nutrient accumulation, because patches with higher vascular plant biomass will transpire more water than their surroundings, and therefore water and nutrients will flow toward these high-density vegetated patches (Chapter 3). If the nutrient accumulation mechanism is switched on, transpiration and evaporation are both explicitly addressed in the model (Table 3). The growth of vascular plants may promote an increase in transpiration rates (Frankl & Schmeidl 2000; Andersen et al. 2005). We assumed that transpiration could be reduced due to water stress (Rietkerk et al. 2004a; Ridolfi et al. 2006; Broksma and Bierkens 2007). Therefore we applied the same water stress function for transpiration as used for plant growth (Table 3). The same water stress function was also used for evaporation. This was done to separate the effects of acrotelm thickness (and the peat accumulation mechanism) and the nutrient accumulation mechanism (Table 3). Hence, evaporation became a function of acrotelm thickness if the peat accumulation and the nutrient accumulation were switched on simultaneously (Table 3). Then, we assumed that the rate of evaporation decreases towards zero as acrotelm thickness increases (Hilbert et al. 2000), and that the maximum evaporation rate is reached when acrotelm thickness is close to zero (Hilbert et al. 2000; Nungesser 2003). To minimize the number of

parameters in the model, we assumed similar shapes for the functions for evaporation and water stress, the latter controlling plant growth and transpiration (Fig. 2c).

Model version	f^*	ΔW_C^*	k^*
(Between 0 and 1)			
a) Null model	$f^* = \frac{W - z - h_2}{h_1 - h_2}$	$\Delta W_C^* = P_{Excess}$	$k^* = k_0$
b) PA	$f^* = \frac{1}{1 + c(A - A_{OPT})^y}$	$\Delta W_C^* = P_{Excess}$	$k^* = k_0$
c) NA	$f^* = \frac{W - z - h_2}{h_1 - h_2}$	$\Delta W_C^* = P - t_V B f^* - E_T f^*$	$k^* = k_0$
d) PA+NA	$f_{Plant} = \frac{1}{1 + c(A - A_{OPT})^y}$	$\Delta W_C^* = P - t_V B f_{Plant} - E_T f_{Evap}$	$k^* = k_0$
	$f_{Evap} = \frac{1}{1 + c \max(0, A)^y}$		
e) WP	$f^* = \frac{W - z - h_2}{h_1 - h_2}$	$\Delta W_C^* = P_{Excess}$	$k^* = \frac{k_{Aopt}}{\left(1 + \left((\max(0, A))^2 - A_{OPT}^2\right)\right)^\beta}$
f) PA+WP	$f^* = \frac{1}{1 + c(A - A_{OPT})^y}$	$\Delta W_C^* = P_{Excess}$	$k^* = \frac{k_{Aopt}}{\left(1 + \left((\max(0, A))^2 - A_{OPT}^2\right)\right)^\beta}$
g) WP+NA	$f^* = \frac{W - z - h_2}{h_1 - h_2}$	$\Delta W_C^* = P - t_V B f^* - E_T f^*$	$k^* = \frac{k_{Aopt}}{\left(1 + \left((\max(0, A))^2 - A_{OPT}^2\right)\right)^\beta}$
h) PA+WP+NA	$f_{Plant} = \frac{1}{1 + c(A - A_{OPT})^y}$	$\Delta W_C^* = P - t_V B f_{Plant} - E_T f_{Evap}$	$k^* = \frac{k_{Aopt}}{\left(1 + \left((\max(0, A))^2 - A_{OPT}^2\right)\right)^\beta}$
	$f_{Evap} = \frac{1}{1 + c \max(0, A)^y}$		

Table 3: Mathematical formulation of the full-factorial analysis of the effects of peat accumulation (PA), water ponding (WP) and nutrient accumulation (NA) on peatland pattern formation. See Table 1 for interpretations of parameters and their assigned value.

Model analyses

We studied the effect of three mechanisms on peatland pattern formation, using a full-factorial design. Hence, we analyzed eight model versions (Table 3), both on flat ground and on peatland slopes. We performed a linear stability analysis for the model versions on flat ground. This analysis is used to identify for each model version the environmental conditions (in terms of nutrients and precipitation regime)

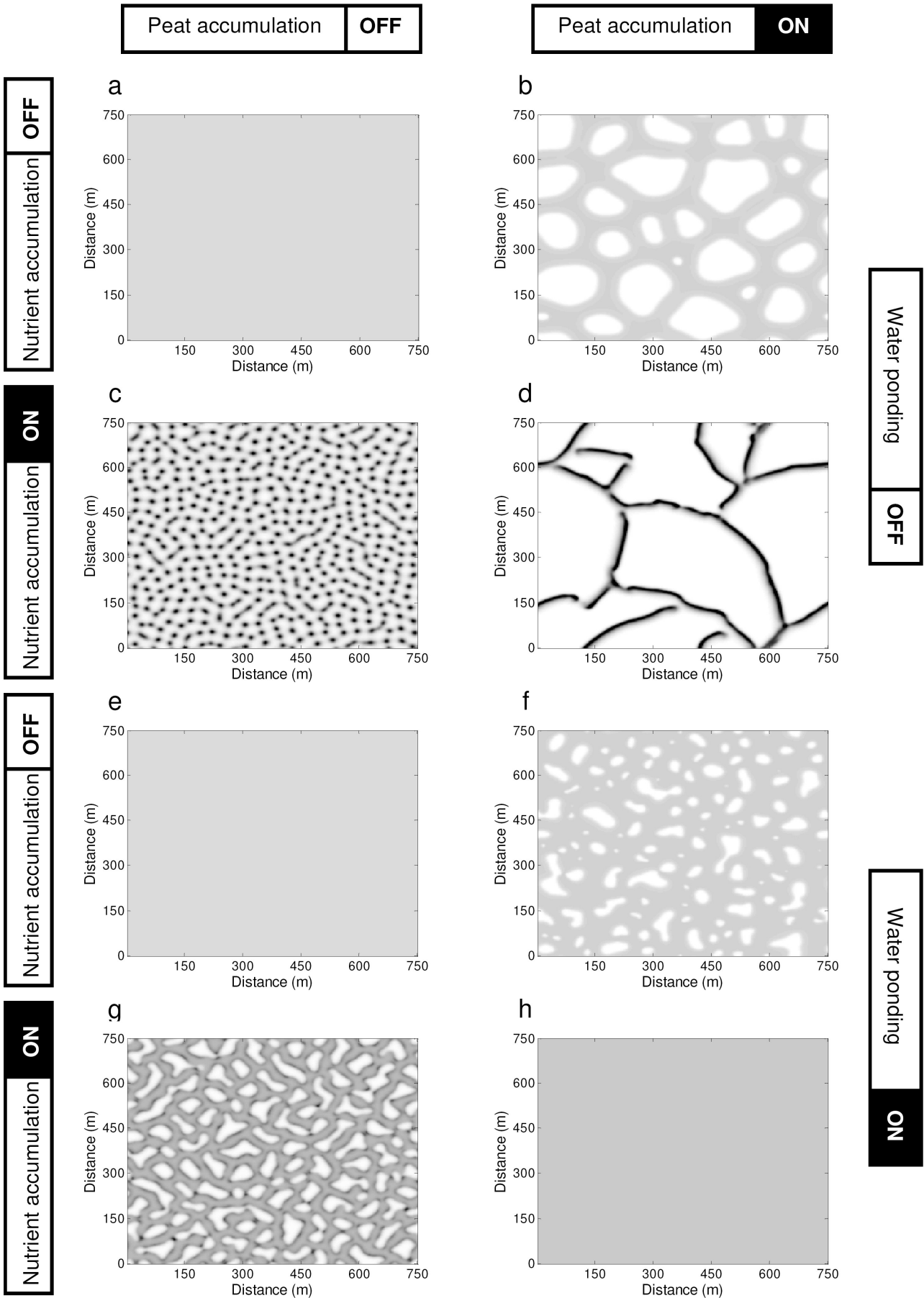
under which pattern formation can occur. The linear stability analysis is presented in appendix 4C. We also performed numerical simulations on a two-dimensional domain to study the emerging patterns (see appendix 4B for details). Subsequently, we tested the sensitivity and robustness of the model results by performing an elasticity analysis (e.g. Hartemink et al. 2008) and by identifying the sensitivity range (Eppinga et al. 2006) of the model parameters. These analyses are presented in 4D. Finally, we compared the spatial scale of the modeled patterns with field observations of patterned peatlands from previous studies (presented in appendix 4E), using a geostatistical method originally developed for the analysis of self-organized spatial fracture patterns on frozen ground (Plug and Werner 2001).

Results

Peatland pattern formation on flat ground

We selected for each model (if possible) a parameterization leading to pattern formation on flat ground (Fig. 3). The null model showed that in the absence of the three mechanisms, the peatland developed into an area that was homogeneously covered with vascular plants (Fig. 3a). Due to the peat accumulation mechanism, sparsely vegetated hollows emerged within a matrix of densely vegetated hummocks (Fig. 3b). The underlying pattern in hydrology revealed that the water level in hollows was lower than in hummocks (see appendix 4F for a detailed overview). Further, the underlying pattern in nutrients revealed higher nutrient concentrations in hollows as compared to hummocks (appendix 4F).

If the nutrient accumulation was switched on, a pattern emerged because of a scale-dependent feedback; areas with higher biomass transpire more water, and hence attract water and nutrients from the surroundings, which further amplifies spatial differences in biomass. This resulted in a pattern of densely vegetated hummocks, surrounded by more sparsely vegetated hollows (Fig. 3c). If the peat accumulation mechanism and the nutrient accumulation mechanism were both switched on expansion of the hollows forced hummocks into the narrow spaces between separate hollows. As a result, the hummocks merged into narrow ridges, forming a net-like or maze structure (Fig. 3d). The underlying pattern in hydrology revealed that the water level under ridges was lower than in hollows (appendix 4F). The underlying pattern in nutrients revealed higher nutrient concentrations in ridges as compared to hollows (appendix 4F).



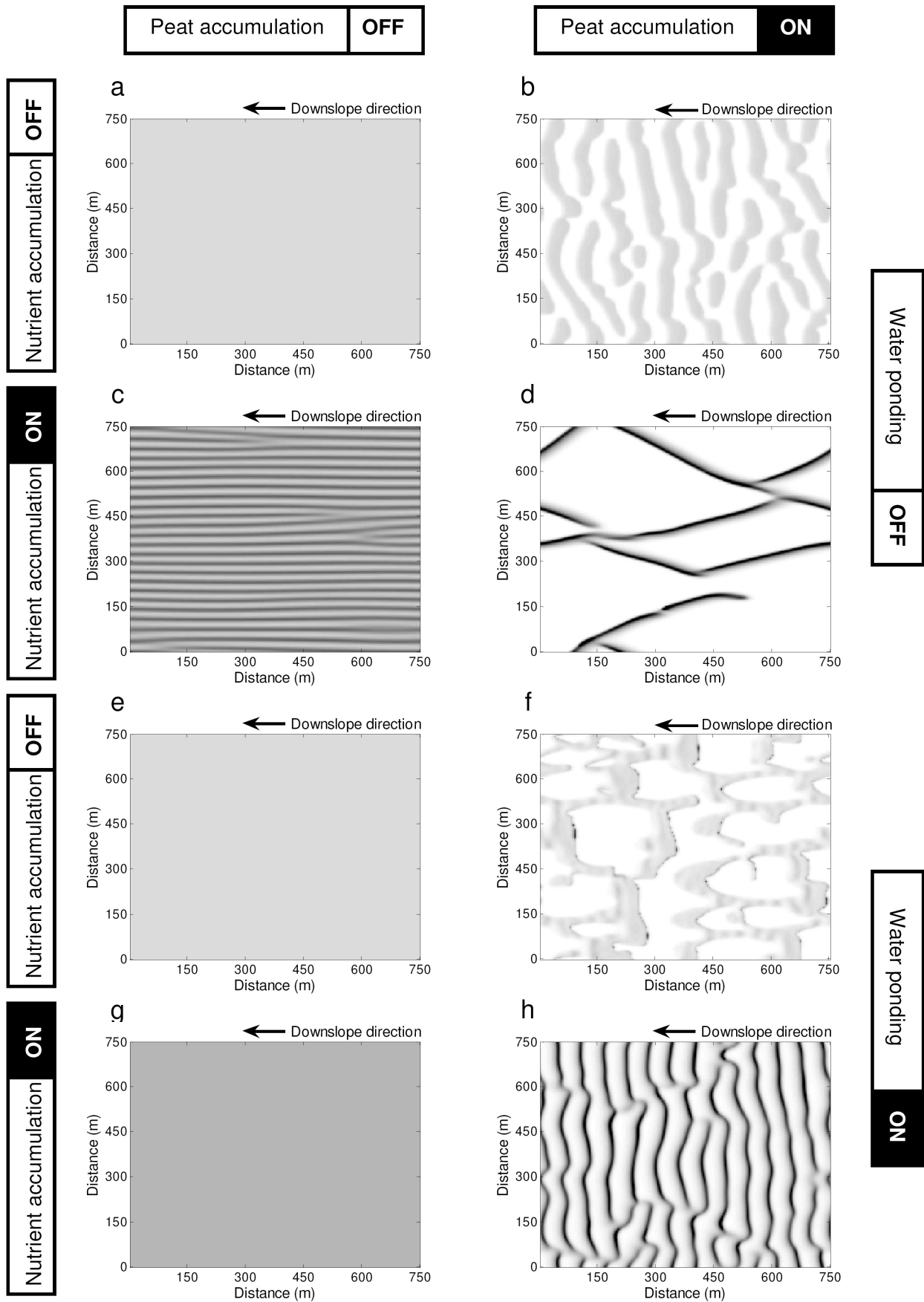
◀ **Figure 3:** Two-dimensional numerical model simulations mimicking peatlands on flat ground. Each panel representing a plan view of the vascular plant biomass distribution on a square peatland area of 750*750 m. Darker colors indicate areas with higher vascular plant biomass, the colormap ranging from white (0 gB.m⁻²) to black (2500 gB.m⁻²). For the simulations the following parameters values were used: $P_{EXCESS} = 0.35$ m, $P = 2$ m, $I_N = 1.7$ gN.m⁻².yr⁻¹ (Brooks 1992; Bobbink et al. 1998; Hilbert et al. 2000; Chapter 3). Other parameter values are reported in appendix 4A. The different panels together show a full-factorial analysis of the effects of peat accumulation, nutrient accumulation and water ponding mechanisms. a) The null model; b) The model with only the peat accumulation mechanism; c) The model with only the nutrient accumulation mechanism; d) The model with both the peat accumulation and the nutrient accumulation mechanisms, e) The model with only the water ponding mechanism; f) The model with both the peat accumulation and the water ponding mechanisms, g) The model with both the water ponding and the nutrient accumulation mechanisms, h) The model with the peat accumulation, water ponding and nutrient accumulation mechanisms.

If only the water ponding mechanism was switched on, no peatland patterning emerged (Fig. 3e). If the water ponding was added to the model with the peat accumulation mechanism, the size of the hollows somewhat decreased, but there was no qualitative change in the patterning (Fig. 3f vs. Fig. 3b). If the water ponding was added to the model with the nutrient accumulation mechanism, the individual hummocks merged to a maze pattern of connected hummocks merging into ridges (Fig. 3g vs. Fig. 3c).

If all three mechanisms were switched on simultaneously, formation of a stable pattern was not possible (Fig. 3h). If the parameterization was set within the parameter region of pattern formation (the Turing instability region, see appendix 4C), a pattern formed initially, but this pattern was not stable and died out, meaning that the system developed to a uniform wet state with no biomass (data not shown). A more detailed explanation of the relation between the modeled mechanisms and the morphology of the emerging patterns on flat ground is described in appendix 4G.

Peatland pattern formation on slopes

We also examined pattern formation on slopes (Fig. 4). Similar to the model simulation on flat ground, the null model showed that in the absence of the three mechanisms, the peatland developed into a slope that was homogeneously covered with vascular plants (Fig. 4a).



◀ **Figure 4:** Two-dimensional numerical model simulations mimicking peatlands on slopes (arrows indicate the downslope direction). Each panel representing a plan view of the vascular plant biomass distribution on a square and sloping peatland area of 750*750 m. Darker colors indicate areas with higher vascular plant biomass, the colormap ranging from white (0 gB.m^{-2}) to black (2500 gB.m^{-2}). For each panel, the downslope direction is from right to left. Parameter values are the same as in Fig. 3, except for Figures 4B and 4F. In these two simulations, stable patterns only formed at lower nutrient input rates, so lower values were used for these two simulations ($1.25 \text{ gN.m}^{-2}.\text{yr}^{-1}$ instead of $1.7 \text{ gN.m}^{-2}.\text{yr}^{-1}$). The different panels together show a full-factorial analysis of the effects of peat accumulation, nutrient accumulation and water ponding mechanisms. a) The null model; b) The model with only the peat accumulation mechanism; c) The model with only the nutrient accumulation mechanism; d) The model with both the peat accumulation and the nutrient accumulation mechanisms, e) The model with only the water ponding mechanism; f) The model with both the peat accumulation and the water ponding mechanisms, g) The model with both the water ponding and the nutrient accumulation mechanisms, h) The model with the peat accumulation, water ponding and nutrient accumulation mechanisms.

Due to the peat accumulation mechanism, a linear ridge-hollow pattern emerged, in which the ridges and hollows were oriented perpendicular to the slope (Fig. 4b). The nutrient accumulation mechanism also drove the formation of a linear ridge-hollow pattern, but in this case the orientation of the stripes was parallel to the slope (Fig. 4c). If the peat accumulation and the nutrient accumulation mechanism were both switched on, an elongated net-like or maze pattern developed, meaning that the large hollows in between the ridges were wider in the direction of the slope (Fig. 4d). Therefore, the dominant orientation of the ridges was also parallel to the slope (Fig. 4d).

If only the water ponding mechanism was switched on, no pattern formation occurred (Fig. 4e). If the water ponding mechanism was added to the model with the peat accumulation mechanism, the dominant orientation of stripes was still perpendicular to the slope, but connecting ridges parallel to the slope also emerged (Fig. 4f). If the water ponding mechanism was added to the model with the nutrient accumulation mechanism, stable pattern formation was not possible (Fig. 4g).

Interestingly, if the water ponding mechanism was added to the model with the nutrient accumulation mechanism and the peat accumulation mechanism (meaning that all three mechanisms were switched on), the orientation of the stripes reversed (Fig. 4h vs. 4d). A more detailed explanation of the relation between the modeled mechanisms and the morphology of the emerging patterns on peatland slopes is described in appendix 4G.

Sensitivity and robustness of the model results

Pattern formation could occur over a large range of nutrient input and precipitation rates. However, the parameter space for model versions without the nutrient accumulation mechanism was quite narrow (appendix 4C), meaning that for a fixed value of net water input rate, for example, pattern formation only occurred in a small range of nutrient input rates. Other parameters that imposed strong constraints on pattern formation were the plant respiration and mortality rates, and the vascular plant transpiration parameter (appendix 4D). The state variables in the model were most sensitive to changes in hydrological conditions as regulated by water input in the system (appendix 4D). Further, the model was also sensitive to parameters related to the vascular plant physiology (appendix 4D). The spatial scales of the modeled patterns were within the observed range in field studies, mostly at the upper end of this range (appendix 4E).

Discussion

Our model results suggest that the structuring mechanism(s) driving peatland surface patterning can be identified by analysis of the underlying patterns in nutrients and hydrology (see appendix 4F for a detailed overview). Until now, such specific predictions were not possible, because this is the first study that explicitly linked spatial surface patterning to underlying patterns in nutrients and hydrology for different (combinations of) structuring mechanisms. It is necessary to take into account underlying patterns in nutrients and hydrology, because the presence or absence of a structuring mechanism cannot be inferred from the surface pattern alone (Rietkerk et al. 2004a; Chapter 2; Fig 3; Fig 4). The presented modeling framework could simulate the variety of peatland patterns that occurs in nature, namely hummock-hollow patterning and maze patterns on flat ground (Fig. 3), but also linear patterns on peatland slopes (Fig. 4). These patterns were generated by a combination of structuring mechanisms that have been proposed and modeled before, but were not yet integrated into a single model. Importantly, the fact that we generated contrasting hypotheses with this approach (appendix 4F) will increase the inferential power of empirical studies on peatland surface patterning, which we will now explain in further detail.

Our study suggests that measuring the nutrient concentration in the mire water under hummocks and in hollows indicates whether the peatland surface pattern is driven by the nutrient accumulation mechanism or not (appendix 4F). In the field, water

samples can be taken at both hummocks and hollows to quantify the difference in nutrient status. An alternative way to quantify the nutrient status in hummocks and hollows is to harvest a plant species that grows both on hummocks and in hollows and measure the nutrient content and stoichiometry in these samples (De Wit et al. 1963; Vermeer and Berendse 1983; Wassen et al. 1995). The presence of the nutrient accumulation mechanism would induce higher nutrient concentrations on hummocks as compared to hollows. In the absence of the nutrient accumulation mechanism, this pattern in nutrients would be reversed. Another way to test the model predictions (appendix 4F) is to measure the height of the water table under hummocks and in hollows. The presence of the nutrient accumulation mechanism would induce lower water tables in hummocks as compared to hollows. In the absence of the nutrient accumulation mechanism, this hydrological pattern would be reversed (appendix 4F). These hydrological measurements are more demanding than nutrient measurements, but even a few measurement points of water table height in hummocks and hollows can provide enough information to accept or reject hypotheses (Chapter 3). Note that both types of measurements are relatively simple and short-term measurements in the field, meaning that longer-term field manipulations can be circumvented. These measurements of nutrients and hydrology have been carried out for a maze-patterned peatland in Western Siberia (Chapter 3). Our new model results have two new implications. First, measurements of nutrients and hydrology can also be used to identify the structuring mechanisms in other types of patterned peatlands, namely hummock-hollow and linearly patterned sloping peatlands (appendix 4F). Second, measurements of nutrients and hydrology can also be used to discriminate between alternative hypotheses (appendix 4F). Therefore, the model study presented here increases the inferential power of future empirical studies on peatland patterning.

Our modeling framework also enabled the investigation of the effect of combinations of mechanisms on peatland patterning. For example, the water ponding mechanism in isolation could not drive pattern formation, but the synergy with the other mechanisms was important on slopes (Fig. 4), because it yielded a different orientation of stripes (perpendicular to the slope, appendix 4G) as compared to stripes that formed due to the nutrient accumulation mechanism only (parallel to the slope, appendix G). Thus, perpendicular-oriented linear patterning on slopes requires either occurrence of the peat accumulation mechanism, or a synergetic combination of peat accumulation, nutrient accumulation and water ponding (Fig. 4, appendix 4G).

The structuring mechanisms driving peatland patterning has been the field of much speculation, but the long time-span of these mechanisms hampers actual experiment (Moore and Bellamy 1974). A common approach to circumvent this problem is inferring past process from current spatial patterns. Interpretations of current patterns benefit from a priori construction of multiple hypotheses (Platt 1964; Loehle 1987), a method of hypothesis testing that differs fundamentally from hypothesis generation based on a posteriori interpretation of data (Belyea and Lancaster 2002). Our model results generated contrasting hypotheses about different structuring mechanisms driving peatland patterning, and how the occurrence of each structuring mechanism would be reflected in surface pattern and underlying patterns in nutrients and hydrology (appendix 4F), which will benefit interpretations of empirical studies on peatland patterning.

Appendix 4A: Null model equations for the case of peatland slopes

In the model simulation on peatland slopes, we included a gradient of angle α in one direction in the impermeable mineral subsoil. The water table height W is expressed relative to the datum, which is a mineral subsoil plane aligned with the slope at angle α . Following Brolsma and Bierkens (2007), the model equations then become:

$$\frac{\partial B}{\partial t} = \frac{g[N]}{s+[N]} Bf^* - bB - dB + D_B \left(\frac{\partial^2 B}{\partial x^2} + \frac{\partial^2 B}{\partial y^2} \right) \quad (\text{I-VII})$$

$$\frac{\partial A}{\partial t} = \frac{dB}{\rho_D} - r_A A - r_W W - \frac{\Delta W_C^* - d_W W}{\theta} - \frac{k^*}{\theta} \left(\frac{\partial}{\partial x} \left(W \left(\frac{\partial W}{\partial x} \right) + W \tan \alpha \right) + \frac{\partial}{\partial y} W \left(\frac{\partial W}{\partial y} \right) \right) \quad \text{If } A \geq 0$$

$$\frac{\partial A}{\partial t} = \frac{dB}{\rho_D} - r_W (A + W) - \frac{\Delta W_C^* - d_W W + oA}{\theta} - \frac{k^*}{\theta} \left(\frac{\partial}{\partial x} \left(W \left(\frac{\partial W}{\partial x} \right) + W \tan \alpha \right) + \frac{\partial}{\partial y} W \left(\frac{\partial W}{\partial y} \right) \right) \quad \text{If } A \leq 0$$

$$\frac{\partial W}{\partial t} = \frac{\Delta W_C^* - d_W W}{\theta} + \frac{k^*}{\theta} \left(\frac{\partial}{\partial x} \left(W \left(\frac{\partial W}{\partial x} \right) + W \tan \alpha \right) + \frac{\partial}{\partial y} W \left(\frac{\partial W}{\partial y} \right) \right) \quad \text{If } A \geq 0$$

$$\frac{\partial W}{\partial t} = \frac{\Delta W_C^* - d_W W + oA}{\theta} + \frac{k^*}{\theta} \left(\frac{\partial}{\partial x} \left(W \left(\frac{\partial W}{\partial x} \right) + W \tan \alpha \right) + \frac{\partial}{\partial y} W \left(\frac{\partial W}{\partial y} \right) \right) \quad \text{If } A \leq 0$$

$$\frac{\partial N}{\partial t} = I_N - r_N N + \rho_D u (r_A A + r_W W) - u \frac{g[N]}{s+[N]} Bf^* + W \theta \left(D_N \left(\frac{\partial^2 [N]}{\partial x^2} + \frac{\partial^2 [N]}{\partial y^2} \right) + \frac{k^*}{\theta} \left(\frac{\partial}{\partial x} \left([N] \left(\frac{\partial W}{\partial x} \right) + [N] \tan \alpha \right) + \frac{\partial}{\partial y} [N] \left(\frac{\partial W}{\partial y} \right) \right) \right) \quad \text{If } A \geq 0$$

$$\frac{\partial N}{\partial t} = I_N - r_N N + \rho_D u (r_W (W + A)) - u \frac{g[N]}{s+[N]} Bf^* + oA[N] + W \theta \left(D_N \left(\frac{\partial^2 [N]}{\partial x^2} + \frac{\partial^2 [N]}{\partial y^2} \right) + \frac{k^*}{\theta} \left(\frac{\partial}{\partial x} \left([N] \left(\frac{\partial W}{\partial x} \right) + [N] \tan \alpha \right) + \frac{\partial}{\partial y} [N] \left(\frac{\partial W}{\partial y} \right) \right) \right) \quad \text{If } A \leq 0$$

Note that in the case of $\alpha = 0$ (no slope), the model equations reduce to the model for flat ground.

Appendix 4B: Model parameterization and initialization

Most parameter values were taken directly from previous model studies (Table B1). For the newly introduced parameters in our model, order-of-magnitude realistic values could be derived from literature, which will now be explained. The value for the maximum relative growth rate was taken from a study that measured growth of the vascular plants *Betula pubescens* and *Pinus sylvestris* in a subarctic environment (Karlsson and Nordell 1987). The nutrient uptake constant was parameterized as half the nutrient concentration that was added in the ‘high nutrient concentration’ treatment of the same experiment (Karlsson and Nordell 1987). The value of the nutrient: carbon ratio for plants was based upon measurements in ombrotrophic Siberian bogs (Yefremov and Yefremova 2001). The overland flow parameter controls the maximum depth of pools, and it was calibrated so that maximum pool depths of 0.4 m were reached in the simulations (Belyea and Lancaster 2002). In the null model, the net water input rate was assigned a typical value of the annual difference between precipitation and losses through evapotranspiration (Brooks 1992; Hilbert et al. 2000). In model versions in which the nutrient accumulation mechanism was switched on, the value of net water input rate was based upon field

data from a maze-patterned plain in the Great Vasyugan Bog, Western Siberia, showing that apart from precipitation (in that area 0.5 m yr^{-1} ; Semenova and Lapshina 2001) there was an additional water input from upland areas of approximately 0.005 m.day^{-1} (Chapter 3). Data on peat bulk density shows large variation, and also the bulk density of peat changes along the depth profile (Belyea and Clymo 2001; Frolking et al. 2001). In all model versions, the peat bulk density controls the acrotelm height increment because of litter input, and the nutrient mass that is released via decomposition. Because both processes mainly occur at the top of the acrotelm, we took a typical value for peat bulk density at the upper part of the acrotelm (Schulze et al. 2002). In model versions with both the peat accumulation and nutrient accumulation mechanisms, we needed parameter values that determine the rate at which evaporation and transpiration decrease when the acrotelm thickness moves away from the optimum. The parameters were set in a way that the ratio of Actual Evapotranspiration (AET) and Potential Evaporation (PET) became very small at an acrotelm thickness of 0.4-0.8 m (Juusela et al. 1970 in: Brooks 1992). Also, these model versions contained a parameter that mainly influences the width of the plateau in the stress function near the optimum value (see Fig. 2C in the main text of Chapter 4). The value of this parameter was set in a way that plants experienced little water stress ($> 75\%$ of optimum) when the distance of the water table is between 0.1-0.5 m, and that evaporation is not much reduced ($> 75\%$ of optimum) if the water table is within 0.2 m of the peatland surface (Kim and Verma 1996). Data on hydraulic conductivity shows large variation (e.g. Waddington and Roulet 1997). For the null model, we followed Reeve et al. (2001), who reported values for hydraulic conductivity that are somewhere at the lower end of the spectrum. For the model with variable conductivity, we adopted the function similar to Romanov (1968) and Ivanov (1981), however, we slightly modified the function because otherwise it yields unlikely high values for hydraulic conductivity in cases of a shallow acrotelm (Van der Schaaf 1999). It is important not to overestimate values for hydraulic conductivity, because this may lead to a bias toward the nutrient accumulation mechanism (Givnish et al. 2008). Instead, the range of hydraulic conductivity in the model was based on the values reported in the study by Givnish et al. (2008): $0.1\text{-}10 \text{ m.day}^{-1}$. The study by Givnish et al. (2008) was not focused on boreal peatlands. Therefore, it is important to note that similar values for hydraulic conductivity have also been measured in hummocks and hollows of boreal peatlands (Waddington and Roulet 1997). In our model simulations, however, these relatively low values of hydraulic conductivity lead to very large differences in hydraulic head (up to two orders of magnitude larger than observed in the field), which has a

stimulating effect on the nutrient flux. So, our results revealed that the value of hydraulic conductivity is mainly affecting the differences in hydraulic head, rather than the nutrient flux. Therefore, we also performed two (one-dimensional, to limit computation time) simulations using a value for hydraulic conductivity at the upper end of the spectrum of measured values (1000 m.day^{-1} , Waddington and Roulet 1997; Ross et al. 2006). In these alternative runs, the differences in hydraulic head in our model closely resembled hummock-hollow differences in hydraulic head as observed in the field (an average hummock-hollow difference of 0.0044 m in the model version with peat accumulation and 0.0065 m in the model version with both peat accumulation and nutrient accumulation mechanisms vs. 0.005 m observed in the field study of Chapter 3). Summarizing, we used relatively low values of hydraulic conductivity to prevent a bias toward the nutrient accumulation mechanism (Givnish et al. 2008). These low values, however, lead to larger differences in hydraulic head than observed in the field. The value for the peatland slope was calculated from field data of a study on patterned blanket bogs in Scotland (Belyea 2007). Finally, we needed the value for acrotelm thickness that provides the optimum growing conditions (and maximal transpiration rates, in case the nutrient accumulation mechanism is switched on) for vascular plants. We used the value for which Belyea and Clymo (2001) reported maximum production rates (Belyea and Clymo 2001), which coincides with the depth at which vascular plants overtake the evaporation losses of peat mosses by transpiration in the conceptual model of Lafleur et al. (2005).

The numerical two-dimensional numerical simulations were run using a spatial grid of 250×250 elements of $3 \times 3 \text{ m}$ each, using forward Euler integration. The numerical simulations were carried out using the Matlab programming environment (Version 7.5.0, Mathworks 2007). With the numerical simulations we studied patterning on both flat ground and slope. All simulations were initialized with a catotelm of 3 m and an available nutrient pool of 5 g.m^{-2} . Subsequently, random spatial heterogeneity was introduced at initialization: in half of the grid cells initial biomass was low (600 gB.m^{-2}), in the other half it was higher (700 gB.m^{-2}). In models with the peat accumulation mechanism but without the nutrient accumulation mechanism, spatial heterogeneity in acrotelm thickness was also introduced: half of the grid cells was set wet (water table 0.3 m above the surface), the other half was set dry (water table 0.3 m below the surface). Without introducing this spatial heterogeneity in acrotelm thickness, these model versions would develop into a uniform hollow state (due to the parameterization). All model simulations were run until stability was reached. For

model simulations on peatland slopes, we included a gradient in one direction in the impermeable mineral subsoil (Brolsma and Bierkens 2007, see appendix 4A for analytical details).

Parameter	Interpretation	Units	Value	References
<i>g</i>	Plant growth rate	yr ⁻¹	2	Karlsson and Nordell (1987)
<i>b</i>	Plant respiration rate	yr ⁻¹	0.2	Rietkerk et al. (2004)
<i>d</i>	Plant mortality rate	yr ⁻¹	0.1	Pastor et al. (2002); Rietkerk et al. (2004)
<i>s</i>	Nutrient saturation constant	g.m ⁻³	10	Karlsson and Nordell (1987)
<i>D_B</i>	Diffusion coefficient biomass	m ² .yr ⁻¹	2	Rietkerk et al. (2004)
<i>ρ_D</i>	Peat dry bulk density	g.m ⁻³	30000	Schulze et al. (2002)
<i>r_A</i>	Acrotelm decomposition rate	yr ⁻¹	0.0025	Hilbert et al. (2000)
<i>r_W</i>	Catotelm decomposition rate	yr ⁻¹	0.00025	Hilbert et al. (2000)
<i>d_W</i>	Drainage parameter	yr ⁻¹	0.05	Hilbert et al. (2000)
<i>o</i>	Overland flow parameter	yr ⁻¹	5	Belyea and Lancaster (2002)
<i>θ</i>	Peat porosity	-	0.92	Nungesser (2003)
<i>I_N</i>	Nutrient input rate	g.m ⁻² .yr ⁻¹	0-5	Bobbink et al. (1998), Rietkerk et al. (2004)
<i>r_N</i>	Nutrient loss rate	yr ⁻¹	0.1	Pastor et al. (2002), Rietkerk et al. (2004)
<i>u</i>	Nutrient content organic matter	g.g ⁻¹	0.01	Yefremov and Yefremova 2001; Rietkerk et al. (2004)
<i>D_N</i>	Diffusion coefficient nutrients	m ² .yr ⁻¹	10	Rietkerk et al. (2004)
<i>P_{EXCESS}</i>	Net water input (for null model)	m.yr ⁻¹	0-2.5	Brooks (1992); Belyea (2007); Chapter 3
<i>A_{OPT}</i>	Optimum distance water table for vegetation growth (for peat accumulation mechanism)	m	0.3	Belyea and Clymo (2001), Lafleur et al. (2005)
<i>c</i>	Controlling decline of evapotranspiration away from optimum (for peat accumulation mechanism)	-	200	Juusela et al. (1970), Brooks (1992)
<i>y</i>	Controlling width of evapotranspiration plateau close to optimum (for peat accumulation mechanism)	m ^y	4	Kim and Verma (1996)
<i>t_v</i>	Maximum transpiration rate (for nutrient accumulation)	m ³ .g ⁻¹ .yr ⁻¹	0.005	Rietkerk et al. (2004)

E_T	mechanism) Maximum evaporation rate (for nutrient accumulation mechanism)	m.yr ⁻¹	0.3	Hilbert et al. (2000)
h_1	Distance to water table below which stress occurs (for nutrient accumulation mechanism)	m	0	Rietkerk et al. (2004)
h_2	Rooting depth (for nutrient accumulation mechanism)	m	-0.5	Rietkerk et al. (2004)
z	Reference height (for nutrient accumulation mechanism)	m	1	Rietkerk et al. (2004)
P	Water input rate (for nutrient accumulation mechanism)	m.yr ⁻¹	0-2.5	Brooks (1992); Belyea (2007); Chapter 3
k^*	Range of hydraulic conductivity (for water ponding mechanism)	m.yr ⁻¹	36.5-3650	Reeve et al. 2001; Givnish et al. (2008)
k_0	Hydraulic conductivity (in null model)	m.yr ⁻¹	500	Reeve et al. 2001
k_{opt}	Hydraulic conductivity when distance to the water table equals AOPT (for water ponding mechanism)	m.yr ⁻¹	3000	Reeve et al. 2001; Givnish et al. (2008)
β	Controlling decline in hydraulic conductivity with increasing acrotelm thickness (for water ponding mechanism)	m ^{-2β}	20	Waddington and Roulet (1997)
α	Angle of peatland slope (see appendix 4A)	Degrees	1.72	Belyea (2007)
B	Vascular plant biomass	g.m ⁻²	-	Model state variable
A	Acrotelm thickness	m	-	Model state variable
W	Water table height	m	-	Model state variable
N	Available nutrient pool	g.m ⁻²	-	Model state variable
$[N]$	Nutrient concentration in the groundwater	g.m ⁻³	-	Model state variable
k^*	Hydraulic conductivity function	m.yr ⁻¹	-	Model function
ΔW_C	Net water input rate	m.yr ⁻¹	-	Model function
f^*	Function(s) for plant water stress and evaporation	-	-	Model function(s)
f_{Plant}	Plant water stress function	-	-	Model function
f_{Evap}	Evaporation function	-	-	Model function

Table B1: Model parameters, state variables and functions and their assigned values.

Appendix 4C: Linear stability analysis

In this appendix, we present the methods and the results of a linear stability analysis of the model versions on flat ground. With this analysis it can be calculated under which environmental conditions (here nutrient and water input regime) peatland patterning may occur.

Methods

Because we studied the effects of three mechanisms that could be switched on or off, the full-factorial analysis comprised eight model versions. The mean field version of each model could be solved implicitly (meaning in terms of the model parameters rather than numerically) using Mathematica (Version 4.1; Wolfram 2004). For each model version, we calculated the environmental conditions (nutrient and water input regime) under which a stable vegetated equilibrium with positive acrotelm thickness (from here referred to as the hummock state) existed. So, this exercise distinguished two parameter regions: a region where the hummock state is unstable and a region where the hummock state is not unstable. The latter region could be subdivided into two parameter regions: a region where the hummock state is stable and a region where pattern formation occurs. We performed for all model versions a linear stability analysis to identify the conditions (nutrient and precipitation regimes) under which pattern formation could occur. The idea of the method is that first, the equilibrium condition is calculated for which the entire peatland area is uniformly covered by hummocks. Then, this uniform hummock-state peatland is slightly perturbed. The shape of this perturbation is a sine-like wave function, meaning that in some areas the state variables are slightly increased, and in other areas the state variables are slightly decreased. So, the perturbation introduces spatial differences in the hummock-state peatland. Subsequently, it can be calculated whether these spatial differences will decrease over time (meaning that the system develops back into the uniform hummock state), or increase over time, meaning that the spatial differences amplify and lead to pattern formation. This latter case is referred to as a Turing instability, which is associated with pattern formation (e.g. HilleRisLambers et al. 2001). So, with the mathematical methods described above, we could distinguish three different cases: 1) The uniform hummock state is unstable; 2) The uniform hummock state is stable; 3) There is a Turing instability, associated with pattern formation. Given the parameter setting, it could be calculated which of the three cases occurred. So, we could obtain a parameter plane of environmental conditions (nutrient and water input regimes), and identified for each of the three cases the

parameter region in which it applied. We obtained such a parameter plane for each of the eight model versions.

It should be noted that the linear stability analysis underestimates the parameter regions for pattern formation, because patterns can also occur outside the linearly unstable region (Rietkerk et al. 2002). For example, in our model hummocks can survive in a patterned state far below the threshold where the homogeneous hummock state becomes unstable (as can be seen in Fig. 3b of the main text of Chapter 4, this pattern forms outside the Turing instability region as shown in Fig. C1b). Neither does the method enable us to distinguish whether patterns are indefinitely stable, because it does not reveal basin boundary collisions (Vandermeer and Yodzis 1999; Scheffer et al. 2001). In our model, a basin boundary collision can occur if in a pattern a number of deep hollows may develop over time (with a maximum depth of 0.4 m), and these hollows can keep expanding until hollows cover the entire peatland area. Despite these shortcomings, the linear stability analysis is suitable to provide a good idea whether patterns can occur in a certain model version, and how pattern formation is linked with nutrient and water input regime. We will now proceed with the mathematical details of the linear stability analysis.

The mathematical details of the linear stability analysis of the null model are presented, because this is the most simple model. The Turing matrix that we will now derive, however, is the same for all model versions. The null model consists of the following reaction equations:

$$F = \frac{dB}{dt} = \frac{g[N]}{s+[N]} Bf^* - bB - dB \quad (\text{I})$$

$$G = \frac{dA}{dt} = \frac{dB}{\rho_D} - r_A A - r_W W - \frac{\Delta W_C^* - d_W W}{\theta} \quad (\text{II})$$

$$H = \frac{dW}{dt} = \frac{\Delta W_C^* - d_W W}{\theta} \quad (\text{III})$$

$$I = \frac{dN}{dt} = I_N - r_N N + \rho_D u (r_A A + r_W W) - u \frac{g[N]}{s+[N]} Bf^* \quad (\text{IV})$$

Linear stability can then be checked with the four eigenvalues of the Jacobian matrix:

$$J = \begin{bmatrix} F_B & F_A & F_W & F_N \\ G_B & G_A & G_W & G_N \\ H_B & H_A & H_W & H_N \\ I_B & I_A & I_W & I_N \end{bmatrix} \quad (\text{V})$$

Where subscripts denote the derivatives. The spatially explicit model consists of the following equations:

$$\begin{aligned} \frac{\partial B}{\partial t} &= \frac{g[N]}{s+[N]} Bf^* - bB - dB + D_B \left(\frac{\partial^2 B}{\partial x^2} + \frac{\partial^2 B}{\partial y^2} \right) & (VI-XIX) \\ \frac{\partial A}{\partial t} &= \frac{dB}{\rho_D} - r_A A - r_w W - \frac{\Delta W_C^* - d_w W}{\theta} - \frac{k^*}{\theta} \left(\frac{\partial}{\partial x} W \left(\frac{\partial W}{\partial x} \right) + \frac{\partial}{\partial y} W \left(\frac{\partial W}{\partial y} \right) \right) \\ \frac{\partial W}{\partial t} &= \frac{\Delta W_C^* - d_w W}{\theta} + \frac{k^*}{\theta} \left(\frac{\partial}{\partial x} W \left(\frac{\partial W}{\partial x} \right) + \frac{\partial}{\partial y} W \left(\frac{\partial W}{\partial y} \right) \right) \\ \frac{\partial N}{\partial t} &= I_N - r_N N + \rho_D u (r_A A + r_w W) - u \frac{g[N]}{s+[N]} Bf^* + W \theta \left(D_N \left(\frac{\partial^2 [N]}{\partial x^2} + \frac{\partial^2 [N]}{\partial y^2} \right) + \frac{k^*}{\theta} \left(\frac{\partial}{\partial x} [N] \left(\frac{\partial W}{\partial x} \right) + \frac{\partial}{\partial y} [N] \left(\frac{\partial W}{\partial y} \right) \right) \right) \end{aligned}$$

Subsequently we introduce a perturbation of the following form:

$$\begin{bmatrix} B \\ A \\ W \\ N \end{bmatrix} = \begin{bmatrix} \hat{B} \\ \hat{A} \\ \hat{W} \\ \hat{N} \end{bmatrix} + \begin{bmatrix} p \\ q \\ r \\ s \end{bmatrix} e^{ikx+iky+\omega t} \quad (X)$$

Where the hats indicate equilibrium solutions for the mean field equations. To each variable a perturbation is added that has the shape of a wave with wavenumber k . We will consider spatially periodic solutions, meaning $\omega=0$ (e.g. Cross and Hohenberg 1993). The stability can still be checked with the Jacobian presented above, only some first-order spatial terms will be included, which we will calculate below.

For diffusion of the biomass:

$$D_B \left(\frac{\partial^2 B}{\partial x^2} + \frac{\partial^2 B}{\partial y^2} \right) = D_B \left(\frac{\partial^2 (\hat{B} + p e^{ikx+iky})}{\partial x^2} + \frac{\partial^2 (\hat{B} + p e^{ikx+iky})}{\partial y^2} \right) = D_B (-pk^2 e^{ikx+iky} - pk^2 e^{ikx+iky}) = D_B (-2pk^2 e^{ikx+iky}) \quad (XI)$$

For the Darcy-flow water transport term:

$$\frac{K}{\theta} \left(\frac{\partial}{\partial x} W \left(\frac{\partial W}{\partial x} \right) + \frac{\partial}{\partial y} W \left(\frac{\partial W}{\partial y} \right) \right) = \frac{K}{\theta} \left(\left(\frac{\partial W}{\partial x} \right)^2 + W \left(\frac{\partial^2 W}{\partial x^2} \right) + \left(\frac{\partial W}{\partial y} \right)^2 + W \left(\frac{\partial^2 W}{\partial y^2} \right) \right) = \dots \quad (XII)$$

$$\frac{K}{\theta} \left((\hat{W} + r e^{ikx+iky}) \left(\frac{\partial^2 (\hat{W} + r e^{ikx+iky})}{\partial x^2} \right) + (\hat{W} + r e^{ikx+iky}) \left(\frac{\partial^2 (\hat{W} + r e^{ikx+iky})}{\partial y^2} \right) \right) + h.o.t. \approx \dots \quad (XIII)$$

$$\frac{K}{\theta} \left(\hat{W} (-rk^2 e^{ikx+iky}) + \hat{W} (-rk^2 e^{ikx+iky}) \right) = \frac{-2K\hat{W}}{\theta} rk^2 e^{ikx+iky} \quad (XIV)$$

(h.o.t. stands for higher order terms)

For the nutrient diffusion term:

$$\begin{aligned}
 W\theta \left(D_N \left(\frac{\partial^2 [N]}{\partial x^2} + \frac{\partial^2 [N]}{\partial y^2} \right) \right) &= D_N \theta W \left(\frac{\partial^2 \left(\frac{N}{\theta W} \right)}{\partial x^2} + \frac{\partial^2 \left(\frac{N}{\theta W} \right)}{\partial y^2} \right) = \dots \quad (\text{XV-XIX}) \\
 D_N \theta W \left(\frac{\partial}{\partial x} \left(\frac{W\theta \frac{\partial N}{\partial x} - N\theta \frac{\partial W}{\partial x}}{W^2 \theta^2} \right) + \frac{\partial}{\partial y} \left(\frac{W\theta \frac{\partial N}{\partial y} - N\theta \frac{\partial W}{\partial y}}{W^2 \theta^2} \right) \right) &= \dots \\
 D_N \theta W \left(\frac{W^2 \theta^2 \left(\theta \frac{\partial W}{\partial x} \frac{\partial N}{\partial x} + W\theta \frac{\partial^2 N}{\partial x^2} - \theta \frac{\partial N}{\partial x} \frac{\partial W}{\partial x} - N\theta \frac{\partial^2 W}{\partial x^2} \right) - 2W \frac{\partial W}{\partial x} \left(W\theta \frac{\partial N}{\partial x} - N\theta \frac{\partial W}{\partial x} \right)}{W^4 \theta^4} \right. &= \dots \\
 \left. + \frac{W^2 \theta^2 \left(\theta \frac{\partial W}{\partial y} \frac{\partial N}{\partial y} + W\theta \frac{\partial^2 N}{\partial y^2} - \theta \frac{\partial N}{\partial y} \frac{\partial W}{\partial y} - N\theta \frac{\partial^2 W}{\partial y^2} \right) - 2W \frac{\partial W}{\partial y} \left(W\theta \frac{\partial N}{\partial y} - N\theta \frac{\partial W}{\partial y} \right)}{W^4 \theta^4} \right) &= \dots \\
 D_N \theta W \left(\frac{\left(W\theta \frac{\partial^2 N}{\partial x^2} - N\theta \frac{\partial^2 W}{\partial x^2} \right)}{W^2 \theta^2} + \frac{\left(W\theta \frac{\partial^2 N}{\partial y^2} - N\theta \frac{\partial^2 W}{\partial y^2} \right)}{W^2 \theta^2} + h.o.t. \right) &\approx \dots \\
 D_N \theta \hat{W} \left(\frac{-k^2}{\theta \hat{W}} s e^{ikx+iky} + \frac{Nk^2}{\theta \hat{W}} r e^{ikx+iky} + \frac{-k^2}{\theta \hat{W}} s e^{ikx+iky} + \frac{Nk^2}{\theta \hat{W}} r e^{ikx+iky} \right) &= -2D_N k^2 s e^{ikx+iky} + \frac{2D_N \hat{N} k^2}{\hat{W}} r e^{ikx+iky}
 \end{aligned}$$

For the nutrient advection term:

$$\begin{aligned}
 KW \left(\frac{\partial}{\partial x} [N] \left(\frac{\partial W}{\partial x} \right) + \frac{\partial}{\partial y} [N] \left(\frac{\partial W}{\partial y} \right) \right) &= KW \left(\frac{\left(\frac{W\theta \frac{\partial N}{\partial x} - N\theta \frac{\partial W}{\partial x}}{W^2 \theta^2} \right) \left(\frac{\partial W}{\partial x} \right) + \frac{N}{\theta W} \left(\frac{\partial^2 W}{\partial x^2} \right) + \dots}{\left(\frac{W\theta \frac{\partial N}{\partial y} - N\theta \frac{\partial W}{\partial y}}{W^2 \theta^2} \right) \left(\frac{\partial W}{\partial y} \right) + \frac{N}{\theta W} \left(\frac{\partial^2 W}{\partial y^2} \right)} \right) = \dots \quad (\text{XX-XXIII}) \\
 KW \left(\frac{N}{\theta W} \left(\frac{\partial^2 W}{\partial x^2} \right) + \frac{N}{\theta W} \left(\frac{\partial^2 W}{\partial y^2} \right) \right) &+ h.o.t. \approx \\
 \frac{K\hat{N}}{\theta} \left(\left(\frac{\partial^2 (\hat{W} + r e^{ikx+iky})}{\partial x^2} \right) + \left(\frac{\partial^2 (\hat{W} + r e^{ikx+iky})}{\partial y^2} \right) \right) &= \frac{-2K\hat{N}}{\theta} k^2 r e^{ikx+iky}
 \end{aligned}$$

Now adding these spatial terms we can disentangle a Turing Matrix and a perturbation Matrix:

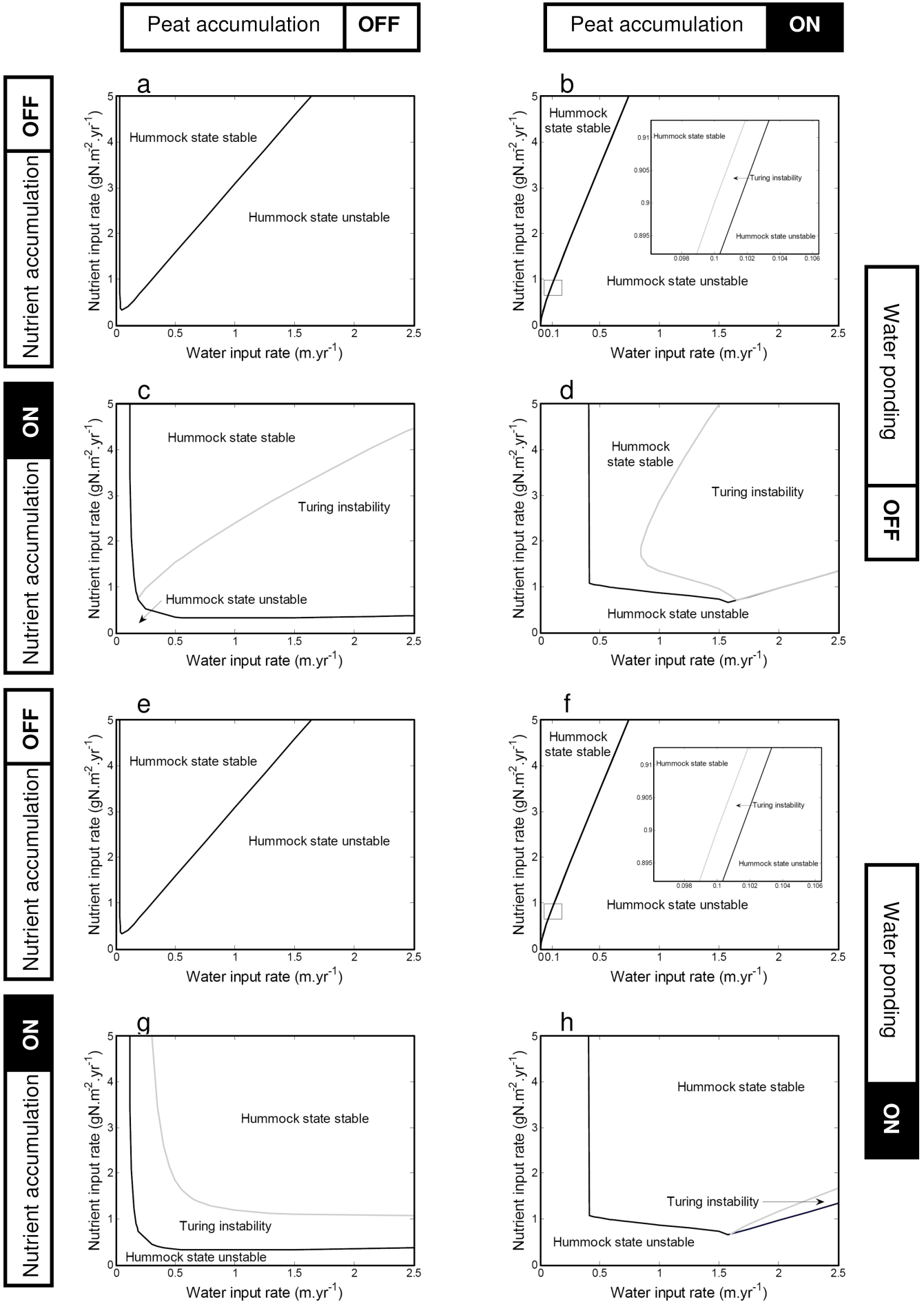
$$\begin{bmatrix} F_B - 2D_B k^2 & F_A & F_W & F_N \\ G_B & G_A & G_W + \frac{2K\hat{W}}{\theta} k^2 & G_N \\ H_B & H_A & H_W - \frac{2K\hat{W}}{\theta} k^2 & H_N \\ I_B & I_A & I_W + \frac{2D_N \hat{N} k^2}{\hat{W}} - \frac{2K\hat{N}}{\theta} k^2 & I_N - 2D_N k^2 \end{bmatrix} * \begin{bmatrix} p \\ q \\ r \\ s \end{bmatrix} e^{ikx+iky} \quad (\text{XXIV})$$

Now the dominant eigenvalue of this Turing matrix as a function of the wavenumber k gives the stability of the equilibrium. We distinguished three possibilities which are indicated by different parameter regions in Figure C1: 1) The dominant eigenvalue is positive at the zero wavenumber, this means that the hummock/ridge equilibrium is unstable. 2) The dominant eigenvalue is always zero, this means that the hummock/ridge equilibrium is always stable. 3) The dominant eigenvalue is positive for a certain band of non-zero wavelengths, this means that spatially heterogeneous perturbations of certain wavelengths will be amplified over time, indicating pattern formation. For the parameter regions where this is the case we use the term ‘‘Turing instability’’ in Figure C1. Note that in the above derivation the hydraulic conductivity was treated as a constant. In the model versions including the water ponding mechanism, hydraulic conductivity is dependent on acrotelm thickness. Apart from including the acrotelm function as indicated in Table 3 of the main text of Chapter 4, the dependency of acrotelm thickness only leads to additional higher order terms, so this dependency does not alter the Turing Matrix of the linear stability analysis.

Results

Pattern formation was not possible in the null model (the model with all three mechanisms switched off, Fig. C1a). The hummock state was stable at low precipitation and high nutrient input rates. The hummock state became unstable if precipitation increased or nutrient input decreased (Fig. C1a).

Due to the peat accumulation mechanism, the hummock state became more sensitive to precipitation, so that the precipitation threshold below which hummocks could survive decreased (Fig. C1b).



▲ Figure C1: *Linear stability analysis of the hummock (or ridge) state as a function of nutrient and precipitation regimes. The different panels together show a full-factorial analysis of the effects of peat accumulation, water ponding and nutrient accumulation mechanisms on the stability of the hummock state. The Turing instability indicates the region within the parameter space in which the hummock state is unstable to spatial perturbations, thereby indicating the possibility for pattern formation. a) The null model; b) The model with only the peat accumulation mechanism; c) The model with only the nutrient accumulation mechanism; d) The model with both the peat accumulation and the nutrient accumulation mechanisms, e) The model with only the water ponding mechanism; f) The model with both the peat accumulation and the water ponding mechanisms, g) The model with both the water ponding and the nutrient accumulation mechanisms, h) The model with the peat accumulation, water ponding and nutrient accumulation mechanisms.*

Also, a parameter region emerged in which the hummock state became unstable for spatially heterogeneous perturbations (referred to as a Turing instability), which means that in this parameter region pattern formation was possible. The size of this parameter region, however, was small (Fig. C1b).

If the nutrient accumulation mechanism was switched on, the parameter region in which the hummock state was stable drastically increased, mainly because vascular plants could survive at high precipitation rates (Fig. C1c vs. Fig. C1a). Also, a relatively large parameter region where pattern formation was possible emerged (Fig. C1c). If both the peat accumulation and the nutrient accumulation mechanisms were switched on, the parameter region for pattern formation slightly shifted toward wetter and more nutrient-rich conditions (Fig. C1d).

The water ponding mechanism did not have a distinct effect when added to the null model (Fig. C1e vs. Fig. C1a), or to the model with the peat accumulation mechanism (Fig. C1f vs. Fig. C1c). In combination with the nutrient accumulation mechanism, however, the water ponding mechanism increased the parameter region for pattern formation at low water input rates, whereas it decreased the parameter region for pattern formation at high water input rates (Fig. C1g vs. C1b). Interestingly, if all three mechanisms were switched on simultaneously, the parameter region for pattern formation was very small (Fig. C1h).

Appendix 4D: Model sensitivity and robustness

Methods to calculate model sensitivity

We performed a local sensitivity analysis, meaning that we examined how the equilibrium state would respond to a change in a parameter value. Note that the

water ponding mechanism cannot be included in a mean field model, because this mechanism influences only hydraulic conductivity. In turn, hydraulic conductivity only affects lateral (spatial) flow processes, which are not included in the mean field model. Further, we used the null model for parameters that were not present in the model with both the peat accumulation and nutrient accumulation mechanisms. For each parameter, we calculated how a change in the parameter value would affect the equilibrium values of the four state variables of the model (an elasticity analysis, e.g. Hartemink et al. 2008):

$$\text{Sensitivity}_{S_i p_j} = p_j \frac{\partial \hat{S}_i}{\partial p_j} \quad (1)$$

In which S denotes a state variable and p a parameter. The hat on S indicates that this is the equilibrium point of the state variable as a function of parameters, which were obtained using Mathematica (Version 4.1; Wolfram 2004). For most parameters we used the equilibrium situation of model version with the peat accumulation and nutrient accumulation mechanisms and the same parameterization as in Figure 3d of the main text of Chapter 4. For the parameters P_{EXCESS} , h_1 , h_2 and z we used the null model with the same parameterization as in Figure 3a of the main text of Chapter 4. The second term in equation (1) indicates the change in the state variable per unit of change in the parameter. The first term in equation (1) standardizes the outcome from an absolute into a relative sensitivity, which enables comparisons between parameters, despite the large variation in absolute parameter values (see Table B1 in appendix 4B).

Results model sensitivity

The results of the sensitivity analysis are listed in Table D1. The state variable vascular plant biomass was most sensitive to the nutrient input rate parameter, the plant respiration rate and the parameter controlling the nutrient content of the organic matter (Table D1). The state variable acrotelm thickness was most sensitive to the parameters controlling the water input rate (Table D1). The state variable groundwater level was also very sensitive to these parameters, but this state variable also had a high sensitivity for plant mortality rate and dry bulk density of the peat (Table D1). The available nutrient pool was most sensitive to water input rate and the vascular plant transpiration rate (if the nutrient accumulation mechanism was switched on). Further, this state variable was also sensitive to a change in the plant growth rate (Table D1). It can be concluded that the state variables in the peatland model are most sensitive to changes in hydrological conditions as regulated by water

input in the system. Further, the model is also sensitive to parameters related to the vascular plant physiology.

Parameter	Interpretation	Sensitivity Vascular plant biomass (g.m-2)	Sensitivity Acrotelm thickness (m)	Sensitivity Groundwater table (m)	Sensitivity Available nutrient pool (g.m-2)
g	Plant growth rate	62	0.06	0.25	-2.0
b	Plant respiration rate	-324	-0.30	-1.3	-0.22
d	Plant mortality rate	-267	-0.20	4.1	-0.40
s	Nutrient saturation constant	-52	-0.05	-0.21	1.7
p_D	Peat dry bulk density	246	0.18	-4.1	1.1
r_A	Acrotelm decomposition rate	197	0.14	-3.3	0.86
r_W	Catotelm decomposition rate	49	0.04	-0.82	0.21
d_W	Drainage parameter	3.12	0.01	-0.09	0.08
θ	Peat porosity	-52	-0.05	-0.21	-0.29
I_N	Nutrient input rate	335	0.31	1.3	1.9
r_N	Nutrient loss rate	-52	-0.05	-0.21	-0.29
u	Nutrient content organic matter	-283	-0.27	1.1	1.6
P_{EXCESS}	Net water input (for null model)	4.04	-0.60	6	-0.08
A_{OPT}	Optimum distance water table for vegetation growth (for peat accumulation mechanism)	127	0.38	-2.1	0.47
c	Controlling decline of evapotranspiration away from optimum (for peat accumulation mechanism)	-18	-0.05	0.31	-0.10
y	Controlling width of evapotranspiration plateau close to optimum (for peat accumulation mechanism)	32	0.09	-0.50	0.14
t_V	Maximum transpiration rate (for nutrient accumulation mechanism)	107	0.45	-3.0	2.7
E_T	Maximum evaporation rate (for nutrient accumulation mechanism)	1.8	0.008	-0.05	0.04
h₁	Distance to water table below which stress occurs (for nutrient accumulation mechanism)	-59	-0.08	0	0.28
h₂	Rooting depth (for nutrient accumulation mechanism)	-27	-0.04	0	0.13
z	Reference height (for nutrient accumulation mechanism)	-5.4	-0.007	0	0.03
P	Water input rate (for nutrient accumulation mechanism)	-111	-0.47	3.2	-2.8

Table D1: Sensitivity of the model as indicated by an elasticity analysis

Methods to calculate robustness of the model results

The sensitivity analysis examined the effect of a change in a parameter value on the equilibrium state of the mean field model solution. To assess the robustness of the model results, we also analyzed for each parameter the range (with a maximum of one order-of-magnitude smaller or larger) in which this parameter could be changed without leading to a qualitatively different model outcome (cf. Eppinga et al. 2006). More specifically, we used the model version with the peat accumulation and nutrient accumulation mechanisms and the parameterization leading to pattern formation as shown in Figure 3d of the main text of Chapter 4. By performing a linear stability analysis as described in appendix 4C we could subsequently analyze for each parameter the range within which pattern formation could occur (while keeping the other parameters at their default values). The sensitivities of the parameters P_{EXCESS} , k_{AOPT} and β were analyzed using the model version with the peat accumulation and water ponding mechanisms (with a linear stability analysis around the point $P_{EXCESS} = 0.222 \text{ m.yr}^{-1}$ and $I_N = 1.7 \text{ g.m}^{-2}.\text{yr}^{-1}$). The sensitivities of the model parameters h_1 , h_2 and z were analyzed using the model version with only the nutrient accumulation and the parameterization leading to pattern formation as shown in Figure 3c of the main text of Chapter 4. The sensitivity ranges of the model parameters are listed in Table D2.

Results model robustness

As shown in Figure C1 in appendix 4C, pattern formation can occur over a large range of nutrient input and precipitation rates. However, the parameter space for model versions without the nutrient accumulation mechanism is quite narrow (Fig. C1d, C1f), meaning that for a fixed value of precipitation excess, for example, pattern formation only occurs in a small range of nutrient input rates. Other parameters that impose strong constraints on pattern formation are the plant respiration and mortality rates, and the vascular plant transpiration parameter (Table D2).

Parameter	Interpretation	Units	Default Value	Low limit pattern formation	High limit pattern formation
g	Plant growth rate	yr ⁻¹	2	0.66	2.60
b	Plant respiration rate	yr ⁻¹	0.2	0.08	0.35
d	Plant mortality rate	yr ⁻¹	0.1	0.08	0.18
s	Nutrient saturation constant	g.m ⁻³	10	7.4	49.1
D_B	Diffusion coefficient biomass	m ² .yr ⁻¹	2	< 0.2	4.7
ρ_D	Peat dry bulk density	g.m ⁻³	3.0*10 ⁴	1.3*10 ⁴	4.3*10 ⁴
r_A	Acrotelm decomposition rate	yr ⁻¹	2.5*10 ⁻³	< 2.5*10 ⁻⁴	3.8*10 ⁻³
r_W	Catotelm decomposition rate	yr ⁻¹	2.5*10 ⁻⁴	< 2.5*10 ⁻⁵	1.0*10 ⁻³
d_W	Drainage parameter	yr ⁻¹	0.05	< 0.005	> 0.5
o	Overland flow parameter	yr ⁻¹	5	n.a.*	n.a.*
θ	Peat porosity	(-)	0.92	< 0.09	1
I_N	Nutrient input rate	g.m ² .yr ⁻¹	1.7	0.97	6.90
r_N	Nutrient loss rate	yr ⁻¹	0.1	< 0.01	0.49
u	Nutrient content organic matter	g.g ⁻¹	0.01	< 0.001	0.019
D_N	Diffusion coefficient nutrients	m ² .yr ⁻¹	10	< 1	19
P_{EXCESS}	Net water input (for null model)	m.yr ⁻¹	0.222	0.221	0.223
A_{OPT}	Optimum distance water table for vegetation growth (for peat accumulation mechanism)	m	0.3	< 0.03	0.59
c	Controlling decline of evapotranspiration away from optimum (for peat accumulation mechanism)	(-)	200	< 20	1730
y	Controlling width of evapotranspiration plateau close to optimum (for peat accumulation mechanism)	m ^y	4	< 3	< 5
t_v	Maximum transpiration rate (for nutrient accumulation mechanism)	m ³ .g ⁻¹ .yr ⁻¹	0.005	0.0035	0.017
E_T	Maximum evaporation rate (for nutrient accumulation mechanism)	m.yr ⁻¹	0.3	< 0.03	> 3
h₁	Distance to water table below which stress occurs (for nutrient accumulation mechanism)	m	0	-0.48	1
h₂	Rooting depth (for nutrient accumulation mechanism)	m	-0.5	-1	-0.02
z	Reference height (for nutrient accumulation mechanism)	m	1	0.29	4.91
P	Water input rate (for nutrient accumulation mechanism)	m.yr ⁻¹	2	0.85	2.99
k₀	Maximal hydraulic conductivity (for water ponding mechanism)	m.yr ⁻¹	500	335	> 5*10 ³
k_{AOPT}	Maximal hydraulic conductivity (for water ponding mechanism)	m.yr ⁻¹	3000	< 300	> 3*10 ⁴
β	Controlling decline in hydraulic conductivity with increasing acrotelm thickness (for water ponding mechanism)	m ^{-2β}	20	< 2	125
α	Steepness of the peatland slope	Degrees	1.72	1.55	> 17.2

Table D2: Robustness of the model results as indicated by the sensitivity range of the model parameters.

Appendix 4E: Comparison of model results with field observations

In this appendix, we calculate some simple statistical metrics of the model results presented in Figures 3 and 4 of the main text of Chapter 4. We compare these results with field observations of patterned peatlands.

Method

A standard approach of spatial pattern analysis is to perform a spectral analysis (Renshaw and Ford 1984; Couteron and Lejeune 2001; Van de Koppel et al. 2005; Barbier et al. 2006). A spectral analysis provides dominant wavelengths within the spatial pattern. In our modeled patterns, however, one wave consists of one hummock/ridge and one hollow. Because we are interested in the characteristic length scales of hummocks/ridges and hollows separately, we used an alternative approach.

We adopted the approach of Plug and Werner (2001), who developed a method for characterizing characteristic length scales in self-organized polygon networks on frozen ground. Each modeled pattern was converted into a Boolean map in which each cell was categorized either as hummock/ridge or hollow (Fig. E1). The criterion to assign the hummock/ridge state to each model grid cell was based on acrotelm thickness, or, for patterns with high biomass, based on a biomass threshold (Table E1; Table E2). This “hummock/ridge-criterion” was chosen in a way that the Boolean maps closely resembled the patterns presented in Figures 3 and 4 of the main text of Chapter 4 (Fig. E1). For each pattern on flat ground, we measured the lengths of hummocks and hollows that were encountered along 1,000 sample lines that dissect the modeled pattern at randomly selected angles and originate from randomly selected locations (Fig. E1; Plug and Werner 2001). For the peatland patterns on slopes, we did not use randomly oriented sample lines, but determined characteristic length scales along 100 sample lines that were oriented parallel to the slope, and 100 sample lines that were oriented perpendicular to the slope (Wu et al. 2006). Hence, this yielded for each pattern a collection of hummock/ridge lengths and a collection of hollow lengths. The characteristic length scales were subsequently determined by taking the median value of each collection (Plug and Werner 2001). The collections were also used to calculate the standard deviations of the characteristic length scales.

1): Biomass distribution as presented in the main text of Chapter 4

2): Converted to a boolean ridge-hollow map, which is dissected by 1,000 random sample lines

3): Along each sample line, the occurrence and the lengths of hummocks, ridges and hollows are measured

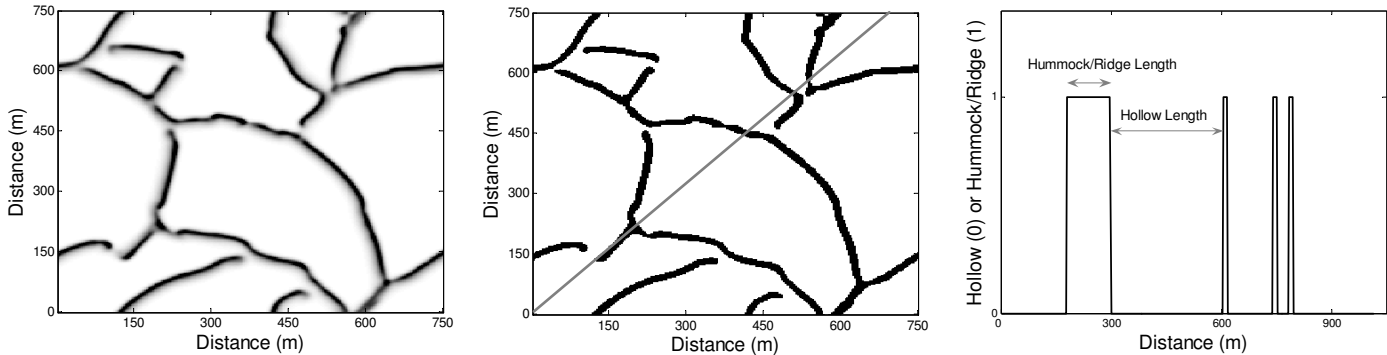


Figure E1: Procedure to assess the characteristic length scale of hummocks/ridges and hollows for the patterns that were presented in the main text of Chapter 4. Here, the model version with the peat accumulation and nutrient accumulation mechanisms on flat ground is used as an example. The model output is converted into a Boolean map. Then, the length of hummocks/ridges and hollows is measured along 1,000 random sample lines (1 sample line is drawn as an illustration) the pattern. This yields for both hummocks/ridges and hollows a characteristic length scale with a standard deviation.

Further, we calculated for each pattern the fraction of the surface that was covered by hummocks/ridges and the fraction that was covered by hollows. Also, for the patterns that contained isolated hollows (Figures 3b,d,f,g and 4f of the main text of Chapter 4), we also calculated for these hollows the average area and its standard deviation.

We compared the statistical metrics obtained from the pattern analyses with values reported in previous studies on real peatland patterns. It is important to note that it is not our intention to explain the patterning of these specific field sites by our model runs. Our model aims to assess the effects of pattern-forming mechanisms in general, and it does not include site-specific conditions (in terms of slope, situation in the catchment area, vegetation type, etc.) of any of the field sites that are mentioned. Instead, the comparison with field data is only to test whether the statistical metrics of the modeled patterns are in the same range as those observed in real peatland patterns.

Characteristic length scales of hummocks/ridges and hollows

For model runs on flat ground, the characteristic length scales of hummocks (12 m) and ridges (18 m) in the models were at the upper end of or slightly higher than the observed range in field observations (Table E1; Foster and King 1984; Nungesser 2003; Chapter 3). The characteristic length scale was higher if the ridges formed a continuous matrix across the model grid (Table E1). For some model runs, the characteristic length scale and area of hollows were similar to observed ranges in sloping peatlands (Belyea and Lancaster 2002). For flat ground, however, it has also been reported that hollows can be much larger, with a characteristic length scale of more than 100 m (Sjörs 1961). Indeed, hollows of this size class could also be observed in some of our model runs on flat ground (Table E1).

For model runs on slopes, two different types of patterns can be distinguished. The first category comprises ridges that are oriented parallel to the slope. Such patterning has been observed in the Florida Everglades (Wu et al. 2006). The modeled patterns had similar characteristic spatial scales in the direction parallel to the slope, but smaller characteristic spatial scales in the direction perpendicular to the slope as compared with observed patterns in the Everglades (Table E2; Wu et al. 2006). It should be noted, however, that the driving mechanism of patterning in the Everglades system (transport of sediment from hollows to hummocks/ridges; Larsen et al. 2007) might be different from the mechanisms considered in this study. The second category comprises ridges and hollows that are oriented perpendicular to the slope. One of these model runs had a characteristic ridge width of 12 m, alternating with wider hollows (characteristic width: 45 m). Smaller ridges alternating with wider hollows are indeed frequently observed in the field (e.g. Sjörs 1961; Foster et al. 1983). The two remaining model runs, however, consisted of ridges and hollows of similar widths (Table E2), the characteristic length scale being larger than usually observed. Further, the model run with the peat accumulation and nutrient accumulation mechanisms exhibited more of a maze-like structure as observed on relatively flat ground in Siberia (Rietkerk et al. 2004a).

The surface cover of ridges and hollows varied substantially between the model runs (roughly between 0.1 – 0.9). Field observations also show that the fraction of hummocks/ridges and hollows can vary substantially, even between peatlands in the same region ((hollow cover between 0.3 and 0.7 in Karofeld 1998; hollow cover roughly between 0.2 and 0.95 in Belyea 2007).

It can be concluded that the statistical metrics of the modeled pattern are in reasonable agreement with field observations, although most of the characteristic spatial scales of the modeled patterns are at the upper end of the observed range in field data. Therefore we think it is important to point out that the spatial scale of the modeled patterns is the result of the chosen values of the three spatial parameters in our model: diffusion speed of the biomass, diffusion speed of the nutrients and the hydraulic conductivity. The aim of this study was to develop a generally applicable model, and not to calibrate the model for one or more specific sites. Therefore, we adopted the values that were used in previous model studies (Rietkerk et al. 2004a; Chapter 2), but in principle the results of a reaction-diffusion model as we studied are scale-invariant (e.g. Othmer and Pate 1980; HilleRisLambers et al. 2001).

Model version	Hummock / ridge criterion	Hummock / ridge cover	Characteristic hummock/ ridge Length (m)	Hollow cover	Characteristic hollow length (m)	Hollow area (m ²)	Comparison with field observations of peatland patterns
a) Null	A > 0	0	-	1	-	-	
b) PA	A > 0	0.65	78 (31)*	0.35	60 (43)	5.7 *10 ³ (5.4 *10 ³)	Hollow areas of 2.3-1930 m ² on Scottish sloping site (Belyea and Lancaster 2002), meaning that observed areas in model are much larger. It has been noted, however, that on flat ground hollows can indeed grow much larger, with characteristic lengths of > 100 m (Sjörs 1961).
c) NA	B > 900	0.18	12 (6)	0.82	39 (42)	-	Nungesser (2003) reported characteristic hummock diameter between 0.48 and 12.4 m, meaning that the model results are at the upper end of this spectrum. A similar range of hummock widths was reported by Foster and King (1984): 3-12 m. Other studies, however, generally report a characteristic length of ~1 m (e.g. Belyea and Clymo 2001; Lafleur et al. 2003).
d) PA+NA	B > 900	0.1	18 (16)	0.9	129 (121)	-	The modeled pattern is slightly larger than observed spatial scales in a maze patterned Siberian peatland (Chapter 3) . In that study, ridges of 1-15 m and hollows of 25-100 m have been observed.
d) WP	A > 0	0	-	1	-	-	-
e) PA+WP	A > 0	0.85	78 (84)*	0.15	18 (14)	6.7 *10 ² (7.1 *10 ²)	Hollow areas of 2-1932 m ² on Scottish sloping site (Belyea and Lancaster 2002), meaning that observed areas in model are within this spectrum.
f) NA+WP	B > 500	0.66	39 (38)*	0.34	24 (16)	1.5 * 10 ³ (8.7 *10 ²)	Hollow areas of 2-1932 m ² on Scottish sloping site (Belyea and Lancaster 2002), meaning that observed areas in model are within this spectrum.
g) PA+NA + WP	A > 0	1	-	0	-	-	-

Table E1: Characteristic length scales of hummocks/ridges and hollows for the modeled patterns on slopes, and comparisons with field observations

Model version	Hummock / ridge criterion	Hummock / ridge cover	Characteristic hummock/ ridge Length (m)	Hollow cover	Characteristic hollow length (m)	Comparison with field observations of peatland patterns
a) Null	A > 0	0	-	1	-	-
b) PA	A > 0	0.56	Perpendicular: 88 (75) Parallel: 48 (12)	0.44	Perpendicular: 68 (68) Parallel: 36 (13)	Frequently observed that on slopes, the length of ridges and hollows is larger than their widths (Moore 1977; Foster and King 1984; Rydin and Jeglum 2006). Similar partitioning of the surface in ridges and hollows has also been observed (Belyea and Malmer 2004), but generally the observed width scales on slopes are smaller (in the orders of 1-10 m wide, Sjörs 1961; Moore 1977 Foster et al. 1983).
c) NA	B > 900	0.47	Perpendicular: 15 (2) Parallel: 750 (120)	0.53	Perpendicular: 18 (3) Parallel: 230 (79)	Patterning parallel to the slope has been observed in the Florida Everglades (Wu et al. 2006). Here, the ridges are > 100 m wide and 100s-1000s m in long, whereas the hollows are 140-360 m wide and 200-1500 m long (Wu et al. 2006). Also, similar cover for ridges was observed in these systems (0.02-0.58). It should be noted, however, that patterning in the Everglades might be driven by other mechanisms (Larsen et al. 2007), which were not considered in this study.
d) PA+NA	A > 0	0.09	Perpendicular: 18 (5) Parallel: 18 (13)	0.91	Perpendicular: 123 (92) Parallel: 129 (130)	Patterning parallel to the slope has been observed in the Florida Everglades (Wu et al. 2006). Here, the ridges are > 100 m wide and 100s-1000s m in long, whereas the hollows are 140-360 m wide and 200-1500 m long (Wu et al. 2006). Also, similar cover for ridges was observed in these systems (0.02-0.58). It should be noted, however, that patterning in the Everglades might be driven by other mechanisms (Larsen et al. 2007), which were not considered in this study.
d) WP	A > 0	0	-	1	-	-
e) PA+WP	A > 0	0.52	Perpendicular: 48 (47) Parallel: 76 (72)	0.48	Perpendicular: 56 (52) Parallel: 76 (59) Hollow area: $9.6 \cdot 10^3 \text{ m}^2$ $(1.7 \cdot 10^4 \text{ m}^2)$	Contradicts frequently reported notion that on slopes, the length of ridges and hollows is larger than their widths (Moore 1977; Foster and King 1984; Rydin and Jeglum 2006). Similar partitioning of the surface in ridge and hollow has also been observed (Belyea and Malmer 2004), but generally the observed width scales on slopes are smaller (in the orders of 1-10 m wide, Sjörs 1961; Moore 1977 Foster et al. 1983). Network structure seems similar to field observations from Siberia (Rietkerk et al. 2004a). Magnitude of hollow areas at upper end of observed range (Rydin and Jeglum 2006).
f) NA+WP	A > 0	1	-	0	-	-
g) PA+NA + WP	B > 900	0.22	Perpendicular: 42 (51) Parallel: 12 (2)	0.78	Perpendicular: 120 (163) Parallel: 45 (12)	Frequently observed that the ridges on slopes are several meters wide, but the hollows can be much wider, and as a result cover a larger fraction of the surface (e.g. Sjörs 1961; Foster et al. 1983; Rydin et al. 2003).

Table E2: Characteristic length scales of hummocks/ridges and hollows for the modeled patterns on slopes, and comparisons with field observations

Appendix 4F: Relation between driving mechanisms and underlying patterns in nutrients and hydrology

In this appendix, we present a Table that summarizes for each model version how the surface pattern is related to the underlying patterns in nutrients and hydrology (Table F1). Because the eight different model versions comprise a full-factorial analysis of the peat accumulation, nutrient accumulation and water ponding mechanisms, the Table summarizes how these driving mechanisms of peatland patterning can be identified by underlying patterns in nutrients and hydrology.

Table F1: Model predictions about how the occurrence of the mechanisms peat accumulation, water ponding and nutrient accumulation are reflected by the underlying patterns in nutrients and hydrology.

Model version	Surface pattern	Biomass Pattern	Pattern in nutrients	Pattern in hydrology
a) Null	Spatially uniform peatland surface on flat grounds and slopes. Either uniform hummock or uniform hollow state, depending on initial conditions	Spatially uniform distribution	Spatially uniform distribution	No differences in water table level
b) PA	On flat ground: Hummocks and hollows, hummocks merging to net or star-like ridges at high nutrient availability. On slopes: Linear ridge-hollow patterns oriented perpendicular to the slope.	Highest biomass on hummocks	Highest nutrient concentrations in hollows	Highest water tables under hummocks
b) NA	On flat ground: Hummocks and hollows, hummocks merging to net or star-like ridges at high nutrient availability. On slopes: Linear ridge-hollow patterns oriented parallel to the slope	Highest biomass on hummocks	Highest nutrient concentration under hummocks	Highest water tables in hollows
c) PA+NA	On flat ground: Hummocks and hollows, hummocks merging to net or star-like ridges at high nutrient availability, but hollows are much larger than ridges. On slopes: Elongated ridge-hollow maze patterns, dominant orientation parallel to the slope.	Highest biomass on hummocks	Highest nutrient concentration under hummocks	Highest water tables in hollows
d) WP	Spatially uniform peatland surface on flat grounds and slopes. Either uniform hummock or uniform hollow state, depending on initial conditions (peatland height)	Spatially uniform distribution	Spatially uniform distribution	No differences in water table level
e) PA+WP	On flat ground: Hummocks and hollows, hummocks merging to net or star-like ridges at high nutrient availability. On slopes: Linear ridge-hollow patterns oriented perpendicular to the slope, with some circular hollows.	Highest biomass on hummocks	Highest nutrient concentrations in hollows	Highest water tables under hummocks.
f) NA+WP	On flat ground: Hummocks and hollows, hummocks merging to net or star-like ridges at high nutrient availability. On slopes: Spatially uniform state, either uniform hummock or uniform hollow state, depending on initial conditions (peatland height)	Flat ground: Highest biomass on hummocks. On slopes: Spatially uniform distribution	Flat ground: Highest nutrient concentration under hummocks. On slopes: Spatially uniform distribution	Flat ground: Highest water tables in hollows. On slopes: Spatially uniform distribution
g) PA+NA+WP	On flat ground: Spatially uniform state, either uniform hummock or uniform hollow state, depending on initial conditions (peatland height). On slopes: Linear ridge-hollow patterns oriented perpendicular to the slope.	Flat ground: Spatially uniform distribution. On slopes: Highest biomass on hummocks	Flat ground: Spatially uniform distribution. On slopes: Highest nutrient concentration under hummocks	Flat ground: Spatially uniform distribution. On slopes: Highest water tables in hollows

Appendix 4G: Development of pattern morphology in the different model versions

In this appendix, we provide a detailed physical explanation of how the peat accumulation (PA), nutrient accumulation (NA) and water ponding (WP) mechanisms drive pattern morphology and the orientation of patterns on slopes. First we discuss patterning on flat ground (Fig. G1), followed by a discussion of patterning on slopes (Fig. G2). In the following, we use the term “hummock” for both hummocks and ridges. Further, the terms “parallel direction” and “perpendicular direction” refer to directions relative to the peatland slope.

The null model can be extended into the model with all three mechanisms via different pathways (Fig. G1, Fig. G2). When all possible pathways are considered, twelve different actions (meaning addition of a particular mechanism to a particular model version) can be distinguished. We will discuss each of these twelve actions for the patterns on flat ground (actions F1-F12 in Fig. G1) and for the patterns on slopes (actions S1-S12 in Fig. G2).

Patterning on flat ground (Fig. G1)

F1) Including PA in the null model: Previous studies have shown that the peat accumulation mechanism may amplify surface microtopography, inducing high-productive dryer patches (hummocks) and low-productive wetter patches (hollows) (Alexandrov 1988; Belyea and Clymo 2001; Larsen et al. 2007). This mechanism, however, is a local feedback (Chapter 2), meaning that it is not directly evident how this mechanism induces spatial coherence between hummocks and hollows (Belyea and Clymo 2001; Rietkerk et al. 2004a; Larsen et al. 2007). In this model version, the water table in hollows is lower than that under hummocks, because water losses are highest from hollows (Foster et al. 1983; Glaser 1992b; Belyea 2007). Hence, patterning emerges when conditions are so wet that hummocks benefit from transport of excess water towards a nearby hollow (Belyea and Clymo 2001). Thus, slight initial differences in biomass and acrotelm thickness may be amplified by the peat accumulation mechanism, creating a surface of hummocks and hollows. Hummocks survive if enough excess water is drained toward a nearby hollow, which constrains hummock size and leads to a spatially consistent pattern of hummocks and hollows (Fig. G1).

F2) Including NA in the null model: Previous studies have explained in detail how the nutrient accumulation mechanism leads to spatial patterning (Rietkerk et al. 2004a; Wetzel et al. 2005; Chapter 3). As compared to the other model versions, it is important to note that water stress does not increase if acrotelm thickness increases. Hence, patches reach very high biomass and high transpiration rates extract nutrients from a relatively large surrounding area, which explains the formation of isolated spots of high biomass (Fig. G1).

F3) Including WP in the null model: Pattern formation does not occur through the water ponding mechanism on flat ground, which is in compliance with previous models focusing on this mechanism (Swanson and Grigal 1988; Couwenberg 2005; Couwenberg and Joosten 2005).

F4) Including NA in the PA model: Inclusion of the nutrient accumulation mechanism reverses the fluxes of water and nutrients. Hummocks benefit from the presence of nearby hollows, in this case as a source of nutrients. Low nutrient availability and the wet conditions in hollows together pose a strong constraint on the expansion possibilities for hummocks, leading to very narrow hummocks being surrounded by large hollow areas (Fig. G1).

F5) Including PA in the NA model: It has been previously explained how the peat accumulation mechanism may amplify the patterning caused by the nutrient accumulation mechanism (Chapters 2 and 3). More specifically, the peat accumulation mechanism induces sharp boundaries between hummocks and hollows as observed in the field (Fig. G1; Chapters 2 and 3). In this model version, pattern formation is in the initial stage governed by the nutrient accumulation mechanism (data not shown). As time proceeds, however, the patches with low biomass become wetter, which results in even less growth and hence a further decrease in biomass (data not shown). Subsequently, the wet hollows expand; forcing the hummocks into narrow strips in between different hollows (Fig. G1). The nutrient accumulation mechanism is driven by fast processes (small-scale water and nutrient flow), which explains the dominance of this mechanism at the start of the model run. The peat accumulation mechanism is driven by the slower process of peat formation, which explains why this mechanism becomes important at a later stage.

F6) Including WP in the PA model: The most important effect of including the water ponding mechanism in the PA model is that it can change the water flux between

hummocks and hollows. Whether the water fluxes increase or decrease depends on the shape of the conductivity function (Fig. 2b in the main text of Chapter 4) that is chosen. In this study, we assumed that the hummocks had a lower conductivity and the hollows a higher conductivity than the null model conductivity (Swanson and Grigal 1988; Couwenberg 2005; Couwenberg and Joosten 2005). The net effect for the chosen parameterization is that the hummocks can drain excess water more effectively toward the hollows, meaning that the hollows are smaller as compared to the model run without the water ponding mechanism (Fig. G1). Thus, depending on the assumed hydraulic conductivity function, the size of the hollows and the hummock-hollow partitioning of the surface may change (Goode 1973; Belyea 2007), but there is no principal difference in the pattern-forming process.

F7) Including PA in the WP model: In this case the peat accumulation mechanism induces pattern formation as discussed in (F1). The hummock-hollow water flux depends on the shape of the hydraulic conductivity function as discussed in (F6).

F8) Including WP in the NA model: The water ponding mechanism decreases the hydraulic conductivity of patches with a thick acrotelm as compared to the null model conductivity (see Fig. 2b of the main text of Chapter 4). Therefore, the water ponding mechanism partly counteracts the nutrient accumulation mechanism. The nutrient accumulation mechanism induces patches of high biomass and a thick acrotelm, but the water ponding mechanism limits the water flow and hence the flow of nutrients toward these patches. This also means that nutrient availability in the surroundings is less depleted. As a result, vegetation biomass spreads out into larger patches of lower biomass, creating a matrix of hummocks, surrounding wetter and low-productive hollows (Fig. G1). The lower nutrient availability in the hollows eventually limits expansion of the hummock matrix.

F9) Including NA in the WP model: In this case the nutrient accumulation mechanism induces pattern formation as discussed in (F2). The water ponding limits the biomass density in patches as discussed in (F8).

F10) Including WP in the PA+NA model: It was previously explained that the dominant water flow in the PA+NA model is driven by the nutrient accumulation mechanism (F5), and that the water ponding mechanism can counteract the hollow-hummock flux of water and nutrients (F8). For the parameter settings that we used in this study, the counteracting effect of the water ponding mechanism outweighs the

effect of the nutrient accumulation mechanism, meaning that no patterning emerges (Fig. G1).

F11) Including NA in the PA+ WP model: The nutrient accumulation mechanism may reverse the flow of water and nutrients as explained in (F4). In this case, however, the water ponding mechanism counterbalances the nutrient accumulation mechanisms as explained in (F8 and F10). As a result, patterning does not emerge.

F12) Including PA in the NA + WP model: For F9-F11 it was argued that the water ponding mechanism counteracts the nutrient accumulation mechanism, but in the NA+WP model patterning did emerge. This may seem contradictory, but inclusion of the peat accumulation in this NA+WP model provides an explanation for this. The model versions discussed in F9-F11 included the peat accumulation mechanism, whereas the NA+ WP model does not. An important aspect of the peat accumulation mechanism is that water stress depends on acrotelm thickness, rather than the absolute height of the water table. In the NA+WP model, vegetated patches have a relatively thick acrotelm, but this does not limit evapotranspiration. If the peat accumulation mechanism is included, however, this relatively thick acrotelm limits evapotranspiration. As a result, the nutrient accumulation mechanism is not strong enough to drive pattern formation (Fig. G1).

Patterning on slopes (Fig. G2)

S1) Including PA in the null model: The peat accumulation mechanism drives patterning of hummocks and hollows. Hummocks locally deplete nutrient concentration; therefore the preferential expansion of hummocks is in the upslope direction, to intercept downward flowing nutrients (Rietkerk et al. 2002, 2004a). The width of hummocks in parallel direction is limited, because the hummock depends on draining excess water in downslope hollows. This means that the presence of a hollow stimulates upslope hummock formation. As a result, hollows also expand preferentially in the perpendicular direction (Foster et al. 1983; Glaser 1992b; Belyea and Lancaster 2002). Thus, a striped hummock-hollow pattern emerges that is oriented in perpendicular direction (Fig. G2).

S2) Including NA in the null model: Due to the presence of a slope, water flow in downslope direction is only to a very limited extent controlled by evapotranspiration. As a result, patches with higher vascular plant biomass and evapotranspiration rates

mainly accumulate nutrients from the surrounding area of equal elevation, which is the perpendicular direction. Subsequently, the nutrient depletion from the surrounding area of equal elevation limits expansion of hummocks in this direction. Patches with higher vascular plant biomass have higher nutrient concentration. These nutrients are partly advected by water in downslope direction, which explains the expansion of hummocks in downslope direction (Ross et al. 2006). Our finding that the nutrient accumulation mechanism induces the formation of ridges parallel to the slope contradicts previous modeling results (Rietkerk et al. 2004a; Chapters 2). In these previous studies, peatland slopes were not modeled explicitly, but the water flow was switched off in one direction (perpendicular to the “slope”). In the current study, we improved this aspect by modeling the slope explicitly, which explained the orientation of the ridges parallel to the slope. Ridges parallel to the peatland slope occur in the Florida Everglades (Wu et al. 2006; Larsen et al. 2007), but here the mechanism of pattern formation may be different (Larsen et al. 2007). Thus, these model results suggest that ridge-hollow patterns perpendicular to peatland slopes cannot be driven by nutrient accumulation only (as suggested in Rietkerk et al. 2004a; Chapter 2).

S3) Including WP in the null model: Including only the water ponding mechanism in the model does not induce pattern formation on slopes. Although the presence of more densely vegetated hummocks would pond up water upslope, this would increase vegetation growth upslope due to the shape of the water stress function in the null model (Rietkerk et al. 2004a). Hence, differences in acrotelm thickness and biomass are damped through this negative feedback. This is in line with previous studies arguing that positive feedback between vegetation and the environment (in this case the water table) is a prerequisite for pattern formation (Couwenberg and Joosten 1999, Couwenberg 2005). In this particular model version, the water ponding mechanism may create differences in water table height, but there is no feedback to plant growth that reinforces these differences.

S4) Including NA in the PA model: Similar to the model version on flat ground (F4), nutrient accumulation reverses the fluxes of water and nutrients. As described in (S2), the preferential expansion of hummocks and hollows also changes, toward the downslope direction. Because hummocks can lose water through transpiration there is no dependency on presence of downslope hollows. Therefore, the expansion in downslope direction is not limited.

S5) Including PA in the NA model: Similar to the model version on flat ground (F5), the peat accumulation mechanism may amplify the patterning caused by the nutrient accumulation mechanism (Chapters 2 and 3). More specifically, the peat accumulation mechanism causes further expansion of wet patches with low biomass, forcing the hummocks into narrow strips with high biomass (similar to observations by Ross et al. 2006). Flows of water and nutrients in this model version, however, are still dominated by gravity-induced downslope flow and evapotranspiration-induced flow in the perpendicular direction. As a result, the main orientation of the hummocks and hollows is in the parallel direction.

S6) Including WP in the PA model: Obviously, the presence of hummocks stimulates the ponding of water upslope when the water ponding mechanism is added to the PA model. Hence, maximum water tables occur on the upslope side of the hummock-hollow boundary. Due to the low hydraulic conductivity of hummocks, water flow in the downslope direction becomes very low for wide hummocks. Hence, this creates the possibility of perpendicular-slope flow of water from hummocks toward hollows. This interaction creates the occurrence of circular pools that are enclosed by perpendicular-oriented and parallel-oriented hummocks (Fig. G2). The size and shape of the hollows and the hummock-hollow partitioning of the surface depends on the ratio of hummock:hollow hydraulic conductivity (Goode 1973; Belyea 2007), and thus on the shape of the hydraulic conductivity function.

S7) Including PA in the WP model: In this case the peat accumulation mechanism induces pattern formation as discussed in (S1). The circle-like shape of some of the enclosed hollows (Fig. G2) can be explained by the water ponding mechanism as discussed in (S6).

S8) Including WP in the NA model: Although this combination of mechanisms does induce pattern formation on flat ground, no patterning occurs on peatland slopes (Fig. G2). Occurrence of the nutrient accumulation mechanism induces the formation of parallel oriented hummocks and hollows (S2, Ross et al. 2006), but in this case the water ponding mechanism limits downslope water flow through hummocks, because of the low hydraulic conductivity. Subsequently, the water flow bypasses the parallel oriented hummocks. Due to rheotrophic effects (Ivanov 1981), the preferential expansion of the hummocks becomes in the perpendicular direction, counteracting the surface patterning as induced by the nutrient accumulation mechanism. As time proceeds, the entire surface is covered by hummocks (Fig. G2). This explanation

clarifies that the absence of patterning depends on the shape of the hydraulic conductivity function (Fig. 2b of the main text of Chapter 4). If larger values of hummock conductivity are assumed, similar patterning as described in (S2) occurs (data not shown).

S9) Including NA in the WP model: In this case patterning does not occur, as described in (S8).

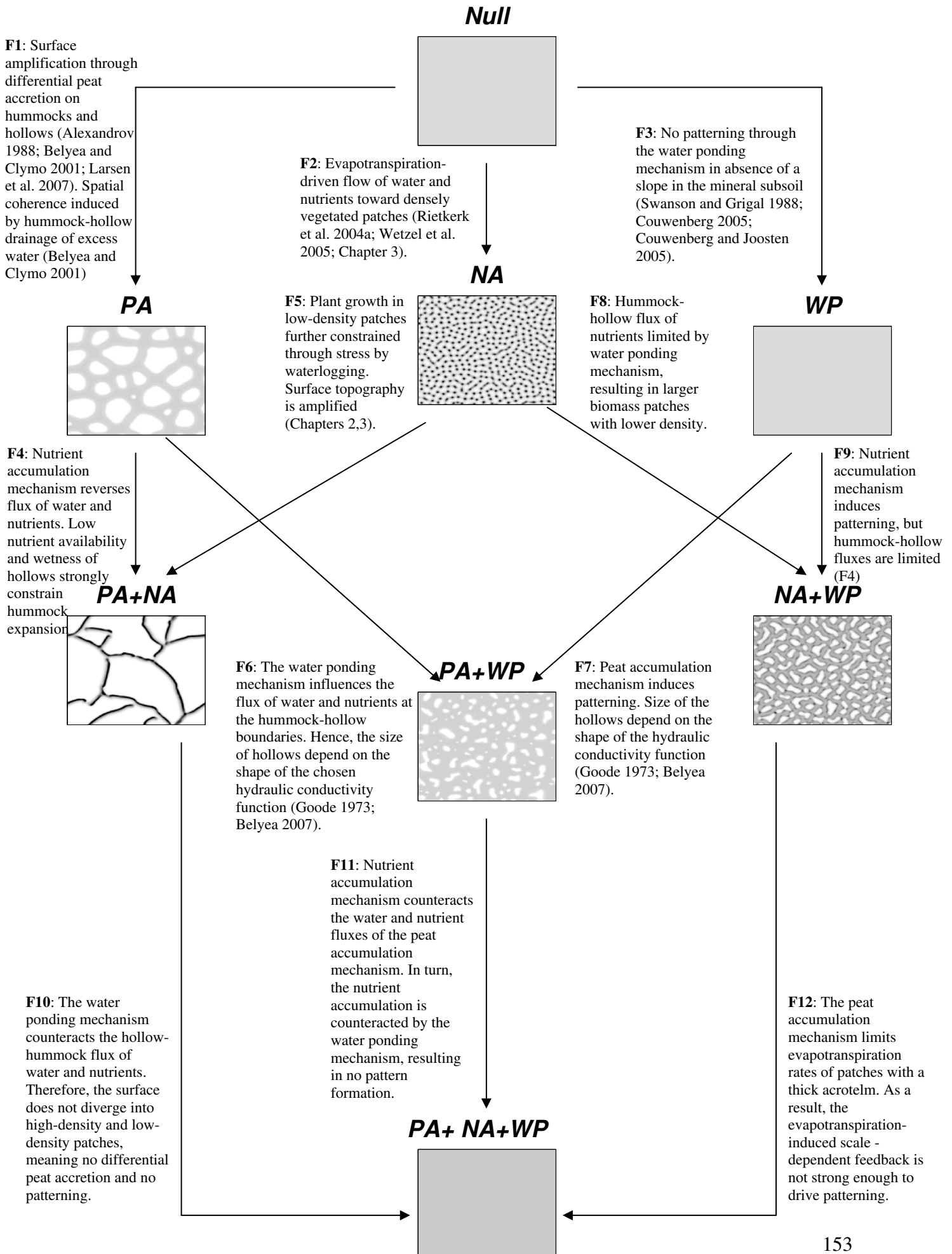
S10) Including WP in the PA+NA model: Interestingly, patterning occurs in this model version, whereas patterning did not occur in the equivalent model version for flat ground (S10). Further, the orientation of the patterning reverses when the water ponding mechanism is included in the PA+NA model (Fig. G2). The downslope expansion of hummocks (S4,S5) is now strongly limited by the low hydraulic conductivity. Upslope expansion of the hummocks is limited because of the high water table at the hummock-hollow boundary due to the water ponding mechanism, and the subsequent hollow deepening due to the peat accumulation mechanism (Belyea and Clymo 2001). Moreover, if the water ponding mechanisms is strong enough, rheotrophic effects (Ivanov 1981) outweigh evapotranspiration-driven depletion effects. As a result, the main mode of hummock expansion then occurs in the perpendicular direction (Foster et al. 1983; Glaser 1992b). Hence, the expansion of hummocks and hollows proceeds in concert, mainly in the perpendicular direction (Fig. G2).

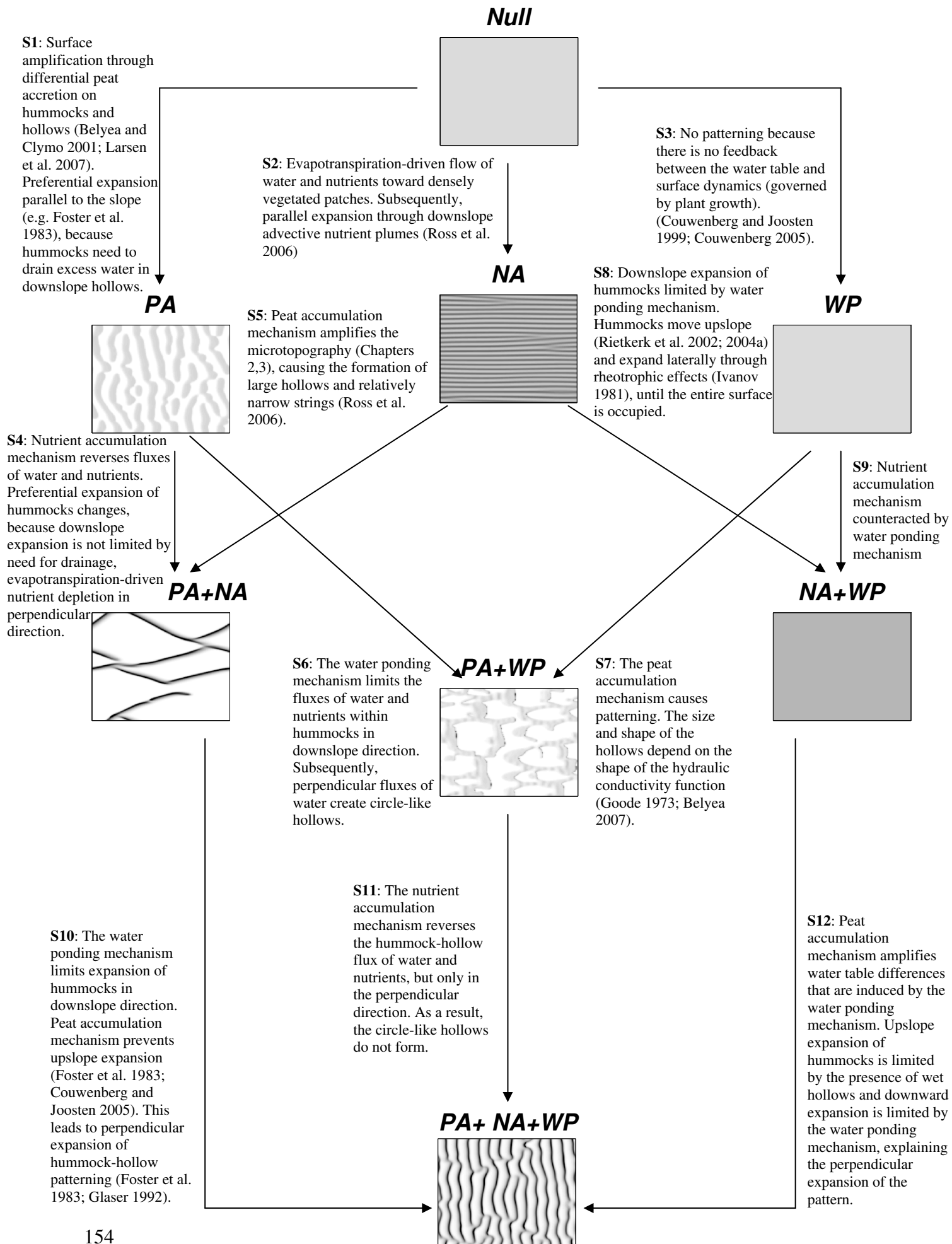
S11) Including NA in the PA+ WP model: The nutrient accumulation mechanism reverses the flow of water and nutrients in perpendicular direction, because the water table in hummocks is lower than hollows on the same elevation of the slope. As a result, there is no water flux from hummocks toward hollows in the perpendicular direction, preventing the formation of the enclosed hollows as described in (S6 and S7).

S12) Including PA in the NA + WP model: The peat accumulation mechanism induces pattern formation in this model, because the water level differences due to the water ponding mechanism are amplified. It was previously described that a combination of the nutrient accumulation mechanism and water ponding mechanism limits the downslope expansion of hummocks and that rheotrophic effects stimulate the expansion of hummocks in the perpendicular direction. The water ponding mechanism induces higher water tables upslope of these hummocks, but the peat

accumulation mechanism is the pivotal mechanism by which these areas develop into sparsely vegetated hollows. As a result, a linear pattern oriented in the perpendicular direction emerges (Fig. G2).

► **Figure G1:** *Schematic overview of the development of peatland pattern morphology on flat ground. Patterns are driven by (combinations of) three different mechanisms: the peat accumulation mechanism, the nutrient accumulation mechanism and the water ponding mechanism.*





◀ **Figure G2:** Schematic overview of the development of peatland pattern morphology on slopes. Patterns are driven by (combinations of) three different mechanisms: the peat accumulation mechanism, the nutrient accumulation mechanism and the water ponding mechanism.

Acknowledgments

The authors would like to thank Laurel Larsen and an anonymous reviewer for many valuable comments that improved the manuscript. Joram van den Boezem is thanked for providing ideas for Figure 1. The research of MBE and MR is supported by a VIDI grant from the Research Council Earth and Life Sciences of the Netherlands Organization of Scientific Research to MR.



5

Resource contrast in patterned peatlands increases along an evapotranspiration gradient

Maarten B. Eppinga, Max Rietkerk, Lisa R. Belyea,
Mats B. Nilsson, Peter C. De Ruiter
& Martin J. Wassen

Resource contrast in patterned peatlands increases along an evapotranspiration gradient

Abstract

1. Spatial surface patterning of hummocks and hollows is a remarkable feature of peatlands, which asks for identification of underlying driving mechanisms.
2. Recent theoretical studies suggest that the drivers of peatland patterning may change with environmental conditions. More specifically, patterning in drainage-dominated peatlands may be driven by a peat accumulation mechanism, whereas patterning in evapotranspiration-dominated peatlands may be driven by a nutrient accumulation mechanism.
3. Theory also predicts that the driving mechanism of a peatland pattern is reflected in the resource contrast between hummocks and hollows. More specifically, occurrence of the peat accumulation mechanism is reflected by a negative resource contrast (meaning lower nutrient availability in hummocks than in hollows), whereas occurrence of the nutrient accumulation mechanism is reflected by a positive resource contrast (higher nutrient availability in hummocks than in hollows).
4. The aim of this study was to empirically test the hypothesis that the resource contrast in patterned peatlands increases from negative to positive along a gradient of increasing importance of evapotranspiration to the water balance.
5. We measured the contrasts in phosphorous, nitrogen and potassium in water and vegetation in three patterned peatlands with a maritime (Scotland), temperate (Sweden) and continental (Siberia) climate.
6. Contrary to our hypothesis, the contrasts for nutrients in mire water showed no trend along the evapotranspiration gradient. The low nutrient concentrations in mire water suggest that nutrient dynamics are not adequately represented by the steady state conditions of the deterministic models of previous theoretical studies.
7. In line with our hypothesis, the contrasts for nutrients in hummock and hollow vegetation showed an increasing trend along the evapotranspiration gradient: contrasts were negative or slightly positive in Scotland, positive in Sweden and strongly positive in Siberia.
8. *Synthesis*: this study presents the first comparison of resource contrasts in patterned ecosystems along an environmental gradient. The results suggest that future climatic changes may affect the ecosystem functioning of patterned peatlands by altering the contribution of pattern-driving mechanisms to the within-system redistribution of water and nutrients.

Introduction

A key challenge in ecosystem ecology is to explain large-scale patterns that emerge from smaller-scale driving mechanisms (Levin 1992; Solé and Bascompte 2006). Spatial patterns of sessile biota that are regular or otherwise coherent are among the most striking large-scale patterns and have been observed in a variety of ecosystems. Examples include savannas (Lejeune et al. 2002), arid ecosystems (Klausmeier 1999), mussel beds (Gascoigne et al. 2005) and marsh tussocks (Crain and Bertness 2005). Large-scale patterning is an important determinant of ecosystem functioning (Wiegand et al. 1998; Van de Koppel et al. 2008) and biodiversity (Levin 2000; Scheffer and Van Nes 2006). To predict how ecosystems respond to changes in external forcing, such as climate change, identification of the smaller-scale driving mechanisms that explain these kinds of spatial ecosystem patterning may be essential (Rietkerk et al. 2004b; Belyea and Baird 2006; Kéfi et al. 2007b; Scanlon et al. 2007). A common small-scale mechanism that can explain patterning in the above examples is concentration of limiting resources by sessile biota (Rietkerk et al. 2004b; Shachak et al. 2008).

Until now, the majority of research on spatial ecosystem patterns comprises theoretical modeling studies (e.g. Von Hardenberg et al. 2001; Meron et al. 2004; Couwenberg and Joosten 2005; Van de Koppel et al. 2005; Pueyo et al. 2008). These modeling studies test whether a hypothesized small-scale mechanism is able to drive the formation of a large-scale ecosystem pattern that is observed in the field. The fact that a mechanism explains a pattern in a model, however, is not evidence that this mechanism drives the pattern in reality (Levin 1992). Therefore, empirical research is necessary to test whether modeled mechanisms are indeed present in the field, and whether these mechanisms are strong enough to be a likely explanation of the observed ecosystem pattern. Moreover, the few empirical studies so far have mainly focused on a single study site with a particular type of ecosystem pattern (e.g. Gascoigne et al. 2005; Barbier et al. 2006; 2008; Van de Koppel and Crain 2006; Chapter 3). However, several mechanisms may be capable of explaining the same ecosystem pattern (Levin 1992; Rietkerk and Van de Koppel 2008) and which of these mechanisms drives pattern formation in reality may change with changing environmental conditions (Carpenter 1996; Scheffer 1999; Chapter 2). One approach to disentangle the influence of several mechanisms is to study a particular type of patterned ecosystem along a gradient of environmental conditions, when it

can be expected that the contribution of the underlying mechanisms to the observed ecosystem pattern will change along this gradient.

Spatial surface and vegetation patterning with a characteristic spatial scale of 10^1 - 10^2 m is also observed in northern peatland ecosystems (Glaser et al. 1981; Foster et al. 1983; Belyea and Lancaster 2002). This pattern consists of elevated, relatively dry and densely vegetated patches (hummocks or ridges), alternating with less elevated and less densely vegetated patches (lawns) or sparsely vegetated wet depressions (hollows). The characteristic spatial scale of the patches is 10^0 - 10^1 m. Peatland patterns of hummocks/ridges, lawns and hollows occur in various spatial arrangements, including scattered individual hummocks, lawns and hollows (e.g. Belyea and Clymo 2001), maze-like arranged ridges within a matrix of hollows (e.g. Rietkerk et al. 2004a) and linear ridge-hollow patterns along the contours of mire slopes (e.g. Sjörs 1961).

In peatlands, most of the incoming precipitation is lost again through either evapotranspiration (ET) or drainage (Ivanov 1981; Ingram 1983; Brooks 1992). The proportion of precipitation lost through ET (from here referred to as the ET:Prec ratio) is constrained by the climate conditions and the peatland slope (Bridgham et al. 1999; Reeve et al. 2000; Belyea and Malmer 2004; Belyea 2007). The ET:Prec ratio therefore varies along climatic gradients. If the climate imposes a low ET:Prec ratio, the water losses in peatlands are dominated by drainage (from here referred to as drainage-dominated). If the climate imposes a high ET:Prec ratio (close to 1), the water losses in peatlands are dominated by ET (from here we referred to as ET-dominated). Under the latter conditions, ET importantly controls mire water movement and thereby constitutes an important mechanism to redistribute nutrients within the mire (Rietkerk et al. 2004a; Wetzel et al. 2005; Ross et al. 2006).

More specifically, model studies suggest that in ET-dominated peatlands, patterning might be driven by a resource concentration mechanism (Rietkerk et al 2004a; Ross et al. 2006; Chapter 2). The presence of vascular plants (in particular trees and shrubs) on hummocks may induce higher ET rates on hummocks as compared to hollows (Takagi et al. 1999; Frankl and Schmeidl 2000; Rietkerk et al. 2004a; Andersen et al. 2005). As a result, water and dissolved nutrients flow from hollows toward hummocks. Subsequently, the nutrients become trapped on the hummocks through uptake by vascular plants. Thus, during their lifespan, vascular plants that grow on hummocks accumulate nutrients originating from outside the hummocks. Nutrients become available again through mineralization of vascular plant litter, but

this only increases nutrient availability on the local scale (within the hummock). Models predict that this local recycling effect outweighs the effect of nutrient uptake, meaning that nutrient concentrations in the mire water under hummocks also increase (Rietkerk et al. 2004a; Chapter 3). This resource concentration mechanism was coined the *nutrient accumulation mechanism* (Rietkerk et al. 2004a).

However, peatland patterning also occurs in regions with a low ET:Prec ratio, which makes it unlikely that patterning in these regions is driven by a resource concentration mechanism, i.e. the nutrient accumulation mechanism. A recent model study (Chapter 4) revealed that peatland patterning could also be driven by a positive feedback between acrotelm thickness and net rate of peat formation (Belyea and Clymo 2001; Larsen et al. 2007). This *peat accumulation mechanism* is expected to be the most important driver of patterning in drainage-dominated peatlands (Chapter 4). Water losses through drainage and overland flow are highest from hollows (Ivanov 1981; Foster and King 1984; Quinton and Roulet 1998; Belyea and Malmer 2004). Due to the peat accumulation mechanism elevated and relatively dry hummocks may form, but in drainage-dominated systems these hummocks can only survive if they can drain excess water toward neighboring hollows (Belyea and Clymo 2001; Chapter 4). Hence, these systems require a net transport of water from hummocks toward hollows. Because the transport of water implies transport of dissolved nutrients as well, this would lead to lower nutrient concentrations in hummocks as compared to hollows (Chapter 4).

A straightforward empirical investigation for the presence of a resource concentration mechanism in patterned ecosystems is to test for the occurrence of resource contrasts (Boeken and Shachak 1994; Shachak et al. 2008; Van der Valk and Warner 2009). For peatlands, resource contrast refers to the hummock-hollow difference (hummock minus hollow) in nutrient availability. We hypothesize that the presence of the nutrient accumulation mechanism is reflected by the resource contrast in patterned peatlands (Chapter 4). More specifically, we hypothesize that in ET-dominated peatlands, patterning is driven by the nutrient accumulation mechanism, which is reflected by a positive resource contrast (nutrient availability is higher in hummocks than in hollows) (Table 1; Rietkerk et al. 2004a). On the other hand, we hypothesize that in drainage-dominated peatlands, patterning is driven by the peat accumulation mechanism, which is reflected by a negative resource contrast (nutrient availability is lower in hummocks than in hollows) (Table 1; Belyea and Clymo 2001; Larsen et al. 2007; Chapter 4).

Study site	Precipitation (P)	Evapo-transpiration (ET)	Importance of Evapo-transpiration (ET:Prec ratio)	Expected main driving mechanism	Expected resource contrast
Inverewe (Scotland)	1700 mm ¹	380 mm (hollows) 250 mm (hummocks/ridges) ¹	0.15-0.22	Peat accumulation mechanism ^{1,2}	Negative (meaning lower nutrient availability in hummocks than in hollows) ²
Degerö Stormyr (Sweden)	520 mm ³ (546-936 mm ^{*,4})	227-337 mm ^{*,4}	0.25-0.62	No data from previous studies available	Larger than in Scotland, smaller than in Siberia
The Great Vasyugan Bog (Siberia)	500 mm ⁵	300-500 mm ⁵	0.60-1.00	Nutrient accumulation mechanism (together with peat accumulation mechanism) ^{2,6,7}	Positive (meaning higher nutrient availability in hummocks than in hollows) ^{** 2,6,7}

Table 1: Overview of the study areas, which comprise a gradient with respect to the importance of evapotranspiration in the water balance. Hypotheses were based upon data available from previous studies. References: 1: Belyea (2007) 2: Chapter 4 (this thesis) 3: Granberg et al. (2001) 4: Sagerfors et al. (in press) 5: Semanova and Lapshina (2001) 6: Chapter 2 (this thesis) 7: Chapter 3 (this thesis)

The aim of this study was to test these hypotheses with empirical data from three study areas in maritime (Scotland), humid temperate (Sweden) and humid continental (Siberia) climates. Due to the climatic differences, the study sites comprise a gradient in the ET:Prec ratio (Table 1). Notably, the Scottish site was part of a previous study presenting field data that was in agreement with a model that assumed higher ET rates for hollows than for ridges (Belyea 2007). Thus, for this Scottish field site it seems reasonable to assume that there is no ET-induced flow of water and nutrients from hollows toward hummocks. In other words, the nutrient accumulation mechanism is likely to be absent in the Scottish site. On the contrary, previous data from the Siberian study site showed the dominance of ET in diurnal water table dynamics and suggested that ET rates were higher on hummocks than in hollows, which indicated the presence of the nutrient accumulation mechanism (Chapter 3). To test whether the resource contrast indeed followed a consistent trend along a gradient in the ET:Prec ratio, we included a third site (in northern Sweden)

where ET is of intermediate importance (Table 1). Thus, based on previous theoretical studies, we expected an increasing trend in resource contrast along the gradient in ET:Prec ratio; from negative in Scotland to positive in Siberia (Table 1).

Material and Methods

Study areas

Inverewe (Ross and Cromarty, Scotland)

Inverewe (57° 46' N, 5° 34' W) lies 3 km from the coast of Loch Ewe, which flows out into the Atlantic Ocean. This study area is situated approximately 30 km southwest of Ullapool (Fig. 1a). Current climate is typically maritime, with a mean annual temperature of ca. 9 °C (Belyea 2007). Compared to the other study areas, the precipitation excess is large: annual precipitation is 1700 mm, whereas the annual ET (from hollows) is 380 mm (Table 1; Belyea 2007). Across the study area several sites of surface patterning occur within generally non-patterned blanket bog (Belyea 2007). The ombrotrophic character of the study area is reflected by low values for pH and alkalinity, but the Ca:Mg ratio of the mire water may indicate some influence of minerogenic water or weathering of the rock outcrops that are present in the study area (Table 2; Bellamy 1959; Wells 1996; Bragazza and Gerdol 1999). The proximity to the Atlantic ocean is reflected in high values of chloride (Cl) and sodium (Na) concentrations in the mire water (Table 2). We sampled two types of patterns in this study area.

The first pattern occurs on relatively flat terrain, and comprises a three-phase mosaic of hummocks, lawns and hollows, irregularly arranged in space (Fig. 1b). The second pattern occurs at peatland slopes within the Inverewe study area. This pattern comprises elevated ridges alternating with wet hollows, both features orientated perpendicular to the slope (Fig. 1c). Vegetation on the ridges and hummocks is characterized by *Rynchospora alba*, *Racomitrium lanuginosum*, *Calluna vulgaris*, *Erica tetralix*, *Molinia caerulea*, *Drosera rotundifolia*, *D. anglica* and *Sphagnum capillifolium*. Vegetation in the lawns and hollows is dominated by *R. alba*, *Carex lasiocarpa*, *C. limosa*, *C. pulicaris*, *Eriophorum angustifolium*, *Narthecium ossifragum*, *Menyanthes trifoliata* and *Utricularia intermedia*. *R. alba* occurred on all ridges, hummocks, lawns and hollows. The measurement period in this study site was from August 9 to August 15 2007.



- ① Scotland: Flat (B) and Slope (C) ② Sweden: Flat (D) and Slope (E) ③ Siberia: Flat from sky (F) and ground (G)

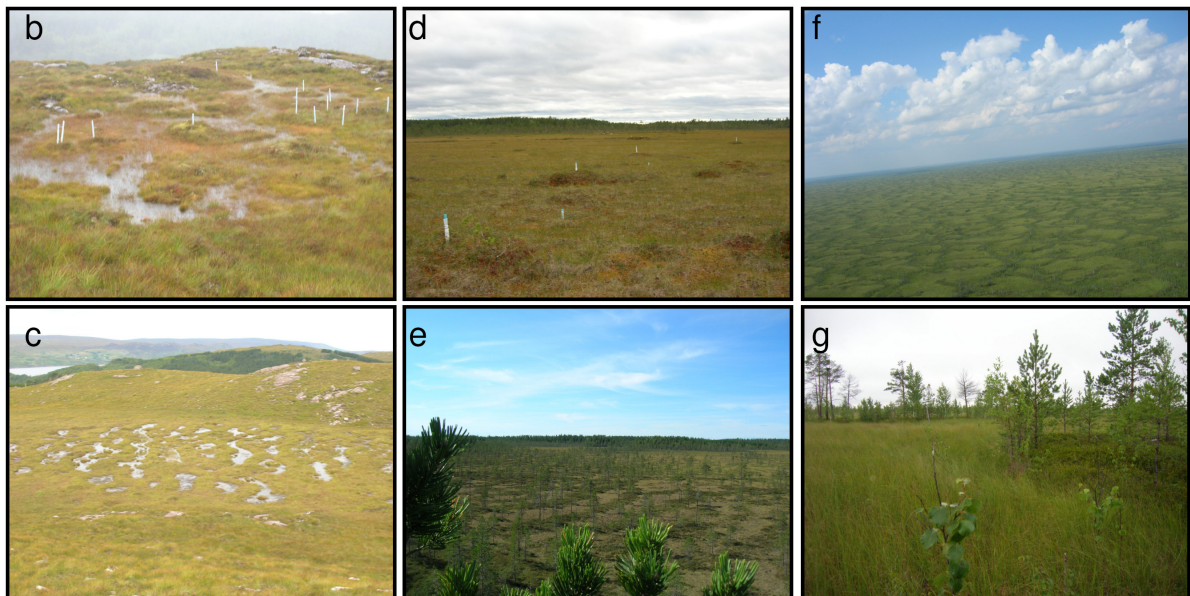


Figure 1: Satellite image showing the study areas (accessed via Google Earth). Three different study areas were sampled: 1) Inverewe, Scotland ($57^{\circ} 46' N$, $5^{\circ} 34' W$) 2) Degerö Stormyr, Sweden ($64^{\circ} 11' N$, $19^{\circ} 33' E$) and 3) The Great Vasyugan Bog, Siberia ($56^{\circ}18' N$, $81^{\circ}28' E$). The sites comprise a gradient with respect to the importance of evapotranspiration in the water balance. The contribution of evapotranspiration to the water balance is small in the maritime climate of Scotland, and large in the humid continental climate of Siberia. In Scotland and Sweden, we sampled two types of patterns: a hummock-hollow pattern on flat ground and a linear hummock-hollow pattern on slopes. In Siberia, we sampled a maze pattern of hummocks and hollows on flat ground.

Pattern Locality	Scotland Flat		Scotland Slope		Sweden Flat		Sweden Slope		Siberia Flat	
	Hummock (n = 24)	Hollow (n = 48)	Hummock (n = 40)	Hollow (n = 40)	Hummock (n = 42)	Hollow (n = 42)	Hummock (n = 42)	Hollow (n = 42)	Hummock (n = 47)	Hollow (n = 36)
Variable										
DWT (cm)	21 (2)	-0.7 (0.7)	12 (1)	-5 (1)	34 (1)	6 (0.5)	36 (1)	3 (0.5)	41 (2)	-7 (1)
pH (-)	4.51 (0.04)	4.53 (0.03)	5.29 (0.10)	4.93 (0.07)	3.73 (0.02)	3.78 (0.02)	3.70 (0.01)	3.69 (0.01)	4.93 (0.12)	5.64 (0.06)
EC ($\mu\text{S}\cdot\text{cm}^{-1}$)	64 (7)	41 (1)	99 (4)	73 (1)	154 (3)	139 (3)	172 (3)	157 (3)	53 (2)	48 (1)
Alkalinity (mmol [HCO₃]⁻ l⁻¹)	0.004 (0.002)	0.002 (0.001)	0.25 (0.04)	0.02 (0.008)	b.d.	b.d.	b.d.	b.d.	0.25 (0.02)	0.34 (0.01)
Ca (mg.l⁻¹)	0.99 (0.14)	0.56 (0.05)	4.09 (0.39)	0.71 (0.03)	1.56 (0.10)	1.16 (0.09)	2.06 (0.08)	1.17 (0.07)	6.15 (0.30)	5.39 (0.15)
Mg (mg.l⁻¹)	0.63 (0.06)	0.44 (0.02)	1.38 (0.06)	1.10 (0.02)	0.37 (0.01)	0.34 (0.01)	0.43 (0.02)	0.37 (0.02)	2.77 (0.08)	2.32 (0.05)
Ca:Mg ratio (mg.mg⁻¹)	1.52 (0.11)	1.27 (0.10)	2.83 (0.20)	0.64 (0.02)	4.31 (0.25)	3.41 (0.23)	4.97 (0.15)	3.30 (0.19)	2.21 (0.09)	2.31 (0.02)
Na (mg.l⁻¹)	8.91 (0.90)	5.84 (0.31)	13.84 (0.51)	9.86 (0.17)	3.96 (0.37)	2.31 (0.25)	6.48 (0.57)	2.18 (0.25)	1.55 (0.05)	1.35 (0.05)
Cl (mg.l⁻¹)	11.15 (0.80)	8.60 (0.40)	18.79 (0.56)	15.96 (0.23)	3.89 (0.25)	2.28 (0.19)	4.24 (0.67)	1.69 (0.17)	b.d.	b.d.

Table 2: Measured average values of water-related variables on hummocks and hollows in five pattern-localities in Scotland (on flat ground and slopes), Sweden (on flat ground and slopes) and Siberia (on flat ground only). DWT means Distance to the Water Table, EC means Electrical Conductivity. Standard errors are given between brackets. b.d. means that all measurements were below the detection limit.

Degerö Stormyr (Västerbotten, Sweden)

Degerö Stormyr (64° 11' N, 19° 33' E) is situated on a highland between the rivers Umeälven and Vindelälven, approximately 70 km west of the Gulf of Bothnia and 300 km east of the Atlantic ocean (Fig. 1a). The study area is part of a complex system of interconnected smaller mires within a total catchment area of ~10 km² (Malmström 1923; Granberg et al. 2001). The study area can be characterized as a mixed mire system: low pH and no alkalinity of the mire water reveals that the conditions are acid (Table 2). However, there is also minerogenic groundwater input (Malmström 1923; Granberg et al. 2001; Sagerfors et al. 2008), which is reflected by relatively high values of the Ca: Mg ratio in the mire water (Table 2). The influence of the Atlantic ocean is reflected in intermediate values of Cl and Na concentrations in the mire water (Table 2). Degerö Stormyr is in a temperate cold humid climate (Nilsson et al.

2008), with a mean monthly temperature ranging between ca. $-12\text{ }^{\circ}\text{C}$ and ca. $+15\text{ }^{\circ}\text{C}$ (Granberg et al. 2001). Long-term annual precipitation is 523 mm (Granberg et al. 2001). Between 2000 and 2005, annual ET in the study area ranged between 227-337 mm (in these years, precipitation varied between 546 mm and 936 mm, Sagerfors et al. in press). We sampled two types of patterns in this study area.

The first pattern occurs on relatively flat terrain, and comprises individual elevated hummocks within a matrix of lower peatland lawn (Fig. 1d). The second pattern occurs on slopes and comprises elevated ridges surrounded by lower lawns, both features orientated perpendicular to the slope (Fig.1e). Vegetation on the perpendicular-slope ridges is characterized by *Pinus sylvestris*, *Andromeda polifolia*, *Betula nana*, *Empetrum nigrum*, *Eriophorum vaginatum*, *Vaccinium oxycoccos*, *Calluna vulgaris*, *Sphagnum balticum*, *S. rubellum* and *S. fuscum*. Trees very rarely occur on the hummocks within the pattern on flat ground. Vegetation on these hummocks is characterized by *E. vaginatum*, *Sphagnum fuscum* and *S. rubellum*. For both patterns on flat ground and slopes, vegetation in the lawns is dominated by *E. vaginatum*, *V. oxycoccos*, *A. polifolia*, *Scheuchzeria palustris*, *Carex limosa*, *Sphagnum balticum*, *S. majus* and *S. lindbergii*. *E. vaginatum* occurred on all ridges, hummocks and lawns. The measurement period in this study area was from August 22 to August 26 2007. A more detailed description of Degerö Stormyr can be found in previous studies (Granberg et al. 2001; Sagerfors 2007; Wiedermann et al. 2007; Nilsson et al. 2008).

The Great Vasyugan Bog (Siberia, Russia)

The Great Vasyugan Bog ($55\text{-}59\text{ }^{\circ}\text{N}$, $76\text{-}83\text{ }^{\circ}\text{E}$) is situated at the water divide between the rivers Ob and Irtysh, approximately 200 km northeast of Novosibirsk (Fig. 1a). The study area is situated about 10 km from the water divide, and the relatively high values of pH, alkalinity and Ca: Mg ratio of the mire water (Table 2) suggest that the area is receiving water from uplands. The absence of marine influence is reflected in low values of Cl and Na concentrations in the mire water (Table 2). Current climate is typically humid continental, with a mean monthly temperature ranging between ca. $-20\text{ }^{\circ}\text{C}$ and ca. $+18\text{ }^{\circ}\text{C}$ (Semenova and Lapshina 2001). Contrary to most regions in the boreal zone, the precipitation excess is small: annual precipitation is 500 mm, whereas the annual ET is 300-500 mm (Semenova and Lapshina 2001). We sampled only one pattern in this study area, on relatively flat terrain.

Patterning in the Siberian study area (56°18 N, 81°28 E) can be characterized as a maze pattern of elevated ridges, embedded in a matrix of waterlogged hollows (Fig. 1f, 1g). Vegetation on the ridges is characterized by *Pinus sylvestris*, *Chamaedaphne calyculata*, *Ledum palustre* and *Sphagnum fuscum*. The vegetation in the hollows is dominated by *Carex lasiocarpa*. In the study area, *C. lasiocarpa* occurred on all ridges and in all hollows. The measurement period in this study area was from July 28 to July 31 2005. A more detailed description of the study area can be found in a previous study (Chapter 3).

Field measurements and laboratory analyses

In Siberia we sampled a peatland pattern on a relatively flat terrain. In Scotland and Sweden, we sampled peatland patterns on both relatively flat terrain and slopes. Thus, in total we sampled five different pattern-localities. We use the term pattern-locality to refer to a combination of pattern ('flat ground' or 'slope') and location (Scotland, Sweden or Siberia). Within pattern-localities on flat ground, field measurements were taken along transect sets, each set consisting of two orthogonal transects through the surface pattern. For the pattern in Siberia, a transect ranged from the middle of one ridge to the middle of the next ridge, so each transect contained the halves of two ridges and the hollow in between. The two orthogonal transects of a set crossed in the centre of the hollow. On each ridge, three measurement points were selected: the centre of the ridge, the edge of the ridge and a point in between these two. The hollow in between these ridges was sampled on five points: the centre, the edges with the two ridges and a point in between the centre and each edge. In the Swedish and Scottish pattern-localities, each microform had only one measurement point. For the pattern on flat ground in Sweden, we sampled three transect sets. Here, the pattern consisted of an irregular two-phase mosaic of hummocks and lawns, so along each transect we sampled these microforms alternately. In Scotland, we sampled two transect sets. Here, the pattern consisted of an irregular three-phase mosaic of hummocks, lawns and hollows, so along each transect there was no regular order in sampling microforms. In both Scotland and Sweden, the orientation of the first transect of a set was selected at random. The second transect of a set was orientated orthogonal to the first. Further, the second transect was selected in such a way that the crossing of the two transects was approximately in the middle of both transects.

For the pattern-localities on peatland slopes (only in Sweden and Scotland) we sampled along transects orientated along the slope of a linearly patterned area.

These patterns consisted of two-phase mosaics, so along each transect we sampled in alternating turns a ridge and a wetter microform (lawn or hollow).

At each measurement point we took a water sample from the upper 5 cm of the water table, which was analyzed in the laboratory for the hydrochemical composition. Methods of laboratory analyses were the same as in Chapter 3, where the sampling campaign for the Siberian pattern-locality is described in detail. The only methodological difference was that we filtered the water samples in Scotland and Sweden (instead of centrifugation in the laboratory, which was done for the Siberian water samples). We performed both procedures (centrifugation and filtration) for 24 samples from Scotland and Sweden, but the different methods did not affect the conclusions of this study. Furthermore, around each measurement point we harvested 10 healthy-looking shoots of vegetation. We focused on harvesting healthy-looking newly grown shoots (meaning from the current growing season), to avoid effects of nutrient resorption processes (Jonasson and Shaver 1999). Within each study area we selected a sedge species (*Cyperaceae*) that was present on all microforms. We selected *Rynchospora alba* in Scotland, *Eriophorum vaginatum* in Sweden and *Carex lasiocarpa* in Siberia. For each vegetation sample, the nutrient content was determined following the procedure described in Chapter 3. The type of nutrient limitation was determined based on thresholds in the N:P, N:K and K:P ratios in the plant tissue (Wassen et al. 1995, 2005; Olde Venterink et al. 2003).

Comparisons and statistical treatment

For nutrient concentrations in the mire water and for nutrient content and nutrient ratios in the plant tissue, we tested for general differences between microforms within each of the five pattern-localities that were sampled for this study. For the pattern on flat ground in Scotland we aggregated the measurements of lawns and hollows into one 'hollow' group. Whether these two groups were lumped or not had no effect on the conclusions of this study, but it eased presentation of the results, because all five pattern-localities then consisted of two microform groups. Statistical analyses were done with the software SPSS (Version 11.0.1, SPSS Inc. 2001). For all comparisons, homogeneity of variances between groups was tested with the Levene test statistic. If variances were homoscedastic at the $\alpha = 0.05$ significance level, differences were tested with one-way ANOVA. Otherwise we turned to the nonparametric Mann-Whitney U test.

Further, we tested whether there were differences in the hummock-hollow resource contrasts between the five pattern-localities with respect to nutrients. For these hummock-hollow differences we could not perform a standard factorial ANOVA approach, for two reasons. First, our study design was imbalanced, because we did not sample a pattern on peatland slopes in Siberia. Second, a factorial ANOVA does not correct for differences in nutrient availability between sites. Therefore, we used an alternative approach by calculating for each pattern-locality a resource contrast, which represents a relative measure of the hummock-hollow difference in nutrient availability. In the following we use the term hummock for both hummocks and ridges, and hollow for both hollows and lawns. The resource contrast (RC) for each pattern-locality was calculated as follows:

$$RC_X = \frac{(X_{HUMMOCK} - X_{HOLLOW})}{X_{HUMMOCK} + X_{HOLLOW}} \quad (I)$$

Where RC_X is a dimensionless unit for the contrast in resource X in a pattern-locality. The value of RC_X can vary between -1 (which means infinitely more resource X in hollows) and 1 (infinitely more resource X in hummocks). Differences in resource contrast between two pattern-localities can be tested by comparing the RC values and their standard deviations. We used a Monte Carlo method (e.g. Sokal and Rohlf 1995) to obtain the standard deviation for each RC . The RC of each pattern-locality is an invariant quantity, but its standard deviation depends on the pair-wise coupling of hummocks and hollows in the numerator of eq. (I). In our study, however, hummocks and hollows were not paired: therefore it was necessary to consider all possible pairs. Hence, we used a Monte Carlo method to randomly select hummock-hollow pairs to calculate a standard deviation of the mean hummock-hollow difference. For the random selection of hummock-hollow pairs we used the random permutation function as implemented in MATLAB (Version 7.5.0, Mathworks 2007). We repeated this procedure 100,000 times, yielding 100,000 standard deviations. The number of iterations was chosen in a way that the average of these standard deviations converged to a constant value, which was used as the standard deviation of the RC . If the hummocks and hollows had an unequal sample size, the RC itself was also calculated using the Monte Carlo procedure described above. We could then test for significant differences between sites using a t-test for two populations. Because multiple comparisons were made for each resource (10 pair-wise comparisons were made between the 5 pattern-localities) we subsequently performed a Bonferroni adjustment.

In the above procedure, it is assumed that measurement points can be seen as independent observations. In other words, it neglects the effect of trends on a larger spatial scale than the current scale of interest. To test the validity of this assumption we also performed the analysis by focusing on hummock-hollow differences between fixed pairs of nearest neighbors. When assigning hummock-hollow pairs in this manner, the standard deviation of the mean hummock-hollow difference may be different from the random procedure if there is a spatial trend that is filtered out (e.g. Rietkerk et al. 2000). In our analysis, however, the change in standard deviations did not qualitatively alter the results. Hence it can be concluded that the effect of spatial trends was very weak as compared to the local hummock-hollow differences in our dataset and that the assumption of independence of measurement points is justified.

Results

First, we determined for all five pattern-localities which nutrient was limiting plant growth in order to focus our analysis on resource contrasts for the limiting nutrient. Then, we tested our hypothesis with the data on nutrients in water and vegetation (Column 6 in Table 1). More specifically, we tested whether there was an increasing trend in resource contrast along the evapotranspiration (ET) gradient (ranging from Scotland to Sweden to Siberia).

Type of nutrient limitation

In all five pattern-localities, the majority of measurement points (84%) indicated phosphorus (P) limitation (Fig. 2). Co-limitation by nitrogen (N), however, did also occur (12.5%, Fig. 2). Co-limitation by potassium (K) was rarely observed (~ 1%, Fig. 2). Vegetation on the hummocks in the Siberian pattern was on average co-limited by N and P, vegetation on all other microforms in all other pattern-localities was on average P-limited. In all pattern-localities, N:P ratios in plants growing on hummocks were significantly lower as compared to hollows (data not shown), suggesting that hollows are more strongly limited by P. It can be concluded that P is the most important nutrient limiting plant growth, so in the following analyses we will focus on P, but we will report the results for N and K as well.

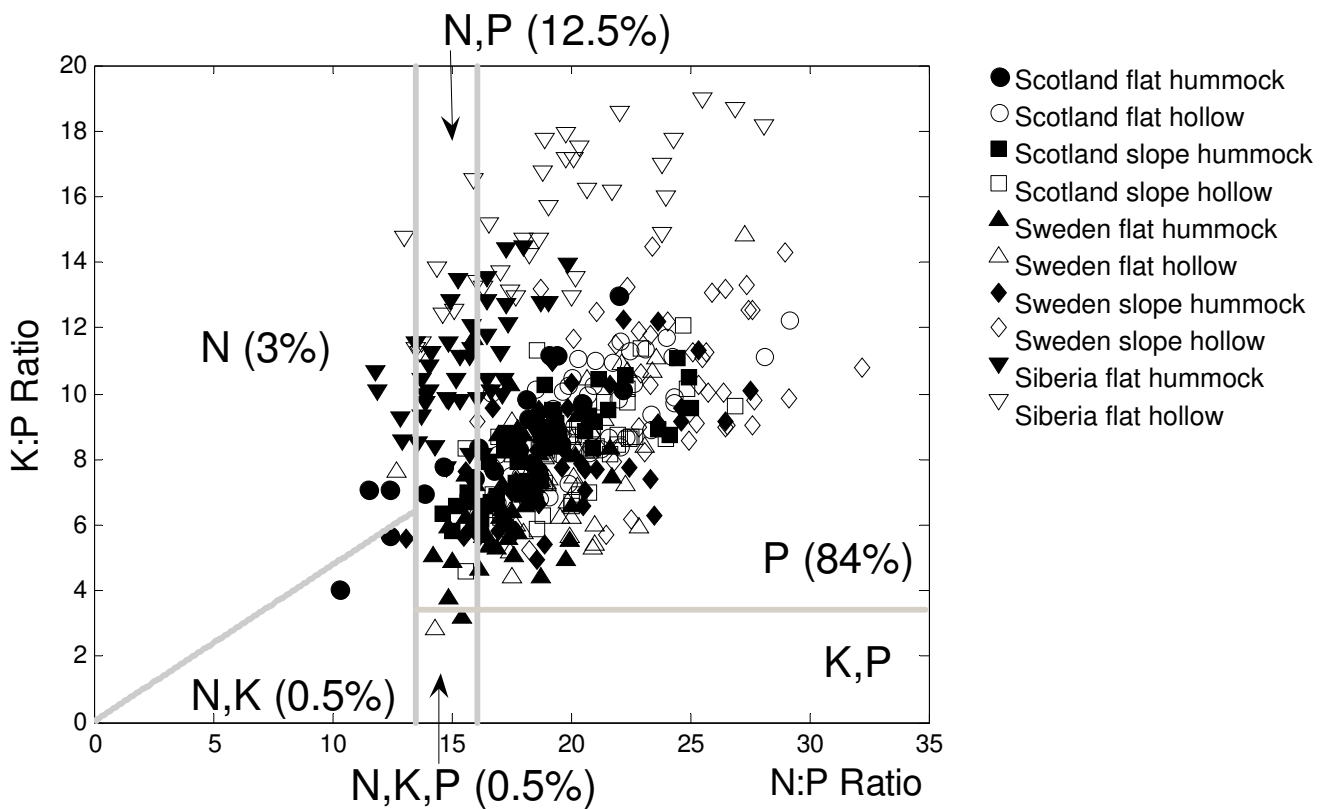


Figure 2: Nutrient ratios within the tissue of plants growing on hummocks (filled symbols) and hollows (open symbols) in different types of patterned peatlands. *Rhynchospora alba* was sampled in Scotland, *Eriophorum vaginatum* in Sweden and *Carex lasiocarpa* in Siberia. The grey lines separate regions with different kinds of nutrient limitation. Letters indicate nitrogen (N), phosphorous (P) or potassium (K) limitation. More than one letter indicates co-limitation of multiple nutrients. Between brackets the occurrence of the type of limitation is given. On average, all three study areas were P-limited. Further, lawns and hollows were more strongly limited by P than hummocks/ridges.

Resource contrast

P concentrations in mire water were very low in the pattern-localities in Sweden (62% of the measurement points below the detection limit of 0.03 mgP l^{-1}) and Scotland (89% below the detection limit). In general, nutrient concentrations were highest in mire water under hummocks (Fig. 3). Further, vegetation growing on hummocks had a higher P content as compared to hollows, but a higher N and K content in hummock vegetation was only observed in the Siberian pattern (Fig. 3).

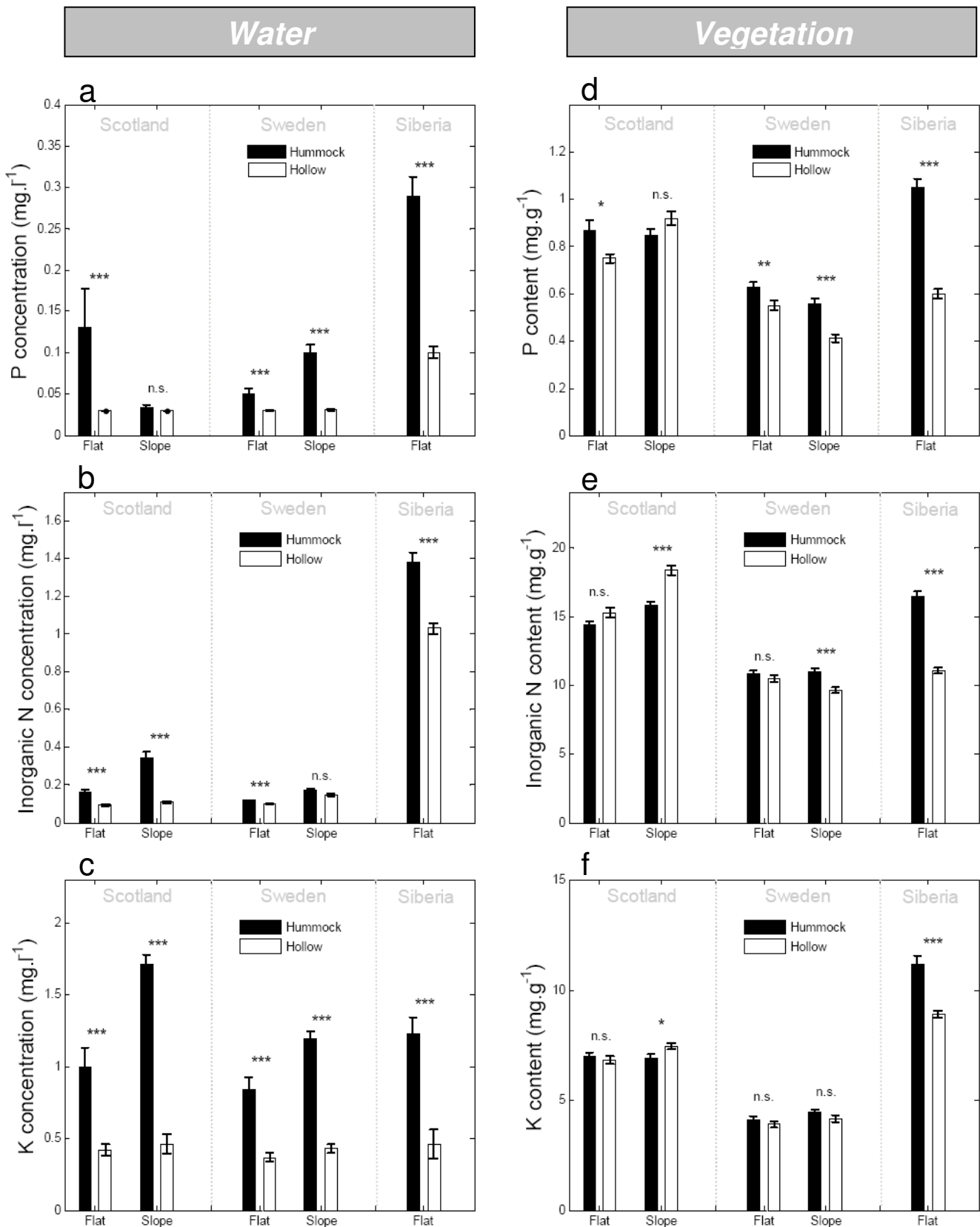


Figure 3: Nutrient concentrations in mire water (a-c) and vegetation (d-f) as measured on hummocks and hollows in patterned peatlands in Scotland, Sweden and Siberia. Black bars represent hummocks and white bars represent hollows. Asterisks indicate significant differences: *** $p < 0.001$, ** $p < 0.01$, and * $p < 0.05$.

There were no trends in the resource contrast for the nutrients in mire water (Fig. 4 a-c). For P, the smallest and largest resource contrast both occurred in Scotland (Fig. 4a), suggesting that the ET gradient had little influence on the contrast in mire water P concentration. Trends were also absent for mire water concentrations of N and K (Fig. 4 b,c). However, there were trends in the resource contrasts for the nutrient content in the vegetation tissue (Fig. 4 d-f). In general, the resource contrast increased along the ET gradient, with low ET:Prec ratio in Scotland to high ET:Prec ratio in Siberia (Fig. 4 d-f). The contrasts were negative (i.e. lower nutrient concentrations in the hummock than in the hollow) or slightly positive in Scotland, positive (i.e. higher nutrient concentrations in the hummock than in the hollow) in Sweden and strongly positive in Siberia (Fig. 4 d-f). This trend was qualitatively the same for vegetation P, N and K content. The only exception occurred for vegetation P content in the Scottish pattern on flat ground, for which the contrast in P content was similar to the Swedish pattern (but still smaller than the Siberian pattern).

Discussion

We will first discuss the issues that arise when comparing model results from previous theoretical studies with the field data gathered in this study. Subsequently, we discuss the implications of our results with respect to the relevance of the nutrient accumulation mechanism for peatland patterning in general.

Comparison of model results with field data

Our results indicated that resource contrasts in the vegetation of hummock-hollow patterned peatlands increase along an ET gradient (from areas with a low ET:Prec ratio to areas with a high ET:Prec ratio) (Table 1; Fig. 4 d-f). At the lower end of the ET gradient, vegetation growing in hollows had equal or higher nutrient content as compared to hummocks, whereas at the upper end of the gradient, nutrient content was much higher in vegetation growing on hummocks (Fig. 4 d-f). These results are in line with the hypothesis that in ET-dominated peatlands, patterning may be driven by a nutrient accumulation mechanism (Rietkerk et al. 2004b; Wetzel et al. 2005, 2009; Ross et al. 2006). Many theoretical studies have shown that such a resource concentration mechanism can induce patterning in a variety of ecosystems (Rietkerk and Van de Koppel 2008), which should be reflected in the presence of pronounced resource contrasts in patterned ecosystems (Boeken and Shachak 1994; Shachak et al. 2008; Van der Valk and Warner 2009). This study is the first comparison of resource contrasts in patterned ecosystems along an environmental gradient.

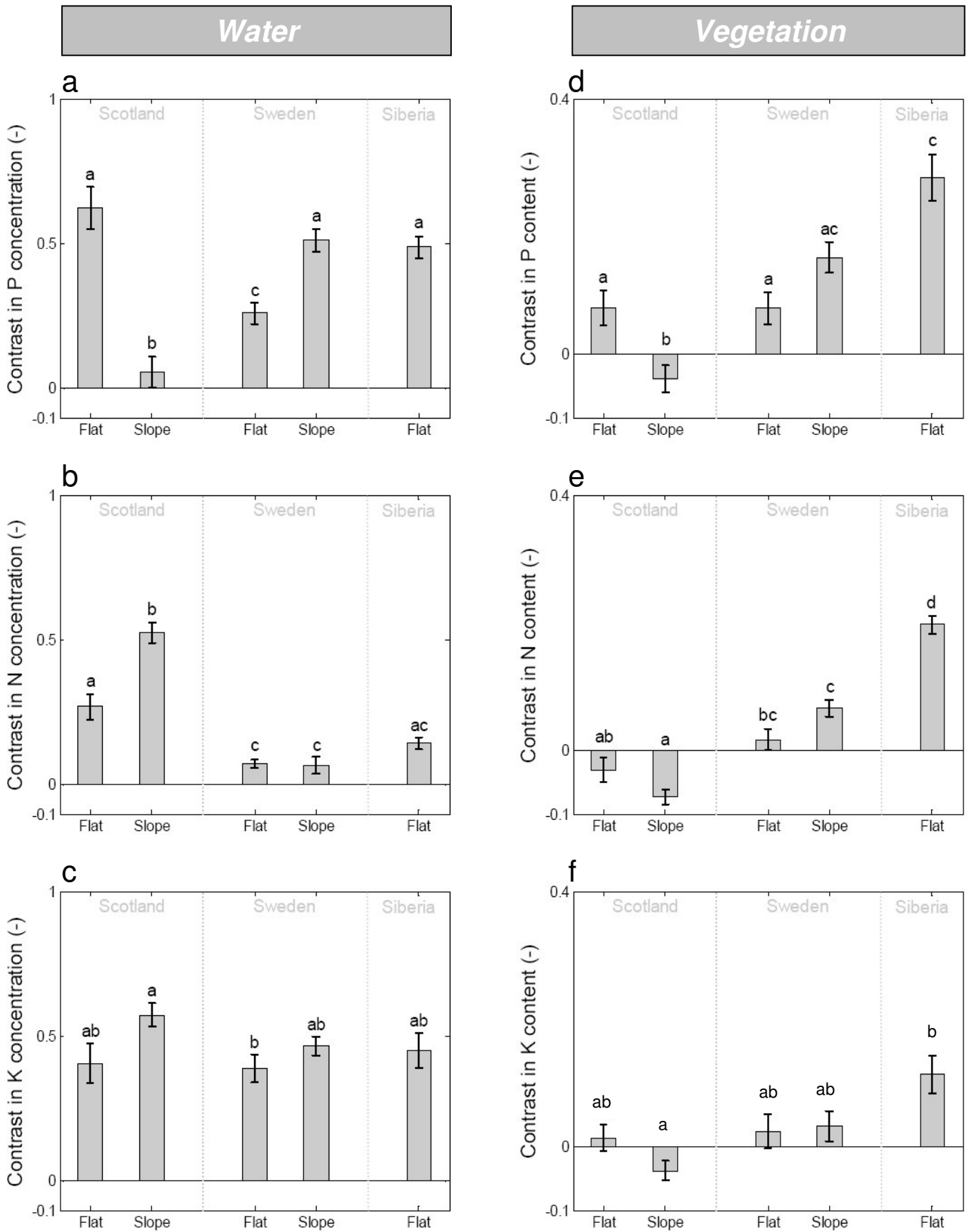


Figure 4: Hummock-hollow resource contrasts, for nutrient concentrations in mire water (A,B,C) and vegetation (D,E,F) as measured on hummocks and hollows in patterned peatlands in Scotland, Sweden and Siberia. In all panels the importance of evapotranspiration increases from left (Scotland) to right (Siberia). Different letters indicate significant differences ($p < 0.05$) between pattern-localities.

Contrary to our expectations, however, there was no trend in the contrasts in mire water nutrient concentrations along the ET gradient (Fig. 3; Fig. 4 a-c). These results emphasize the importance of a comparative approach across regions. In a previous study on the maze-patterned peatland in Siberia, the higher nutrient concentrations in mire water on hummocks were interpreted as evidence for the nutrient accumulation mechanism (Chapter 3). By comparing this Siberian study site with patterned peatlands in Scotland and Sweden, the present study revealed that resource contrasts were qualitatively similar in systems where the nutrient accumulation mechanism is probably less important (the Swedish site) or absent (the Scottish site). Similarly, the previous study interpreted higher values of electrical conductivity (EC) and sodium (Na) concentrations in the mire water on hummocks as indicators for higher ET rates (Chapter 3), but the same phenomenon was observed in the Scottish and Swedish pattern-localities (Table 2). Summarizing, the comparison with patterned peatlands in Scotland and Sweden reveals that the underlying pattern in hydrochemistry in Siberia cannot be interpreted as support for the nutrient accumulation mechanism.

The hypotheses that were tested in the present study were based upon a model that assumes a continuous plant uptake of nutrients and continuous availability of the dissolved nutrient pool (Chapter 4). In nutrient-poor sites as sampled in this study, however, the dissolved nutrient pool may be orders of magnitude smaller than annual nutrient uptake by plants (Bridgham et al. 2001). Therefore, nutrient availability is determined by the nutrient replenishment rate rather than the actual size of the dissolved nutrient pool at a certain moment (Binkley and Hart 1989; Bridgham et al. 2001). Under such nutrient-limited conditions, annual vegetation shoots may give a more reliable indication of the average availability of the limiting nutrient during the growing season (De Wit 1963; Vermeer and Berendse 1983; Craft et al. 1995; Wassen et al. 1995; U.S. EPA 2002).

An interesting observation in all three study sites is that the nutrient stoichiometry in the shoots indicated limitation by P rather than N (Olde Venterink et al. 2003; Wassen et al. 2005). In general, N is considered to be more often the limiting nutrient in mires (e.g. Aerts et al. 1995; Malmer et al. 1997), and increased plant growth has also been observed in N-addition experiments in one of our study sites (Gunnarsson et al. 2004; Wiedermann et al. 2007). Therefore, it is important to note that there may be interactive effects between N-addition and P-availability, for example through

increased phosphatase-activity of mire plants such as *Eriophorum vaginatum* (Kroehler and Linkins 1988; Olander and Vitousek 2000; Turner et al. 2003).

Further, previous studies suggested that EC and Na concentration in mire water are reliable indicators for ET rates (McCarthy et al. 1993; Bleuten 2001), because ET may induce concentration of ions that are not taken up by plants. These studies considered systems that were mainly fed by single ground- or surface water-source (McCarthy et al. 1993; Bleuten 2001). In the Scottish and Swedish sites of this study, however, precipitation is also an important water input source. The larger leaf area of the more densely vegetated hummocks may lead to greater interception losses (i.e., evaporation of water stored on the leaves). As a result, the water that enters the hummock through stemflow and throughflow may have a higher concentration of ions than the precipitation that directly enters the hollows (Miranda et al. 1984; Bobbink et al. 1992). In other words, the ionic concentration in Scottish and Swedish sites is not only influenced by water and nutrient redistribution processes in the peat layer, but also by interception processes from precipitation. Therefore, the concentration of conservative ions in these systems may be less suitable indicators for ET-induced water flow within the peat layer.

The above considerations of the limitations of the mire water chemistry data outline an important discrepancy between theoretical models and real ecosystem functioning. The hypotheses in this study were based upon the equilibrium (steady state) condition in deterministic models. In practice, however, ecosystems undergo external forcing, and it is more appropriate to think of an ecosystem having a dynamic regime rather than it being in a constant stable state (Scheffer et al. 2001; Scheffer and Carpenter 2003). In this study, we adopted a snapshot approach: at a specific moment in time, we measured the nutrient distribution in patterned peatlands, and analyzed the spatial variability in terms of resource contrasts. In a dynamic ecosystem regime, however, conditions are always subject to temporal variability. Thus, to link model predictions to field data, a snapshot approach requires that the temporal variability is filtered out, which means that the key variables should reflect a longer-term average. Note that this is the case for the annual tissue of vegetation (Wassen et al. 1995, 2005; Olde Venterink et al. 2003), but not for the dissolved nutrient pools (Bridgham et al. 2001). More generally, we think that our snapshot approach is also valuable to test model hypotheses in other patterned ecosystems as well, but suggest that a snapshot approach can only be used for key-variables that represent a longer-term average of the ecosystem's conditions.

Further, our results agree with other recent empirical research suggesting that future models on pattern formation in peatlands would benefit from a more detailed description of precipitation and interception processes (Robroek et al. 2007 a,b).

The role of the nutrient accumulation mechanism in peatland patterning

Our vegetation data revealed that the resource contrast increased along an evapotranspiration gradient (Table 1; Fig. 4 d-f). Previous theoretical studies suggest that such a positive resource contrast reflects occurrence of the nutrient accumulation mechanism. A next step would be to determine at what value of the ET:Prec ratio the nutrient accumulation mechanism might become important for peatland patterning. The Swedish pattern-localities are interesting in this respect. Trees in particular may stimulate ET rates (Frankl and Schmeidl 2000; Rietkerk et al. 2004a). Resource contrasts for phosphorous (P) and nitrogen (N) in vegetation tended to be slightly higher in the pattern with trees, but this difference was not significant (Fig. 4 d,e). Our measurement period took place relatively late in the growing season, when ET rates may be close to the yearly maximum (Sagerfors et al. 2008). During this period, ET losses may exceed inputs via precipitation (Sagerfors 2007). We speculate that during this short period, there might be some nutrient accumulation on hummocks, but this occurs not long or strongly enough to drive pattern formation and amplification of resource contrasts. This could imply that the Swedish pattern-localities are close to the threshold where the nutrient accumulation mechanism may become relevant for peatland pattern formation. Based on this assumption, we hypothesize that the nutrient accumulation mechanism may become relevant in peatlands with a considerable tree and shrub cover and with an ET:Prec ratio of at least ca. 0.6 (on an annual basis). This threshold value agrees well with other patterned wetland ecosystems where the nutrient accumulation mechanism may drive pattern formation. Based on measurements of diurnal dynamics in water table level, the nutrient accumulation mechanism may also occur on a patterned slope of a Swedish bog (ET/Prec 0.92 – 1.28 for 1996-1997, Kellner and Halldin 2002), in tree islands and surrounding sloughs in the Florida Everglades (ET/Prec 0.7 – 1.2, German 2000; Reed and Ross 2004) and in tree islands and the surrounding swamps in the Okavango Delta (ET/Prec ~ 3, McCarthy et al. 1993; McCarthy and Ellery 1994). It should be noted that an ET:Prec ratio of ca. 0.6 or higher would be a rather strong climatic constraint, excluding the relevance of the nutrient accumulation mechanism for many patterned peatlands, especially in maritime climates (Fig. 5). On the other hand, this threshold would suggest that the nutrient accumulation may be relevant in three of the four largest peatland regions in

the world: the West Siberian basin, the Pripyat basin and the Glacial lake Agassiz (Glaser et al. 2004).

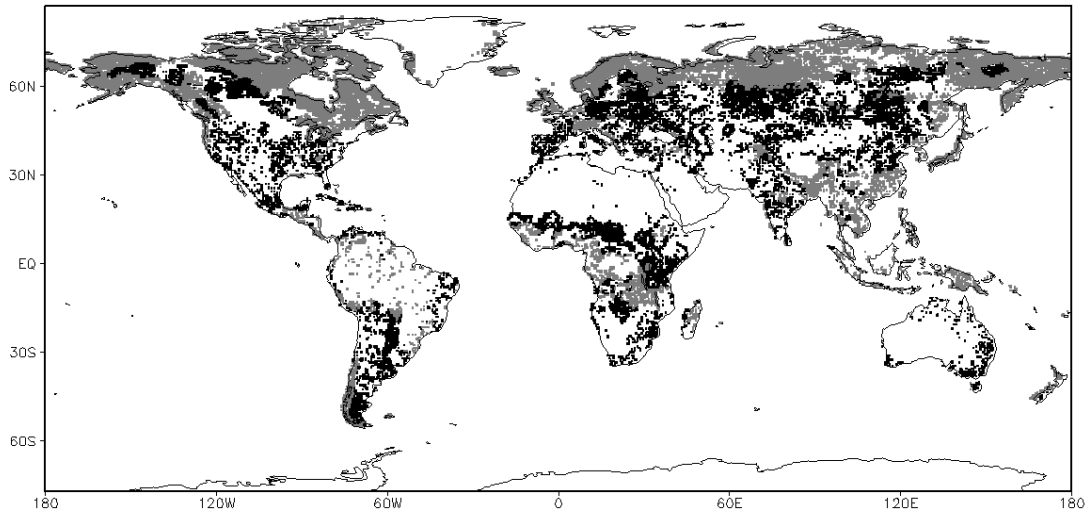


Figure 5: Map showing the global distribution of peatland ecosystems (grey and black areas), and the peatland areas where the nutrient accumulation mechanism might affect peatland patterning (black areas). In these areas the long-term annual average evapotranspiration/precipitation ratio is larger than 0.6. The following data sources were used: Lehner and Döll (2004) for wetland cover, Mitchell et al. (2004) for long-term annual average precipitation, Fekete et al. (2002) for long-term annual evapotranspiration.

It should be noted, however, that an essential component of the nutrient accumulation mechanism is the entrapment of nutrients on ridges through uptake by vascular plants (Chapter 3). Moreover, there is likely to be strong seasonal variation in the partitioning of drainage and ET losses (Seppälä and Koutaniemi 1985; Price and Moloney 1994; Quinton and Roulet 1998; Admiral and Lafleur 2007). More specifically, the annual ET:Prec ratio may be reduced by spring floods (e.g. through snowmelt) and relatively wet fall periods with reduced ET. This means that during the vascular plant growing season, the ET:Prec ratio may even need to exceed the value of ca. 0.6 to create the potential for the nutrient accumulation mechanism. Further, the duration of the vascular plant growing season also needs to be long enough to create substantial differences in nutrient status between microforms. Therefore, a promising direction for future studies would be to estimate the potential for the nutrient accumulation mechanism more precisely by taking into account the following two components: the ET:Prec ratio for the vascular plant growing season, and the duration of this vascular plant growing season.

Conclusions

We presented the first study that compared the resource contrasts between hummocks and hollows of patterned peatlands in maritime, humid temperate and humid continental climates. Our results suggest that the presence of the nutrient accumulation mechanism may amplify resource contrasts in the vegetation of patterned peatlands (Fig. 4 d-f), which may be of particular importance in peatlands with a considerable cover of shrubs and trees and relatively little precipitation excess (Fig. 5). Further, peatlands worldwide are affected by changing patterns in precipitation and ET (Meehl et al. 2007) and changes in temperature that may affect the length of the vascular plant growing season (Backéus 1985; Chapter 2). The results of this study suggest that these changes may affect the ecosystem functioning of patterned peatlands by altering the contribution of pattern-driving mechanisms to redistribution of water and nutrients.

Acknowledgments

We thank Rob Dewar and the National Trust for Scotland for granting access to the Inverewe field site. We thank Helen de Waard, Gijs Nobbe, Arnold van Dijk and Dineke van de Meent for help with the laboratory analyses, and Wladimir Bleuten, Wiebe Borren, Olga Pisarenko, Andrej Korolyuk, Jan Hrupacék and Frans Wassen for assistance in the field, and Hugo de Boer for assistance with preparing Figure 5. The research of MBE and MR is supported by a VIDI grant from the Research Council Earth and Life Sciences of the Netherlands Organization of Scientific Research (NWO-ALW) to MR.

6

Synthesis and Perspectives

Maarten B. Eppinga

Synthesis and Perspectives

Ecosystems are increasingly exposed to gradual changes in climate, nutrient loading and biotic exploitation (Vitousek et al. 1997; Kareiva et al. 2007). How ecosystems respond to these changes is one of the frontiers in ecology and environmental science. Ecosystems may respond in a smooth and gradual way to changes in environmental conditions, but evidence is growing that the response will be different for ecosystems that are governed by positive feedback mechanisms. Due to positive feedback mechanisms, environmental thresholds may emerge and ecosystems may undergo so-called catastrophic shifts in ecosystem structure and functioning when these environmental thresholds are passed. Once a shift has occurred, it may be difficult to restore the previous ecosystem state due to hysteretic effects. Hence, it is desirable to know whether an ecosystem is close to an environmental threshold. A recent idea is that in terrestrial ecosystems, patchiness of sessile biota may be the result of spatial self-organization (Rietkerk et al. 2004b). Such self-organized patchiness may indicate proximity to environmental thresholds (Fig. 1; Rietkerk et al. 2004b).

This notion suggests that the feedback mechanism that drives self-organized patchiness is (at least in part) the same mechanism that induces alternate stable ecosystem states and the possibility of catastrophic shifts from one state to the other. This feedback mechanism can be characterized as a resource concentration mechanism: the presence of a consumer increases resource availability locally by harvesting resources from a surrounding area. This means that resources are depleted in this surrounding area. Thus, there is a short-range positive feedback and a longer-range negative feedback, referred to as a scale-dependent feedback. Vegetation patchiness has also been observed in peatland ecosystems. These peatland patterns consist of densely vegetated hummocks and sparsely vegetated hollows. Although peatland patterning has attracted a lot of attention of researchers during the last century, the driving mechanisms remain elusive. The striking resemblance with patchiness in other ecosystems generated the idea that peatland patterning may be driven by a resource concentration mechanism. Vascular plants may increase evapotranspiration, thereby inducing water and nutrient flow towards densely vegetated patches (Rietkerk et al. 2004a). The aim of this thesis was to test whether peatland patterning is driven by a resource concentration mechanism, and whether peatland patterns serve as an indicator to environmental thresholds.

The approach to reach this aim consisted of a combination of theoretical and empirical studies. From here, I will briefly recapitulate the findings of Chapters 2-5 by answering the research questions that were raised in Chapter 1. At the end of this section I will also discuss the final research question, whether self-organized patchiness in peatlands could serve as an indicator for catastrophic shifts. Thereafter, I will provide a perspective on how further research could contribute to better predict the response of patterned peatlands to climate change. In the last section I will discuss in what way this work may contribute to ecosystem theory.

Vegetation Cover

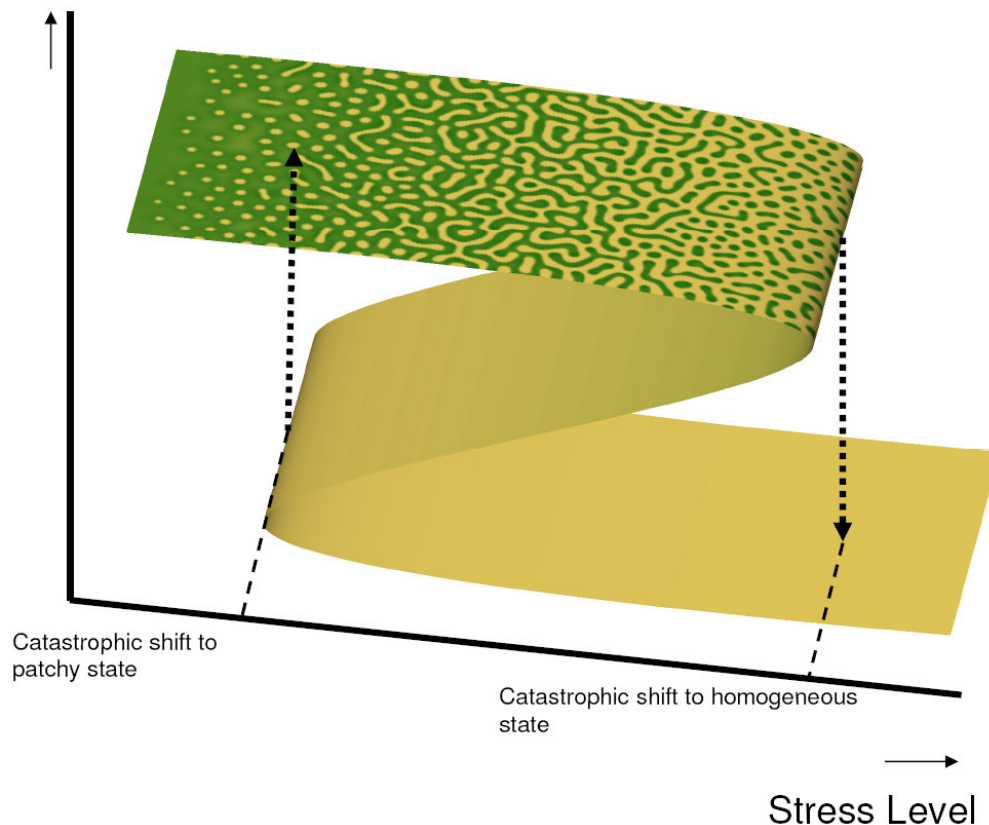


Figure 1: Conceptual model illustrating that self-organized patchiness may serve as an indicator for catastrophic ecosystem shifts (figure based upon Rietkerk et al., 2004b).

Synthesis of previous chapters

Are theoretical concepts for complex (eco)systems relevant for the case of spatial patterning of peatland ecosystems?

In Chapter 2 of this thesis, we concluded that the answer to the first research question is yes; the concepts of positive feedback, alternate stable states and catastrophic shift are relevant for peatland ecosystems. This conclusion was based upon a review of empirical studies of peatland ecosystems. The results of this review were also used to expand a model previously developed by Rietkerk et al. (2004a).

The expanded model results suggested that hummocks are not only characterized by higher biomass, but also by higher nutrient availability and lower water tables as compared to hollows (Fig. 2). Obviously, the latter model predictions cannot be checked with aerial photographs but require empirical field observations.

Does field data from patterned peatlands corroborate with predictions of models that mimic a nutrient accumulation mechanism?

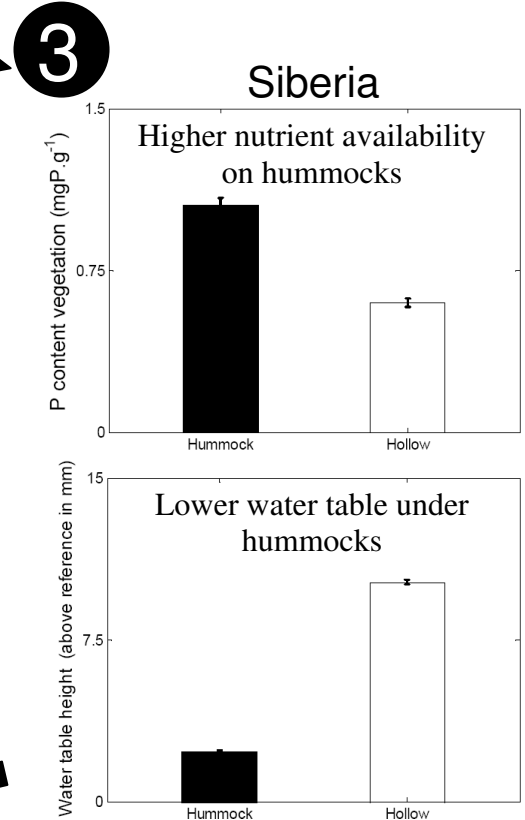
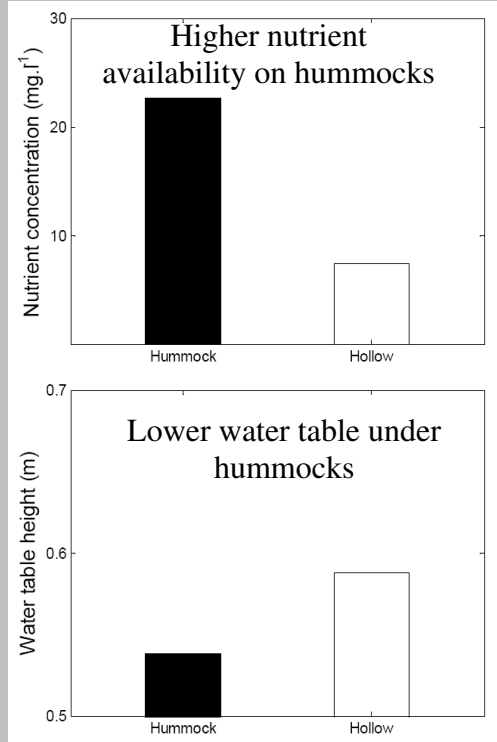
Empirical testing of the model results of Chapter 2 is essential to gain confidence in the relevance of the modeled nutrient accumulation mechanism for real ecosystem patterning. In Chapter 3, we performed such an empirical test in a patterned peatland in Siberia. The empirical test was very straightforward: to check whether the spatial pattern in nutrients and hydrology agreed with the model predictions. The empirical results agreed qualitatively with the model predictions: nutrient availability was higher and the water table was lower under hummocks as compared to hollows (Fig. 2). However, the research question could not be simply answered with yes. Although the data corroborated model predictions, it also revealed that two other proposed mechanisms for peatland patterning, the peat accumulation mechanism and the water ponding mechanism (Box I), may play a role in the formation of the patterns. More, specifically, the peat accumulation mechanism may amplify the differences between hummocks and hollows in acrotelm thickness and create sharp boundaries between the microforms. The water ponding mechanism may influence the distance between hummocks, and this mechanism becomes more important with increasing slope.

► **Figure 2:** Summary of the results presented in this thesis. In Chapter 2, a mathematical model revealed that the presence of an evapotranspiration-induced scale-dependent feedback (i.e. the nutrient accumulation mechanism) would be reflected by higher nutrient concentrations and lower water tables under hummocks. In Chapter 3, this hypothesis was tested with field data from a maze-patterned peatland in Siberia. In Chapter 4, an alternative hypothesis was derived with an extended mathematical model that could also explain peatland pattern formation in regions where evapotranspiration is only a small component in the water balance. More specifically, the model predicts that the hummock-hollow difference in nutrient availability increases with increasing importance of evapotranspiration. In Chapter 5, field data from patterned peatlands in Scotland, Sweden and Siberia was found to agree with this hypothesis.

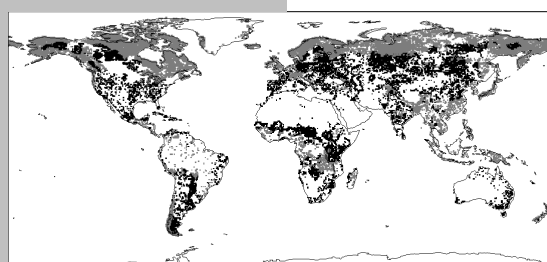
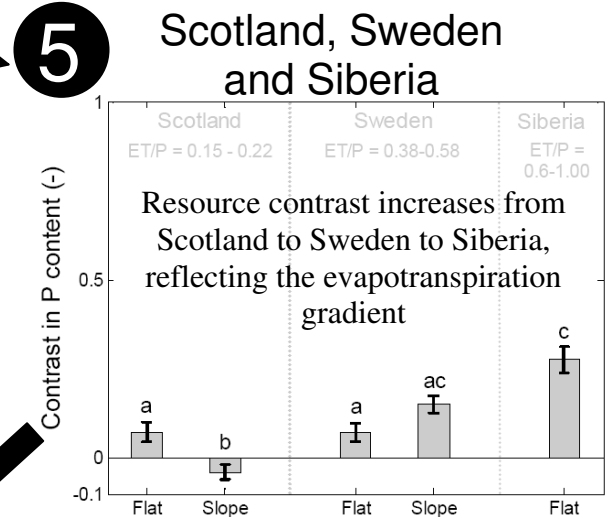
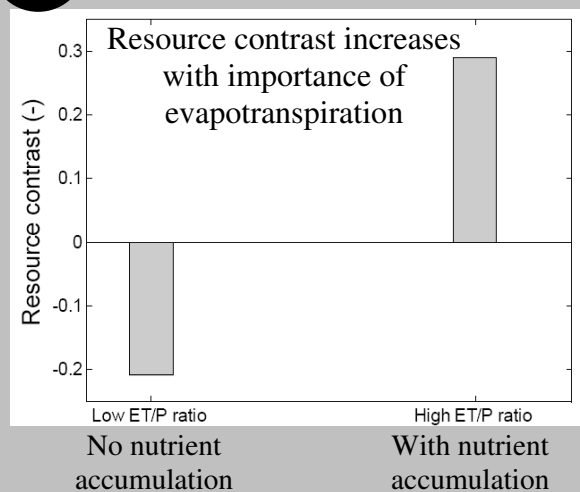
Models

Data

2 Variation within patterned peatland



4 Variation between patterned peatlands



Black and grey areas show the regions where peatlands occur. Based on field measurements the nutrient accumulation mechanism is only expected in the black areas.

Box I: Three mechanisms of peatland patterning

The nutrient accumulation mechanism: This mechanism implies that because of higher evapotranspiration rates, there is a net flow of water and dissolved nutrients toward densely vegetated hummocks (Rietkerk et al. 2004a). Subsequently, the nutrients become trapped on hummocks through uptake by vascular plants. Thus, during their lifespan, vascular plants that grow on hummocks accumulate nutrients originating from outside the hummock. Nutrients become available again through mineralization of vascular plant litter, but this only increases nutrient availability on the local scale at which the litter is deposited (within the hummock). Models predict that this local recycling effect outweighs the effect of nutrient uptake (Chapter 3), meaning that nutrient concentrations in the mire water under hummocks also increase. Because higher nutrient availability will lead to an increase in vascular plant biomass, the nutrient accumulation mechanism is a self-reinforcing process.

The peat accumulation mechanism: This mechanism relates to the fact that plant growth in peatlands is limited by water stress. Water stress occurs both at high water tables because of waterlogging and at low water tables because of desiccation. Because plant production determines the organic matter input into the peat layer, peat growth is optimal at intermediate acrotelm thickness. As proposed by Belyea and Clymo (2001), this implies that below the optimum acrotelm thickness for plant growth, there is a positive feedback between net rate of peat formation and acrotelm thickness. This positive feedback explains how peatland microforms may develop either into a wet, sparsely vegetated, low-productive state or a dry, densely vegetated, high-productive state. Thus, slight differences between wetter and dryer sites may further amplify and lead to spatial patterning of sharply bounded microforms (Sjörs 1990; Belyea and Clymo 2001).

The water ponding mechanism: This mechanism was first proposed by Kulczyński (1949), and relates to a lower hydraulic conductivity of hummocks as compared to hollows. As a result of lower hydraulic conductivity, water may accumulate upslope of hummocks, which stimulates the formation of hollows. Later model studies (Swanson and Grigal 1988; Couwenberg 2005; Couwenberg and Joosten 2005) show that such water ponding mechanism indeed explains spatial hummock-hollow patterning, provided that the slope of the peatland exceeds a critical angle. Hence, the water ponding mechanism is a possible explanation for the formation of hummock-hollow patterns on peatland slopes.

Which key variables can discriminate the nutrient accumulation mechanism from alternative mechanisms as crucial drivers for peatland patterning?

The results of Chapter 2 and Chapter 3 suggest that self-organized patchiness in peatland ecosystems may be driven by an evapotranspiration-induced scale-dependent feedback, i.e. the nutrient accumulation mechanism. Patchiness in peatlands, however, is also observed in climatic regions where evapotranspiration is of minor importance in the water balance. The model study presented in Chapter 4 provided an explanation for this apparent contradiction. Similar types of peatland patterning may be driven by different (combinations of) mechanisms. The results suggested that nutrients and hydrology are the key variables that can discriminate between patterns as driven by the nutrient accumulation mechanism and as driven by other mechanisms (Fig. 2). This answer to the research question paved the way for another empirical test. If the nutrient pattern as observed in Siberia indeed reflects

the presence of the nutrient accumulation mechanism, the nutrient pattern should be different in peatlands where the nutrient accumulation mechanism is likely to be absent.

Is the presence or absence of the nutrient accumulation mechanism indeed reflected in field data on the spatial variation of key variables in patterned peatlands?

In Chapter 5, we quantified the resource contrast (difference in nutrient availability between hummocks and hollows) for five pattern-localities in Scotland, Sweden and Siberia. We found that the resource contrast in vegetation increased along the evapotranspiration gradient (Fig. 2). This agreed with the findings in Chapter 4. The data on nutrient concentration in the water, however, did not agree with the hypothesis, in that no trends in resource contrast were found. The very low nutrient concentrations and the role of interception processes in the study sites may explain this discrepancy. Thus, the answer to the research question is: yes, but only in the nutrient content of the vegetation. This suggests that the adopted 'snapshot approach' (Hanski 1994; Ter Braak et al. 1998) is valuable to test model hypotheses in patterned ecosystems, but it can only be used for key variables that represent a longer-term average of ecosystem conditions.

These answers to the four of the research questions will now be combined to address the final research question: *What potential catastrophic shifts could occur in peatland ecosystems and can spatial patterns serve as an indicator of proximity to such shifts?*

What kinds of shifts occur in peatlands, and can patterns indicate these shifts?

Peatlands form by the build-up of an organic matter layer, either on mineral soil or through overgrowth of a lake. Pattern formation starts after a substantial peat layer has already been built up (Foster et al. 1983; Charman 1995; Karofeld 1998; Belyea 2007). More specifically, hollows or pools develop as secondary features on the peat layer. Previous research suggests that during the Holocene, the onset of hollow formation has been triggered by a change in external conditions, namely increasing climate wetness (Karofeld 1998; Belyea and Malmer 2004). During wetter periods the water table rises in the aerobic upper layer of peat, the acrotelm. Note that the acrotelm consists of plant litter that has accumulated over a period of many decades. This means that a climate-induced water table rise may induce a large change in acrotelm thickness as compared to year-to-year variation in biomass production of the vegetation. This movement of the water table closer to the surface may be

reinforced by a reduced rate of plant production (Belyea and Clymo 2001). The pattern-forming mechanisms that were studied in this thesis (Box I) explain why peatlands may not respond in a uniform way to increases in climate wetness, but develop into a pattern of dryer hummocks and wetter hollows. Over time, the hollows increase in size and become deeper (Foster et al. 1983; Belyea and Clymo 2001; Belyea and Lancaster 2002). The formation of hollows has major consequences for peatland ecosystem functioning in terms of hydrological flow paths (Foster et al. 1983; Quinton and Roulet 1998), vegetation composition (Svensson 1988; Sjörs 1990) and carbon sequestration rate (Belyea and Malmer 2004).

Thus, in the case of hollow formation due to increased climate wetness as observed in the past, the transition from unpatterned to patterned peatland is already a shift that is difficult to reverse (Belyea 2007). This means that for this case the occurrence of peatland patterns do not serve as an indicator of proximity to catastrophic shifts, but rather that the shift has already happened. I will now proceed, however, with a case for which I think that peatland patterns may possibly serve as an indicator for catastrophic shifts.

The results of Chapter 4 suggest that the occurrence of the nutrient accumulation mechanism may also lead to hollow formation due to nutrient deficiency in low density patches. In the peatlands of the Florida Everglades, nutrients may be concentrated on densely vegetated tree hummock islands in a matrix of surrounding wet hollows or sloughs (Wetzel et al. 2005). In this system, tree hummock islands only cover 3% of the surface, but sequester 67% of the incoming nutrients (Wetzel et al. 2009). This patterning may be partly driven by the nutrient accumulation mechanism (Reed and Ross 2004; Wetzel et al. 2005, 2009; Ross et al. 2006; Larsen et al. 2007). The nutrient accumulation mechanism involves subtle gradients in water level between hummocks and hollows (Chapter 3) that are driven by differences in evapotranspiration. The water flows in the Everglades system, however, have been altered by drainage activities during the last century. Therefore, the nutrient accumulation mechanism may be less effective, which could explain the observed decline of tree islands in the system (Wetzel et al. 2009). Once tree islands have disappeared, the vegetation becomes homogeneous cattail vegetation (Wetzel et al. 2009). Thus, in the Florida Everglades a system with a very low density of tree islands surrounded by wet sloughs may be indicative of proximity to a shift toward more homogeneous cattail vegetation. This shift would be driven by manmade alterations of the hydrological system.

It is not unlikely that the surface structure of many peatlands will become affected by the current global change. Current climate change creates environmental conditions that have not yet occurred during the Holocene period of peatland development. More specifically, the rapid increase in temperature together with increasing nutrient loadings to peatlands creates an unprecedented advantage for vascular plants in the competition with *Sphagnum* mosses (Ohlson et al. 2001; Malmer et al. 2003; Chapter 2). An increase in vascular plant cover may be reinforced by creating dryer conditions through increasing evapotranspiration rates (Souch et al. 1998; Takagi et al. 1999; Frankl and Schmeidl 2000; Andersen et al. 2005; Chapter 2). Due to global change, the response of peatlands to global change may be reinforced due to internal feedback mechanisms. These feedbacks, however, are not considered in the global models that are currently used to develop future climate scenarios (Limpens et al. 2008). I will now discuss some perspectives that are related to this issue.

Peatlands and climate change

During the Holocene, peatlands have acted as a large sink of carbon. About thirty percent of the global terrestrial carbon pool is stored in peatlands (Gorham 1991). A growing body of research suggests that changes in environmental conditions, such as climate change, may alter peatland-atmosphere carbon fluxes (Yu et al. 2001; Heikkinen et al. 2004; Turunen et al. 2004; Ise et al. 2008). Model studies suggest that a shift from a *Sphagnum*-dominated state to a vascular plant-dominated state may lead to a decrease of the carbon stock that has been sequestered in the past (Fig. 3a; Pastor et al. 2002; Heijmans et al. 2008; Chapter 2).

The models compare carbon storage in different equilibrium states (Fig. 3a). Most pristine peatlands, however, are still growing in height (Joosten and Clarke 2002), meaning that they have not yet reached the equilibrium condition (Clymo 1984). For example, Borren (2007) estimated that for the Bakchar bog in Western Siberia it will still take at least thousands of years before an equilibrium height will be reached. This means that peatlands may be still (far) away from their equilibrium amount of stored carbon. Hence, a shift from the *Sphagnum*-dominated state toward the vascular plant-dominated state does not necessarily imply a rapid decrease of the carbon stock (Fig. 3b). In theory, the carbon storage could even increase on the short-term due to higher plant growth rates (Fig. 3b, 3c). This exemplifies that the long timescale of peatland development complicates the application of equilibrium states. More specifically, predicted losses of the carbon stock due to a vegetation shift, as predicted by equilibrium models, need to be interpreted with caution.

Therefore, it is a more promising perspective to examine the response of peatlands to climate change in terms of changes in carbon fluxes, rather than changes in carbon stocks due to shifts in equilibrium states. Carbon fluxes in peatlands are mainly determined by the peatland surface pattern, which comprises the combination of acrotelm thickness and the vegetation (Belyea and Baird 2006). Many studies implicitly consider that the peatland surface pattern will respond in a uniform manner to climate change, i.e. either a uniform thickening or a thinning of the acrotelm (Weltzin 2000; Cramer et al. 2001; Davidson and Janssens 2006). However, due to spatial feedback processes, as studied in this thesis (Box I), the peatland surface structure is more likely to respond to climate change through spatial reorganization. More specifically, the cover of hummocks and hollows may change. Such a change in the peatland surface pattern may have a much larger effect on carbon sequestration rate than changes of carbon sequestration within hummocks or hollows (Belyea and Malmer 2004), but this is overlooked when only non-spatial interactions are being considered.

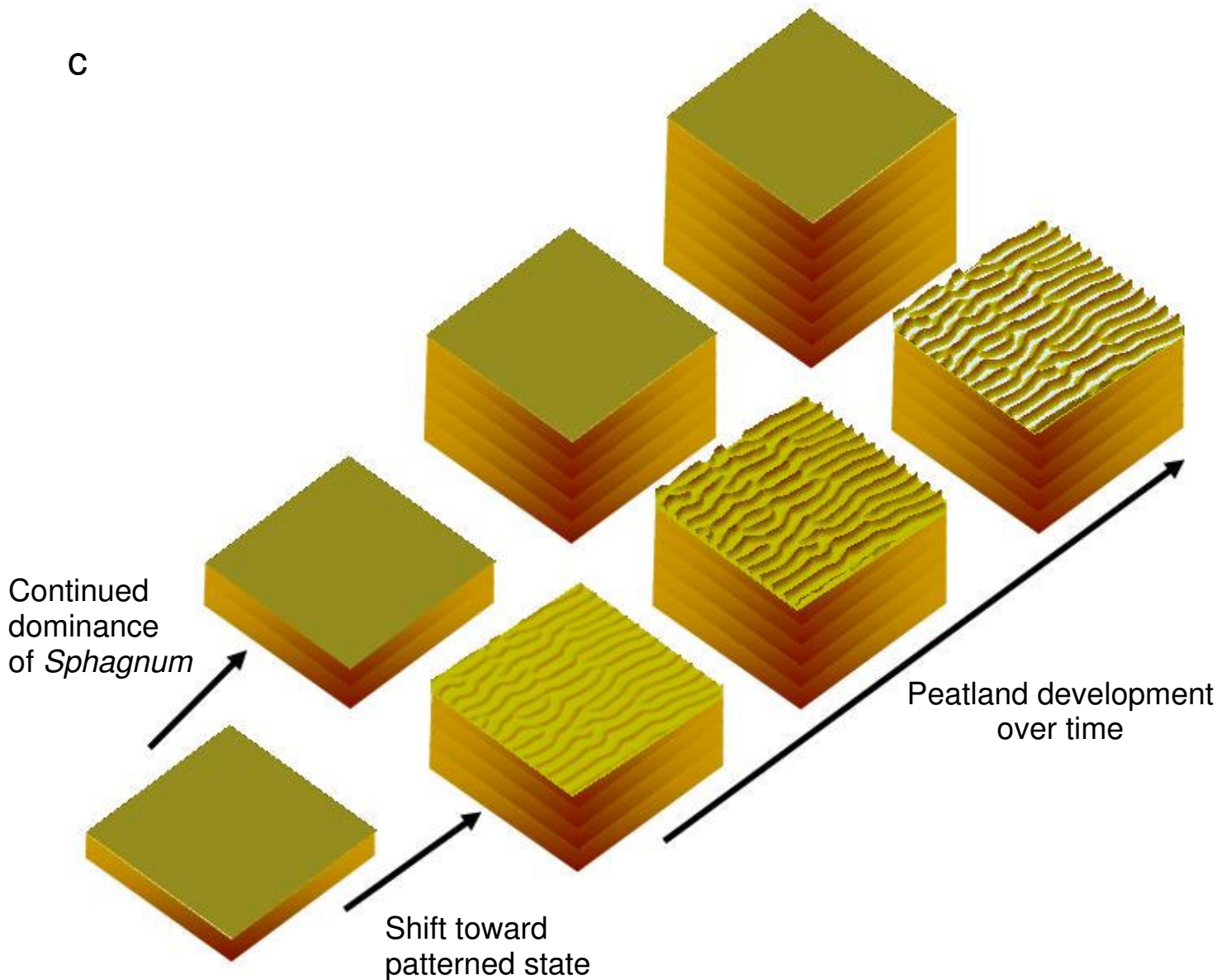
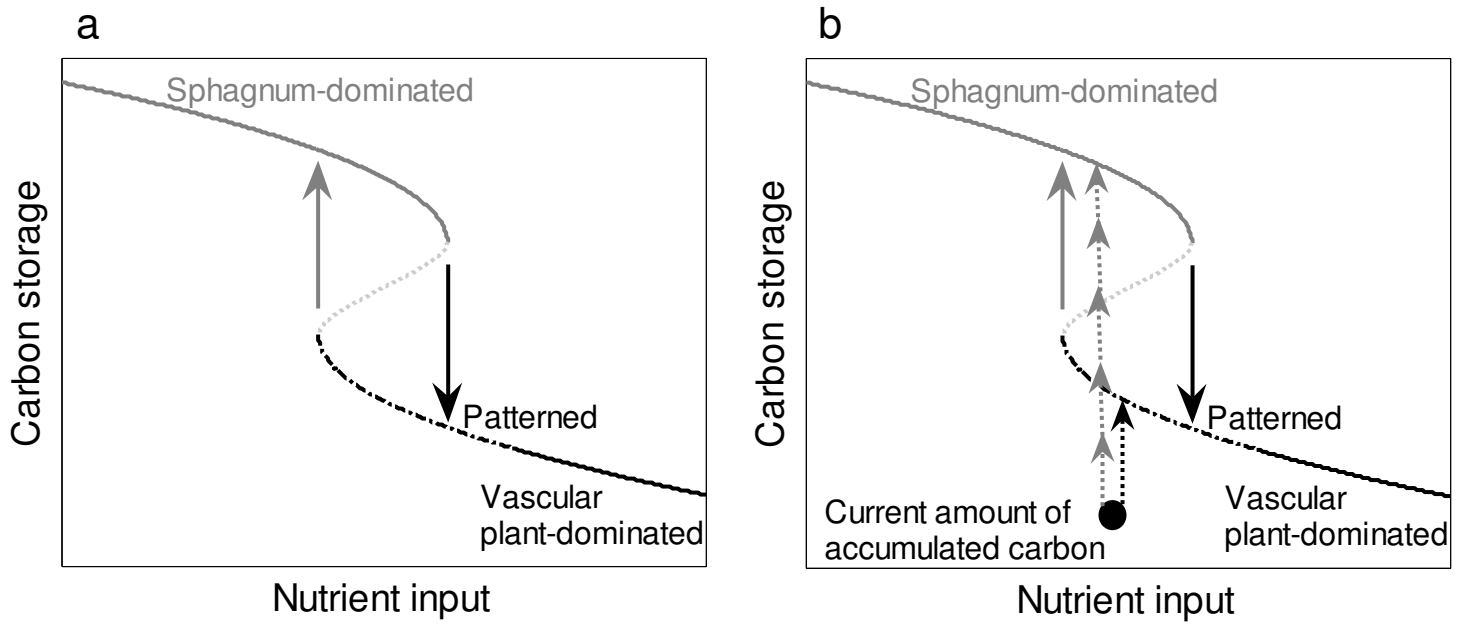
Furthermore, the work in this thesis suggests that the dominant pattern-forming mechanism may change due to changing environmental conditions (Chapter 5). Until now, models have not addressed such a possible change in peatland ecosystem functioning. The work in this thesis has been focused on the effects of three mechanisms on peatland surface patterning. Until now, the models that have been developed were designed to disentangle the effects of the mechanisms (Chapter 4). To predict for particular peatland regions whether there may be a change of the dominant pattern-forming mechanism, subsequent models could be improved by letting the strength of the three mechanisms (and possibly other mechanisms) depend entirely on the environmental conditions. In such a model the climatic parameters (notably temperature and atmospheric carbon dioxide concentration) need to be directly incorporated. As a result, the presence or absence of mechanisms would emerge from the environmental/climatic conditions, rather than the a priori on/off switching of mechanisms (as done in Chapter 4). Nevertheless, I will now briefly explore the potential consequences of climate change on the importance of the nutrient accumulation mechanism for peatlands, based on the findings in the previous chapters.

Based on current climate predictions (Fig. 4), the ratio between evapotranspiration and precipitation is expected to increase in most regions of the northern hemisphere (Fig. 4a). Based on the results of Chapter 5, we proposed that the nutrient accumulation mechanism may become important in peatlands if the

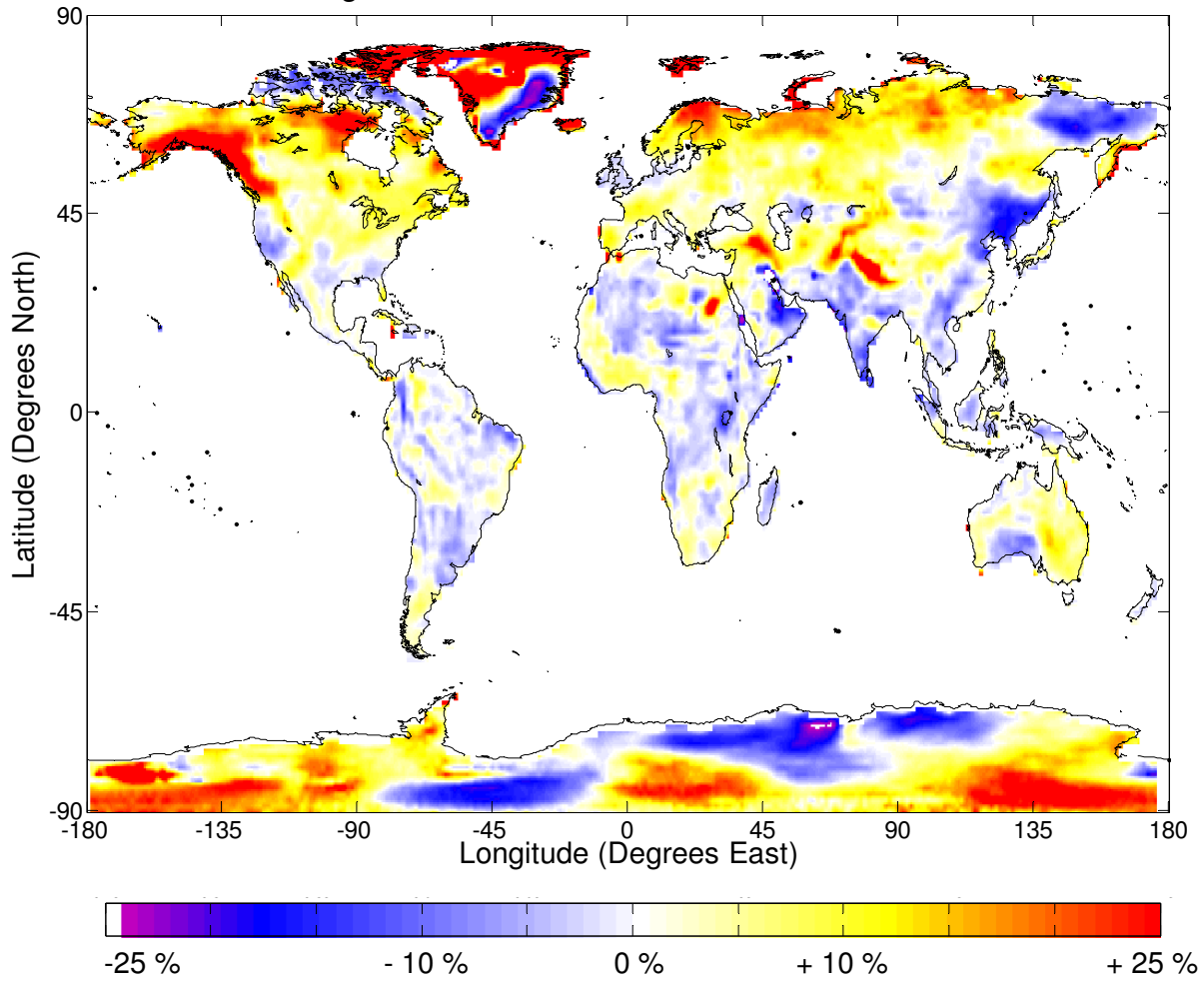
evapotranspiration : precipitation ratio exceeds a value of 0.6 (Chapter 5). Given the projected climate change, this implies that the nutrient accumulation mechanism may become more relevant for a larger region of peatlands, especially on the northern hemisphere (Fig. 4b). This predicted effect of climate change is most pronounced in Siberia, and Canada (Fig. 4b). Climate predictions also suggest an opposite trend for the southern hemisphere, where there may be a decrease in the area in which peatlands are affected by the nutrient accumulation (Fig. 4b).

Occurrence of the nutrient accumulation mechanism would lead to a strong differentiation of the peatland surface structure into high hummocks and wet hollows (Chapter 4). The carbon sequestration rate is very low for both these microforms (Belyea and Clymo 2001). Therefore, I speculate that in the coming century the nutrient accumulation mechanism may become more important for a larger region of peatlands on the northern hemisphere, especially in Siberia and Canada (Fig. 4). A more pronounced nutrient accumulation mechanism may lead to an initial increase in carbon sequestration due to the establishment of shrubs and trees on peatlands (Fig. 3c). On a longer term, however, carbon sequestration rates may decrease due to formation of slowly sequestering high hummocks and wet hollows, and due to the formation of easily decomposable litter by vascular plants.

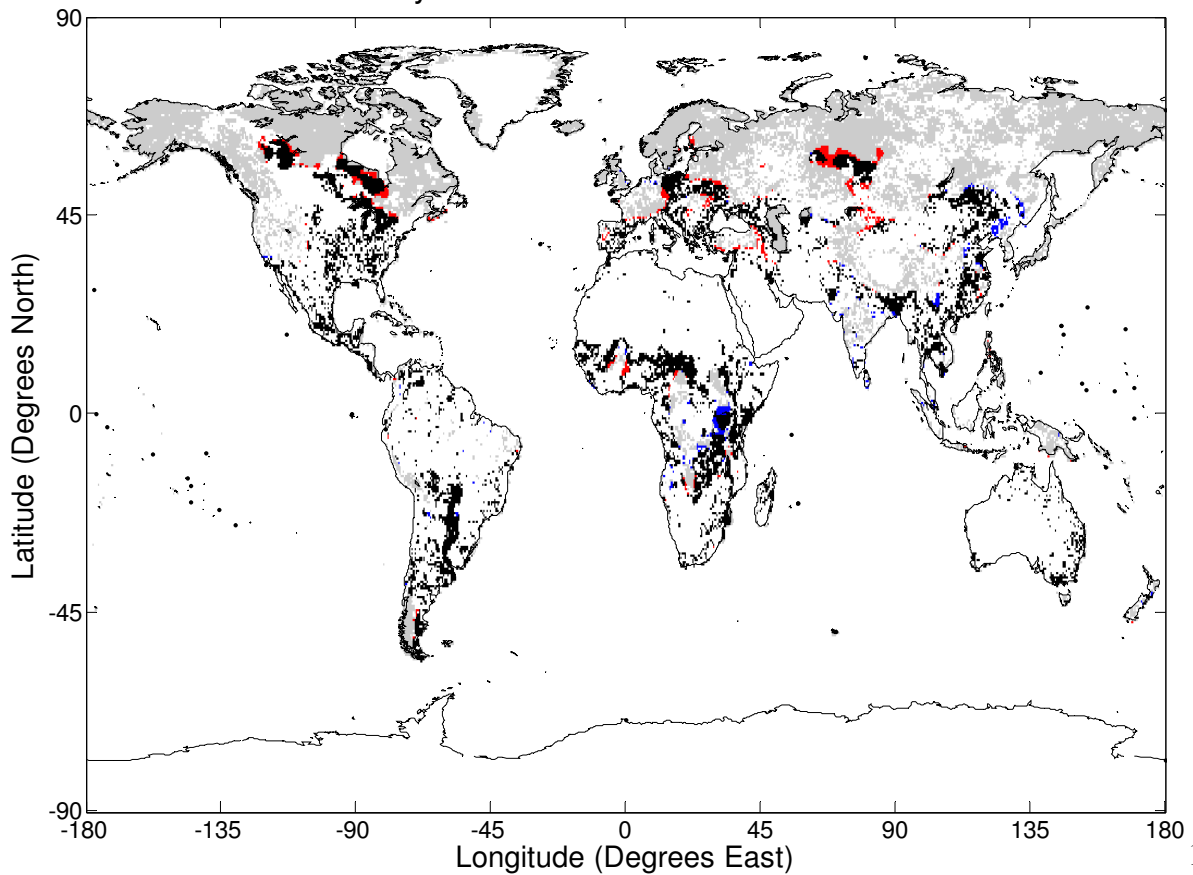
▼ **Figure 3:** *Conceptual diagrams on the response of peatlands to climate change. In Figs. 3a and 3b, increasing nutrient input is used as a forcing parameter (as in Chapter 2), but the same response could be drawn for decreasing precipitation, or increasing temperature. a) At low nutrient input rates, peatlands may be Sphagnum-dominated. If nutrient input increases from this point, there may be a shift toward a patterned state. Note that with the current developments in climate and nutrient loading, patterns are not very suitable to indicate catastrophic shifts, but rather indicate that the shift has already happened. In equilibrium, more carbon will be stored in the Sphagnum-dominated state. b) Peatland development occurs very slowly, and most natural peatlands are still actively growing, meaning that the current carbon storage may be less than the equilibrium storage of either state. Therefore, equilibrium concepts should be applied with caution. The black dot indicates a hypothetical amount of carbon storage. If this peatland would be Sphagnum-dominated, it would slowly accumulate more carbon, but it may lead to a large amount of carbon being stored on the long term. If there would be a vegetation shift from Sphagnum to vascular plants, the faster growing vascular plant species may increase the carbon storage on the short-term, but it may lead to a lower amount of carbon being stored on the longer term. c) A graphical illustration for the two carbon accumulation pathways that are shown in Fig. 3b. From the bottom left toward the top right indicates the development of a peatland over time. A shift from a homogeneous Sphagnum-dominated vegetation cover toward a patterned state may initially increase carbon sequestration rates, but the equilibrium carbon storage may be less than the storage capacity of the uniform state.*



Change in the ET/Prec ratio between 2009 and 2099



Effect of climate change on the distribution of peatlands that could possibly be affected by the nutrient accumulation mechanism



▲ **Figure 4:** *The effect of climate change on the role of the nutrient accumulation mechanism in peatlands. a) Due to climate change, the ratio between evapotranspiration and precipitation (ET/Prec ratio) is expected to increase in most parts of the northern hemisphere. The graph displays the projected change in ET/Prec ratio for the period 2090-2099 as compared to the period 2000-2009. For each period, the average precipitation and average evapotranspiration rate was determined based on the 120 monthly means of the period. The data comprise the predictions of 30 global climate models for the SRES A1B scenario, as assembled by the Climate Variability Working Group (21st century CCSM3 Large Ensemble Project). These multi-model predictions have also been used in the Fourth Assessment Report of the IPCC (Meehl et al. 2007). Comparing the 2090-2099 period with the 2000-2009 period then yielded the predicted changes. b) The effect of climate change on the distribution of peatlands that could possibly be affected by the nutrient accumulation mechanism. In Chapter 5 an ET/Prec ratio of 0.6 was proposed as a threshold value for the occurrence of the nutrient accumulation mechanism. The colored areas indicate the global distribution of peatlands (data from Lehner and Döll 2004). The grey areas indicate peatlands where the nutrient accumulation is not expected to be important. The black areas indicate the areas where the nutrient accumulation is currently present, and also predicted to be present in the 2090-2099 period. The blue areas indicate peatland regions where the importance of nutrient accumulation may vanish. Finally, the red areas indicate peatlands where the nutrient accumulation mechanism may not be currently present, but it may become important in these areas during the 21st century. Especially in Siberia and Canada, the nutrient accumulation may become more important.*

Implications for ecosystem theory

Stability and hysteresis in ecosystem models and their relevance for real ecosystems

The three concepts positive feedback, alternate stable states and catastrophic shifts have been introduced in ecology and environmental science by means of non-spatial mathematical models (e.g. Lotka 1925; Volterra 1926; Holling 1973; Noy-Meir 1975; May 1977; DeAngelis and Waterhouse 1987). These theoretical studies show that the three concepts are closely related with the concept of (ecosystem) stability. Stability has been used and defined in many ways (Grimm and Wissel 1997), but in this paragraph I will use stability to refer to the ability of an ecosystem to recover from disturbances. In the following, I would like to discuss two stability-related issues that arise from the work presented in this thesis. First, I will show that assessment of catastrophic shifts in spatially explicit models is not straightforward, because such an assessment depends on which variables are considered. Second, I will argue that the mathematical analyses of stability in models cannot be directly interpreted as analogues for stability in real ecosystems.

In non-spatial models that exhibit alternate stable states, ecosystem equilibria typically change little in response to a gradual change in environmental conditions. In contrast, if the environmental conditions reach a threshold there is a large response

by shifting toward another equilibrium. A similar contrast occurs in spatially explicit models. For example, in a spatially explicit arid ecosystem model, the vegetation density within patches changes very little in response to a gradual decrease in rainfall (Fig. 5; Rietkerk et al. 2002). At the environmental threshold, however, the patches disappear and the system develops to a bare state (Fig. 5a). If rainfall increases again, the vegetation may not recover at the same threshold as where the vegetation disappeared (Fig. 5a). Hence it can be concluded that there is a catastrophic shift from a system with densely vegetated patches toward a bare state (Rietkerk et al. 2002; Kéfi et al. 2008). The exact same model results, however, can also be interpreted in a different way, leading to a different conclusion (Janssen et al. 2008). As mentioned above, the density within patches changes little toward the tipping point (Fig. 5a). There is, however, a gradual decline in the area that is covered by these patches (Fig. 5b). Thus, when focusing on vegetation cover, one could conclude that spatial heterogeneity smoothens the response of ecosystems to a gradual change in environmental conditions (Van Nes and Scheffer 2005; Janssen et al. 2008), and prevents the occurrence of catastrophic shifts (Groen 2007; Janssen et al. 2008).

This example illustrates that the assessment of catastrophic shifts in spatially explicit models is not straightforward. Whether there is a shift or just a gradual decline may depend on the ecosystem variables that are analyzed (Fig. 5a vs. Fig. 5b). The concept of hysteresis, however, is straightforward. In the above example, the hysteresis effect is revealed in both analyses (Fig. 5a, b). Theoretically, a catastrophic shift can occur due to a gradual change in environmental conditions only, without other disturbances (e.g. Scheffer et al. 2001). Even in the “practice” of model simulations, however, shifts do not always occur in this manner (Chapter 1). Although a gradual decline in environmental conditions paves the way toward shifting to another equilibrium, the final push is exerted by a disturbance (Fig. 5c; Chapter 1). It is difficult to develop robust measures that indicate whether an ecosystem shift is ‘large’ or ‘small’, and whether the pushing disturbance is ‘large’ or ‘small’. This problem can be circumvented by focusing on hysteretic effects, including the ability of an ecosystem to return to equilibrium after a disturbance. This leads to the second issue: how relevant are the mathematical methods to analyze hysteresis and stability in spatially explicit models for predicting the response of real ecosystems to environmental change?

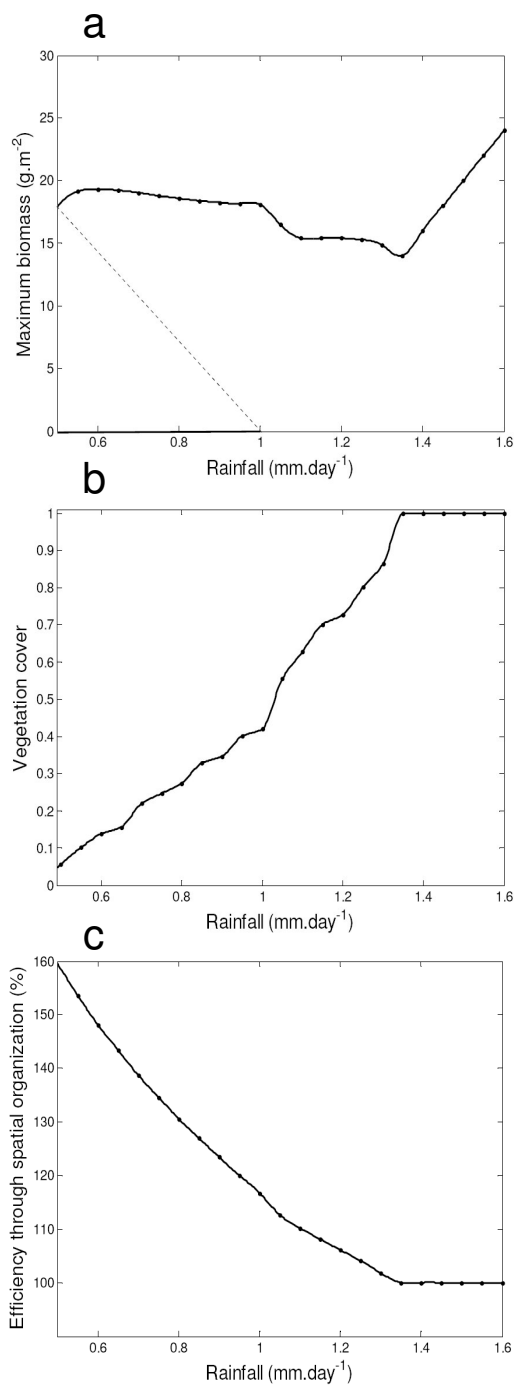


Figure 5: Different panels explaining how researchers have published different interpretations of the same model (the arid ecosystem model of Rietkerk et al. 2002). a) The top panel shows a large shift in maximum biomass at the extinction point, which has been interpreted as a catastrophic shift (e.g. Rietkerk et al. 2002). b) If the vegetation cover is plotted, there is a general decrease in cover toward zero (e.g. Janssen et al. 2008). Note the difference with the conceptual model in Fig. 1. At the (theoretical) extinction point one spot of vegetation survives in an infinite matrix (Morgan et al. 2000). The gradual decline in cover has been interpreted as a smoothing or a loss of the catastrophic shift (Van Nes and Scheffer 2005; Groen 2007; Janssen et al. 2008). c) This smoothing, however, comes at a cost: vegetation becomes more and more dependent on the spatial organization for survival. This is indicated in the bottom panel. Towards the extinction point, the vegetation becomes much more effective in harvesting water as compared to the situation in which the same amount of vegetation were distributed homogeneously (indicated with 100% in the diagram).

Spatially explicit reaction-diffusion model studies, which are frequently used to explore ecosystem pattern formation, usually determine the stability of uniform states with a linear stability analysis. Lyapunov (1892) called this the indirect method of stability analysis, which is less sophisticated and yields less information than the direct method. The direct method, however, is often too difficult to utilize for ecosystem models (Justus 2006). A linear stability analysis determines whether an ecosystem state will return to equilibrium after a perturbation. In a linear stability

analysis, however, the perturbation is assumed to be infinitely small. Here arises a discrepancy with real ecosystems, where disturbances are not infinitely small. If a cellular automata model formalism is used, however, the minimal perturbation may be a discrete entity that is relatively large (e.g. the smallest perturbation may be the introduction of an individual plant or other ecosystem engineer). This is an important difference, because alternate stable states arise if there is a critical density of the engineer below which the ecosystem engineering mechanism fails. This means that if the perturbation in the stability analysis exceeds this critical engineer density, there are no alternate stable states in the model. An example of such a situation was described in Kéfi et al. (2007a). In that study, the familiar sequence of vegetation patterns (gaps, labyrinths, spots) can be observed, but for some parameter settings the ecosystem engineering mechanism already occurs if a single individual is introduced, excluding the possibility of alternate stable states (Kéfi 2008).

It is evident that in reaction-diffusion models, the mathematical perturbation (in principle infinitely small) is much smaller than the realistic or relevant ecological perturbation. This is not very important for systems in which there is only one globally attracting stable equilibrium (e.g. Neutel et al. 1994). It is a problem, however, for systems that possibly exhibit alternate stable states. The predicted sizes of hysteresis loops or even predictions on the presence or absence of alternate stable states may depend on the magnitude of the perturbation that was used in the analysis. For example, Morgan et al. (2000) derived the 'singular' solution for a reaction-diffusion model of pattern formation, which has also been applied to pattern formation in arid ecosystems (Klausmeier 1999). In ecological terms, the singular solution could be viewed as the extinction threshold for vegetation. They showed that at this point, one single peak of consumers/vegetation biomass persists within an infinite matrix of bare soil. If one would define this biomass peak as being one individual, there would be no hysteresis in this model, meaning that vegetation would always be able to re-establish if conditions were to improve again. On the contrary, a linear stability analysis of the bare state in this model suggests that this state is always stable, meaning that vegetation would never be able to re-establish if conditions were to improve again. Thus, conclusions about hysteresis may entirely depend on the definition of an individual (the minimal perturbation) in a reaction-diffusion model.

Altogether, the issues discussed in this paragraph stress the fact that model predictions on stability and the possibility of catastrophic shifts and hysteresis are

closely linked to the model formulation and mathematical methods of model analysis. These methods have been directly adopted from physics (Lyapunov 1892). Although these methods have serious shortcomings (May 1973; Hastings 1988), theoretical model studies that used these methods have certainly increased the conceptual understanding of the response of ecosystems to changing environmental conditions (Chapter 1). However, the next step will be to predict the response of real ecosystems to projected environmental changes. In my view, it is the task of ecologists and environmental scientists to develop new methods that provide a better link between stability in models and stability of real ecosystems. These methods should better account for the strong temporal variation of environmental parameters and strong disturbances of state variables due to extreme events.

The necessity of combining theoretical and empirical approaches in pattern-oriented research

This thesis is part of a project that investigated whether self-organized patchiness that is driven by a resource concentration mechanism could serve as an indicator for catastrophic shifts between alternate stable states in peatland and arid ecosystems (Rietkerk et al. 2004b; Kéfi 2008). The limitation to the resource concentration mechanism is crucial, because recent research has shown that the same types of self-organized patchiness also occur in models without a resource concentration mechanism that do not exhibit alternate stable states (Van de Koppel and Crain 2006; Chapter 1). This means that observing patchiness in the field cannot be directly used as an indicator of catastrophic ecosystem shifts. Empirical evidence that this patchiness is caused by a resource concentration mechanism is a second necessary requirement. Because the driving mechanism of self-organized patchiness may change with environmental conditions (Chapters 2, 4, 5), it is very difficult to directly link self-organized patchiness with catastrophic shifts without site-specific empirical investigation. On the other hand, theoretical models are needed to generalize and reconcile empirical results from different sites, and to be able to predict future ecosystem development.

Despite the necessity to combine theoretical and empirical approaches to examine a possible link between ecosystem patterning and alternate stable states, empirical evidence for this link is rather limited so far. This is not surprising, given the requirements for showing alternate stable states in ecosystems. First, stability of any ecosystem state requires self-maintenance in time and space for at least one complete turnover of species (Connell and Sousa 1983; Schröder et al. 2005). For example, given the lifespan of especially trees and shrubs in peatlands and arid

ecosystems, this criterion would imply that manipulation experiments should be run for many decades before conclusions about stability of observed ecosystem states can be drawn. Therefore, the possibilities for experimental tests for discontinuity and non-recovery (Schröder et al. 2005) will be very limited. Schröder et al. (2005) suggest that evidence for alternate stable states can also be found in divergence of states due to experimentally manipulated initial conditions, or divergence of states in replicates due to stochastic events. I think that the most promising possibilities for testing for alternate stable states in peatland and arid ecosystems lies in this line of experimental approaches. Theoretical models suggest that especially under harsh conditions, peatland and arid ecosystems may crucially depend on the degree of spatial organization (Fig. 5c; Rietkerk et al. 2002; Kéfi et al. 2007b; Chapter 2). Hence, one could use an experimental setup in which the same amount of vegetation is distributed in each experimental unit, but in each unit the spatial configuration is different. Theory predicts that more organized units should be able to survive and maybe even increase in biomass and vegetation cover, whereas randomly planted vegetation may not be able to survive and therefore decrease in biomass and cover. The above considerations indicated that such experiments should run very long to convincingly show stability of states, but on the short term divergent developments would already be a strong test for alternate stable states. Even for such experiments, however, the required effort would be enormous. The size of each experimental unit should be large enough to encompass all relevant spatial processes, meaning that each unit should be the size of at least a number of characteristic pattern wavelengths. Characteristic wavelengths in peatland and arid ecosystems typically vary between 1 m and 100 m, meaning that experimental research seems only comprehensible for patterns at the smaller end of this range.

Alternatively, it has been suggested that evidence for alternate stable states can also be found in field data (Scheffer and Carpenter 2003, but see Peterson 1984). The increasing availability of high-resolution aerial photographs may create the possibility of creating long-term timeseries of the spatial organization of vegetation at specific sites (Kéfi 2008). Especially when these vegetation timeseries can be linked with the environmental variable of interest, it may be possible to link jumps in the ecosystem states to changes in environmental conditions. This approach has been adopted previously by Barbier et al. (2006), who correlated long-term rainfall data to vegetation cover of a semi-arid ecosystem. In that study, however, there was a general decline in rainfall, which excludes the possibility of identifying a hysteresis effect. The ideal situation to identify a hysteresis effect would be if there is a short-

term anomaly in the environmental variable of interest, after which external conditions return back to normal. If the ecosystem jumps to a new state during the anomaly and does not return to the previous state, it would make a strong case for the occurrence of alternate stable states.

Further, the occurrence of sharp boundaries in the landscape (and the resulting multimodal frequency distribution) can be used as a spatial analogue of jumps in timeseries (Scheffer and Carpenter 2003). Part of the work in this thesis and other studies contradicts this notion. Sharply bounded vegetation patchiness may be observed on a relatively small spatial scale, but in my view it is incorrect to interpret this as two independent systems being in alternate stable states. Due to spatial processes, patches cannot be seen as independent units, because their existence and maintenance may depend on source-sink relations with surrounding patches. Hence, the relevant spatial scale to assess stability is larger than the scale of individual patches. At this spatial scale, a self-organized patchy state may be the only stable state under the given environmental conditions (Chapter 2). In other words, sharply bounded patchiness can also be observed in the absence of alternate stable states. Although sharply bounded patches clearly indicate the presence of positive and scale-dependent feedbacks (Wilson and Agnew 1992; Chapters 1-2), not all types of spatial feedbacks that create patchiness induce alternate stable ecosystem states (Chapter 1). On the other hand, the resource concentration mechanism is a type of spatial feedback that can induce alternate stable states (Chapter 1), provided that conditions are too harsh to support a uniform vegetation cover. The presence of a resource concentration mechanism may be reflected in multimodality of resource availability, which is similar to the resource contrast concept that we used in Chapter 5. Thus, the multimodality criterion of Scheffer and Carpenter (2003) may be useful for the case of peatland and arid ecosystems, provided that the variable of interest is mechanistically linked to a resource concentration mechanism.

Self-organized patchiness: key to unraveling the ecosystem or an odd peculiarity?

Many examples of self-organized patchiness have recently been discovered, but these patterns may be more the exception than the rule (Herben and Hara 2003). The first study on the global biogeography of a patterned ecosystem (arid ecosystems) suggested that approximately 0.4 % of the area covered by arid ecosystems contain self-organized vegetation patchiness (Deblauwe et al. 2008). This raises the question: is the study of self-organized patchiness key to

understanding general ecosystem functioning or is it the study of a peculiar exception? There are three possible answers to this question. First, self-organized patchiness might be a peculiarity and the pattern-driving mechanisms may not be relevant for the vast majority of the particular type of ecosystem. Second, the mechanisms of pattern formation may be relevant for a larger region than the current region of visible patterns, but due to the current environmental conditions of these sites (too benign or too harsh) patterns may be absent. Third, the mechanisms of pattern formation may occur in a larger region than the current region of visible patterns, but due spatial or temporal variability in environmental conditions, the pattern may not be clearly regular or visible.

To gain insight which (combination) of these answers is most likely, future modeling efforts could be aimed at predicting the presence and also the absence of patterns for a certain region. Deblauwe et al. (2008) made predictions on the presence or absence of patterns with statistical regression models. A similar suggestion was made in Chapter 5, where we presented the ratio between evapotranspiration and precipitation as a requirement for peatland patterning driven by the nutrient accumulation mechanism. More insight, however, would be gained if one would use a parameterized process-based model to predict the presence and absence of patterns. Using process-based models, one could test to what extent the presence-absence predictions of patterns improve when site-specific factors (e.g. topography) or temporal variability (e.g. in rainfall) are taken into account. This kind of research could identify the importance of pattern-forming mechanisms as compared to variability between sites and stochasticity.

Link with general ecological theory

In his classical MacArthur award lecture, Levin (1992) points out that “*the demonstration that a specific mechanism can in theory give rise to a range of observed patterns is not proof that that mechanism is indeed responsible for those patterns.*” Theoretical studies, however, provide a valuable advancement by creating a catalogue of possible mechanisms (Levin 1992), which may reveal what kind of subsequent empirical work is needed to accept or reject alternative hypotheses. In this thesis, alternative mechanisms have been modeled and compared within a single framework (Chapter 4), and subsequent empirical work has been undertaken to show that along an environmental gradient, the dominant pattern-forming mechanism may change (Chapter 5, Fig. 1). The mechanisms of pattern formation that have been studied in this thesis have in common that they are induced by the

presence or absence of a functional species group, which is in line with the “ecosystem engineering” concept (Jones et al. 1994, 1997). An ecosystem engineer modulates the availability of resources to other species (Jones et al. 1994). In peatlands, both *Sphagnum* mosses and vascular plants strongly influence the availability of water, nutrients, light and other growth-related factors for the other functional group (Chapter 2). Until now, explicit mathematical models of ecosystem engineers are still rather primitive (Hastings et al. 2007). Models usually focus on a single ecosystem engineer, and models of specific physical mechanisms have mainly been developed for relatively straightforward mechanisms in arid environments (Hastings et al. 2007). In this thesis, we have contributed to the modeling of ecosystem engineers in two ways. First, we developed a spatially explicit model for competition between two ecosystem engineers (Chapter 2). Second, we developed a spatially explicit model framework for peatlands in which multiple engineer-induced physical mechanisms could be studied (Chapter 4).

A fascinating puzzle for ecologists and environmental scientists is the high biodiversity of many ecosystems, whereas ecological theory predicts that the maximum number of competing species cannot exceed the number of limiting resources of an ecosystem (Hardin 1960, Tilman 1982). One of the proposed solutions to this paradox is spatial heterogeneity in abiotic habitat factors (Hutchinson 1961; Tilman 1980, 1982). The work in this thesis exemplifies that ecosystem engineers can induce a scale-dependent feedback, and thereby actively create such spatial heterogeneity themselves. Vascular plants may create high-density patches (Chapters 2-4), but thereby also create low-density patches, which provide opportunities for other species (Chapter 2). An even more interesting phenomenon can be observed in the model with only the peat accumulation mechanism as presented in Chapter 4. In this model, the dependence of vascular plant growth on water availability is described by an optimum curve. Under wet conditions, vascular plants cannot survive in a uniform hummock cover, because the water supply is too high. Hence, each vascular plant-dominated hummock requires the presence of a nearby hollow, to which excess water can be drained (Chapter 4). Our empirical work in this thesis was not aimed to confirm this facilitative effect in patterned peatlands, but it certainly has potential to explain the very frequently observed coexistence of hummocks and hollows.

Outlook to future research

To predict the response of terrestrial ecosystems to future global change, small-scale spatial interactions between organisms and their environment cannot be ignored. The work in this thesis has focused on linking spatially explicit model predictions for peatland ecosystems with real-world observations. This is necessary to gain more confidence in model-based predictions of future ecosystem states. We used two methods to link models and field data: snapshot-based mapping of state variables within one site and between-site comparisons of resource contrasts. These methods are relatively easy to apply. Therefore, we think that the methods are promising approaches to apply in other spatially patterned ecosystems as well. In one of the first scientific descriptions of self-organized patchiness in arid ecosystems, Macfadyen (1950) wrote: “*They [self-organized vegetation patterns] are manifestly within the province of botany and ecology; the essential background concerns geomorphology and meteorology; the causes as I believe must be investigated by physics and mathematics; and the whole matter must be studied on air photographs.*” Much of Macfadyen’s statement is in line with recent research in this field. The work presented in this thesis, however, suggests that studying solely air photographs may not be sufficient to identify underlying structuring mechanisms: several mechanisms may be capable of explaining the same vegetation and surface pattern (Chapter 2, 4). Therefore, analyzing other ecosystem state variables may provide a tool to distinguish several candidate mechanisms (Chapters 3, 5).

The work in this thesis has emphasized the importance of the spatial surface structure of peatlands for the ecosystem functioning. Hence, peatland surface patterning provides a good starting point for future studies on the effect of climate change on peatlands. In this thesis, we have paid particular attention to the nutrient accumulation mechanism as a driver of peatland surface patterning. Climate predictions and our field data suggest that this mechanism may become more important in a larger region of peatlands in the coming century, possibly affecting the peatland-atmosphere carbon fluxes.

Further, the study of complex ecosystems is in my view most fruitfully pursued when focusing on the phenomenon of hysteresis. Here, a key challenge for ecologists and environmental scientists is to develop measures of ecosystem stability and hysteresis that are not only mathematically sound, but also adequately addressing the environmental variations that real ecosystems are continuously exposed to.

Changes in climate affect ecosystems. In turn, altered nutrient and carbon cycles will feed back to climate. For example, a change in carbon storage capacity of peatlands could potentially have a large effect on atmospheric carbon concentrations. Yet, global climate models currently ignore the role of peatlands in the global carbon and nutrient cycles, causing considerable uncertainty in future climate projections. Further, the response of peatlands and other ecosystems to climate change may strongly depend on the types of internal feedbacks that are present (Chapters 2, 4), and the importance of feedbacks may vary between sites (Chapter 5). With respect to peatlands, I hope that the spatially explicit models that were developed and empirically tested in this thesis provide a suitable starting point toward site-specific predictions of the response of these ecosystems to climate change.



References

References

A

- Aaby, B. 1994. Monitoring Danish raised bogs. Pages 284-300 in: *Mires and man: mire conservation in a densely populated country – the Swiss experience*. Grünig, A. (editor). Swiss Federal Institute for Forest, Snow and landscape Research, Birmensdorf.
- Admiral, S.W. and Lafleur, P.M. 2007. Partitioning of latent heat flux at a northern peatland. *Aquatic Botany* **86**: 107-116.
- Aerts, R., Logtestijn, R., Van Staalduinen, M. and Toet, S. 1995. Nitrogen supply effects on productivity and potential leaf litter decay of *Carex* species from peatlands differing in nutrient limitation. *Oecologia* **104**: 447-453.
- Aerts, R., Wallén, B. and Malmer, N. 1992. Growth-limiting nutrients in Sphagnum dominated bogs subject to low and high atmospheric nitrogen supply. *Journal of Ecology* **80**: 131-140.
- Agnew, A.D.Q., Wilson, J.B. and Sykes, M.T. 1993. A Vegetation Switch as the Cause of a Forest Mire Ecotone in New-Zealand. *Journal of Vegetation Science* **4**: 273-278.
- Allee, W.C. 1931. Co-operation among animals. *American Journal of Sociology* **37**: 386-398.
- Alexandrov, G.A. 1988. A spatially distributed model of raised bog relief. Pages 41–53 in: *Wetland Modelling (Developments in Environmental Modelling, v.12)*. Mitsch, W.J., Straskaba, M. and Jørgensen, S.E. (editors). Elsevier, Amsterdam.
- Alexandrov, G.A. and Logofet, D.O. 1994. Raised mire succession as modeled by multiple equilibria and dissipative structures. Pages 585-592 in: *Global wetlands: old world and new*. Mitsch, W.J. (editor). Elsevier, Amsterdam.
- Almer, B., Dickson, W., Ekstrom, C., Hornstrom, E. and Miller, U. 1974. Effects of acidification on Swedish lakes. *Ambio* **3**: 30-36.
- Andersen, H.E., Hansen, S. and Jensen, H.E. 2005. Evapotranspiration from a riparian fen wetland. *Nordic Hydrology* **36**: 121-135.
- Auer, V. 1920. Ueber die Entstehung der Straenge auf den Torfmooren. *Acta Forestalia Fennica* **12**: 1-145. (In German).

B

- Backéus, I. 1985. Aboveground production and growth dynamics of vascular bog plants in Central Sweden. *Acta Phytogeographica Suecica* **74**: 5-102.
- Backéus, I. 1986. Production and depth distribution of fine roots in a boreal open bog. *Annales Botanici Fennici* **27**:261-265.
- Backéus, I. 1989. Flarks in the Maloti, Lesotho. *Geografiska Annaler A* **71**:105-111.
- Barbier, N., Couteron, P., Lefever, R., Deblauwe, V. and Lejeune, O. 2008. Spatial decoupling of facilitation and competition at the origin of gapped vegetation patterns. *Ecology* **89**: 1521-1531.
- Barbier, N., Couteron, P., Lejoly, J., Deblauwe, V. and Lejeune, O. 2006. Self-organized vegetation patterning as a fingerprint of climate and human impact on semi-arid ecosystems. *Journal of Ecology* **94**: 537-547.
- Begon, M., Harper, J.L. and Townsend, C.R. 1990. *Ecology: individuals, populations and communities*. Blackwell Scientific, Oxford.
- Bellamy, D.J. 1959. Occurrence of *Schoenus nigricans* L. on ombrogenous peats. *Nature* **184**: 1590-1591.
- Beltman, B. and Rouwenhorst, T.G. 1994. Impact on soil fertility by replacement of hydrologically different water types. Pages 33-39 in: *Hydrological, chemical and biological processes of transformation and transport of contaminants in aquatic environments (Proceedings of the Rostov-on-Don Symposium, May 1993)*. Peters, N.E., Allan, R.J. and Tsirkunov, V.V. (editors). IAHS Press, Wallingford.

- Belyea, L.R. 1996. Separating the effects of litter quality and microenvironment on decomposition rates in a patterned peatland. *Oikos* **77**: 529-539.
- Belyea, L.R. 2007. Climatic and topographic limits to the abundance of bog pools. *Hydrological Processes* **21**:675-687.
- Belyea, L.R. and Baird, A.J. 2006. Beyond “the limits to peat bog growth”: Cross-scale feedback in peatland development. *Ecological Monographs* **76**: 299-322.
- Belyea, L.R. and Clymo, R.S. 2001. Feedback control of the rate of peat formation. *Proceedings of the Royal Society of London B* **268**: 1315-1321.
- Belyea, L.R. and Lancaster, J. 2002. Inferring landscape dynamics of bog pools from scaling relationships and spatial patterns. *Journal of Ecology* **90**: 223-234.
- Belyea, L.R. and Malmer, N. 2004. Carbon sequestration in peatland: patterns and mechanisms of response to climate change. *Global Change Biology* **10**: 1043-1052.
- Berendse, F., Van Breemen, N., Rydin, H., Buttler, A., Heijmans, M., Hoosbeek, M.R., Lee, J.A., Mitchell, E., Saarinen, T., Vasander, H. and Wallén, B. 2001. Raised atmospheric CO₂ levels and increased N deposition cause shifts in plant species composition and production in Sphagnum bogs. *Global Change Biology* **7**: 591–598.
- Berryman, A.A. 2002. Population: a central concept for ecology? *Oikos* **97**: 439-442.
- Bertness, M.D. and Callaway, R.M. 1994. Positive interactions in communities. *Trends in Ecology and Evolution* **9**: 191-193.
- Bertness, M.D. and Leonard, G.H. 1997. The role of positive interactions in communities: lessons from intertidal habitats. *Ecology* **78**: 1976-1989.
- Bertness, M.D., Trussel, G.C., Ewanchuk, P.J. and Silliman, B.R. 2002. Do alternate community stable states exist on rocky shores in the Gulf of Maine? *Ecology* **83**: 3434-3448.
- Biggs, R., Carpenter, S.R. and Brock, W.A. 2009. Turning back from the brink: detecting an impending regime shift in time to avert it. *Proceedings of the National Academy of Sciences USA* **106**: 826-831.
- Binkley, D. and Hart, S.C. 1989. The components of nitrogen availability in forest soils. *Advances in Soil Science* **10**: 57–112.
- Bleuten, W. 2001. Hydrochemistry. Pages 38-42 in: *Carbon storage and atmospheric exchange by West Siberian peatlands*. Bleuten, W. and Lapshina, E.D. (editors). Department of Physical Geography Utrecht University, Utrecht.
- Boatman, D.J. and Tomlinson, R.W. 1973. The Silver Flowe. I. Structural and hydrological features of Birshie Bog and their bearing on pool formation. *Journal of Ecology* **61**:653-666.
- Bobbink, R., Heil, G.W. and Raessen, M.B.A.G. 1992. Atmospheric deposition and canopy exchange processes in heathland ecosystems. *Environmental Pollution* **75**: 29-37.
- Bobbink, R., Hornung, M. and Roelofs, J.G.M. 1998. The effects of air-borne nitrogen pollutants on species diversity in natural and semi-natural European vegetation. *Journal of Ecology* **86**: 717-738.
- Boeken, B. and Shachak, M. 1994. Desert plant communities in human-made patches – Implications for management. *Ecological Applications* **4**: 702-716.
- Borren, W. 2007. *Carbon exchange in Western Siberian watershed mires and implications for the greenhouse effect: a spatial temporal modelling approach*. PhD thesis. Utrecht University, Utrecht.
- Borren, W. and Bleuten, W. 2006. Simulating Holocene carbon accumulation in a western Siberian watershed mire using a three-dimensional dynamic modeling approach. *Water Resources Research* **42**: 12413.
- Bragazza, L., Alber, R. and Gerdol, R. 1998. Seasonal pore water chemistry in hummocks and hollows in a poor-mire in the southern Alps (Italy). *Wetlands* **18**: 320-328.
- Bragazza, L. and Gerdol, R. 1999. Hydrology, groundwater chemistry and peat chemistry in relation to habitat conditions in a mire on the south-eastern Alps of Italy. *Plant Ecology* **144**: 243-256.

- Bragazza, L., Siffi, C., Iacumin, P. and Gerdol, R. 2007. Mass loss and nutrient release during litter decay in peatland: The role of microbial adaptability to litter chemistry. *Soil Biology and Biochemistry* **39**:257-267.
- Bridgham, S.D., Johnston, C.A., Pastor, J. and Updegraff, K. 1995. Potential feedbacks of northern wetlands on climate-change – an outline of an approach to predict climate-change impact. *BioScience* **45**: 262-274.
- Bridgham, S.D., Pastor, J., Updegraff, K., Malterer, T.J., Johnson, K., Harth, C. and Chen, J. 1999. Ecosystem control over temperature and energy flux in northern peatlands. *Ecological Applications* **9**: 1345-1358.
- Bridgham, S.D., Updegraff, K. and Pastor, J. 2001. A comparison of nutrient availability indices along an ombrotrophic-minerotrophic gradient in Minnesota wetlands. *Soil Science Society of America Journal* **65**: 259-269.
- Brolsma, R.J., and Bierkens, M.F.P. 2007. Groundwater-soil-vegetation dynamics in a temperate forest ecosystem along a slope. *Water Resources Research* **43**: 01414.
- Brooks, K.N. 1992. Surface hydrology. Pages 153-162 in: *The patterned peatlands of Minnesota*. Wright Jr., H.E., Coffin, B.A. and Aaseng, N.D. (editors). University of Minnesota press, Minneapolis.
- Brown, R.J.E. 1968. Occurrence of permafrost in Canadian peatlands. Pages 174-181 in: *Proceedings of the 3rd International Peat Congress, Quebec*. Lafleur, C. and Butler, J. (editors). National research council of Canada, Ottawa.
- Bruno, J.F., Stachowitz, J.J. and Bertness, M.D. 2003. Inclusion of facilitation into ecological theory. *Trends in Ecology and Evolution* **18**:119-125.

C

- Carpenter, S.R. 1996. Microcosm experiments have limited relevance for community and ecosystem ecology. *Ecology* **77**: 677-680.
- Carpenter, S.R. 2001. Alternate states of ecosystems: evidence and some implications. Pages 357-383 in: *Ecology: achievement and challenge*. Press, M.C., Huntly, N.J. and Levin, S.A. Blackwell Scientific Publishing, London.
- Carpenter, S.R. and Brock, W.A. 2006. Rising variance: a leading indicator of ecological transition. *Ecology Letters* **9**: 311-318.
- Carpenter, S.R., Brock, W.A., Cole, J.J., Kitchell, J.F. and Pace, M.L. 2008. Leading indicators of trophic cascade. *Ecology Letters* **11**: 128-138.
- Casparie, W.A. 1972. Bog development in southeastern Drenthe, the Netherlands. *Vegetatio* **25**: 1-271.
- Chamberlin, T.C. 1890. The method of multiple working hypotheses, *Science* **15**: 92-97. (Reprinted in 1965: *Science* **148**: 754-759).
- Charman, D.J. 1995. Patterned fen development in northern Scotland: hypothesis testing and comparison with ombrotrophic blanket peats. *Journal of Quaternary Science* **10**: 327-342.
- Charman, D.J. 2002. *Peatlands and environmental change*. Wiley, London.
- Clymo, R.S. 1964. The origin of acidity in Sphagnum bogs. *Bryology* **67**:427-431.
- Clymo, R.S. 1970. The growth of Sphagnum: methods of measurement. *Journal of Ecology* **58**: 13-49.
- Clymo, R.S. 1984. The limits to peat bog growth. *Philosophical Transactions of the Royal Society of London B* **303**: 605-654.
- Clymo, R.S. and Hayward, P.M. 1982. The ecology of Sphagnum. Pages 229-289 in: *Bryophyte ecology*. Smith, A.J.E. (editor). Chapman and Hall, London.
- Connell, J.H. and Sousa, W.P. 1983. On the evidence needed to judge ecological stability or persistence. *The American Naturalist* **121**: 789-824.
- Costanza, R., d' Arge, R., De Groot, R., Farber, S., Grasso, M., Hannon, B., Limburg, K., Naeem, S., O' Neill, R.V., Paruelo, J., Raskin, R.G., Sutton, P. and Van den Belt, M.

1998. The value of the world' s ecosystem services and natural capital. *Ecological Economics* **25**: 3-15.
- Coulson, J.C. and Butterfield, J. 1978. An investigation of the biotic factors determining the rates of plant decomposition on blanket bog. *Journal of Ecology* **66**: 631–650.
- Couteron, P. and Lejeune, O. 2001. Periodic spotted patterns in semi-arid vegetation explained by a propagation-inhibition model. *Journal of Ecology* **89**: 616-628.
- Couwenberg, J. 2005. A simulation model of mire patterning – revisited. *Ecography* **28**: 653-661.
- Couwenberg, J. and Joosten, H. 1999. Pools as missing links: the role of nothing in the being of mires. Pages 87-102 in: *Patterned mires and mire pools: origin and development, flora and fauna*. Standen, V., Tallis, J. and Meade, R. (editors). British Ecological Society, London.
- Couwenberg, J. and Joosten, H. 2005. Self-organization in raised bog patterning: the origin of microtope zonation and mesotope diversity. *Journal of Ecology* **93**:1238-1248.
- Craft, C.B., Vymazal, J. and Richardson, C.J. 1995. Response of Everglades plant communities to nitrogen and phosphorus additions. *Wetlands* **15**:258-271.
- Crain, C.M. and Bertness, M.D. 2005. Community impacts of a tussock sedge: is ecosystem engineering important in benign habitats? *Ecology* **86**: 2695-2704.
- Cramer, W., Bondeau, A., Woodward, F.I., Prentice, I.C., Betts, R.A., Brovkin, V., Cox, P.M., Fisher, V., Foley, J.A., Friend, A.D., Kucharik, C., Lomas, M.R., Ramankutty, N., Sitch, S., Smith, B., White, A. and Young-Molling, C. 2000. Global response of terrestrial ecosystem structure and function to CO₂ and climate change: results from six dynamic global global vegetation models. *Global Change Biology* **7**: 357-373.
- Cross, M.C. and Hohenberg, P.C. 1993. Pattern formation outside of equilibrium. *Reviews of Modern Physics* **65**: 851-1112.

D

- Dakos, V., Scheffer, M., Van Nes, E.H., Brovkin, V., Petoukhov, V. and Held, H. 2008. Slowing down as an early warning signal for abrupt climate change. *Proceedings of the National Academy of Sciences USA* **105**: 14308-14312.
- Davidson, E.A. and Janssens, I.A. 2006. Temperature sensitivity of soil carbon decomposition and feedbacks to climate change. *Nature* **440**: 165-173.
- Davis, S.M. 1991. Growth, decomposition and nutrient retention of *Cladium jamaicense* Crantz and *Typha domingensis* Pers. in the Florida Everglades. *Aquatic Botany* **40**: 203-224.
- DeAngelis, D.L. 1992. *Dynamics of nutrient cycling and food webs*. Chapman and Hall, London.
- DeAngelis, D.L. and Post, W.M. 1991. Positive feedback and ecosystem organization. Pages 155-178 in: *Theoretical studies of ecosystems: the network perspective*. Higashi, M. and Burns, T.P. (editors). Cambridge University Press, Cambridge.
- DeAngelis, D.L. and Waterhouse, J.C. 1987. Equilibrium and nonequilibrium concepts in ecological models. *Ecological Monographs* **57**: 1-21.
- DeAngelis, D.L., Post, W.M. and Travis, C.C. 1986. *Positive feedback in natural systems*. Springer, New York.
- Deblauwe, V., Barbier, N., Couteron, P., Lejeune, O. and Bogaert, J. 2008. The global biogeography of semi-arid periodic vegetation patterns. *Global Ecology and Biogeography* **17**: 715-723.
- De Roos, A.M. and Persson, L. 2002. Size-dependent life-history traits promote catastrophic collapses of top predators. *Proceedings of the National Academy of Sciences USA* **99**: 12907-12912.

- De Roos, A.M., McCauley, E. and Wilson, W.G. 1998. Pattern formation and the spatial scale of interaction between predators and their prey. *Theoretical Population Biology* **53**: 108-130.
- De Wit, C.T., Dijkshoorn, W. and Noggle, J.G. 1963. *Ionic balance and growth of plants*. Verslagen van Landbouwkundige Onderzoeken 69.15. Pudoc, Wageningen.
- Didham, R.K., Watts, C.H. and Norton, D.A. 2005. Are systems with strong underlying abiotic regimes more likely to exhibit alternate stable states? *Oikos* **110**: 409-416.

E

- Edelstein-Keshet, L. 1988. *Mathematical models in biology*. Random House/Birkhäuser Mathematics Series, New York.
- Edom, F. 2001. Moorlandschaften aus hydrologischer Sicht (chorische Betrachtung). Pages 185-225 in: *Landschaftsökologische Moorkunde*. Succow, M. and Joosten, H. (editors). Schweizerbart, Stuttgart. (In German).
- Ehrlich, P.R. and Ehrlich, A.H. 1981. *Extinction: the causes and consequences of the disappearance of species*. Random House, New York.
- Elton, C.S. 1958. *The ecology of invasions by animals and plants*. Methuen, London.
- Eppinga, M.B., Rietkerk, M., Dekker, S.C., De Ruiter, P.C. and Van der Putten, W.H. 2006. Accumulation of local pathogens: a new hypothesis to explain exotic plant invasions. *Oikos* **114**:168-176.

F

- Feddes, R. A., Kowalik, P.J. and Zaradny, H. 1978. *Simulation of field water use and crop yield*. Simulation Monograph. Pudoc, Wageningen.
- Fekete, B. M., Vorosmarty, C.J. and Grabs, W. 2002. High-resolution fields of global runoff combining observed river discharge and simulated water balances. *Global Biogeochemical Cycles* **16**: 1-10.
- Fitter, A.H. and Hay, R.K.M. 1983. *Environmental physiology of plants*. Academic Press, London.
- Foster, D.R. and King, G.A. 1984. Landscape features, vegetation and developmental history of a patterned fen in south-eastern Labrador, Canada. *Journal of Ecology* **72**:115-143.
- Foster, D.R., King, G.A., Glaser, P.H. and Wright Jr., H.E. 1983. Origin of string patterns in boreal peatlands. *Nature* **306**: 256-258.
- Frankl, R. and Schmeidl, H. 2000. Vegetation change in a South German raised bog. Ecosystem engineering by plant species, vegetation switch or ecosystem level feedback mechanisms? *Flora* **195**: 267-276.
- Frenzel, B. 1983. Mires-repositories of climatic information or self-perpetuating ecosystems? Pages 35-67 in: *Mires: swamp, bog, fen, and moor, Ecosystems of the world 4*. Gore, A.J.P. (editor). Elsevier, New York.
- Frolking, S., Roulet, N.T., Moore, T.R., Richard, P.J.H., Lavoie, M. and Muller, S.D. 2001. Modelling northern peatland decomposition and peat accumulation. *Ecosystems* **4**: 479-498.
- Fukami, T. and Lee, W.G. 2006. Alternate stable states, trait dispersion and ecological restoration. *Oikos* **113**: 353-356.

G

- Gascoigne, J.C., Beadman, H.A., Saurel, C. and Kaiser, M.J. 2005. Density dependence, spatial scale and patterning in sessile biota. *Oecologia* **145**: 371-381.
- German, E.R. 2000. *Regional evaluation of evapotranspiration in the Everglades*. U.S. Geological Survey Water-Resources Investigations Report 00-4217, Tallahassee.

- Givnish, T.J., Volin, J.C., Owen, V.D., Volin, V.C., Muss, J.D. and Glaser, P.H. 2008. Vegetation differentiation in the patterned landscape of the central Everglades: importance of local and landscape drivers. *Global Ecology and Biogeography* **17**: 384-402.
- Glaser, P.H. 1987. The development of streamlined bog islands in the continental interior of North America. *Arctic and Alpine Research* **19**:402-413.
- Glaser, P.H. 1992a. Peat landforms. Pages 3-14 in: *The patterned peatlands of Minnesota*. Wright Jr., H.E., Coffin, B.A. and Aaseng, N.D. (editors). University of Minnesota press, Minneapolis.
- Glaser, P.H. 1992b. Ecological development of patterned peatlands. Pages 27-42 in: *The patterned peatlands of Minnesota*. Wright Jr., H.E., Coffin, B.A. and Aaseng, N.E. (editors). University of Minnesota press, Minneapolis.
- Glaser, P.H., Siegel, D.I., Reeve, A.S., Janssens, J.A. and Janecky, D.R. 2004. Tectonic drivers for vegetation patterning and landscape evolution in the Albany River region of the Hudson Bay Lowlands. *Journal of Ecology* **92**:1054-1070.
- Glaser, P.H., Wheeler, G.A., Gorham, E. and Wright Jr., H.E. 1981. The patterned mires of the Red Lake Peatland, northern Minnesota: Vegetation, water chemistry and landforms. *Journal of Ecology* **78**:1021-1048.
- Goode, D.A. 1973. The significance of physical hydrology in the morphological classification of mires. Pages 10-20 in: *Classification of Peat and Peatlands. Proceedings of the IPS Symposium, Glasgow*. International Peat Society, Glasgow.
- Gorham, E. 1991. Northern peatlands: Role in the carbon cycle and probable responses to climatic warming. *Ecological Applications* **1**: 182-195.
- Gorham, E., Underwood, J.K., Martinand, F.B. and Ogden, J.G. 1986. Natural and anthropogenic causes of lake acidification in Nova Scotia. *Nature* **324**:451-453.
- Granberg, G., Sundh, I., Svensson, B.H. and Nilsson, M. 2001. Effects of temperature, and nitrogen and sulfur deposition, on methane emission from a boreal mire. *Ecology* **82**:1982-1998.
- Grimm, V. and Wissel, C. 1997. Babel, or the ecological stability discussions: an inventory and analysis of terminology and a guide for avoiding confusion. *Oecologia* **109**: 323-334.
- Groen, T.A. 2007. *Spatial matters: how spatial patterns and processes affect savanna dynamics*. PhD thesis. Wageningen University, Wageningen.
- Gunnarsson, U., Granberg, G. and Nilsson, M. 2004. Growth, production and interspecific competition in Sphagnum: effects of temperature, nitrogen and sulphur treatments on a boreal mire. *New Phytologist* **163**: 349-359.
- Gunnarsson, U., Malmer, N. and Rydin, H. 2002. Dynamics or constancy in Sphagnum dominated mire ecosystems? A 40-year study. *Ecography* **25**: 685-704.
- Gunnarsson, U. and Rydin, H. 1998. Demography and recruitment of Scots pine on raised bogs in eastern Sweden and relationships to microhabitat differentiation. *Wetlands* **18**:133-141.
- Gunnarsson, U., Rydin, H. and Sjörs, H. 2000. Diversity and pH changes after 50 years on the boreal mire Skattlösbergs Stormosse, Central Sweden. *Journal of Vegetation Science* **11**:277-286.
- Guttal, V. and Jayaprakash, C. 2008. Changing skewness: an early warning signal for regime shifts in ecosystems. *Ecology Letters* **11**: 450-460.

H

- Hanski, I. 1994. A practical model of metapopulation dynamics. *Journal of Animal Ecology* **63**: 151-162.
- Hardin, G. 1960. The competitive exclusion principle. *Science* **131**: 1292-1297.

- Hartemink, N.A., Randolph, S.E., Davis, S.A. and Heesterbeek, J.A.P. 2008. The basic reproduction number for complex disease systems: defining R0 for tick-borne infections. *The American Naturalist* **171**: 743-754.
- Hassell, M.P., Comins, H.N. and May, R.M. 1994. Species coexistence and self-organizing spatial dynamics. *Nature* **370**: 290-292.
- Hastings, A. 1988. Food web theory and stability. *Ecology* **69**: 1665-1668.
- Hastings, A., Byers, J.E., Crooks, J.A., Cuddington, K., Jones, C.G., Lambrinos, J.G., Talley, T.S. and Wilson, W.G. 2007. Ecosystem engineering in space and time. *Ecology Letters* **10**: 153-164.
- Hayward, P.M. and Clymo, R.S. 1983. The growth of Sphagnum: experiments on, and simulation of, some effects of light flux and water-table depth. *Journal of Ecology* **71**: 845-863.
- Heffernan, J.B. 2008. Wetlands as an alternative stable states in desert streams. *Ecology* **89**: 1261-1271.
- Heijmans, M.M.P.D., Arp, W.J. and Berendse, F. 2001. Effects of elevated CO2 and vascular plants on evapotranspiration in bog vegetation. *Global Change Biology* **7**: 817-827.
- Heijmans, M.M.P.D., Klees, H. and Berendse, F. 2002. Competition between Sphagnum magellanicum and Eriophorum angustifolium as affected by raised CO2 and increased N deposition. *Oikos* **97**: 415-425.
- Heijmans, M.M.P.D., Mauquoy, D., Van Geel, B. and Berendse, F. 2008. Long-term effects of climate change on vegetation and carbon dynamics in peat bogs. *Journal of Vegetation Science* **19**: 307-320.
- Heikkinen, J.E.P., Virtanen, T., Huttunen, J.T., Elsakov, V. and Martikainen, P.J. 2004. Carbon balance in east European tundra. *Global Biogeochemical Cycles* **18**: 1023.
- Heinselman, M.L. 1963. Forest sites, bog processes and peatland types in the Glacial Lake Agassiz region, Minnesota. *Ecological Monographs* **33**:327-374.
- Hemond, H.F. 1980. Biogeochemistry of Thoreau's bog, Concord, Massachusetts. *Ecological Monographs* **50**:507-526.
- Herben, T. and Hara, T. 2003. Spatial pattern formation in plant communities. Pages 223-235 in: *Morphogenesis and pattern formation in biological systems – models and experiments*. Sekimura, T., Noji, S., Ueno, N. and Maini, P.K. (editors). Springer-Verlag, Tokyo.
- Hiemstra, C.A., Liston, G.E. and Reiners, W.A. 2006. Observing, modelling, and validating snow redistribution by wind in a Wyoming upper treeline landscape. *Ecological Modelling* **197**: 35-51.
- Hilbert, D.W., Roulet, N. and Moore, T. 2000. Modelling and analysis of peatlands as dynamical systems. *Journal of Ecology* **88**: 230-242.
- HilleRisLambers, R., Rietkerk, M., Van den Bosch, F., Prins, H.H.T. and De Kroon, H. 2001. Vegetation pattern formation in semi-arid grazing systems. *Ecology* **82**: 50-61.
- Hobbie, S.E. 1996. Temperature and plant species control over litter decomposition in Alaskan tundra. *Ecological Monographs* **66**: 503-522.
- Holden, J. 2005. Peatland hydrology and carbon release: why small-scale process matters. *Philosophical Transactions of the Royal Society of London A* **363**: 2891- 2913.
- Holden, J. and Burt, T.P. 2003. Hydrological studies on blanket peat: the significance of the acrotelm-catotelm model. *Journal of Ecology* **91**:86-102.
- Holling, C.S. 1959. Some characteristics of simple types of predation and parasitism. *Canadian Entomologist* **91**: 385-398.
- Holling, C.S. 1973. Resilience and stability of ecological systems. *Annual Review of Ecology and Systematics* **4**: 1-23.
- Holling, C.S. 1996. Engineering resilience versus ecological resilience. Pages 31-43 in: *Engineering with ecological constraints*. Schulze, P.C. (editor). National Academy Press, Washington.

Houghton, J.T.L., Meira Filho, L.G., Callender, B.A., Harris, A., Kattenberg, A. and Maskell, K. (editors). 1995. *Climate change 1995: the science of climate change*. Cambridge University Press, Cambridge.

Hutchinson, G.E. 1961. The paradox of the plankton. *The American Naturalist* **95**: 137-145.

I

Ingram, H.A.P. 1978. Soil layers in mires: function and terminology. *European Journal of Soil Science* **29**: 224-227.

Ingram, H.A.P. 1982. Size and shape in raised mire ecosystems: a geophysical model. *Nature* **297**: 300-303.

Ingram, H.A.P. 1983. Hydrology. Pages 67-158 in: *Ecosystems of the World 4A. Mires: Swamp, Bog, Fen and Moor*. Gore, A.J.P. (editor). Elsevier, New York.

Ise, T., Dunn, A.L., Wofsy, S.C. and Moorcroft, P.R. 2008. High sensitivity of peat decomposition to climate change through water-table feedback. *Nature Geosciences* **1**: 763-766.

Ivanov, K.E. 1981. *Water Movement in Mirelands* (Vodoobmen v bolotnykh landshaftakh). Translated by Thomson, A. and Ingram, H.A.P. Academic Press, London.

J

Janssen, R.H.H., Meinders, M.B.J., Van Nes, E.H. and Scheffer, M. 2008. Microscale vegetation-soil feedback boosts hysteresis in a regional vegetation-climate system. *Global Change Biology* **14**: 1104-1112.

Johnson, L.C. and Damman, A.W.H. 1993. Decay and its regulation in Sphagnum peatlands. *Advances in Bryology* **5**: 249-296.

Jones, C.G., Lawton, J.H. and Shachak, M. 1994. Organisms as ecosystem engineers. *Oikos* **69**: 373-386.

Jones, C.G., Lawton, J.H. and Shachak, M. 1997. Positive and negative effects of organisms as physical ecosystem engineers. *Ecology* **78**: 1946-1957.

Jonasson, S. and Shaver, G.R. 1999. Within-stand nutrient cycling in arctic and boreal wetlands. *Ecology* **80**: 2139-2150.

Joosten, H. and Clarke, D. 2002. *Wise use of mires and peatlands – background and principles including a framework for decision making*. International Mire Conservation Group and International Peat Society, Saarijärvi.

Justus, J. 2006. Ecological and Lyapunov stability. Contributed paper to: *Philosophy of Science Association, 20th biennial meeting*, Vancouver.

Juusela, T.S., Kaunisto, S. and Mustonen, S. 1970. On factors affecting evapotranspiration from peat (Turpeesta Tapahtuvann Haidhduntaan Vaikuttavista Tekijosta). *Communicationes Instituti Forestalis Fenniae* **67**: 1-45. (In Finnish).

K

Kareiva, P., Watts, S., McDonald, R. and Boucher, T. 2007. Domesticated nature: shaping landscapes and ecosystems for human welfare. *Science* **316**: 1866-1869.

Karlsson, P.S. and Nordell, K.O. 1987. Growth of *Betula pubescens* and *Pinus sylvestris* seedlings in a subarctic environment. *Functional Ecology* **1**: 37-44.

Karofeld, E. 1998. The dynamics of the formation and development of hollows in raised bogs in Estonia. *The Holocene* **8**: 715-722.

Kéfi, S. 2008. *Reading the signs: spatial vegetation patterns, arid ecosystems and desertification*. PhD thesis. Utrecht University, Utrecht.

Kéfi, S., Rietkerk, M., Van Baalen, M. and Loreau, M. 2007a. Local facilitation, bistability and transitions in arid ecosystems. *Theoretical Population Biology* **71**: 367-379.

- Kéfi, S., Rietkerk, M., Alados, C.L., Pueyo, Y., ElAich, A., Papanastasis, V. and De Ruiter, P.C. 2007b. Spatial vegetation patterns and imminent desertification in arid ecosystems. *Nature* **449**: 213-218.
- Kellner, E. and Halldin, S. 2002. Water budget and surface-layer water storage in a Sphagnum bog in central Sweden. *Hydrological Processes* **16**: 87-103.
- Kim, J. and Verma, S.B. 1996. Surface exchange of water vapour between an open Sphagnum fen and the atmosphere. *Boundary-Layer Meteorology* **79**: 243-264.
- Klausmeier, C.A. 1999. Regular and irregular patterns in semiarid vegetation. *Science* **284**: 1826-1828.
- Köppisch, D. 2001. Stoffumsetzungsprozesse. Pages 18-37 in: *Landschaftsökologische Moorkunde*. Succow, M. and Joosten, H. (editors). Schweizerbart, Stuttgart. (In German).
- Kroehler, C.J. and Linkins, A.E. 1988. The root surface phosphatases of *Eriophorum vaginatum*: effects of temperature, pH, substrate concentration and inorganic phosphorous. *Plant and Soil* **105**: 3-10.
- Kulczyński, S. 1949. Peat bogs of Polesie. *Memoirs de l'academie Polonaise des sciences et des lettres B* **15**: 1-356.
- Kuznetsov, Y. 1995. *Elements of Applied Bifurcation Theory*. Springer-Verlag, New York.

L

- Lafleur, P.M., Hember, R.A., Admiral, S.W. and Roulet, N.T. 2005. Annual and seasonal variability in evapotranspiration and water table at a shrub-covered bog in southern Ontario, Canada. *Hydrological Processes* **19**: 3533-3550.
- Lafleur, P.M., Roulet, N.T., Bubier, J.L., Frolking, S. and Moore, T.R. 2003. Interannual variability in the peatland-atmosphere carbon dioxide exchange at an ombrotrophic bog. *Global Biogeochemical Cycles* **17**: 1036.
- Laiho, R. and Finer, L. 1996. Change in root biomass after water-level drawdown on pine mires in southern Finland. *Scandinavian Journal of Forest Research* **11**:251-260.
- Lamers, L.P.M., Bobbink, R. and Roelofs, J.G.M. 2000. Natural nitrogen filter fails in polluted raised bogs. *Global Change Biology* **6**: 583-586.
- Lapshina, E.D., Mouldiyarov, E.Y. and Vasiliev, S.V. 2001a. Analyses of key area studies. Pages 23-37 in: *Carbon storage and atmospheric exchange by West Siberian peatlands*. Bleuten, W. and Lapshina, E.D. (editors). Department of Physical Geography Utrecht University, Utrecht
- Lapshina, E.D., Polgova, N.N. and Mouldiyarov, E.Y. 2001b. Pattern of development and carbon accumulation in homogeneous Sphagnum fuscum-peat deposit on the south of West Siberia. Pages 101-104 in: *West Siberian peatlands and carbon cycle: past and present. Proceedings of the International Field Symposium (Noyabirsk, August 18–22, 2001)*. Vasiliev, S.V., Titlyanova, A.A. and Velichko, A.A. (editors). Agenstvo Sibprint, Novosibirsk.
- Larsen, L.G., Harvey, J.W. and Crimaldi, J.P. 2007. A delicate balance: ecohydrological feedbacks governing landscape morphology in a lotic peatland. *Ecological Monographs* **77**: 591-614.
- Lehner, B. and Döll, P. 2004. Development and validation of a global database of lakes, reservoirs and wetlands. *Journal of Hydrology* **296**: 1-22.
- Lejeune, O., Tlidi, M. and Coutron, P. 2002. Localized vegetation patches: a self-organized response to resource scarcity. *Physical Review E* **66**:010901-1.
- Levin, S.A. 1992. The problem of pattern and scale in ecology. *Ecology* **73**: 1943-1967.
- Levin, S.A. 1998. Ecosystems and the biosphere as complex adaptive systems. *Ecosystems* **1**: 431-436.
- Levin, S.A. 2000. Multiple scales and the maintenance of biodiversity. *Ecosystems* **3**: 498-506.

- Levin, S.A. and Segel, L.A. 1985. Pattern generation in time and aspect. *SIAM Review* **27**: 45-67.
- Lewontin, R.C. 1969. The meaning of stability. *Brookhaven Symposium in Biology* **22**:13-24.
- Limpens, J., Berendse, F., Blodau, C., Canadell, J.G., Freeman, C., Holden, J., Roulet, N., Rydin, H. and Schaepman-Strub, G. 2008. Peatlands and the carbon cycle: from local processes to global implications- a synthesis. *Biogeosciences* **5**: 1475-1491.
- Limpens, J., Berendse, F. and Klees, H. 2003. N deposition affects N availability in interstitial water, growth of Sphagnum and invasion of vascular plants in bog vegetation. *New Phytologist* **157**: 339-347.
- Loehle, C. 1989. Catastrophe theory in ecology: a critical review and an example of the butterfly catastrophe. *Ecological Modelling* **49**:125-152.
- Loehle, D. 1987. Hypothesis testing in ecology: Psychological aspects and the importance of theory maturation. *Quarterly Review of Biology* **62**: 397-409.
- Logofet, D.O. and Alexandrov, G.A. 1988. Interference between Mosses and Trees in the framework of a dynamic model of carbon and nitrogen cycling in a mesotrophic bog ecosystem. Pages 55-67 in: *Wetland Modelling (Developments in Environmental Modelling, v.12)*. Mitsch, W.J., Straskaba, M. and Jørgensen, S.E. (editors.). Elsevier, Amsterdam.
- Lotka, A.J. 1925. *Elements of physical biology*. Williams and Wilkins, Baltimore.
- Lyapunov, A.M. 1892. *The general problem of the stability of motion* (Obshchaya zadacha ob ustoichivosti dvizheniya). PhD thesis. Translated by Fuller, A.T. 1992. Taylor and Francis, London.

M

- Macfadyen, W.A. 1950. Vegetation patterns in the semi-desert plains of British Somaliland. *Geographical Journal* **116**: 199-210.
- Malmer, N. 1962. Studies on mire vegetation in the Archaean area of southwestern Götaland. I. Vegetation and habitat conditions on the Åkhult mire. *Opera Botanica* **7**: 1-322.
- Malmer, N., Albinsson, C., Svensson, B.M. and Wallén, B. 2003. Interferences between Sphagnum and vascular plants: effects on plant community structure and peat formation. *Oikos* **100**: 469-482.
- Malmer, N., Svensson, B.M. and Wallén, B. 1994. Interactions between Sphagnum Mosses and Field Layer Vascular Plants in the Development of Peat-Forming Systems. *Folia Geobotanica et Phytotaxonomica* **29**:483-496.
- Malmer, N., Svensson, G. and Wallén, B. 1997. Mass balance and nitrogen accumulation in hummocks on a South Swedish bog during the late Holocene. *Ecography* **20**: 535-549.
- Malmström, C. 1923. *Degerö Stormyr. En botanisk, hydrologisk och utvecklingshistorisk undersökning över ett nordsvenskt myrkomplex*. PhD thesis. Uppsala University, Uppsala. (In Swedish with German summary).
- Mark, A.F., Johnson, P.N., Dickinson, K.J.M. and McGlone, M.S. 1995. Southern hemisphere patterned mires, with emphasis on southern New Zealand. *Journal of the Royal Society of New Zealand* **25**: 23-54.
- Maron, J.L. and Harrison, S. 1997. Spatial pattern formation in an insect host-parasitoid system. *Science* **278**: 1619-1621.
- Marschner, H. 1995. *Mineral nutrition of higher plants*. Academic Press, London.
- Mason, N.W.H., Wilson, J.B. and Steel, J.B. 2007. Are alternate stable states more likely in high stress environments? Logic and available evidence do not support Didham et al. 2005. *Oikos* **116**: 353-357.
- May, R.M. 1973. *Complexity and stability in model ecosystems*. Princeton University Press, Princeton.

- May, R.M. 1977. Thresholds and breakpoints in ecosystems with a multiplicity of stable states. *Nature* **269**: 471-477.
- Mayer, A.L. and Rietkerk, M. 2004. The dynamic regime concept for ecosystem management and restoration. *BioScience* **54**: 1013-1020.
- McCarthy, T.S. and Ellery, W. N. 1994. The effect of vegetation on soil and ground water chemistry and hydrology of islands in the seasonal swamps of the Okavango fan, Botswana. *Journal of Hydrology* **154**: 169-193.
- McCarthy, T.S., Ellery, W.N. and Ellery, K. 1993. Vegetation-induced, subsurface precipitation of carbonate as an aggradational process in the permanent swamps of the Okavango (delta) fan, Botswana. *Chemical Geology* **107**: 111-131.
- Meadows, D.H., Meadows, D.L., Randers, J. and Behrens, W.W. 1972. *The limits to growth*. Potomac, Washington.
- Meehl, G.A., Stocker, T.F. , Collins, W.D., Friedlingstein, P., Gaye, A.T., Gregory, J.M., Kitoh, A., Knutti, R., Murphy, J.M., Noda, A., Raper, S.C.B., Watterson, I.G., Weaver A.J. and Zhao, Z.-C. 2007. Global Climate Projections. Pages 747-845 in: *Climate Change 2007: The Physical Science Basis. Contribution of Working Group I to the Fourth Assessment Report of the Intergovernmental Panel on Climate Change*. Solomon, S., Qin, D., Manning, M., Chen, Z., Marquis, M., Averyt, K.B., Tignor, M. and Miller, H.L. (editors). Cambridge University Press, Cambridge.
- Meijer, M.L. and Hoesper, H. 1997. Effects of biomanipulation in the large and shallow Lake Wolderwijd, The Netherlands. *Hydrobiologia* **342**: 335-349.
- Meinhardt, H. 1995. *The algorithmic beauty of sea shells*. Springer-Verlag, Berlin.
- Meron, E., Gilad, E., Von Hardenberg, J., Shachak, M. and Zarmi, Y. 2004. Vegetation patterns along a rainfall gradient. *Chaos, Solitons and Fractals* **19**: 367-376.
- Miranda, A.C., Jarvis, P.G. and Grace, J. 1984. Transpiration and evaporation from heather Moorland. *Boundary Layer Meteorology* **28**: 227-243.
- Mitchell, T.D., Carter, T.R., Jones, P.D., Hulme, M. and New, M. 2004. *A comprehensive set of high resolution grids of monthly climate for Europe and the globe: the observed record (1901-2000) and 16 scenarios (2001-2100)*. Tyndall Centre Working Paper 55.
- Moore, P.D. 1977. Stratigraphy and pollen analysis of Claish Moss, north-west Scotland:significance for the origin of surface-pools and forest history. *Journal of Ecology* **65**: 365-397.
- Moore, P.D. and Bellamy, D.J. 1974. *Peatlands*. Elek Science, London.
- Moore, T.R., Bubier, J.L. and Bledzki, L. 2007. Litter decomposition in temperate peatland ecosystems: the effect of substrate and site. *Ecosystems* **10**: 949-963.
- Morgan, D.S., Doelman, A. and Kaper, T.J. 2000. Stationary periodic patterns in the 1D Gray-Scott model. *Methods and Applications of Analysis* **7**: 105-150.
- Murray, J.D. 1989. *Mathematical biology*. Springer-Verlag, Berlin.
- Murray, K.J., Tenhunen, J.D. and Nowak, R.S. 1993. Photoinhibition as a control on photosynthesis and production of Sphagnum mosses. *Oecologia* **96**:200-207.

N

- Neutel, A.M., Heesterbeek, J.A.P. and De Ruiter, P.C. 2002. Stability in real food webs: Weak links in long loops. *Science* **296**: 1120-1123.
- Neutel, A.M., Heesterbeek, J.A.P., Van de Koppel, J., Hoenderboom, G., Vos, A., Kaldeway, C., Berendse, F. and De Ruiter, P.C. 2007. Reconciling complexity with stability in naturally assembling food webs. *Nature* **449**: 599-602.
- Neutel, A.M., Roerdink, J.B.T.M. and De Ruiter, P.C. 1994. Global stability of 2-level detritus decomposer food chains. *Journal of Theoretical Biology* **171**: 351-353.
- Nicolis, G. and Prigogine, I. 1977. *Self-organization in non-equilibrium systems*. Wiley, New York.

- Nilsson, A. 1899. Några drag ur de svenska växtsamhällenas utvecklingshistoria. *Botaniska Notiser* **1899**: 123-135. (In Swedish).
- Nilsson, M.B., Sagerfors, J., Buffam, I., Laudon, H., Eriksson, T., Grelle, A., Klemedtsson, L., Weslien, P. and Lindroth, A. 2008. Contemporary carbon accumulation in an oligotrophic minerogenic mire – a significant sink after accounting for all C-fluxes. *Global Change Biology* **14**: 2317-2332.
- Noe, G.B., Childers, D.L. and Jones, R.D. 2001. Phosphorus biogeochemistry and the impact of phosphorus enrichment: why is the Everglades so unique? *Ecosystems* **4**: 603-624.
- Noy-Meir, I. 1975. Stability of grazing systems: an application of predator-prey graphs. *Journal of Ecology* **63**: 459-481.
- Nungesser, M.K. 2003. Modelling microtopography in boreal peatlands: hummocks and hollows. *Ecological Modelling* **165**:175-207.
- Nystrom, M., Folke, C. and Moberg, F. 2000. Coral reef disturbance and resilience in a human-dominated environment. *Trends in Ecology and Evolution* **15**: 413-417.

O

- Odum, H.T. 1971. *Environment, Power, and Society*. Wiley, New York.
- Ohlson, M. and Økland, R.H. 1998. Spatial variation in rates of carbon and nitrogen accumulation in a boreal bog. *Ecology* **79**: 2745-2758.
- Ohlson, M., Økland, R.H., Nordbakken, J-F. and Dahlberg, B. 2001. Fatal interactions between Scots pine and Sphagnum mosses in bog ecosystems. *Oikos* **94**: 425-432.
- Økland, R.H. 1990. A phytoecological study of the mire Northern Kisselbergmosen, SE Norway. II. Identification of gradients by detrended (canonical) correspondence analysis. *Nordic Journal of Botany* **10**:79-108.
- Okubo, A. 1989. *Diffusion and ecological problems: mathematical models*. Springer-Verlag, New York.
- Olander, L.P. and Vitousek, P.M. 2000. Regulation of soil phosphatase and chitinase activity by N and P availability. *Biogeochemistry* **49**: 175-191.
- Olde Venterink, H.G.M., Wassen, M.J., Verkroost, A.W.M. and De Ruiter, P.C. 2003. Species richness-productivity patterns differ between N, P and K limited wetlands. *Ecology* **84**: 2191-2199.
- Othmer, H.G. and Pate, E. 1980. Scale-invariance in reaction-diffusion models of pattern formation. *Proceedings of the National Academy of Sciences USA* **77**: 4180-4184.

P

- Pastor, J., Peckham, B., Bridgman, S., Weltzin, J. and Chen, J. 2002. Plant community dynamics, nutrient cycling, and alternative stable equilibria in peatlands. *The American Naturalist* **160**: 553-568.
- Patterson, C.C. 1965. Contaminated and natural lead environments of man. *Archives of Environmental Health* **11**: 344-360.
- Pearsall, W.H. 1956. Two blanket bogs in Sutherland. *Journal of Ecology* **44**: 493-516.
- Peterson, C.H. 1984. Does a rigorous criterion for environmental identity preclude the existence of multiple stable points? *The American Naturalist* **124**: 127-133.
- Pimm, S.L. and Pimm, J.W. 1982. Resource use, competition and resource availability in Hawaiian honeycreepers. *Ecology* **63**: 1468-1480.
- Platt, J.R. 1964. Strong inference. *Science* **146**: 347–353.
- Plug, L.J. and Werner, B.T. 2001. Fracture networks in frozen ground. *Journal of Geophysical Research* **106**: 8599-8613.
- Popper, K.R. 1968. *Conjectures and refutations: the growth of scientific knowledge*. Harper and Row, New York.

- Post, W.M., Emmanuel, W.R., Zinke, P.J. and Stangenberger, A.G. 1982. Soil carbon pools and world wildlife zones. *Nature* **298**: 156-159.
- Post, W.M., Pastor, J., Zinke, P.J. and Stangenberger, A.G. 1985. Global patterns of soil nitrogen storage. *Nature* **317**: 613-616.
- Price, J.S. and Moloney, D.A. 1994. Hydrology of a patterned bog-fen complex. *Nordic Hydrology* **25**: 313-330.
- Pueyo, Y., Kéfi, S. and Rietkerk, M. 2008. Dispersal strategies and spatial organization of vegetation in arid ecosystems. *Oikos* **117**: 1522-1532.

Q

- Quinn, J.F. and Dunham, A.E. 1983. On hypothesis testing in ecology and evolution. *The American Naturalist* **122**: 602-617.
- Quinton, W.L. and Roulet, N.T. 1998. Spring and summer runoff hydrology of a subarctic patterned wetland. *Arctic and Alpine Research* **30**: 285-294.

R

- Radforth, N. W. 1969. Environmental and structural differentials in peatland development. Pages 87-104 in: *Environments of coal deposition*. Dapples, E. C. and Hopkins, M. E. (editors). Geological Society of America, Boulder.
- Ramsar Convention on wetlands. 1971. UN Treaty Series no. 14583.
- Redbo-Torstensson, P. 1994. Variation in plastic response to a salinity gradient within a population of the halophytic plant *Spergularia marina*. *Oikos* **70**: 349-358.
- Reed, D.L. and Ross, M.S. 2004. Hydrological variation among and within tree islands of Shark Slough. Pages 5-17 in: *Tree islands in the Shark Slough landscape: Interactions of vegetation, hydrology and soils*. Ross, M.S. and Jones, D.T. (editors). Southeast Environmental Research Center Florida International University, Miami.
- Reeve, A.S., Siegel, D.I. and Glaser, P.H. 1996. Geochemical controls on peatland pore-water from the Hudson Bay Lowlands: a multivariate and statistical approach. *Journal of Hydrology* **181**: 285-304.
- Reeve, A.S., Siegel, D.I. and Glaser, P.H. 2000. Simulating vertical flow in large peatlands. *Journal of Hydrology* **227**: 207-217.
- Reeve, A. S., Siegel, D.I. and Glaser, P.H. 2001. Simulating dispersive mixing in large peatlands. *Journal of Hydrology* **242**:103-114.
- Reichman, O.J. and Seabloom, E.W. 2002. Ecosystem engineering: a trivialized concept? Response from Reichman and Seabloom. *Trends in Ecology and Evolution* **17**: 308.
- Renshaw, E. and Ford, E.D. 1984. The description of spatial pattern using two-dimensional spectral analysis. *Vegetatio* **56**: 113-123.
- Ricker, W.E. 1963. Big effects from small causes: two examples from fish population dynamics. *Journal of the Fisheries Research Board of Canada* **20**: 257-264.
- Ridolfi, L., D'Odorico, P. and Laio, F. 2006. Effect of vegetation-water feedbacks on the stability and resilience of plant ecosystems. *Water Resources Research* **42**: 01201.
- Rietkerk, M. and Van de Koppel, J. 2008. Regular pattern formation in real ecosystems. *Trends in Ecology and Evolution* **23**: 169-175.
- Rietkerk, M., Boerlijst, M.C., Van Langevelde, F., HilleRisLambers, R., Van de Koppel, J., Kumar, L., Prins, H.H.T. and De Roos, A.M. 2002. Self-organization of vegetation in arid ecosystems. *The American Naturalist* **160**: 524-530.
- Rietkerk, M., Dekker, S.C., Wassen, M.J., Verkroost, A.W.M. and Bierkens, M.F.P. 2004a. A putative mechanism for bog patterning. *The American Naturalist* **163**: 699-708.
- Rietkerk, M., Dekker, S.C., De Ruiter, P.C. and Van de Koppel, J. 2004b. Self-organized patchiness and catastrophic shifts in ecosystems. *Science* **305**: 1926-1929.

- Rietkerk, M., Ketner, P., Burger, J., Hoorens, B. and Olf, H. 2000. Multiscale soil and vegetation patchiness along a gradient of herbivore impact in a semi-arid grazing system in West Africa. *Plant Ecology* **148**: 207-224.
- Rietkerk, M., Van den Bosch, F. and Van de Koppel, J. 1997. Site-specific properties and irreversible vegetation changes in semi-arid grazing systems. *Oikos* **80**: 241-252.
- Rinaldi, S. and Scheffer, M. 2000. Geometric analysis of ecological models with slow and fast processes. *Ecosystems* **3**: 507-521.
- Robroek, B.J.M., Limpens, J., Breeuwer, A., Crushell, P. and Schouten, M.G.C. 2007a. Interspecific competition between Sphagnum mosses at different water tables. *Functional Ecology* **21**: 805-812.
- Robroek, B.J.M., Limpens, J., Breeuwer, A., Van Ruijven, J. and Schouten, M.G.C. 2007b. Precipitation determines the persistence of hollow Sphagnum species on hummocks. *Wetlands* **27**: 979-986.
- Rodriguez-Iturbe, I. and Porporato, A. 2004. *Ecohydrology of water-controlled ecosystems: Soil moisture and plant dynamics*. Cambridge University Press, Cambridge.
- Roelofs, J.G.M. 1986. The effect of airborne sulphur and nitrogen deposition on aquatic and terrestrial heathland vegetation. *Experientia* **42**: 372-377.
- Rohani, P., Lewis, T.J., Grünbaum, D. and Ruxton, G.D. 1997. Spatial self-organisation in ecology: pretty patterns or robust reality? *Trends in Ecology and Evolution* **12**: 70-74.
- Romanov, V.V. 1968. *Hydrophysics of bogs*. Israel Program for Scientific Translations.
- Rosenzweig, M.L. 1971. Paradox of enrichment: destabilization of exploitation ecosystems in ecological time. *Science* **171**: 385-387.
- Ross, M.S., Mitchell-Bruker, S., Sah, J.P., Stothoff, S., Ruiz, P.L., Reed, D.L., Jayachandran, K. and Coultas, C.L. 2006. Interaction of hydrology and nutrient limitation in the Ridge and Slough landscape of the southern Everglades. *Hydrobiologia* **569**: 37-59.
- Roulet, N.T., Lafleur, P.M., Richard, P.J., Moore, T.R., Humphreys, E.R. and Bubier, J. 2007. Contemporary carbon balance and late Holocene carbon accumulation in a northern peatland. *Global Change Biology* **13**: 397-411.
- Roughgarden, J. 1983. Competition and theory in community ecology. *The American Naturalist* **122**: 583-601.
- Rutter, A.J. 1963. Studies in the water relations of *Pinus sylvestris* in plantation conditions. I: Measurements of rainfall and interception. *Journal of Ecology* **51**: 191-203.
- Rycroft, D.W., Williams, D.J.A. and Ingram, H.A.P. 1975. The transmission of water through peat. I: Review. *Journal of Ecology* **63**: 535-556.
- Rydin, H. and Clymo, R.S. 1989. Transport of carbon and phosphorus-compounds about Sphagnum. *Proceedings of the Royal Society of London B* **237**: 63-84.
- Rydin, H. and Jeglum, J.K. 2006. *The biology of peatlands*. Oxford University Press, Oxford.
- Rydin, H. and McDonald, A.J.S. 1985. Tolerance of Sphagnum to water level. *Journal of Bryology* **13**: 571-578.

S

- Sagerfors, J. 2007. *Land-atmosphere exchange of CO₂, water and energy at a boreal minerotrophic mire*. PhD thesis. Swedish University of Agricultural Sciences, Umeå.
- Sagerfors, J., Lindroth, A., Buffam, I., Grelle, A., Klemetsson, L., Laudon, H. and Nilsson, M. (In press). Water budget and energy partitioning of a boreal, minerogenic mire. *Journal of Geophysical Research- Atmospheres*, (in press).
- Sagerfors, J., Lindroth, A., Grelle, A., Klemetsson, L., Weslien, P. and Nilsson, M. (2008) Annual CO₂ exchange between a nutrient-poor, minerotrophic, boreal mire and the atmosphere. *Journal of Geophysical Research – Biogeosciences* **113**: G01001.
- Sakaguchi, Y. 1980. On the genesis of banks and hollows in peat bogs: an explanation by a thatch line theory. *Bulletin of the Department of Geography University of Tokyo* **12**: 35-58.

- Scanlon, T.S., Caylor, K.K., Levin, S.A. and Rodriguez-Iturbe, I. 2007. Positive feedbacks promote power-law clustering of Kalahari vegetation. *Nature* **449**: 209-212.
- Scheffer, M. 1999. Searching explanations of nature in the mirror world of math. *Conservation Ecology* **3**: 11.
- Scheffer, M. and Carpenter, S.R. 2003. Catastrophic regime shifts in ecosystems: linking theory to observation. *Trends in Ecology and Evolution* **18**:648-656.
- Scheffer, M. and Van Nes, E.H. 2006. Self-organized similarity, the evolutionary emergence of groups of similar species. *Proceedings of the National Academy of Sciences USA* **103**: 6230-6235.
- Scheffer, M., Carpenter, S.R., Foley, J.A., Folke, C. and Walker, B. 2001. Catastrophic shifts in ecosystems. *Nature* **413**: 591-596.
- Scheffer, M., Hosper, S.H., Meijer, M.L., Moss, E. and Jeppesen, E. 1993. Alternative equilibria in shallow lakes. *Trends in Ecology and Evolution* **8**: 275-279.
- Schot, P.P. and Dijst, M. 2000. Development of a generic framework for integrated physical planning. Contribution no. 145 in: *Proceedings from the 4th International conference on GIS and environmental modelling*. University of Colorado, Colorado.
- Schröder, A., Persson, L. and De Roos, A.M. 2005. Direct experimental evidence for alternative stable states: a review. *Oikos* **110**: 3-19.
- Schulze, E.D., Prokuschkin, A., Arneith, A., Knorre, N. and Vaganov, E.A. 2002. Net ecosystem productivity and peat accumulation in a Siberian Aapa mire. *Tellus B* **54**: 531-536.
- Shachak, M., Boeken, B., Groner, E., Kadmon, R., Lubin, Y., Meron, E., Ne'eman, G., Perevolotsky, A., Shkedy, Y. and Ungar, E.D. 2008. Woody species as landscape modulators and their effect on biodiversity patterns. *BioScience* **58**: 209-221.
- Shaver, G.R., Johnson, L.C., Cades, D.H., Murray, G., Laundre, J.A., Rastetter, E.B., Nadelhoffer, K.J. and Giblin, A.E. 1998. Biomass and CO₂ flux in wet sedge tundras: responses to nutrients, temperature and light. *Ecological Monographs* **68**: 75-97.
- Shaver, G.R. and Melillo, J.M. 1984. Nutrient budgets of marsh plants: efficiency concepts and relation to availability. *Ecology* **65**: 1491-1510.
- Shimoyama, K., Hiyama, T., Fukushima, Y. and Inoue, G. 2004. Controls on evapotranspiration in a west Siberian bog. *Journal of Geophysical Research* **109**: D08111.
- Semenova, N.M. and Lapshina, E.D. 2001. Description of the West Siberian plain. Pages 10-22 in: *Carbon storage and atmospheric exchange by West Siberian peatlands*. Bleuten, W. and Lapshina, E.D. (editors). Department of Physical Geography Utrecht University, Utrecht.
- Seppälä, M. and Koutaniemi, L. 1985. Formation of a string and pool topography as expressed by morphology, stratigraphy and current processes on a mire in Kuusamo, Finland. *Boreas* **14**: 287-309.
- Siegel, D.I., Glaser, P.H., So, J., Janecky, D.R. 2006. The dynamic balance between organic acids and circumneutral groundwater in a large boreal peat basin. *Journal of Hydrology* **320**: 421-431.
- Sjörs, H. 1961. Surface patterns in boreal peatland. *Endeavour* **20**: 217-223.
- Sjörs, H. 1983. Mires of Sweden. Pages 69-94 in: *Ecosystems of the world 4B. Mires: swamps, bog, fen and moor*. Gore, A.J.P. (editor). Elsevier, Amsterdam.
- Sjörs, H. 1990. Divergent succession in mires, a comparative study. *Aquilo Serio Botanica* **28**: 67-77.
- Sokal, R.R. and Rohlf, F.J. 1995. *Biometry*. Third edition. WH Freeman and Company, New York.
- Solander, D. 1983. Biomass and shoot production of *Carex rostrata* and *Equisetum fluviatile* in unfertilized and fertilized subarctic lakes. *Aquatic Botany* **15**: 349-366.
- Solé, R.V. and Bascompte, J. 2006. *Self-organization in complex ecosystems*. Princeton University press, Princeton.

- Souch, C., Susan, C., Grimmond, B. and Wolfe, C.P. 1998. Evapotranspiration rates from wetlands with different disturbance histories: Indiana Dunes National Lakeshore. *Wetlands* **18**: 216-229.
- Suding, K.N., Gross, K.L. and Houseman, G.R. 2004. Alternative states and positive feedbacks in restoration ecology. *Trends in Ecology and Evolution* **19**: 46-53.
- Svensson, B.M. 1995. Competition between *Sphagnum fuscum* and *Drosera rotundifolia*: a case of ecosystem engineering. *Oikos* **74**: 205-212.
- Svensson, G. 1988. Bog development and environmental conditions as shown by the stratigraphy of Store Mosse mire in southern Sweden. *Boreas* **17**: 89-111.
- Swanson, D.K. and Grigal, D.F. 1988. A simulation model of mire patterning. *Oikos* **53**: 309-314.

T

- Takagi, K., Tsuboya, T. and Takahashi, H. 1999. Effect of the invasion of vascular plants on heat and water balance in the Sarobetsu Mire, Northern Japan. *Wetlands* **19**: 246-254.
- Ter Braak, C.J.F., Hanski, I. and Verboom, J. 1998. The incidence function approach to modeling of metapopulation dynamics. Pages 167-188 in: *Modeling spatiotemporal dynamics in ecology*. Bascompte, J. and Solé, R.V. (editors). Springer-Verlag, Berlin.
- Thom, R. 1975. *Structural stability and morphogenesis: An outline of a general theory of models*. Benjamin Cummings, Reading, Massachusetts.
- Tilman, D. 1980. Resources: a graphical-mechanistic approach to competition and predation. *The American Naturalist* **116**: 362-393.
- Tilman, D. 1982. *Resource competition and community structure*. Princeton University Press, Princeton.
- Tricart, J. 1969. *Geomorphology of cold environments*. Macmillan, London.
- Turing, A.M. 1952. The chemical basis of morphogenesis. *Philosophical Transactions of the Royal Society of London B* **237**: 37-72.
- Turner, B.L., Chudek, J.A., Whitton, B.A. and Baxter, R. 2003. Phosphorous composition of upland soils polluted by long-term atmospheric nitrogen decomposition. *Biogeochemistry* **65**: 259-274.
- Turunen, J., Roulet, N.T. and Moore, T.R. 2004. Nitrogen deposition and increased carbon accumulation in ombrotrophic peat bogs in eastern Canada. *Global Biogeochemical Cycles* **18**: 3002.

U

- UNEP. 1992. *Global biodiversity strategy: guidelines for action to save, study and use earth's biotic wealth sustainably and equitably*. WRI, Washington DC.
- U.S. EPA. 2002. *Methods for Evaluating Wetland Condition: Vegetation-Based Indicators of Wetland Nutrient Enrichment*. Office of Water, U.S. Environmental Protection Agency, Washington DC.

V

- Van Breemen, N. 1995. How *Sphagnum* bogs down other plants. *Trends in Ecology and Evolution* **10**: 270-275.
- Van de Koppel, J. and Crain, C.M. 2006. Scale-dependent inhibition drives regular tussock spacing in a freshwater marsh. *The American Naturalist* **168**: E136-E147.
- Van de Koppel, J., Gascoigne, J.C., Theraulaz, G., Rietkerk, M., Mooij, W.M. and Herman, P.M.J. 2008. Experimental evidence for spatial self-organization and its emergent effects in mussel bed ecosystems. *Science* **322**: 739-742.
- Van de Koppel, J., Herman, P.M.J., Thoolen, P. and Heip, C.H.R. 2001. Do alternate stable states occur in natural ecosystems? Evidence from a tidal flat. *Ecology* **82**: 3449-3461.

- Van de Koppel, J., Rietkerk, M., Dankers, N. and Herman, P.M.J. 2005. Scale-dependent feedback and regular spatial patterns in young mussel beds. *The American Naturalist* **165**: E66-E77.
- Vandermeer, J. and Yodzis, P. 1999. Basin boundary collisions as a model of discontinuous change in ecosystems. *Ecology* **80**: 1817-1827.
- Van der Schaaf, S. 1999. *Analysis of the hydrology of raised bogs in the Irish Midlands –A case study of Raheenmore Bog and Clara Bog*. PhD thesis. Wageningen University, Wageningen.
- Van der Valk, A.G. and Warner, B.G. 2009. The development of patterned mosaic landscapes: an overview. *Plant Ecology* **200**: 1-7.
- Van Langevelde, F., Van de Vijver, C.A.D.M., Kumar, L., Van de Koppel, J., De Ridder, N., Van Andel, J., Skidmore, A.K., Hearne, J.W., Stroosnijder, L., Prins, H.H.T. and Rietkerk, M. 2003. Effects of fire and herbivory on the stability of savanna ecosystems. *Ecology* **84**: 337-350.
- Van Nes, E.H. and Scheffer, M. 2005. Implications of spatial heterogeneity for catastrophic regime shifts in ecosystems. *Ecology* **86**: 1797-1807.
- Van Nes, E.H. and Scheffer, M. 2007. Slow recovery from perturbations as a generic indicator of a nearby catastrophic shift. *The American Naturalist* **169**: 738-747.
- Van Wesenbeeck, B.K., Eppinga, M.B., Rietkerk, M. and Van de Koppel, J. 2007. Negative species interactions through ecosystem engineering. Pages 51-61 in: *Thresholds and shifts*. Van Wesenbeeck, B.K. PhD thesis. Rijksuniversiteit Groningen, Groningen.
- Vasiliev, S.V., Kosykh, N.P. and Mironycheva-Tokareva, N.P. 2001. Actual carbon accumulation by crop measurement. Pages 87-96 in: *Carbon storage and atmospheric exchange by West Siberian peatlands*. Bleuten, W. and Lapshina, E.D. (editors). Department of Physical Geography Utrecht University, Utrecht
- Verhoeven, J.T.A. and Schmitz, M.B. 1991. Control of plant growth by nitrogen and phosphorus in mesotrophic fens. *Biogeochemistry* **12**:135-148.
- Verkroost, A.W.M. 1997. *Syllabus praktijkopdracht interdisciplinaire en theoretische aspecten van de milieukunde*. Utrecht University, Utrecht. (In Dutch)
- Vermeer, J.G. and Berendse, F. 1983. The relationship between nutrient availability, shoot biomass and species richness in grassland and wetland communities. *Vegetatio* **53**: 121-126.
- Verry, E.S. and Urban, N.R. 1992. Nutrient cycling at Marcell Bog, Minnesota. *Suo* **43**: 147–153.
- Vitousek, P.M., Mooney, H.A., Lubchenco, J. and Melillo, J.M. 1997. Human domination of earth's ecosystems. *Science* **277**: 494-499.
- Volterra, V. 1926. Variations and fluctuations of the numbers of individuals in animal species living together. Reprinted in 1931 in: *Animal Ecology*. Chapman, R.N. (editor). McGraw Hill, New York.
- Von Hardenberg, J., Meron, E., Shachak, M. and Zarmi, Y. 2001. Diversity of vegetation patterns and desertification. *Physical Review Letters* **87**: 198101.
- VROM. 1991. *Natuurbeleidsplan*. Ministerie van VROM, The Hague. (In Dutch)

W

- Waddington, J.M. and Roulet, N.T. 1997. Groundwater flow and dissolved carbon movement in a boreal peatland. *Journal of Hydrology* **191**:122-138.
- Walker, D. and Walker, P.M. 1961. Stratigraphic evidence of regeneration in some Irish bogs. *Journal of Ecology* **49**: 169-185.
- Wallén, B. 1987. Growth pattern and distribution of biomass of *Calluna vulgaris* on an ombrotrophic peat bog. *Holarctic Ecology* **10**: 73-79.
- Wallén, B., Falkengren-Grerup, U. and Malmer, N. 1988. Biomass, productivity and relative rate of photosynthesis of *Sphagnum* at different water levels. *Holarctic Ecology* **11**: 70–76.

- Wassen, M.J. and Joosten, J.H.J. 1996. In search of a hydrological explanation for vegetation changes along a fen gradient in the Biebrza Upper Basin (Poland). *Vegetatio* **124**: 191-209.
- Wassen, M.J., Olde Venterink, H.G.M. and De Swart, E.O.A.M. 1995. Nutrient concentrations in mire vegetation as a measure of nutrient limitation in mire ecosystems. *Journal of Vegetation Science* **6**: 5-16.
- Wassen, M.J., Olde Venterink, H.G.M., Lapshina, E.D. and Tanneberger, F. 2005. Endangered plants persist under phosphorus limitation. *Nature* **437**: 547-550.
- Wells, E.D. 1996. Classification of peatland vegetation in Atlantic Canada. *Journal of Vegetation Science* **7**: 847-878.
- Weiner, J. 1995. On the practice of ecology. *Journal of Ecology* **83**: 153-158.
- Weltzin, J.F., Pastor, J., Harth, C., Bridgham, S.D., Updegraff, K. and Chapin, C.T. 2000. Response of bog and fen plant communities to warming and water-table manipulations. *Ecology* **81**: 3464-3478.
- Werner, B.T. 1999. Complexity in natural landform patterns. *Science* **284**: 102-104.
- Wetzel, P.R., Van der Valk, A.G., Newman, S., Gawlik, D.E., Troxler-Gann, T., Coronado-Molina, C.A., Childers, D.L. and Sklar, F.H. 2005. Maintaining tree islands in the Everglades: nutrient redistribution is the key. *Frontiers in Ecology and the Environment* **3**: 370-376.
- Wetzel, P.R., Van der Valk, A.G., Newman, S., Gawlik, D.E., Troxler-Gann, T., Coronado-Molina, C.A., Childers, D.L. and Sklar, F.H. 2009. Heterogeneity of phosphorus distribution in a patterned landscape, the Florida Everglades. *Plant Ecology* **200**: 83-90.
- Wiedermann, M.M., Nordin, A., Gunnarsson, U., Nilsson, M.B. and Ericson, L. 2007. Global change shifts vegetation and plant-parasite interactions in a boreal mire. *Ecology* **88**: 454-464.
- Wiegand, T., Moloney, K.A. and Milton, S.J. 1998. Population dynamics, disturbance and pattern evolution: identifying the fundamental scales of organization in a model ecosystem. *The American Naturalist* **152**: 321-337.
- Williams, G.P. 1970. The thermal regime of a Sphagnum peat bog. Pages 195-200 in: *Proceedings of the Third International Peat Congress, Quebec*. International Peat Society, Quebec.
- Williams, P.J. 1959. Arctic 'vegetation arcs'. *The Geographical Journal* **125**: 144-145.
- Wilson, C.L. and Matthews, W.H. (editors). 1970. *Man's impact on the global environment: assessment and recommendation for actions*. MIT press, Massachusetts.
- Wilson, J.B. and Agnew, A.D.Q. 1992. Positive-feedback switches in plant-communities. *Advances in Ecological Research* **23**: 263-336.
- Wu, Y., Wang, N. and Rutchey, K. 2006. An analysis of spatial complexity of ridge and slough patterns in the Everglades ecosystem. *Ecological Complexity* **3**: 183-192.

Y

- Yefremov, S. P., and Yefremova, T.T. 2001. Stocks and forms of deposited carbon and nitrogen in bog ecosystems of West Siberia. Pages 148-151 in: *West Siberian peatlands and carbon cycle: past and present. Proceedings of the International Field Symposium (Noyabrsk, August 18-22, 2001)*. Vasiliev, S.V., Titlyanova, A.A. and Velichko, A.A. (editors). Aгенство Sibprint, Novosibirsk.
- Yu, Z.C., Campbell, I.D., Vitt, D.H. and Apps, M.J. 2001. Modelling long-term peatland dynamics. I. Concepts, review, and proposed design. *Ecological Modelling* **145**: 197-210.

Z

- Zeeman, E.C. 1976. Catastrophe theory. *Scientific American* **234**: 65-83.



Summary

&

Nederlandse Samenvatting

Summary

Predicting how gradual changes in abiotic conditions affect ecosystem functioning is a key challenge in ecology and environmental science. For many ecosystems, the response to gradual changes may not be smooth, but rapid and sometimes even irreversible shifts in ecosystem states may occur. Early warning signals for such catastrophic shifts are difficult to obtain. Recent research suggests that so-called self-organized patchiness (regular spatial vegetation patterning) in ecosystems can serve as an indicator that such sudden changes may occur. Peatlands are among the ecosystems that show self-organized patchiness. More specifically, the patterning in peatlands consists of a spatially coherent structure of densely vegetated hummocks and more sparsely vegetated hollows. Research on this patchiness has focused on typical linear patterns along the contours of peatland slopes. More recently, aerial photographs from relatively flat ground in Siberia revealed peatlands with so-called maze patterning, because this type of patchiness somewhat resembles the corridors of a maze. This striking self-organized patchiness has amazed many peatland scientists, but the driving mechanisms of peatland patchiness still remain elusive. This thesis investigates underlying mechanisms that explain self-organized patchiness (such as maze patterns) in peatlands, and whether this patchiness could serve as an indicator for proximity to catastrophic shifts in peatland ecosystem states. A combination of theoretical and empirical approaches is used. Three alternative mechanisms for pattern formation are considered: evapotranspiration-induced nutrient transport (*nutrient accumulation mechanism*), differential peat accretion (*peat accumulation mechanism*), and water obstruction by denser peat layers (*water ponding mechanism*).

First, a literature review reveals that empirical evidence supports the view that peatland dynamics may be governed by catastrophic shifts. The results from the review are also used to expand a previously developed model of peatland pattern formation. The expanded model results suggest that the nutrient accumulation mechanism leads to a regular pattern of hummocks with high biomass and hollows with low biomass, similar to peatland patterns observed in the field (by means of aerial photographs). Moreover, the model predicts that hummocks have higher nutrient availability and lower water tables as compared to hollows. Obviously, the latter model predictions cannot be checked with aerial photographs but require empirical field measurements.

Second, such measurements are carried out in a patterned peatland in Siberia. In this peatland, the largest undisturbed bog-fen complex in the world, we test whether existing spatial patterns in nutrients and hydrology agree with model predictions. The empirical results agree qualitatively: nutrient availability is higher and the water table is lower under hummocks as compared to hollows. Although the data corroborates model predictions, it also reveals that the peat accumulation and water ponding mechanisms may both play a role in the formation of the patterns.

Third, a theoretical study is carried out to infer how field data can reveal which (combination) of the three mechanisms is actually driving pattern formation. Therefore, we integrate existing models into a new model framework in which each of the three mechanisms can be switched on or off, creating the possibility of a full-factorial analysis. The model results show that the water ponding mechanism alone does not lead to pattern formation. Further, the results suggest that nutrients and hydrology are the key variables that can discriminate whether patterns are driven by the nutrient accumulation mechanism or the peat accumulation mechanism. This result paves the way for another empirical test. If the nutrient pattern as observed in Siberia indeed reflects the presence of the nutrient accumulation mechanism, the nutrient pattern should be different in peatlands where the alternative mechanism, i.e. the peat accumulation mechanism, is the main driver of pattern formation.

Fourth, we test the new model predictions. We measure spatial nutrient patterns in patterned peatlands in Scotland and Sweden, and compare these results with the data from Siberia. Due to climatic differences, the peat accumulation mechanism may be most important in Scotland and Sweden. According to the model predictions, this would be reflected by the highest nutrient concentrations occurring in hollows. Nutrient data from vegetation samples indeed agree with these predictions. The data on nutrient concentration in the water, however, do not agree with the hypothesis. The very low nutrient concentrations in the study sites may explain this discrepancy, and suggest that future modeling efforts should focus on including more detail about the dynamics of nutrient uptake by plants.

We conclude that the potential importance of the nutrient accumulation mechanism for peatland patterning depends on climatic conditions. Nutrient accumulation may be particularly important in peatlands where most water leaves the system through evapotranspiration. Alternatively, if most water is lost via drainage or overland flow, the peat accumulation mechanism may be more important. Global climate models project for most peatland regions an increasing importance of evapotranspiration

during the coming century, with the strongest increases being projected for Siberia and Canada. Based on the results in this thesis, we speculate that the nutrient accumulation may become the main driver of pattern formation in parts of these regions. We also conclude that a shift from an unpatterned state without hummocks and hollows toward a patterned state with hummocks and hollows already comprises a catastrophic shift in ecosystem functioning that is difficult to reverse. This means that a pattern cannot be used as an indicator of proximity to a catastrophic shift, but rather indicates that the shift has already happened.

Moreover, the very slow development of peatlands calls for caution when applying equilibrium concepts, which are used in most mathematical models of pattern formation, to peatland dynamics. Investigation of the mechanisms that drive self-organized patchiness in ecosystems is a promising approach to increase our understanding of ecosystem functioning, and the response of ecosystems to changing abiotic conditions. This thesis shows how studies on pattern formation need to include both theoretical and empirical approaches, because the driving mechanisms of self-organized patchiness may change with climatic regions and may therefore be site-specific. This means that theory is necessary to scale empirical findings up to larger regions, but empirical testing of such theoretical predictions remains necessary.

Samenvatting

Wereldwijd staan ecosystemen bloot aan veranderingen in de omgeving, bijvoorbeeld veranderingen in klimaat of landgebruik. Een belangrijk vraagstuk binnen de ecologie en de milieuwetenschappen is hoe ecosystemen reageren op zulke geleidelijke veranderingen. Duidelijk is dat ecosystemen op allerlei verschillende manieren kunnen reageren. Een bijzondere manier van reageren is wanneer ecosystemen niet of nauwelijks reageren op geleidelijke veranderingen, totdat er een bepaalde drempelwaarde wordt overschreden. Op dat moment vindt er een snelle en plotselinge omslag in het ecosysteem plaats die moeilijk is terug te draaien. Het is daarom wenselijk om signalen te ontdekken die kunnen aangeven wanneer een ecosysteem in de buurt van zo'n drempelwaarde en een omslag komt. Tot nu toe is het lastig gebleken om dit soort signalen te vinden. Recent onderzoek suggereert echter dat in sommige ecosystemen die in de buurt van een omslag komen, er ruimtelijk regelmatige structuren gevormd worden door de vegetatie. Computermodellen verklaren dat binnen zo'n ruimtelijk regelmatige structuur de groeiomstandigheden voor de vegetatie beter zijn dan wanneer er geen ruimtelijke ordening is. Het ontstaan van een ruimtelijk regelmatig patroon zou er dus op kunnen duiden dat de omstandigheden voor de vegetatie moeilijk geworden zijn, en dat er een drempelwaarde genaderd wordt waarbij het ecosysteem omslaat naar een situatie zonder vegetatie (denk bijvoorbeeld aan verwoestijning).

Ruimtelijk regelmatige structuren in de vegetatie zijn ook waargenomen in veengebieden. Deze structuren bestaan uit drogere plekken met relatief veel vegetatie (bulten) en nattere plekken met relatief weinig vegetatie (slenken). In veengebieden met een helling organiseren de bulten en de slenken zich in strepen, waardoor er een zebra-achtig patroon ontstaat. Deze strepen staan loodrecht op de helling van het veen. In relatief vlakke veengebieden vormen de bulten een labyrint patroon dat is omgeven door slenken. De ruimtelijke regelmaat van deze veenpatronen heeft veel onderzoekers gefascineerd, en zijn daarom veelvuldig beschreven in de literatuur. Het is echter nog steeds onduidelijk welke processen zorgen voor de vorming van deze ruimtelijk regelmatige structuren in veengebieden.

Venen zijn relatief natte ecosystemen, wat betekent dat een deel van het dode plantenmateriaal terecht komt onder de grondwaterstand. Hier kan het plantenmateriaal nauwelijks worden verteerd door bacteriën. Dit heeft als gevolg dat met het verstrijken van de tijd een dikke laag plantenmateriaal ophoopt als veen. Omdat planten koolstofdioxide opnemen uit de lucht, vormt ook het veen een

belangrijke opslag van koolstof. De ontwikkeling van veengebieden de afgelopen 14.000 jaar heeft ertoe geleid dat op dit moment ongeveer 30% van alle op land opgeslagen koolstof zich in venen bevindt. Een omslag in veengebieden zou grote gevolgen kunnen hebben voor de waterhuishouding en de afbraaksnelheid van het veenmateriaal. Daarmee zou een omslag in veengebieden gevolgen kunnen hebben voor de koolstof-opslag functie die venen tot nu toe hebben gehad. Het is dus nuttig om te kijken of ruimtelijk regelmatige vegetatiestructuren in veengebieden een signaal zijn voor het naderen van zo'n mogelijke omslag. In dit proefschrift worden mogelijke processen voor patroonvorming in venen onderzocht, en ook of deze patronen een signaal zijn voor het naderen van drempelwaardes en omslagen in het veensysteem. Ik heb hierin voor een combinatie van modellering en empirie gekozen. Het onderzoek maakt gebruik van computermodellen waarin verschillende processen kunnen worden onderzocht, en ook worden de voorspellingen van de computermodellen getest met metingen in veensystemen. De uitkomsten van de metingen kunnen dan weer aanwijzingen geven hoe de modellen kunnen worden verbeterd. Het onderzoek beschouwt drie mogelijke verklaringen voor de patroonvorming in venen.

De eerste mogelijke verklaring is dat de patroonvorming in venen wordt bepaald door de dikte van de veenlaag boven de grondwaterstand. De bovenste veenlaag is dus de afstand van het veenoppervlak tot het grondwater. De dikte van deze laag bepaald in belangrijke mate de groeiomstandigheden voor planten. Echter, de plantengroei beïnvloedt weer de dikte van de bovenste veenlaag. Er bestaat dus een wederkerige relatie, die zichzelf kan versterken. Als de dikte van de bovenste veenlaag toeneemt, kunnen planten beter groeien. Als planten beter groeien, wordt er meer plantenmateriaal toegevoegd aan de bovenste veenlaag, waardoor deze nog dikker wordt. Uiteindelijk leidt dit tot de vorming van een bult, een relatief droge plek met veel biomassa. De relatie kan echter ook de andere kant op ontwikkelen: als de dikte van de bovenste veenlaag afneemt groeien planten slechter, daardoor wordt er minder plantenmateriaal toegevoegd aan de bovenste veenlaag, waardoor de dikte hiervan verder afneemt. Uiteindelijk leidt dit tot de vorming van een slenk, een relatief natte plek met weinig biomassa. De relatie tussen bovenste veenlaag en plantengroei kan dus zowel bult- als slenkvorming in venen verklaren.

De tweede mogelijke verklaring is dat de patroonvorming in venen wordt veroorzaakt doordat water minder makkelijk door bulten kan stromen dan door slenken. Dit betekent dat wanneer een bult zich vormt op een veenhelling deze fungeert als een

dam, waardoor water kan ophopen hoger op de helling. Deze ophoping van water leidt dan tot de vorming van een slenk. Als deze slenk groot genoeg is, zorgt deze voor voldoende afwatering zodat hoger op de helling weer een nieuwe bult kan vormen, waarna het proces zich weer herhaalt. Modellen hebben laten zien dat deze damfunctie van bulten de patroonvorming op veenhellingen kan verklaren.

De derde mogelijke verklaring is dat de patroonvorming in venen wordt veroorzaakt door een transport van voedingsstoffen van slenken naar bulten. De vegetatie op bulten kan ervoor zorgen dat er meer water verdampt op bulten dan in slenken. Het extra waterverlies wordt dan weer aangevuld met water uit de bodem, dat dan van slenken naar bulten stroomt. Omdat voedingsstoffen opgelost zijn in dit water ontstaat er dus een transport van voedingsstoffen van slenken naar bulten. Ook dit is een zichzelf versterkend proces, omdat een extra toevoer aan voedingsstoffen leidt tot extra plantengroei, en extra plantengroei leidt weer tot meer verdamping en meer aanvoer van voedingsstoffen.

Het eerste inhoudelijke hoofdstuk van het proefschrift laat een overzicht zien van de bestaande literatuur. Hieruit komt naar voren dat eerdere veldstudies suggereren dat er inderdaad plotselinge omslagen in veengebieden plaats kunnen vinden als het gevolg van geleidelijke veranderingen. De resultaten van het literatuuroverzicht worden ook gebruikt om een bestaand computermodel uit te breiden. Met dit model wordt de derde verklaring voor patroonvorming (transport van voedingsstoffen van bulten naar slenken) nader onderzocht. De modelresultaten laten zien dat dit mechanisme inderdaad leidt tot regelmatige patroonvorming van bulten en slenken, zoals ook is waargenomen op luchtfoto's. De modelresultaten suggereren ook dat op de bulten de beschikbaarheid van voedingsstoffen hoger is en de grondwaterstand lager dan die in slenken. Omdat deze laatste modelvoorspellingen niet meer getest kunnen worden met luchtfoto's is veldonderzoek nodig om deze modelresultaten te testen.

In het tweede inhoudelijke hoofdstuk worden deze veldmetingen verricht in een veengebied met regelmatige labyrint-patronen in Siberië. In dit veengebied, het grootste ongestoorde veengebied ter wereld, testen we of de verdeling van voedingsstoffen en de grondwaterstanden in bulten en slenken overeenkomt met de modelvoorspellingen uit het vorige hoofdstuk. De meetresultaten komen in kwalitatieve zin overeen met de modelvoorspellingen: in bulten is de beschikbaarheid van voedingsstoffen hoger en de grondwaterstand lager dan in slenken. De metingen

laten ook zien dat de twee andere verklaringen voor patroonvorming mogelijk ook een rol spelen in het onderzochte Siberische veengebied.

In het derde inhoudelijke hoofdstuk wordt een computermodel gebruikt om te onderzoeken hoe meetgegevens in een veengebied met patroon uitsluitel kunnen geven over welk (of welke combinatie) van de drie verklarende processen daadwerkelijk zorgt voor de patroonvorming in dat gebied. In het nieuwe computermodel worden bestaande modellen gecombineerd. In het nieuwe model kan elk van de drie verklarende processen aan of uit worden gezet. Op deze manier kan systematisch worden nagegaan hoe ieder verklarend proces de patroonvorming, waterhuishouding en verdeling van voedingsstoffen van een veengebied beïnvloedt. De resultaten laten zien dat de damfunctie van bulten geen afdoende verklaring biedt voor patroonvorming. Verder laten de resultaten zien dat als patroonvorming wordt veroorzaakt door de relatie tussen plantengroei en de bovenste veenlaag, de beschikbaarheid van voedingsstoffen lager en de waterstand hoger is in bulten dan in slenken. Dit is precies tegenovergesteld aan patronen veroorzaakt door het transport van voedingsstoffen gedreven door verdamping. Daarmee laten de modelresultaten zien dat het verklarende proces van patroonvorming wordt weerspiegeld in de waterhuishouding en verdeling van voedingsstoffen binnen venen. Dit resultaat biedt mogelijkheden voor verder onderzoek in het veld. Als de patroonvorming in het Siberische veengebied inderdaad wordt veroorzaakt door transport van voedingsstoffen door verdamping, dan zou de waterhuishouding en de verdeling van voedingsstoffen in dit gebied anders zijn dan in gebieden waar patroonvorming wordt veroorzaakt door het andere verklarende proces (de relatie tussen de plantengroei en dikte van de bovenste veenlaag).

In het vierde inhoudelijke hoofdstuk testen we de resultaten van het nieuwe model in het veld. We meten de verdeling van voedingsstoffen in venen met patronen in Schotland en Zweden, en vergelijken deze met de eerder gemeten data in Siberië. Omdat er grote verschillen zijn in het klimaat tussen deze gebieden, veronderstellen we dat ook de rol van verdampingsprocessen in deze gebieden verschilt. In Siberie is verdamping erg belangrijk, en daarom kan mogelijk ook de patroonvorming in dit gebied ontstaan door verschillen in verdamping tussen bulten en slenken. In Schotland speelt verdamping echter een veel kleinere rol. Het is daarom onwaarschijnlijk dat de patroonvorming in dit gebied gedreven wordt door verdamping. Onze modelresultaten uit het vorige hoofdstuk suggereren dat deze verschillen ook weerspiegeld worden in de verdeling van voedingsstoffen in deze

gebieden. De verdeling van voedingsstoffen, zoals gemeten in de vegetatie, komen overeen met de voorspellingen van het model. Echter, de verdeling van voedingsstoffen gemeten in het water komen niet overeen met de modelvoorspellingen. De zeer lage beschikbaarheid van voedingsstoffen in het water vormen een mogelijke verklaring voor het verschil tussen modelvoorspellingen en veldmetingen, en laat zien dat toekomstige modellen meer aandacht moeten schenken aan het proces van opname van voedingsstoffen door de vegetatie.

In het afsluitende hoofdstuk wordt geconcludeerd dat de rol van verdamping in de patroonvorming in venen afhangt van het klimaat. Verdamping kan vooral een rol spelen in veengebieden als het een belangrijke bijdrage levert aan het totale waterverlies van het veen. In veengebieden waar het meeste water het systeem verlaat door andere processen, zoals drainage of afstroming, kan vooral de relatie tussen plantengroei en dikte van de bovenste veenlaag belangrijk zijn voor de patroonvorming. Wereldwijde klimaatmodellen voorspellen dat door klimaatverandering verdamping een belangrijkere rol gaat spelen in de waterhuishouding van veel veengebieden. Vooral in Siberië en Canada zijn er gebieden waar verdamping belangrijker gaat worden. Op basis van de resultaten in dit proefschrift speculeer ik dat hierdoor patroonvorming kan ontstaan, dat is gedreven door transport van voedingsstoffen door verdamping.

Een andere belangrijke vraag in dit proefschrift is of patroonvorming in venen een signaal zijn dat het systeem in de buurt van een drempelwaarde en een plotselinge omslag komt. In het afsluitende hoofdstuk wordt echter geconcludeerd dat een verandering van een patroonloze toestand zonder bulten en slenken naar een patroon toestand met bulten en slenken op zichzelf al een omslag is die moeilijk is terug te draaien. In het geval van veengebieden is deze verandering dus al de plotselinge omslag zelf, en is het dus geen signaal voor een aankomende omslag.

De resultaten van het proefschrift suggereren verder dat er een belangrijk verschil is tussen hoe computermodellen de veengebieden representeren en echte veengebieden. In de gemodelleerde gebieden is een variabele zoals koolstofopslag gedefinieerd voor het moment dat veengebieden volledig ontwikkeld zijn. De zeer trage ontwikkeling van natuurlijke veengebieden zorgen ervoor dat in de praktijk deze eindtoestanden vaak nog niet zijn bereikt. Daarom moet enige voorzichtigheid in acht worden genomen bij de interpretatie van modelresultaten over de gevolgen van plotselinge omslagen voor bijvoorbeeld de hoeveelheid opgeslagen koolstof in

veengebieden. Mijn computermodellen zijn daarom beter bruikbaar voor het voorspellen van processen op de kortere termijn, zoals patroonvorming en het veranderen van patronen door fluctuaties in het klimaat. Het onderzoeken van de verklarende processen van ruimtelijk regelmatige patroonvorming in ecosystemen is een belangrijke stap in de richting van het beter begrijpen van het functioneren van ecosystemen in het algemeen, dus deze processen kunnen nog steeds belangrijk zijn in gebieden waar de ruimtelijke patroonvorming (op het oog) minder aanwezig is. Het beter begrijpen van het functioneren van ecosystemen kan vervolgens helpen in het beter voorspellen hoe deze systemen in de toekomst zullen reageren op geleidelijke veranderingen in klimaat of menselijke invloed. Het werk in dit proefschrift laat zien dat bij dergelijk onderzoek een combinatie van theorie en empirie waardevol kan zijn, omdat de redenen voor patroonvorming afhangen van het lokale klimaat. Dit betekent dus dat het verklarende proces voor patroonvorming per gebied verschillend kan zijn. Theorie is daarom nodig om empirische gegevens te kunnen opschalen naar een groter gebied, maar het is ook nodig om deze theoretische voorspellingen empirisch te testen.



Personal notes

Nawoord

“aMazing pattern...wat bedoel je daar nou mee?” “Er staat een typefout in je titel!” Na een aantal van dit soort reacties op de titel van dit proefschrift werd het me duidelijk dat de dubbele betekenis van aMazing misschien toch niet zo duidelijk was als ik zelf hoopte. Daarom volgt hier alsnog een korte toelichting. Het startpunt van mijn onderzoek in 2004 waren recente foto's uit Siberië, waarop te zien was dat in dit gebied bomen groeien in een labyrint-achtig patroon ('maze pattern' in het Engels). Op de foto's was dus 'a mazing pattern' te zien. Ik zag deze foto's voor het eerst in het VIDI-onderzoeksvoorstel van Max:



*Foto's van Siberische
expeditie door Bleuten,
Lapshina & Wassen*

Ik was meteen enorm geboeid door deze foto's, ik vond het patroon geweldig en verbazingwekkend, 'amazing' dus. Waarom zouden bomen op zo'n ruimtelijk georganiseerde manier gaan groeien? En dat was zo ongeveer de vraag waarvoor een PhD-student gezocht werd. Ik hoefde dan ook niet lang na te denken om te solliciteren, en ben erg blij met de mogelijkheid die ik heb gekregen om een proefschrift over patronen in venen te schrijven.

Het schrijven van een proefschrift is 'a mazing process': de route loopt (gelukkig!) niet in een rechte lijn van het begin naar het eindpunt, maar je slaat ook wel eens paden in die doodlopen en je dus weer een nieuw pad moet bedenken. Maar ik heb mijn PhD periode ook zeker als 'amazing' ervaren: ik heb met ontzettend veel plezier in een geweldige omgeving kunnen puzzelen met dit onderwerp. Ik vind het eigenlijk jammer dat het al afgelopen is! De lastige klus voor dit hoofdstukje is nu om iedereen te bedanken die de PhD periode voor mij zo amazing hebben gemaakt. Allereerst wil ik graag mijn begeleiders Max, Peter en Martin bedanken.

Max, bedankt voor al je enthousiasme waarmee je mijn eerste stappen op de weg naar zelfstandig onderzoeker hebt begeleid. Jouw enthousiasme heeft zeker aanstekelijk gewerkt! Ik kon altijd bij je binnen lopen om wat dan ook te bespreken, maar je gaf ook het vertrouwen om me een tijdje te laten puzzelen als ik daar behoefte aan had. Ik heb bewondering voor de grondigheid waarmee je altijd weer het werk van mij en je andere studenten bestudeert, en dat je altijd met een frisse blik naar stukken kan blijven kijken, ook als je ze al tig keer hebt gelezen. Wat ik ook

erg plezierig heb gevonden is dat je ontzettend duidelijk kunt uitleggen wat je bedoelt; je bent onnavolgbaar goed te volgen. Ik hoop dan ook dat mijn schrijfstijl na onze samenwerking de afgelopen jaren een beetje geMaximized is.

Peter, mijn interesse voor wetenschappelijk onderzoek in het algemeen en modelleren in het bijzonder is ontstaan dankzij jouw cursus milieusysteemanalyse en modellen. Hierin leerde ik van jou dat simpele modellen kunnen helpen om de wereld om ons heen (en Walt Disney tekenfilms) beter te begrijpen. Ik vond het erg leuk om vervolgens een aantal keer jouw assistent te mogen zijn in dezelfde cursus. Als promotor van mijn onderzoek daagde je me uit om de link tussen modelleren en empirie te smeden, en dat ook op te schrijven op een manier die zowel theoretici als empirici aanspreekt. Ook stimuleerde je het bekijken van de consequenties van ons onderzoek in bredere zin. Bedankt voor de tijd die je hebt geïnvesteerd in mijn ontwikkeling in het geven van onderwijs en het doen van onderzoek.

Martin, bedankt voor het delen van jouw kennis over veengebieden en ervaring in het doen van empirische wetenschap. Wat ik van jou op deze vlakken geleerd heb is denk ik zichtbaar in dit proefschrift. Voor mij was het hoogtepunt van onze samenwerking de drie weken dat we samen (met Frans) veldwerk hebben gedaan in Schotland en Zweden. In die tijd hebben we erg veel werk verzet, maar tegelijkertijd het plezier gehad van twee vrienden die op vakantie zijn. Gedurende mijn PhD periode heb jij steeds meer extra bestuurstaken gekregen. Ik vind het daarom bijzonder dat je enthousiasme, betrokkenheid en persoonlijke aandacht als promotor van mijn onderzoek onveranderd groot is gebleven.

Max, Peter en Martin jullie vormen een geweldig team als begeleiders! Ik hoop dan ook dat onze wegen nog vaak mogen kruisen.

I have also enjoyed the collaboration with other scientists from outside our own department. I would like to thank Wladimir Bleuten, Wiebe Borren, Elena Lapshina, Mats Nilsson and Lisa Belyea for our field expeditions and collaboration afterwards. Laurel Larsen is thanked for her comments on various sections of this thesis, which improved these sections significantly. Finally, I have enjoyed the interactions with several NIOO members. I would like to explicitly mention the interactions with Johan Van de Koppel, who was always enthusiastically involved in questions on all kinds of topics, such as bimodality (“aahh, ik had net een programmaatje geschreven dat...”), which I actually benefited from in Chapter 3.

Ik heb het bij milieuwetenschappen altijd enorm naar mijn zin gehad! Tijdens de studietijd was het erg gezellig met mijn jaargenoten, wat ook blijkt uit het feit dat onze beruchte pokersessies nog steeds met regelmaat (toch, OC?) plaatsvinden. Ik wil in het bijzonder Vincent bedanken, die ook mijn gehele PhD periode in de buurt is gebleven om zo nu en dan ff een bakkie te doen. Na de studie werden mijn docenten en werkgroepbegeleiders ineens collega's, en ook hen wil ik allemaal graag bedanken voor de gezellige sfeer op de 11^{de} de afgelopen jaren. Met name de jaarlijkse uitjes, de AiO etentjes, borrels en het maken van de filmpjes zullen me bijblijven. Ik heb in mijn PhD periode behoorlijk wat kamergenoten versleten, daarom wil ik graag de kamergenoten bedanken die het het langst met mij hebben kunnen uithouden. Sonia, ik vind het erg leuk dat onze interessante discussies over cirkels, stickyness en loss terms deels terecht zijn gekomen in jouw proefschrift, en dat ook mijn eerste en laatste hoofdstuk geïnspireerd zijn door onze kamerdiscussies. Remko, ik denk dat ons record op de Copernicus-koffiekaartenlijst nog wel een paar jaar stand houdt. Bedankt voor alle gezellige gesprekken die we hielden tijdens het opdrinken van de koffie en thee. Hugo, als Prof. Oleg McNoleg weer een nieuw paper uitheeft kom ik zeker weer langs om het met je te bediscussiëren. Ik vond het erg gezellig samen op de kamer, en bedankt voor je hulp bij het maken van de world maps in dit proefschrift en het wegwijs maken in de .csv-wereld van klimaatdata!

Maar ja, collega's, hoe leuk en gezellig jullie ook allemaal mogen zijn, mijn favoriete collega is toch echt Roos. Lieve Roos, ik ben heel blij met de bijzondere band die wij de afgelopen jaren hebben opgebouwd. Onwijs bedankt voor alles!

Op cv's zie je wel eens een categorie 'memberships'. Mijn meest waardevolle membership is dat van de Magnificent Se7en & Co, mijn highschool matties die mijn hele PhD periode alle verhalen over patronen, papers, de helikopter en modelruns hebben moeten aanhoren. Daan & Johanna, Johan & Femke, Jos, Lili, Marianne, Wilco & Lieke, Willem & Corlijn, Wouter & Bernadette, we gaan proosten met een glaasje/flesje Raki!

Tenslotte wil ik graag mijn ouders, broers en zus bedanken. Pa, Ma, Kaz, Wout en Juud, jullie hebben me laten zien dat je iets kunt bereiken als je je schouders eronder zet, handen uit de mouwen steekt en beide benen op de grond houdt.

Bedankt allemaal!

Maarten, mei 2009

Curriculum Vitae

Maarten Eppinga was born on the 15th of June 1982 in Woerden, The Netherlands. He grew up in the nearby village of Linschoten, and obtained his high school degree at the Kalsbeek College in Woerden. In the year 2000 he started his academic studies with a propaedeutic in Physics and Astronomy at Utrecht University, which he finished in 2002. Meanwhile, he had started with a doctoral study programme in Environmental Sciences, also at Utrecht University. He obtained the Masters degree in 2004 (cum laude). The subject of his master thesis was the role of soil organisms in driving plant community processes, such as succession and invasion. This modelling study was carried out under the supervision of Max Rietkerk, Stefan Dekker and Peter De Ruiter from Utrecht University and Wim Van der Putten from the Netherlands Institute of Ecology. Also in 2004, he started working on this PhD thesis on self-organization in peatland ecosystems, at the department of Environmental Sciences at Utrecht University. From January until August 2008, he also held a position of lecturer in Environmental Sciences (0.2 fte) at the same department. During his PhD period the times that were not spent on modelling were used to analyze and carry out field measurements in Scotland (in collaboration with Lisa Belyea), Sweden (in collaboration with Mats Nilsson) and Siberia (in collaboration with Wiebe Borren, Elena Lapshina and Wladimir Bleuten). During his PhD period, he also acted as a reviewer for the journals *Plant Ecology*, *Ecoscience*, *Applied Soil Ecology*, *Ecography* and *Ecology Letters*.

Peer-reviewed publications

6. Van der Putten, W.H., Bardgett, R.D., De Ruiter, P.C., Hol, W.H.G., Meyer, K.M., Bezemer, T.M., Bradford, M.A., Christensen, S., Eppinga, M.B., Fukami, T., Hemerik, L., Molofsky, J., Schädler, M., Scherber, C., Strauss, S.Y., Vos, M. and Wardle, D.A. In press. Empirical and theoretical challenges in aboveground-belowground ecology. *Oecologia*, in press.
5. Eppinga, M.B., De Ruiter, P.C., Wassen, M.J. and Rietkerk, M. In press. Nutrients and hydrology indicate the driving mechanisms of peatland surface patterning. *The American Naturalist*, 173, 803-818.
4. Eppinga, M.B., Rietkerk, M., Wassen, M.J. and De Ruiter, P.C. 2009. Linking habitat modification to catastrophic shifts and vegetation patterns in bogs. *Plant Ecology*, 200, 53-68.
3. Robroek, B.J.M., Eppinga, M.B., Limpens, J., Wassen, M.J. and Schouten, M.G.C. 2009. Bog restoration in the Netherlands: more than just a dream. *Landschap* 26: 17-26. (In Dutch with English summary).
2. Eppinga, M.B., Rietkerk, M., Borren, W., Lapshina, E.D., Bleuten, W. and Wassen, M.J. 2008. Regular surface patterning of peatlands: confronting theory with field data. *Ecosystems* 11: 520-536.
1. Eppinga, M.B., Rietkerk, M., Dekker, S.C., De Ruiter, P.C. and Van der Putten, W.H. 2006. Accumulation of local pathogens: a new hypothesis to explain exotic plant invasions. *Oikos* 114: 168-176.